Non-Invasive diagnostic techniques for the detection of acetabular component loosening in total hip replacement.

Alshuhri, Abdullah

Award date:
2016

Awarding institution:
University of Bath

Non-Invasive diagnostic techniques for the detection of acetabular component loosening in total hip replacement.

Abdullah Aziz Alshuhri

A thesis submitted for the degree of Doctor of Philosophy

University of Bath

Centre for Orthopaedic Biomechanics

Department of Mechanical Engineering

September 2016

Abstract

Total hip replacement is a human surgical intervention with the aim of pain relief and function restoration, with a survival rate of ≥ 90% at ten years. Currently, imaging techniques are the primary diagnostic and follow-up method, but are unreliable for early loosening detection. Vibrometry has been proposed as an alternative, more sensitive method for loosening diagnosis.

Despite the fact that acetabular cups have a higher revision rate over femoral components, most of the existing vibrometry literature is stem related. A limited number of studies have examined cup loosening without defining the loosening level detected. Hence, the present study aimed to investigate the feasibility of detecting acetabular cup loosening using vibrometry, and to define the earliest loosening phase that could be accurately detected.

Three objectives were devised to address this aim. Firstly, a simplified set-up with minimal boundary conditions utilising Sawbones blocks. Secondly, a complex bone geometry was examined by utilising a Sawbones hemi-pelvis, and thirdly a more clinically relevant experiment was tested by using a composite femur and hemi-pelvis.

Loosening was demonstrated by a reduction in the fundamental frequency and an increase in the magnitude of the related harmonics. By quantifying the magnitude of the harmonics in relation to the fundamental frequency, it was found that the harmonic ratio would increase, corresponding to the degree of loosening. These findings support the existing vibrometry literature. In the first objective the minimum detected simulated loosening was 1mm zone 2 loosening within the frequency range 2000-2500Hz. For the second and third objectives this was 1mm spherical acetabular cup loosening within the range 500-1500Hz. Hence, the study suggests that vibrometry has the potential to diagnose early acetabular cup loosening. This study is therefore novel because it has defined the minimum acetabular cup loosening level that can be reliably detected, alongside the favourable frequency range.

Acknowledgements

I would like to thank my supervisors, Dr. James Cunningham and Professor Tony Miles, for their support and guidance throughout my PhD. I would also like to acknowledge the support of Nick Waywell and the instrumentation team for all their help with the experimental work undertaken. Special thanks to Sam Horrocks from Stryker for providing the femoral and acetabular components. I also wish to acknowledge the Centre for Orthopaedic Biomechanics team; especially Tim Holsgrove, Samantha Wright, Lisa Coles, and Emilie Crosnier for their guidance. Special thanks go to the Medical Devices Sector at the Saudi Food and Drug Authority for funding my PhD. Also, a special thanks to my wife Zainah and the rest of my extended family for their endless love and support.

Table of Contents

Abstract I

Acknowledgements III

Table of Contents 1

List of Figures 5

List of Tables 11

List of Abbreviation 13

Chapter 1 – Introduction 15

1.1 Background 16

1.2 Report Structure 17

Chapter 2 – Total hip replacement 19

2.1 Introduction 20

2.2 Hip joint 21

2.2.1 Articulate Cartilage 22

2.2.2 Ligaments 22

2.2.3 Muscles 23

2.2.4 Pathologies Outline 25

2.3 Total hip replacement 27

2.3.1 History 27

2.3.2 Fixation 31

2.3.3 Materials and components (state of the art) 34

2.3.4 National Joint Registries 36

2.3.5 Failure and revision 37

2.4 THR Loosening diagnosis 39

2.4.1 Imagining 41

2.4.2 Non-imaging 46

2.5 Literature review summary 77

Chapter 3 – Aim and Objectives 79

3.1 Aim 80

3.2 Research questions 80

3.3 Research objectives 80

Chapter 4 – Research Methodology 83

4.1 Introduction 84

4.2 Vibrometry concept in detecting loosening 85

4.2.1 Study Design 89

4.3 Excitation System 91

4.4 Measurement Techniques 92

4.4.1 Accelerometer 92
4.4.2 Ultrasound 92
4.4.3 Signal measurement 94
4.5 Signal Analysis Technique (Spectrum Analysis) 94
4.5.1 Frequency Spectrum Analysis 96
4.5.2 Harmonic Ratio 97
4.5.3 Statistical Analysis 98
4.6 Summary 99
Chapter 5 –The First Objective (Sawbones blocks Cup Loosening) 101
5.1 Introduction 102
5.2 First Case Study: Late Spherical Loosening 103
5.2.1 Materials and Methods 104
5.2.2 Measurement and Analysis 111
5.2.3 First Case Study Discussion 119
5.3 Second Case Study: Early Spherical Loosening 121
5.3.1 Materials and Methods 122
5.3.2 Measurement and analysis 127
5.3.3 Second Case Study Discussion 132
5.4 Third Case Study: Early Zone Loosening 134
5.4.1 Materials and Methods 135
5.4.2 Measurement and analysis 138
5.4.3 Third Case Study Discussion 144
5.5 Overall Discussion 145
5.6 Conclusion 148
Chapter 6 – The Second Objective (Sawbones Hemi-Pelvis Acetabular Cup Loosening) 149
6.1 Introduction 150
6.2 Fourth Case Study: Hemi-pelvis acetabular cup loosening 151
6.2.1 Materials and Methods 152
6.2.2 Measurement and analysis 161
6.2.3 Discussion 174
6.2.4 Conclusion 176
Chapter 7 – The Third Objective (Sawbones Femur and Hemi-Pelvis Cup Loosening) 177
7.1 Introduction 178
7.2 Fifth Case Study: Femur and Hemi-pelvis Cup Loosening 179
7.2.1 Materials and Methods 179
7.2.2 Measurement and analysis 185
7.2.3 Discussion 200

7.2.4 Conclusion....203
Chapter 8 – Discussion....205
8.1 Discussion....206
Chapter 9 – Conclusion and future work....215
9.1 Conclusion....216
9.2 Future work....218
Reference....221
Appendix A: LabVIEW Code....239
Appendix B: FFT Algorithm....243
Appendix C: Pelvis Specimen Fixation....245
Appendix D: Muscle Simulation Approach....247
Appendix E: Results....249
Appendix F: Publications....261

List of Figures

Figure 2-1: The hip joint bones (Femoral and Pelvis), based on an illustration from [24]. 21

Figure 2-2: The natural hip joint, based on an illustration from [24]. 22

Figure 2-3: Hip joint ligaments, based on an illustration from [24, 29]. 23

Figure 2-4: Hip joint muscle groups, based on an illustration from [29]. 24

Figure 2-5: Hip range of motion, based on an illustration from [30]. 24

Figure 2-6: Historical development of the hip replacement, based on source [42] with permission. 29

Figure 2-7: Overview of THR fixation methods. a) Cementless, b) Cemented, c) Hybrid (cemented stem and cementless cup), d) Reverse Hybrid (Cement cup and cementless stem), based on an illustration from [41]. 33

Figure 2-8: THR primary fixation trend between 2003 and 2014 from NJR 12th annual report [32]. 34

Figure 2-9: THR components illustration, from source [46] with permission. 35

Figure 2-10: The THR loosening zones. a) Anteroposterior view showing the stem first 7 loosening zones and the acetabular cup three loosening zones and, b) Lateral view illustrating the other 7 stem loosening zones. Based on an illustration from [97]. 40

Figure 2-11: The frequency responses reflecting cement healing; a) Chung *et al.* (1979)[141], b) Poss *et al*. (1984)[142]. Illustrations modified by the author. 51

Figure 2-12: The *in vivo* test setting , source [10] with permission 53

Figure 2-13: The FFT response of the secure and loose prosthesis, source [10] with permission. 53

Figure 2-14: Li *et al* (1996) explaining the principle of distinction between secure and loose implants through the (FFT) spectral analysis (not from specimen data just an example), source [12] with permission. 54

Figure 2-15: Li *et al* (1996) secure and loose femoral component spectral analysis, source [12] with permission. 55

Figure 2-16: The two different types of bone tests; a) Sawbones setup, b) Tufnol setup, source [145] with permission. 57

Figure 2-17: The two sensors Sawbones FFT response of the loose prosthesis at driving frequency of 400Hz, showing the higher signal magnitude for the ultrasound (y-axis); a) Accelerometer, b) Ultrasound, source [145] with permission. 57

Figure 2-18: The Sawbones model setup for the combined stem cup loosening, a) the model and excitation setup, b) the location of the three used accelerometers, source [8] with permission. 58

Figure 2-19: The accelerometers average spectral response; clearly illustrating the peak shift with relation to the three simulated conditions, source [8] with permission. 59

Figure 2-20: The new proposed shockwaves excitation, a) the shockwave source, b) the excitation location used, source [5] with permission. 60

Figure 2-21: Perez *et al*.'s experiment setup and results. a) the setup sketch , b) the frequency response (grey line: average secure stem response, bold line: average loose stem response), source [15] with permission. 61

Figure 2-22: The first wireless vibrometry system; a) the system concept, b) the imbedded sensor in the femoral head, c) the time domain response at 150Hz excitation (upper figure for the secure output – lower figure for the loose condition), source [152] with permission. 62

Figure 2-23: The acoustic-mechanical methods concept diagram, source [121]. 65

Figure 2-24: The frequency response of two of the simulated conditions, a) stable (with micromotion reading of 20 µm) and, b) unstable implant (with micromotion reading of 200 µm), source [167, 170] with permission. 68

Figure 2-25: The applied torque and micromotion relation for the experimental and finite element model, source [171] with permission. 68

Figure 2-26: The FES cementless stem osseointegration simulation (a) stem-bone bonding process during the 25 weeks, b) the resonance frequency values during the simulation, source [15], with permission. 70

Figure 4-1: The patient setup under vibrometry assessment; A) Rosenstein et al. [10] with permission, B) Georgiou and Cunningham [9]with permission. 86

Figure 4-2: Rosenstein et al. [10] clinical study results for the secure implant (a) and for the loose condition (b), with permission. 87

Figure 4-3: Georgiou and Cunningham [9] clinical study results for the secure implant (a) and for the loose condition (b), with permission. 87

Figure 4-4: Frequency Spectrum Analysis concept in detecting Acetabular cup loosening, source [194], with permission. 88

Figure 4-5: The Study three Objectives 90

Figure 4-6: The Frequency Spectrum (FFT) analysis. 96

Figure 4-7: The periodical signal spectrum analysis: Fundamental frequency (F), 1st harmonic (2F), 2nd harmonic (3F), etc. 97

Figure 5-1: The polyurethane solid foam and the excitation and measurement techniques used, source [194], with permission, ... 103

Figure 5-2: Case study three conditions (1mm press-fit, 2mm spherical loose and 4mm spherical loose), source [194], with permission. 104

Figure 5-3: The instrument used to create the loosening cavity and the silicone layer. 106

Figure 5-4: The system ste-up ; Sawbones block, excitaion, and measurment method, source [194], with permission. 107

Figure 5-5: The protocol of testing for the spherical late loosening. 110

Figure 5-6: FFT spectrum analysis at driving signal 200Hz, source [194], with permission. 113

Figure 5-7: The harmonic ratio for the ultrasound signal at 200Hz driving frequency. The ultrasound probe sensitivity was (0.5V/KHz). 114

Figure 5-8: The harmonic ratio of the different simulated condition for both measurement techniques. Graphs a, c, e and g were obtained using the accelerometer sensor for the

comparison between the conditions; (secure, 2 and 4 mm loose), (secure and 2mm loose), (secure and 4 mm loose) and (2 and 4mm loose), respectively . Graphs b, d, f and h show the same sequence of comparisons using the ultrasound probe measurement technique. * Mann-Whitney test $p < 0.05$, n = sample size, source [194], with permission. 117

Figure 5-9: The early spherical loosening testing set-up. 121

Figure 5-10: Case study two three conditions (1mm press-fit, 1mm spherical silicone loose and 1 mm spherical clear loose). 122

Figure 5-11: Steps taken to mimic loosening that was a 1mm radiolucent line equivalent using the silicone. 124

Figure 5-12: The Sawbones block showing the added 1mm silicone layer. 124

Figure 5-13: Early loosening set-up showing the additional aluminium frame used for the sensors alignment. 126

Figure 5-14: The accelerometer coupling to sawbone surface, a) using a petro-wax material for the late loosening case study, b) using the screw-fixation coupling for the early loosening case study 126

Figure 5-15:The accelerometer first harmonic magnitude response to the three simulated condition at the driving frequencies 1050 Hz, 1100 Hz and 1150 Hz. ** Mann-Whitney test $p < 0.05$, n = sample size .Source (27). 128

Figure 5-16:The ultrasound second harmonic magnitude response to the three simulated condition at the driving frequencies 800 Hz, 950 Hz and 1050 Hz.* and ** Mann-Whitney test $p < 0.05$, n = sample size. Source (27). 129

Figure 5-17: The accelerometer first harmonic ratio to the three simulated condition at the driving frequencies 800 Hz and 1150 Hz.* and ** Mann-Whitney test $p < 0.05$, n = sample size. 130

Figure 5-18:The ultrasound second harmonic ratio to the three simulated condition at the driving frequencies 800 Hz ,950 Hz and 1000 Hz.* and ** Mann-Whitney test $p < 0.05$, n = sample size. 131

Figure 5-19: The Sawbones testing set-up for the zone loosening case study. 134

Figure 5-20: The acetabular cup early zone loosening conditions. 135

Figure 5-21: The simulated acetabular cup zone loosening conditions. 136

Figure 5-22: The accelerometer first harmonic ratio comparison for the different simulated conditions. * Mann-Whitney test $p < 0.05$, n = sample size. 141

Figure 5-23: The ultrasound first harmonic ratio comparison for the different simulated conditions. * Mann-Whitney test $p < 0.05$, n = sample size. 142

Figure 6-1: The hemi-pelvis three simulated conditions.....150

Figure 6-2: The Hemi-pelvis case study three conditions (1mm press-fit, 1mm and 2mm spherical loose) 152

Figure 6-3: The hemi-pelvis acetabular cup cavity CNC machining process, Graphs a, b, c and d show the holding base and the screw formation. Graphs e and f show the same base being held by angle plate in preparation for the machining. 153

Figure 6-4: Steps taken to mimic loosening that was 1mm and 2mm spherical. 155

Figure 6-5: The silicone layer set-up, the preparation stage to left and on the right the silicone curing stage 155

Figure 6-6: The hemi-pelvis set-up (with the two mediums) 157

Figure 6-7: The two medium set-up testing..... 159

Figure 6-8: The accelerometer fundamental frequency magnitude response to the three simulated condition at the driving frequencies 200 Hz, 300 Hz and 350 Hz. * Mann-Whitney test $p < 0.05$, n = sample size. 162

Figure 6-9: The ultrasound first harmonic magnitude response to the three simulated condition at the driving frequencies 1250 Hz, 1450 Hz and 1500 Hz. * Mann-Whitney test $p < 0.05$, n = sample size. 163

Figure 6-10: The accelerometer second harmonic magnitude response to the three simulated condition at the driving frequencies 550 Hz, 600 Hz, 700 Hz and 1250 Hz. * Mann-Whitney test $p < 0.05$, n = sample size. 164

Figure 6-11: The ultrasound third harmonic magnitude response to the three simulated condition at the driving frequencies 900 Hz, 1100 Hz and 1450 Hz. * Mann-Whitney test $p < 0.05$, n = sample size. 165

Figure 6-12: The Accelerometer first harmonic ratio comparison for the different simulated conditions with air medium. * Mann-Whitney test $p < 0.05$, n = sample size. 169

Figure 6-13: The ultrasound first harmonic ratio comparison for the different simulated conditions with air medium. * Mann-Whitney test $p < 0.05$, n = sample size. 170

Figure 6-14: The water medium ultrasound first harmonic ratio comparison for the different simulated conditions. * Mann-Whitney test $p < 0.05$, n = sample size. 171

Figure 7-1: The femur and hemi-pelvis Sawbones three simulated conditions. 178

Figure 7-2: The testing set-up for both mediums; a) foam support air medium, b) water medium set-up. 182

Figure 7-3: The two medium support approaches. 184

Figure 7-4: The femur accelerometer fundamental frequency magnitude response to the three simulated condition at the driving frequencies 1250 Hz, 1300 Hz and 1400 Hz. * Mann-Whitney test $p < 0.05$, n = sample size. 186

Figure 7-5: The femur accelerometer first harmonic magnitude response to the three simulated condition at the driving frequencies 1200 Hz, 1250 Hz and 1500 Hz. * Mann-Whitney test $p < 0.05$, n = sample size. 187

Figure 7-6: The pelvis accelerometer second harmonic magnitude response to the three simulated condition at the driving frequencies 1300 Hz, 1450 Hz and 1500 Hz. * Mann-Whitney test $p < 0.05$, n = sample size. 188

Figure 7-7: The pelvis accelerometer third harmonic magnitude response to the three simulated condition at the driving frequencies 1150 Hz, 1400 Hz and 1500 Hz. * Mann-Whitney test $p < 0.05$, n = sample size. 189

Figure 7-8: The ultrasound fundamental frequency magnitude response to the three simulated condition at the driving frequencies 1250 Hz, 1300 Hz and 1400 Hz with the two mediums a) air medium, b) water medium. * Mann-Whitney test $p < 0.05$, n = sample size. 190

Figure 7-9: The femur accelerometer first harmonic ratio comparison for the different simulated conditions with air medium. * Mann-Whitney test $p < 0.05$, n = sample size. 194

Figure 7-10: The pelvis accelerometer first harmonic ratio comparison for the different simulated conditions with air medium. * Mann-Whitney test $p < 0.05$, n = sample size. 195

Figure 7-11: The ultrasound first harmonic ratio comparison for the different simulated conditions with air medium. * Mann-Whitney test $p < 0.05$, n = sample size. 198

Figure 7-12: The water medium ultrasound first harmonic ratio comparison for the different simulated conditions. * Mann-Whitney test $p < 0.05$, n = sample size. 199

Figure A-1: The LabVIEW code. 239

Figure A-2: The LabVIEW code filter configuration. 240

Figure A-3: The LabVIEW code power spectrum configuration. 240

Figure A-4: The LabVIEW code peak search configuration. 241

Figure C-1: The FFT analysis for the two pelvis coupling approaches, revealing that the screw fixation give additional unexplained harmonics in the frequency spectrum. 245

Figure D-1: The muscle simulation set-up.....247

List of Tables

Table 2-1: THR components and their up-to-date used materials, source [46]. 36

Table 2-2: THR loosening diagnosis approach, based on [100] 41

Table 2-3: The different imaging modalities used for THR loosening diagnosis comparisons. 42

Table 2-4: THR loosening non-imaging techniques. 46

Table 2-5: Joint Infection Screening Indicators, source [25]. 47

Table 2-6: The THR vibration analysis literature overview. 50

Table 2-7: The Acoustic prosperities of some of the soft tissue components, source [181]. 74

Table 2-8: The acoustic properties of hard and soft tissue substitutes, source [181]. 76

Table 5-1: The first harmonic ratio comparison between the simulated conditions with the significant value being highlighted, ...118

Table E-1: The accelerometer response comparison between the simulated conditions with the significant value being highlighted, NA = where the signal is not significant or do not support the main finding pattern. 249

Table E-2: The ultrasound response comparison between the simulated conditions with the significant value being highlighted, NA = where the signal is not significant or do not support the main finding pattern. 250

Table E-3: The accelerometer response comparison between the simulated conditions with the significant value being highlighted, NA = where the signal is not significant or do not support the main finding pattern. 251

Table E-4: The ultrasound response comparison between the simulated conditions with the significant value being highlighted, NA = where the signal is not significant or do not support the main finding pattern. 252

Table E-5: The air medium accelerometer response comparison between the simulated conditions with the significant value being highlighted, NA = where the signal is not significant or do not support the main finding pattern. 253

Table E-6: The air medium ultrasound response comparison between the simulated conditions with the significant value being highlighted, NA = where the signal is not significant or do not support the main finding pattern. 254

Table E-7: The water medium ultrasound response comparison between the simulated conditions with the significant value being highlighted, NA = where the signal is not significant or do not support the main finding pattern. 255

Table E-8: The air medium femur accelerometer response comparison between the simulated conditions with the significant value being highlighted, NA = where the signal is not significant or do not support the main finding pattern. 256

Table E-9: The air medium pelvis accelerometer response comparison between the simulated conditions with the significant value being highlighted, NA = where the signal is not significant or do not support the main finding pattern. 257

Table E-10: The air medium ultrasound response comparison between the simulated conditions with the significant value being highlighted, NA = where the signal is not significant or do not support the main finding pattern. 258

Table E-11: The water medium ultrasound response comparison between the simulated conditions with the significant value being highlighted, NA = where the signal is not significant or do not support the main finding pattern. 259

List of Abbreviation

THR	Total Hip Replacement
NJR	National Joint Registry
MIS	Minimally invasive surgery
Vibrometry	Vibration analysis
FFT	Fast Fourier Transform
UHMWPE	Ultra- High Molecular Weight Polyethylene
CoCrMo	Cobalt-Chromium
Ti-alloys	Titanium alloys
XLPE	Cross-linked polyethylene
BMI	Body mass index
FDG-PET	Fluorodeoxyglucose positron emission tomography
RSA	Radiostereometric
NDT	Non-destructive testing
ESR	Erythrocyte sedimentation rate
CRP	C-reactive protein
WBC	White blood cell count
TFOI	Trans-femoral Osseointegration
CNC	Computerised numerically controlled

Chapter 1 – Introduction

1.1 Background

Total hip replacement (THR) is a human surgical intervention which has the aim of pain relief and function restoration. THR has come a long way since it was introduced by Charnley in the early 1960s, and was subsequently nominated as the operation of the century. There are over a million THR operations a year, with younger and more active patients now being treated due to the high success rate that reaches up to 95% at ten years [1]. However, despite the high success rate implants do fail with a rate of 4% to 10% at ten years, according to various national registries. Also recognising Aseptic loosening to be the primary failure factor [2-4].

Imaging techniques are the main postoperative assessment follow-up means of identifying loosening. However, these techniques have a low detection rate for early loosening [5-7], particularly for the acetabular cup component [8]. Vibrometry has been proposed as an alternative, more sensitive method for THR loosening diagnosis [9]. Clinical studies [9, 10], *in-vitro* studies [11, 12] and finite element studies [13-15] have all supported the vibrometry approach with positive findings, but were mainly focused on the stem component. A few others have explored the detection of acetabular cup loosening [5, 8, 9, 16] and were able to distinguish it from the stable condition, but without defining the loosening level detected. The aim of this study is to address this gap in the literature by investigating the viability of detecting acetabular component loosening using vibrometry, and to define the earliest loosening phase that can be accurately detected.

The thesis attempted to address the research aim through a series of case studies that vary in complexity, which can be grouped under three objectives. Firstly, the development of acetabular cup loosening through the use of Sawbones blocks, as an initial simplified setup with minimum boundary conditions. Secondly, attempting to accommodate complex bone geometry through utilising a Sawbones hemi-pelvis. Thirdly, to create a more clinically relevant experiment by using Sawbones femur and hemi-pelvis composite bones.

1.2 Report Structure

The thesis is divided into nine Chapters which can broadly be categorised into background and experimental sections. The background sections include the introduction, literature review, and the project aim. This is followed by the experimental chapters, which focus on the research methodology, experiment results, discussions, conclusion and further work.

The literature review in Chapter 2 cover the relevant background to hip joint anatomy, function, pathology, history and development of THR. There is also a detailed investigation of the current state of the art loosening diagnosis techniques and comparisons are drawn with other new emerging technologies. Subsequently, the current study aim and objectives explained in Chapter 3.

The experimental work is conducted in six chapters. Chapter 4 explains the research methodology and the practical steps that were used in the carrying out the experiments relating to the three objectives. For objective one (Sawbones blocks), the experiment set-up justification, results and related discussion is presented in Chapter 5, followed by objectives two (Sawbones hemi-pelvis) and three (Sawbones femur and hemi-pelvis) in Chapters 6 and 7, respectively. In Chapter 8, an overall discussion of the work is then presented, which highlights the study's main findings and relates the study to the literature. Finally, conclusions are drawn from the project and suggestions made for further work in Chapter 9.

Chapter 2 – Total hip replacement

2.1 Introduction

This chapter covers the literature review, justifying the aim and objectives of the current project. This chapter will open with an overall look at the normal hip joint anatomy, structure and will outline the most reported pathological factors. This will be followed by a general overview of the total hip replacement (THR) history and development up to the current state of the art practise. Different fixation techniques, components, materials used and the most prevalent failure factors will be discussed.

Aseptic loosening has been the primary factor for THR failure since the early 1980s [4]. Thus, the current conventional loosening diagnosis techniques have been explored and compared, leading to new emerging techniques. Structural testing is one of these proposed diagnostic method, in the form of vibration analysis, which this study is exploring. This chapter will cover how this concept was introduced and how it evolved to be used in the orthopaedic field, in addition to where it is mostly commonly used.

Despite the fact that acetabular cups have a higher revision rate over femoral components [17-21], the majority of the existing vibrometry loosening diagnostic literature [6, 9-13, 22, 23] is stem related. A limited number of studies [5, 8, 9, 16] have explored the detection of acetabular cup loosening. They detected late cup loosening, but did not specify the earliest detectable threshold, which this study is attempting to address.

2.2 Hip joint

Human anatomy consists of different subsystems that enable it to perform its functions. They are dependent upon each other through a complex, interacting network. For example, the body's mobility mostly depends on two systems: the Skeletal and Muscular systems. Each system has various internal components that work coherently together to generate specific movements. Due to the scope of the present project, focus will be placed on the hip joint in the following sections.

The hip joint is a three degrees of freedom type joint that is located between the pelvis and femur bones, with cartilage and synovial membrane in between for support (Figure 2-1). The femoral head is attached to the pelvis at the acetabular region with a combination of ligaments and muscles, which are important for joint movement and stability. The ligaments mainly support the joint through the weight bearing situation, whereas muscles are the movement stimulators [24].

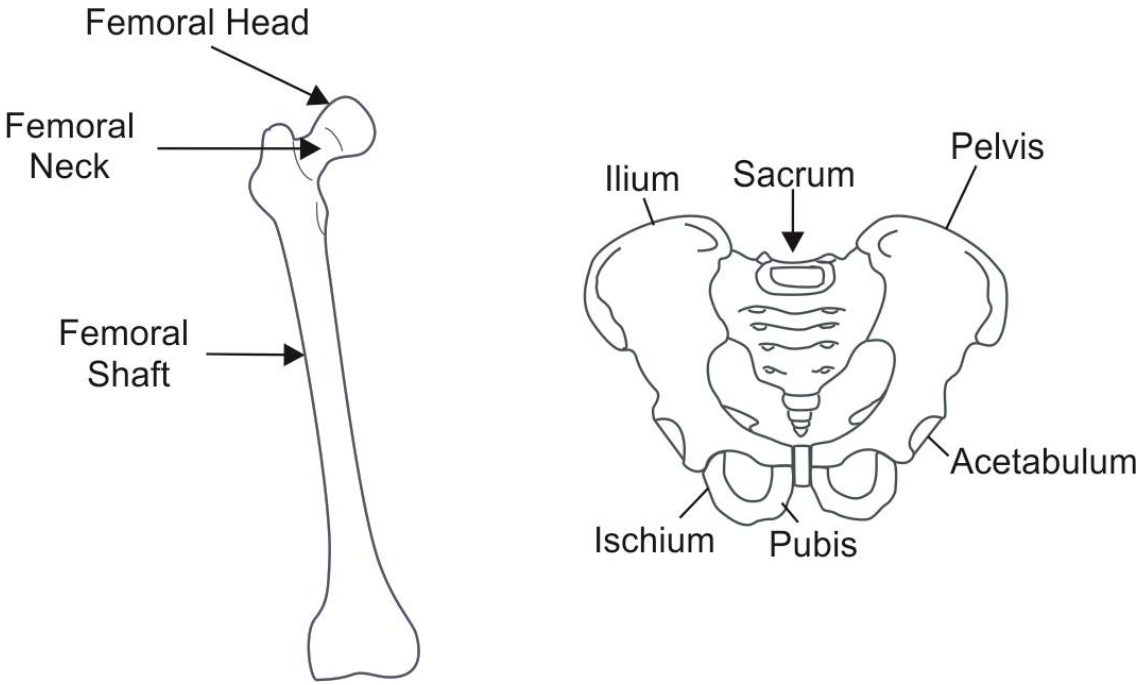

Figure 2-1: The hip joint bones (Femoral and Pelvis), based on an illustration from [24].

2.2.1 Articulate Cartilage

The load transfer and wide range of motion of the hip joint would not be possible without the articulate cartilage. This is a specific type of tissue (hyaline) that tolerates high loads without failure, allowing the hip joint to withstand cyclic loading equivalent to three times human body weight when walking [25] and up to eight-times the body weight when stumbling [26]. This articular cartilage covers the femoral head and the acetabular inner surface with synovial fluid in between, which is maintained with the fibrous capsule (Figure 2-2).

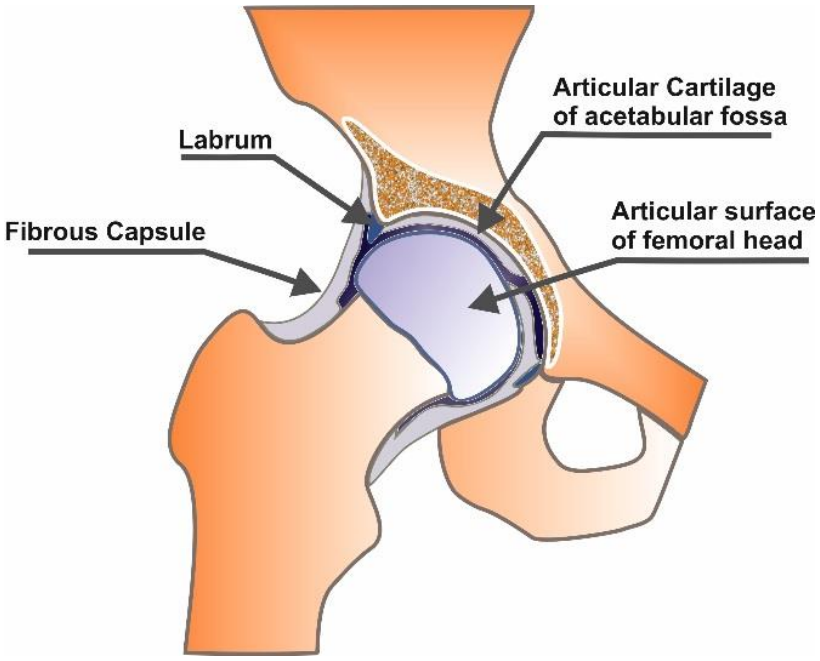

Figure 2-2: The natural hip joint, based on an illustration from [24].

2.2.2 Ligaments

The hip joint alignment and support are largely dependent on five ligaments; Iliofemoral, Pubofemoral, Ischiofemoral, Ligamentum teres, and Transverse acetabular ligament, as shown in Figure 2-3. The two main anterior ligaments are Iliofemoral and Pubofemoral, which shield the hip joint from hyperextension, excessive abduction and medial rotation. On the posterior side, the Ischiofemoral ligament protects the joint from excessive medial rotation. An internal ligament connects the acetabular fossa and femoral head fovea, known as the Ligamentum teres (Ligament of head of femur). Lastly, the Transverse acetabular

ligament is positioned on the acetabular cartilage free distal area, where nerves and vessels enter to nourish the joint [27, 28].

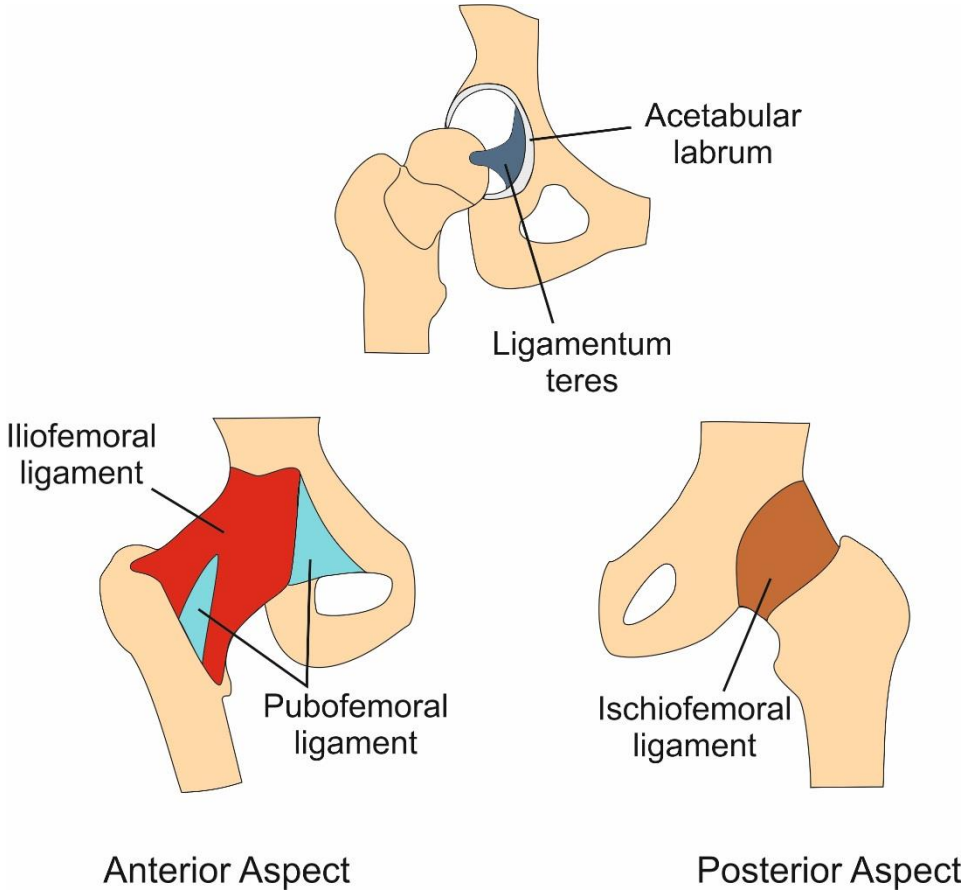

Figure 2-3: Hip joint ligaments, based on an illustration from [24, 29].

2.2.3 Muscles

The hip joint has a wide range of motion that is largely stimulated and controlled by various muscle groups around the joint. These movements are flexion, extension, abduction, adduction, lateral rotation, and medial rotation. They can be divided according to the body axis and the various muscle groups involved, as illustrated in Figure 2-4 and Figure 2-5.

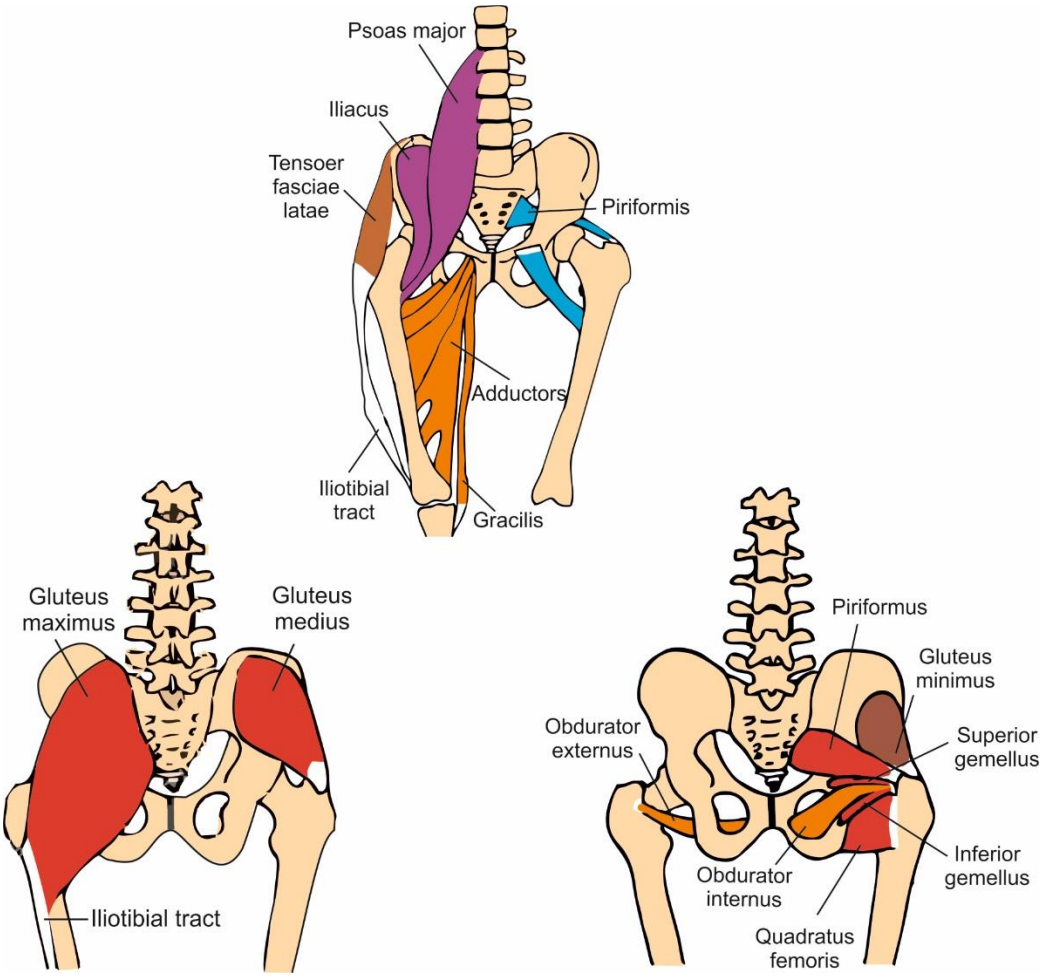

Figure 2-4: Hip joint muscle groups, based on an illustration from [29].

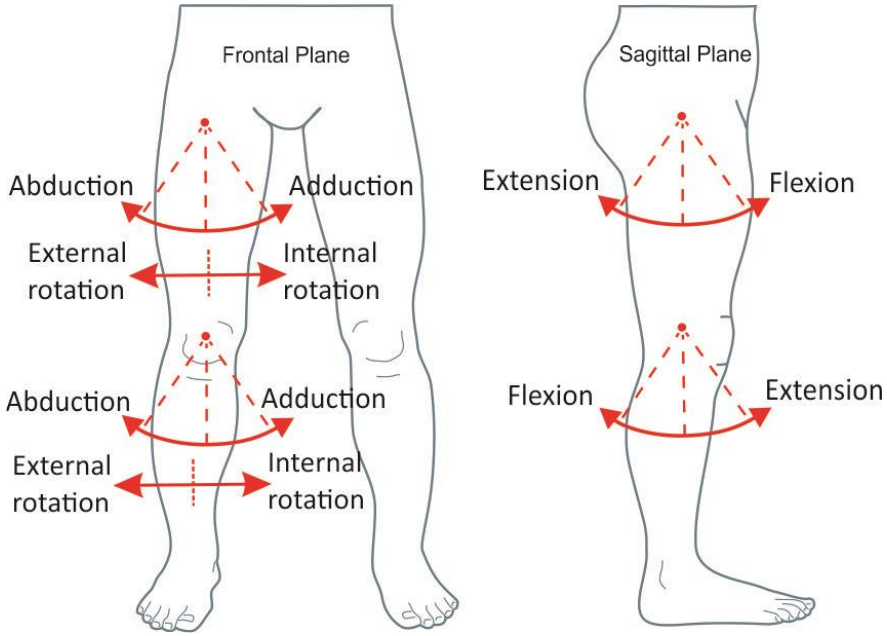

Figure 2-5: Hip range of motion, based on an illustration from [30].

For instance, the sagittal plane has two hip joint motions: flexion and extension. Flexion motion is executed by the muscle group of the psoas major, iliacus, pectineus, rectus femoris, and sartorius. Extension motion is facilitated by the gluteus maximus and hamstring muscles (semimembranous, semitendinosus and biceps femoris).

Likewise, on the frontal plane, there are two motions: adduction and abduction. Abduction is achieved by the gluteus maximus, gluteus medius, and gluteus minimus. Adduction utilises the adductors longus, brevis and magnus, pectineus and gracillis.

Finally, there are two motions on the horizontal plane: lateral and medial rotation. Lateral rotation uses the gluteus maximus, piriformis, obturator internus and externus, gemellus superior and interior, and the quadratus femoris. Medial rotation uses the gluteus medius and minimus, tensor fasciae latae, psoas major, and iliacus [31].

2.2.4 Pathologies Outline

The function of the hip joint is to ensure co-operation between its different elements, making it possible to withstand cyclic loading equivalent to three times human body weight [25]. Due to the joint's location and function, damage could leave patients with pain and reduction in mobility. Generally, hip joint pathological factors have been traced by different national joint registries and categorised according to their prevalence. However, in certain situations, a combination of factors could exist. Selected failure factors will be addressed according to their frequently and severity.

Osteoarthritis (OA) is the most well-known contributing factor for hip joint failure. In fact, according to various joints registries, it has been the primary surgical indicator for the last decade [4, 32, 33]. This condition causes the gradual degeneration of the articular cartilage layer, causing the bone surfaces to rub against each other, leading to pain and disability [34].

Femur neck fracture is the second common factor for hip joint failure [4, 32, 33, 35]. Femoral neck fractures mostly happen at the proximal area near the hip joint. Annually, about 77,000 cases occur in the UK, with an estimated increase that is largely affecting older people [36]. Reports have shown that women are more likely to sustain a fracture than men [37].

Osteonecrosis of the femoral head is the next most important factor [4, 32, 33, 35]. This condition is also known as avascular necrosis, which occurs as the result of lowered or absent

blood supply that causes an inadequate level of bone nutrients. As a consequence, bone cells die. This sequence of events causes the subchondral bone to collapse, affecting the joint function and triggering severe restricting pain [38].

Dysplasia of the hip is a musculoskeletal condition that commonly affects younger patients, mostly at birth (new bones). The femoral head is not held tightly to the acetabular cup cavity leaving it more prevalent to dislocation. This is also known as developmental dysplasia of the hip (DDH) or congenital hip dislocation which, even if treated early, could be an indicator of later hip osteoarthritis [39].

Rheumatoid arthritis (RA) is another noticeable pathological factor that causes patients discomfort and disability. This condition is an autoimmune disease, whereby the body attacks itself and in this case the hip joint. As a result of the immune system attacking the joint, it becomes inflamed and damaged. This causes the cartilage to wear out and exposes the joint to pain and limited function [40].

Other less frequent factors also exist, such as trauma and infection [4, 32, 35]. These can happen in isolated cases but, when combined with other factors, they accelerate joint failure. In some of cases, surgical intervention is needed, which involves removing the failed element and damaged tissue and implanting an artificial component where applicable. This intervention is a safe and effective procedure that has been undertaken for more than two decades, and commonly referred to as total hip replacement (THR).

2.3 Total hip replacement

Over a million THR surgeries are conducted annually around the world; a number that is likely to increase [1, 41]. THR is a human intervention which has the aim of pain relief and function restoration. It has gone through different stages of development involving various sizes, shapes and materials, as well as different fixation methods. However, the goal remains the same.

2.3.1 History

Carnochan was the first to suggest the idea of replacing hip joints with artificial components in 1840. He initially experimented with wooden blocks. Then he decided to seek more biocompatible materials, such as skin, fascia, muscle, pig bladders and gold foil, but these were not successful. In 1890, Gluck attempted to replace the femoral head with an ivory femoral stem (ball and socket joint), which was fixed with nickel-plate screws to the bone. Later, this was faced with biocompatibility complications [42].

In 1923, Smith-Petersen presented the Mold Arthroplasty, which used glass with the intention of achieving better biocompatibility. The Mold Arthroplasty process involved covering the femoral head with a modelled "cup-like" piece of glass. However, the fragile characteristics of glass had cataclysmic consequences. As a result, other materials were subsequently investigated, such as celluloid, Bakelite, Pyrex, and Vitallium [42]. It wasn't until 1937, when Smith-Petersen used Vitallium (cobalt-chromium alloy), inspired by its use in dentistry, that he discovered this material delivers ten years of good clinical results [43]. This represented the earliest version of what is known today as prosthesis resurfacing [44].

The initial metal-on-metal (MOM) arthroplasty was introduced by Wiles in 1938, which resembled existing modern procedures [42, 45]. The material used, stainless steel, was intended to replace both the femoral head and the acetabular cup [44-46]. The Judet brothers, Jean and Robert, also attempted to replace the femoral head in 1938 with an acrylic material, with the intention of producing a smoother surface. However, the acrylic implant came loose after implantation; causing them to research further and present the first short-stem prosthesis in 1946. The short stem prosthesis was made of Poly-methyl-methacrylate (PMMA) and, later, was designed with Vitallium, which had some success. Subsequently,

Haboush, inspired by the work of the Judet brothers, used "fast setting dental acrylic" to fix the prosthesis to the bone [42].

Then, in 1939, Bohlman and Austin T. Moore collaborated to present a prosthesis that replaced the femoral head (Hemiarthroplasty). The Austin-Moore prosthesis had a Vitallium metallic stem that was placed into the medullary cavity of the femur. This performed well, and was further developed during the 1950s to have a longer stem with a self-locking feature. Subsequently, Mckee-Farrar, during the 1950s, utilised the Austin-Moore prosthesis and designed a total hip, metal-on-metal (MoM) prosthesis using screw fixation. This was referred to as the McKee Ring Prosthesis. In the 1960s, another improved design was introduced that used cement fixation instead of screws. This became known as the Mckee-Farrar Prosthesis [42, 44].

John Charnley, a brilliant surgeon, revolutionised THR surgery with his low friction arthroplasty concept in the late 1950s. Charnley pursued the use of substitute materials with low wear characteristics that could replace both sides of the hip joint. Initial attempts included Teflon and acrylic, but these had to be rejected because of the wear produced [42]. It was not until the early 1960s that Charnley introduced the stainless steel stem and polyethylene cup. This was later known as the metal-on-polyethylene (MoP) hip implant replacement [47]. The two components (stem and cup) were fixed by bone cement PMMA (Poly-methyl-methacrylate) that provided a firm and secure fixation [48]. Subsequently, the pursuit of even lower wear material led to the use of High Molecular Weight Polyethylene (HMWPE), followed by cross-linked UHMWPE. Both were more wear-resilient than previously used materials [49, 50]. The MoP hip replacement gradually grew in popularity during the 1970s, due to its success in relieving pain and recovering joint function (Figure 2-6). It managed to phase out previous MoM implants that had sensitivity issues [46].

Figure 2-6: Historical development of the hip replacement, based on source [42] with permission.

During the 1970s, despite the growing popularity and long-time survival of the MoP implant, it was noted that, with time, the Polyethylene tended to wear. This produced micro-sized debris that eventually caused infection and loosening [42, 51]. This triggered interest in the study of so called "Polyethylene disease" and aseptic loosening, in order to understand the problem and produce more wear-resistant materials that the body could tolerate [44, 52]. One attempt, the ceramic on ceramic (CoC) hip implant, was introduced in the 1970s. The high wear resistance of this implant was one of its major advantages, but the downside included its fragility and a noticeable squeak during movement. In the 1980s, a second generation MoM prostheses was presented. This had relative success compared to its previous iteration but, even at its peak, it could not supersede the success of the MoP implant [48].

In the 1990s, hip resurfacing saw the introduction of a third-generation metal-on-metal hip replacement, which was introduced to overcome previous implant wear concerns and a growing younger patient group [53]. The resurfacing procedure had a reported success rate in the medical literature similar to the Birmingham hip replacement [46]. However, this procedure had advantages and disadvantages [54]. Bone preservation was the main

advantage, since resurfacing involved removal of less bone stock. This made it suitable for younger and more active patient groups [41]. It also made it easier to revise later on, if necessary [55]. Hip resurfacing usually involves larger femoral heads that add more stability and wear endurance [56]. Nevertheless, a non-negligible percentage of femoral neck fracture and metallic sensitivity was reported [57].

Then, in the early 2000s, a minimally invasive surgery (MIS) concept was introduced to hip arthroplasty [58]. MIS is when the surgery incision is 10 cm or less [59], and which can be conducted by a single-incision (posterior or anterior) [58] or a two-incision technique [60]. Since the early introduction of the MIS THR technique, its potential benefits compared to traditional approaches remain the subject of debate. The main advocated benefits included the reduction of blood loss and pain, a shorter hospital stay, and shorter rehabilitation times [61]. On the other hand, some downsides have been observed in number of reports. These include acetabular cup malposition, a poor fit of the stem component, and femoral fractures [58, 60]. Despite the increased attention that MIS has had from surgeons and the public over its short term benefits, more studies are needed to understand the long term outcomes [60].

Advancements in the material sciences, alongside public awareness, represent new opportunities and challenges for THR in the future. Present THR techniques have shown good outcomes with regards to pain relief and cost effectiveness. However, an increasing concern comes from the decrease in the average age of patients, which in turn implies more active lifestyles and higher expectations. These challenges will drive the future of THR towards more wear-resistant biocompatible materials, more tissue and bone reservation measures, and possible computer navigation assistance [41].

2.3.2 Fixation

Osseointegration (structural and functional) between the implant and the bone is the ultimate goal that fixation attempts to achieve [62]. Fixation methods in the area of orthopaedics usually fall into one of the following categories: cementless, cemented, or hybrid (one side cemented while the other is not). There is current debate about the best fixation methods within the field of orthopaedics. We will examine these methods and the different arguments.

2.3.2.1 Cemented

Bone cement was made with the initial intention of promoting better osseointegration between the implant and bone surface. However, it does not bond but rather acts as filler. Initially, it emerged from the chemical industry in the 1920s by Otto Rohm and was subsequently utilised in dentistry in the 1930s [63]. It was not until the late 1940s that bone cement was used in hip replacements, following the work of Scales and Herschell [64], Judet and Judet [65], and Haboush [66]. They used Polymethylmethacrylate (PMMA), also known as acrylic bone cement [67]. However, bone cement gained its peak of popularity after the Charnley THR introduction in the 1960s and its relative success, compared to others at that time, in fixing the cup and the stem using PMMA [63, 68].

In addition to bone cement acting as grout between the bone and the implant, it was noticeable that patients suffered less postoperative pain when compared with previous cementless techniques. Another advocated advantage was the reduced rehabilitation period, since the cement technique meant that patients were able to apply load sooner than with cementless techniques [46]. However, several concerns and potential drawbacks were recognised. One concern was that, if the cement was not evenly applied, localised stress may cause it to crack and generate small particles, which would cause irritation between the bone and implant. Also, PMMA is known to have exothermic properties; producing heat that can, in extreme cases, damage bone tissue, leading to bone necrosis [67, 69]. Even with these concerns, bone cement is generally accepted as the gold standard for THR fixation in patients over 65 years of age [70].

2.3.2.2 Cementless (Press-fit)

During the early 1950s, THR fixation development began with a cementless technique (press-fit) with the aid of screw fixation. However, these early cementless THRs resulted in poor results, leaving orthopaedic surgeons in pursuit of alternative means of fixation [49]. Bone cement was popularised in the 1960s by Charnley and grew in popularity as it was endorsed as a method of fixation. During that period, cementing techniques and implant design were not yet fully mature, resulting in early poor outcomes. Due to their lack of clear understanding, questions were raised about the suitability of bone cement. This suspicion caused another shift back to cementless fixation during the 1970s but, at that time, most implant surfaces were smooth. This meant that the possibility of osseointegration between the bone and the implant was poor, eventually leading to implant loosening [70]. However, in the early 1980s, the lack of bonding was resolved by material engineering, through the introduction of porous surfaces that allowed bone tissue to grow into the implant surface. This allowed greater bond stability. In fact, according to Hailer *et al*. [70], surface pore sizes between 100 and 200 μm displayed the best bone ingrowth outcomes. The most common materials used as porous surfaces to promote bone ingrowth are usually titanium fibre mesh, cobalt-chromium beds, and titanium plasma spray [49].

The popularity of cementless fixations grew, as they offered the same results of pain relief and implant stability as the cemented method, but with more reported features. One of the advantages of the cementless, porous surface technique is that it provides a better adhesive option due to the bone ingrowth, rather than the filling effect of the bone cement. Also, the operation procedure usually consumes less time than the cemented [70]. However, cementless THRs demand more operation precision and a longer rehabilitation period in order to achieve the desired purpose [71]. For the above reasons, orthopaedic practice usually utilises cementless fixation with younger age groups, while using cement fixation with older patients.

2.3.2.3 Fixation Summary

The debate around which method of fixation achieves the best osseointegration still exists. However, each technique has progressed since their early introduction and both now have more favourable results [72] . In fact, these two methods have been combined, producing what is known as a hybrid design. This is a combination of the cemented and cementless components (Figure 2-7) [73]. According to the annual reports of the Swedish and British National Joint Registries [4, 32],THR cementless and hybrid are growing in popularity and possibly shaping the future fixation state of the art (Figure 2-8).

In the short term, cemented fixation outperforms the cementless technique. In the long term, however, cement fixation is inferior because, with age, cement weakens and the cementless bond becomes stronger [74]. Patients' related factors, such as age and pathological condition, remain the main influence on which technique is chosen by surgeons. Younger and more active patients are likely to have the cementless fixation, while older patients (age >65) tend to have cemented implants [70].

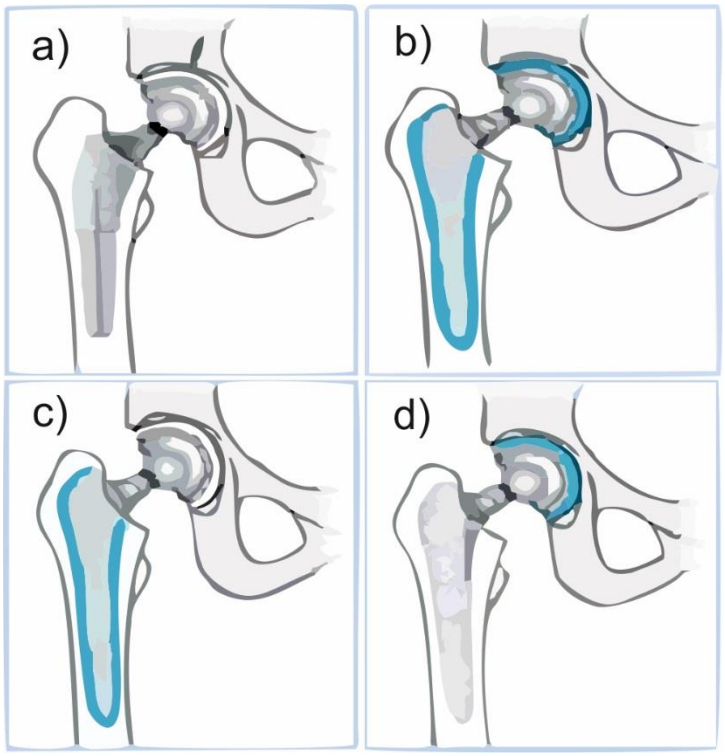

Figure 2-7: Overview of THR fixation methods. a) Cementless, b) Cemented, c) Hybrid (cemented stem and cementless cup), d) Reverse Hybrid (Cement cup and cementless stem), based on an illustration from [41].

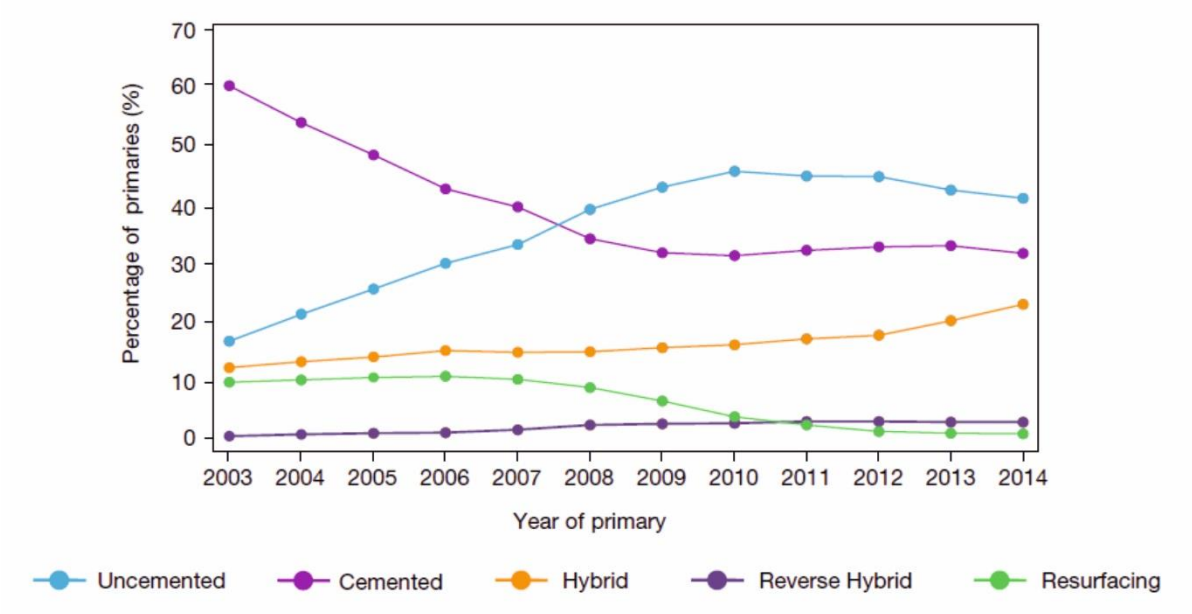

Figure 2-8: THR primary fixation trend between 2003 and 2014 from NJR 12th annual report [32].

2.3.3 Materials and components (state of the art)

The current practice of hip prosthesis is a result of cumulative knowledge that many surgeons and research groups have contributed towards over the last century. In the next section, an overview is provided of the current components and materials of hip prosthesis.

2.3.3.1 THR Components

A THR is mainly made up of four components (stem, head, cup, and shell) where each has a variety of sizes, materials and surface structures that need to be carefully selected in order to suit the patient's needs (Figure 2-9). The most important component is the stem, because of its high load exposure that directly affects implant stability and load transfer. Due to the high strength requirements, the stem is commonly made of metal with an emphasis on length, neck angle, and cross section design features [46]. The next important component is the implant head, due to the major role it plays in defining the range of motion. The head is size dependent and can range between 20 mm to 60mm [75] and can be made of either metal or ceramic. Larger femoral heads are promoted to add more stability and reduce the risk of postoperative dislocation, however they are also linked to higher volumetric wear, especially with large femoral heads on polyethylene [76] .The third component is the acetabular cup liner, which is usually made of polymer and is concave in form and located between the implant head and shell (see Figure 2-9). However, the liner material and thickness is dictated by the implant's head and shell size. Finally, the acetabular cup's shell is usually made of

titanium and has an important impact on the implant's stability and osseointegration. The shell's surface design and material are made with the intention of achieving the best bond between the cup and the bone [46]. These components are coupled and fixed in an operation that usually takes several hours, where initial stability and precision determine the implant's survival pattern

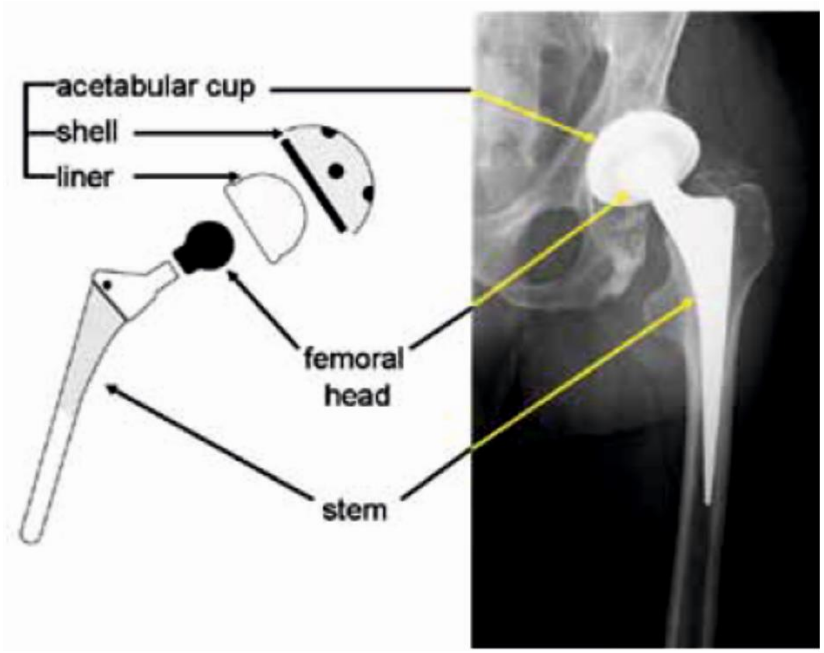

Figure 2-9: THR components illustration, from source [46] with permission.

2.3.3.2 THR Materials

Total hip replacement consists of different components, where each requires a different mechanical feature to sustain its existence in the hostile human (mechanical and chemical) environment. In order to obtain the ultimate resemblance to the human hip joint, improvements have continued to take place since the earliest THR attempts. Amongst the earliest materials used were wood, glass, and rubber. These all had poor outcomes which then led to the use of materials like polymer, metal, and ceramic that still exist to this day [42]. Metal and ceramic are commonly used as hard bearing, while polymer is used as soft bearing [77]. Since early development, these groups have been used either alone or interlinked in various implant components. This was until the existing pattern was released, as shown in

Table 2-1. In addition, these materials are commonly coated with a bioactive layer, which is done in pursuit of more osseointegration between the bone and implant. The most commonly

used metals are stainless steel, titanium, or cobalt chromium; while the polymer is either UHMWPE[1] or cross-linked UHMWPE. The ceramic material could be alumina, zirconia, or an alumina zirconia composite. However, the materials selection process remains influenced by patients' related factors (age and pathological conditions) and fixation method used (cemented or cementless) [46].

Table 2-1: THR components and their up-to-date used materials, source [46].

Components	Material category	Most used material
Femoral stem	Metal	CoCrMo-Wrought, Ti-alloys, Stainless Steel
Femoral head	Metal	CoCrMo-cast, Stainless Steel
	Ceramic	Alumina, Zirconia
Acetabular cup liner	Polymer	UHMWPW,XLPE
	Metal	CoCrMo-cast
	Ceramic	Alumina, Zirconia
Acetabular cup shell	Metal	Pure Titanium, Stainless Steel

2.3.4 National Joint Registries

National registries has shown to be an integral part of the THR follow-up. They serve to highlight different surgical approaches, fixation techniques, and failure factors, among other important data. Some registries have databases that can be traced back to 1987, as is the case for the Swedish National Arthroplasty registry. Such data has been vital for the continuous improvement of THR clinical outcomes, which leads registries to expand to cover other joint replacements, such the knee, ankle, elbow and shoulder. Currently, there are more than thirteen national joint registries and other countries are following; either under or through local orthopaedic surgeon associations [78]. These registries continue to gather cumulative clinical data follow-up, which can be a powerful tool in the assessment of new technologies and complications that otherwise would take much longer to be detected and managed. This is true for the example of the DePuy Articular Surface Replacement (ASR) XL Acetabular System and Birmingham Hip Resurfacing (BHR) implants. These implants were a large

1- Ultra- High Molecular Weight Polyethylene

diameter, metal-on-metal THR, promoting the advantage of increased range of motion, reduce wear rate, and enhancing stability over existed implants [79]. Despite these advantages, the Australian Registry, in their 2009 Annual Report, highlighted the first signs of clinical complications showing a higher failure rate compared to similar implants, leading to the manufacturer having to recall the implants in March 2010 [80]. THR history has been better documented with national registries showing the variation of surgical techniques, implant selection and fixation trends through the years and relating these to clinical outcomes.

2.3.5 Failure and revision

The THR procedure is one of the most successful, safe, and cost effective medical interventions of the past century. However, implants can and do fail due to human, mechanical and biological factors; leaving patients in some cases with unbearable pain and disability. In these cases, revision is needed, which involves removing the failed implant and damaged tissue and re-implanting new components. THR revision is a safe and effective procedure but comes at a cost of the loss of bone tissue. Generally, failure factors tend to be related to the patient, implant, or surgery [81]. Selected primary THR failures factors will now be addressed according to their frequently and severity.

Aseptic loosening and osteolysis are the primary reasons for THR revision. In fact, according to the Swedish hip arthroplasty registry [4] annual reports, aseptic loosening has been the primary factor for THR failure since the early 1980s. Artificial joint implants tend to wear down over time and yield debris that is very small in size. These small particles cause inflammation between the bone and implant, causing bone tissue to degenerate, leading to instability and loosening [44]. Likewise, poor primary fixation could also lead to aseptic loosening [82]. Osteolysis and aseptic loosening usually occur 10 to 20 years after operation, which make them long-term issues [83, 84].

Dislocation is another reason for primary revisions and is usually considered as an early failure factor, since it normally takes place within the first few years of the THR [81]. This factor is the second in the table of reasons for primary THR failure in the Swedish and Australian arthroplasty registry [4, 33], showing the big impact it has on implant failures. Certain patients that are older, or female, or have had a previous THR revisions, could be

more vulnerable to dislocation. Also inexperienced surgeons could also increase the risk of dislocation, either by poor fixation or choosing the incorrect THR component size or alignment [85]. Most dislocation cases can be treated conservatively, but if this is not successful, surgery may be needed to recover and maintain stability [86].

Deep infection is the next most serious reason for THR revisions, according to the Swedish hip arthroplasty registry [4]. Most cases occur in the early stages and are usually instigated by bacterial contamination at the time of the operation. Deep infection can be challenging to diagnose and differentiate from loosening [87]. The treatment management approach is determined by the infection level; however, most surgeons perform revisions alongside antibiotic treatment [88].

Preiprosthetic fracture comes next in most of the existing literature [32, 89, 90]. These fractures take place around the embedded implant and can be caused by a variety of reasons. THR osteolysis or infection can frequently produce preiprosthetic fractures, because they weaken the osseointegration between the bone and implant. However, these type of fractures also can be caused by low energy trauma from normal everyday activities [91]. Preiprosthetic fractures are classified according to the fracture location and treated accordingly. The method for restoring the alignment and stability could be either conservative or surgical [89].

Pain is another noticeable reason for revision. According the British National Joint Registry 2015 Annual Report, pain holds the second place in the reasons for hip revision [32]. Generally, pain location and degree is treated as a symptom of THR failure factors, such as loosening, dislocation, osteolysis, or a fracture. However, when no clear causative factor is present and chronic pain remains, this presents the surgeon with a dilemma: they can find no direct cause for the pain which limits treatment options [92]. Disturbing the mechanical load transfer and micro-motion throughout the gait cycle have been suggested as possible causes of pain [93]. Treatment choices for post-operation chronic pain are initially conservative but, if the pain remain and increases, surgical intervention may be necessary [92].

Other less frequent revision factors also exist that can be generality correlated to the patient, implant, or surgery. These occur less often but, when combined with other factors, they could accelerate failure rate [85]. Patient-related factors include age, gender, body mass index (BMI) and whether they have already had a revision, which, in most cases less can be done

towered. For example patients who are older, female, and with a higher BMI are more prone to THR failure than others. Implant-related issues are concentrated on the materials and implant design that may cause uneven loading, resulting in pain or even fractures. On the other hand, surgical factors are more manageable and if identified can be reduced. These could include the surgical approach, experience of the surgeon, component choice, alignment, and soft tissue management [86]. Taking everything into consideration, THR failure is rarely caused by an isolated factor but, in fact, normally results from two or more factors. Therefore, diagnosis has to be accurate in order to identify suitable treatment management.

2.4 THR Loosening diagnosis

When analysing THR failure factors, it becomes clear how important diagnostic techniques are in orthopaedics. Throughout the first ten years of THR, around 10% of all implants are projected to fail [94, 95]. Femoral and acetabular component aseptic loosening has been shown to be the dominant long-term failure factor [46, 84], which is manifested in the Joint National Registries Annual Reports [4, 32, 33, 35]. However, acetabular cup revisions occurred twice as frequently as femoral component revisions [19, 21].

The criteria for identifying loosening for THR components are not universally agreed upon [25]. However, the zone classifications proposed by DeLee and Charnley [96] are the most commonly used and clinically accepted [97]. This classification system is based on radiograph (anteroposterior and lateral) examinations and the presence of radiolucent line. The radiolucent line is the dark area between the bone and cement interface or the cement and implant, which appears in radiograph follow-up as an indication for loosening. There are fourteen femoral zones. The first seven zones can be examined in the anteroposterior radiography alongside the three acetabular cup zones, while the next seven femoral zones are in the lateral radiography [98], as shown in Figure 2-10. These zones were mainly intended for cemented implants but are also generally adopted to cementless, with the addition of migration criteria [97].

The clinical pattern of acetabular cup loosening is mainly instigated by wear debris. The debris size, if below a certain critical threshold (<10µm), could cause a sequence of biological activities leading to aseptic loosening [84, 99]. The sequence is a result of the wear debris, which activates macrophages (a type of white blood cell), that release cytokine, resulting in more osteolytic activity (bone degradation) around the implant, thus leading to failure [84].

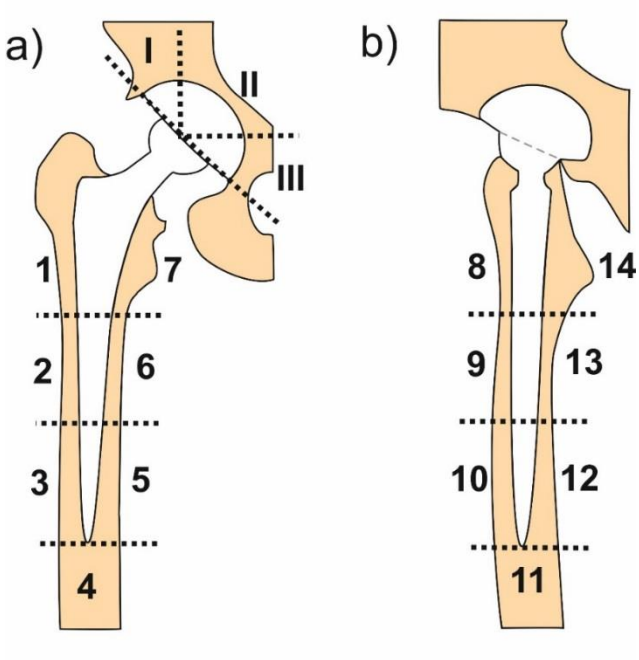

Figure 2-10: The THR loosening zones. a) Anteroposterior view showing the stem first 7 loosening zones and the acetabular cup three loosening zones and, b) Lateral view illustrating the other 7 stem loosening zones. Based on an illustration from [97].

Early and accurate diagnosis is of crucial importance for both patients and healthcare providers, because it reduces patient discomfort and disability, while also reducing physicians' misused time and costs. The diagnosis approaches are generally categorised into two groups, conventional imaging and non-imaging approaches (see Table 2-2). The next sections will address the state of the art of current diagnosis techniques and will compare conventional approaches with other emerging techniques.

Table 2-2: THR loosening diagnosis approach, based on [100]

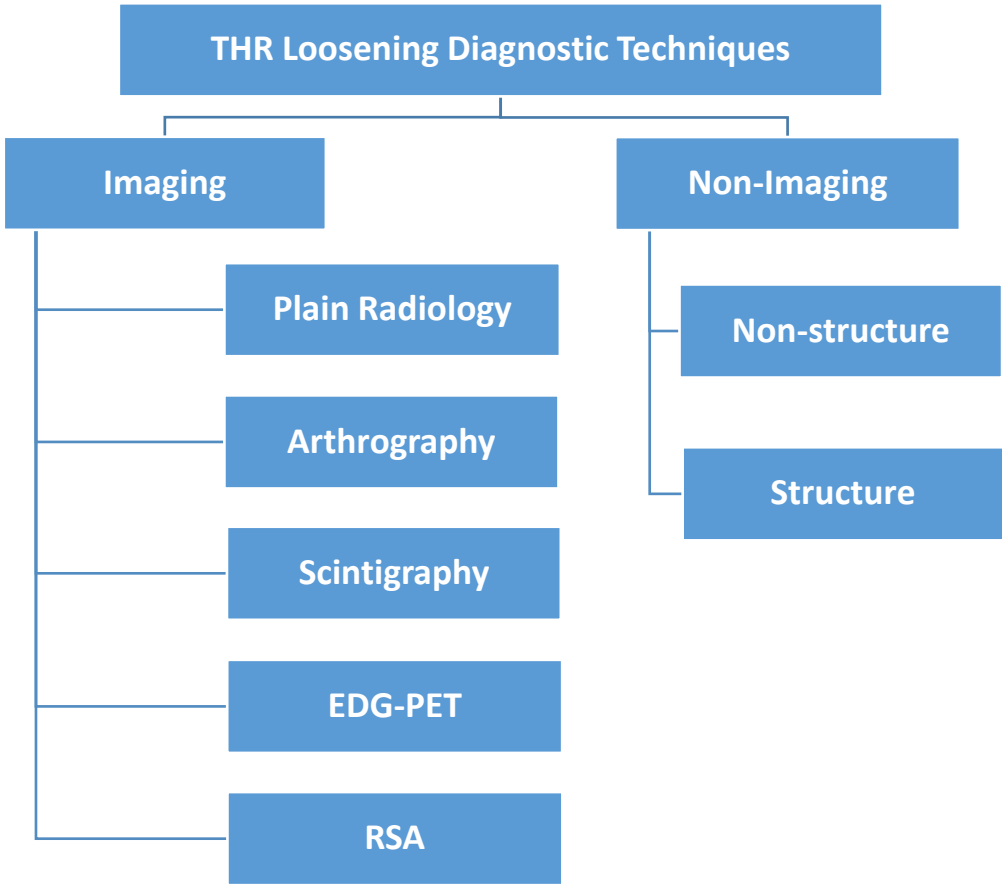

2.4.1 Imagining

Radiological imaging is the most commonly used diagnosis method. This is the main method that junior surgeons are trained in during their training programs and, therefore, the technique they are most familiar with. However, imaging radiology consists of different sub-techniques that can be used according to the diagnosis needs (see Table 2-2). They generally inspect the bone and implant for osseointegration, failure, or fractures [101]. In this section, the sub imaging approaches, their features and limitations will be covered, as illustrated in Table 2-3.

Table 2-3: The different imaging modalities used for THR loosening diagnosis comparisons.

	Modality	Concept	Advantage	Disadvantage
Imaging Diagnosis	Plain Radiology	X-Ray imaging (Radiolucent line) : Space between the bone and the implant [25]	Cost effective and availability [102, 103]	Radiation exposure , Heavily experience-dependent [103, 104]
	Arthrography	(Plain Radiology + contrast agents) = more accuracy imaging (via fluoroscopy , CT or MRI) [100]	Higher sensitivity [95, 104]	Radiation exposure and relatively complex procedure [100]
	Scintigraphy	(Gamma Camera + isotopes) = observe bone metabolic rate [105]	Diagnosing a variety of pathological diagnoses of which musculoskeletal disorders is one [105]	Low specificity, radiation exposure, high cost, and relatively complex procedure [106]
	FDG-PET	(Similar to Scintigraphy + monitor labelled glucose instead of isotope)[100]	Distinguish between infection and loosening [107]	Nuclear, expensive [108]
	RSA	(Two Plain Radiology sources + two detectors) for 3D imaging construction [109]	Enables early detection of implant migration [110, 111] and measurement of polymer wear [112, 113]	Expensive and complicated procedure [113]

2.4.1.1 Plain Radiology

Musculoskeletal system disorders are primarily examined using conventional radiology imaging, due to cost effectiveness and availability of this technique [102]. Also, this is used as one of the main post-operative follow-up procedures [86, 114]. The accurate diagnosis of loosening using this technique is heavily experience-dependent and is usually viewed by either Anteroposterior and/or Lateral views of the hip and/or pelvis region [25, 104].

The radiology criteria for THR loosening include component position, alignment and the presence of a radiolucent line. The first two can be identified by matching the THR side with the opposite side; while the radiolucent line, if present, can be identified as a space between

the bone and the implant. For example, more than 2mm of radiolucent line could indicate a loose or migrated component [101]. Conventional radiology is an accurate diagnostic method; however, certain conditions could go undetected, leaving patients with unresolved pain. In such cases, other imaging techniques need to be considered [100].

2.4.1.2 Arthrography

Arthrography is an imagining modality similar to conventional radiology, but with the use of contrast agents. The contrast agent role in arthrography is to enhance the imaging accuracy, in order to identify what could not be detected using plain radiology [115]. These agents are injected into the joint while a conventional x-ray is taken, which makes it an invasive method for the patient. There are different approaches by which arthrography could be conducted; commonly fluoroscopy but also computed tomographic (CT) or magnetic resonance imaging (MRI) can be used. Attempts to enhance this technique resulted in the introduction of digital subtraction arthrography (DSA). This reveals more accurate images but represents a more complicated procedure than typical arthrography.

Contrast agent diffusion around the joint is the main criteria for arthrography in identifying different failure conditions [116]. This technique has shown higher sensitivity and specificity in diagnosing results compared with plain radiology of about 4%, according to Temmerman *et al.* [104]. The correctly identified (true positive[2]) proportions are referred to as a sensitivity, whereas the true negative[3] as a specificity. However, other studies have stated that arthrography resolution could be compromised by patient motion through the imaging process and, as such, may not be able to reliably detect aseptic loosening [100].

2.4.1.3 Scintigraphy

Hip loosening can also be detected by nuclear medicine, using the Scintigraphy imaging method. This technique involves the use of a radioisotope that is introduced into the blood stream, then detected by a gamma camera, which monitors the uptake of the radioisotope, reflecting bone metabolism. After the isotope is injected, a period of two to six hours is

2- True positive = when patient has the disease or condition.

3- True negative = when patient does not have the disease or condition.

required before imaging, in order to achieve more vivid bone imagining. Patient fluid intake (hydration) before imaging can also contribute to the imaging clarity [105, 117].

Scintigraphy imaging for detecting muscle-skeleton abnormality is achieved through observing the higher rate of isotope uptake that reflects a higher bone metabolic rate. If observed, this could mean that bone growth is being generated by the body to overcome reduced stability, which could be a result from joint infection or loosening. Isotope intake is dictated by blood flow and new bone growth rate, while the imaging period is age dependent, meaning older patients may need a double exposure time compared to younger adults, for whom the waiting time is typically two hours [100, 105].

The scintigraphy imaging method has shown a potential for diagnosing a variety of pathological diagnoses, of which musculoskeletal disorders is one. In regards to hip loosening detection, it has reported high sensitivity of up to 88% but with the downside of specificity as low as 50% [104]. The low specificity, radiation exposure, high cost, and relatively complex procedure are potential disadvantages that could lead surgeons to pursue better options [106].

2.4.1.4 EDG-PET

Fluorodeoxyglucose positron emission tomography (FDG-PET) is another nuclear imaging technique that operates along the same principles as Scintigraphy. However, FDG-PET has shown superior results in distinguishing between infection and loose joints, which has historically been challenging because of the analogous early clinical indications they both hold. In fact, PET scanning enables early infection detection before any radiology symptoms are even present [107, 118].

FDG-PET imaging operates on the principle that an infected joint increases energy intake due to the higher activity of the leukocytes and macrophages blood cells. These increased energy intakes are reflected by the higher radiolabeled glucose (FDG) consumption, which is detected by the tomography imaging [108].

PET scanning has many advantages over similar imaging methods for loosening detection, including the fact that it is a non-invasive method, with a relatively shorter exposure time, and higher accuracy rates with a reported average sensitivity of 85% and a specificity of 90% [106, 108]. However, FDG-PET has the disadvantage of being expensive, and this could prevent its widespread use [108].

2.4.1.5 RSA

Building on plain radiology, Selvik *et al*. [119] introduced radiostereometric analysis (RSA) imaging. RSA provides a precise three-dimensional (3D) image that enables early detection of implant migration, which would not be possible with other methods [110, 111].

RSA's system principle of constructing the 3D image is to use two plain radiology sources and two detectors, with known locations, at the same time, targeting the Tantalum marked implant. These Tantalum markers are inserted surgically around the implant in order to define its location for the 3D imaging construction [109]. However, the surgically invasive procedure needed to implant the markers was considered a disadvantage to the RSA system, which later was overcome by the model-based RSA system that eliminates such intervention [113]. Through the early cup migration RSA measurement, the likelihood of late aseptic loosening can be predicted [120].

RSA imaging has a promising future because of the high accuracy of this technique. It is already regarded as the gold standard in the measurement of *in vivo* THR polymer wear [112, 113]. In fact, RSA measurement of THR loosening has reported translation and rotation accuracy of 0.2mm and 0.5 degrees respectively [110]. However, the high cost and the complicated nature of the RSA system has contributed to it being used much less than any of the previously discussed imaging modalities [113], leaving the prospect of either enhancing earlier modalities to make them more accurate and user-friendly, or exploring non-radiological methods. These will be covered subsequently.

2.4.2 Non-imaging

In the conventional imaging methods of diagnosing prosthesis loosening, some limitations and shortcomings are evident. Even with a sensitivity and specificity of up to 80%, a revision operation on a perfect hip endoprosthesis may still be possible [121]. Consequently, new techniques have been developed and proposed on the basis of non-destructive testing (NDT), which is well established in some industrial fields, such as aerospace and automobile sectors [122]. The non-imaging techniques include two subcategories: non-structural and structural testing, which will elaborated on next (Table 2-4).

Table 2-4: THR loosening non-imaging techniques.

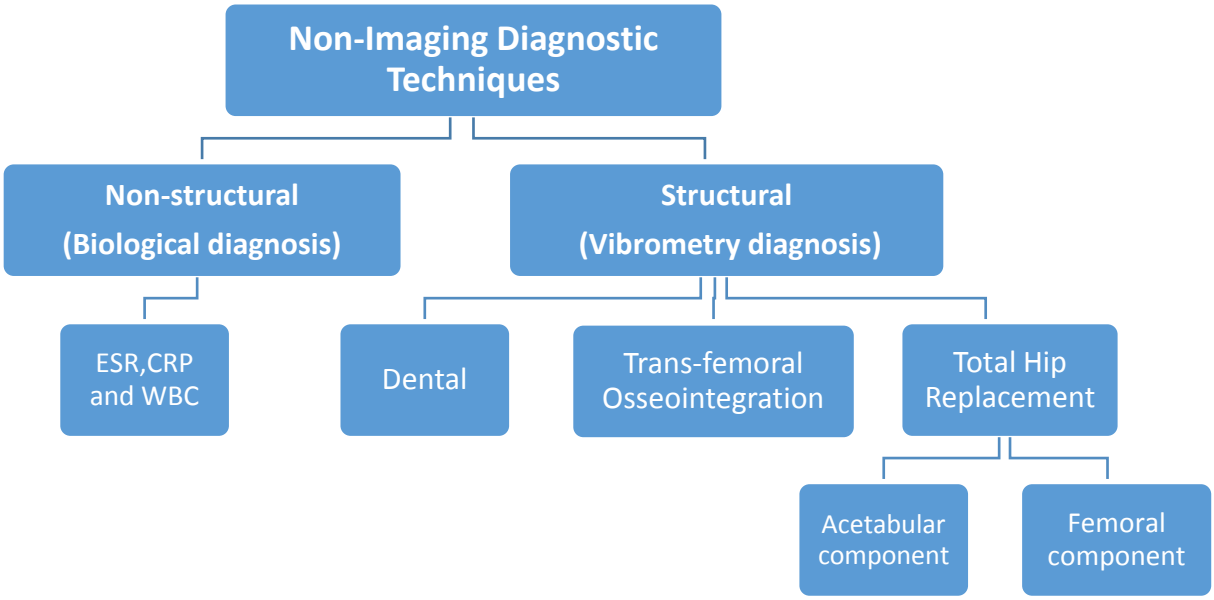

2.4.2.1 Non-structural (biological diagnosis)

Due to the similar early clinical indications of THR loosening and infection, certain tests are initially needed to make this differential diagnosis [25]. This is possible through a series of blood tests that include the reading of the erythrocyte sedimentation rate (ESR), C-reactive protein (CRP) and Synovial fluid white blood cell count (WBC) [123]. Inflammation is highly probable if the readings for all of these biological indicators exceed certain sensitivity limits, as seen in Table 2-5. In normal (non-infected) patients, these indicators return to their normal rate 3 weeks after hip surgery for the CRP, and up to one year for the ESR. The aspiration WBC test is not recommended before two weeks after antibiotic treatment is finished [25].

Table 2-5: Joint Infection Screening Indicators, source [25].

Laboratory Indicator	Sensitivity limit
ESR	> 30 mm/hr
CRP	> 10 mg/L
Aspirate WBC	> 3000 leukocytes/mL)

2.4.2.2 Structural (Vibrometry diagnosis)

Vibration analysis is a mechanical NDT technique that is widely used in the inspection of composite materials and structural integrity and has been successfully expanded into the arena of biomechanics [8, 124]. Vibrometry mainly measures the response to low-frequency excitation reflected from the targeted surface or structure [125]. Long bone property assessment, fracture healing monitoring, osseointegration and stability monitoring are all applications of vibration analysis in biomechanics [8]. However, the most widespread use was initially in the field of dentistry, following the studies of Meredith *et al.*[126, 127], which gave way to further research. Since then, many research groups have used vibration analysis for detecting prosthetic loosening via different measurement and excitation techniques [128]. In the following sections, we will further discuss some of the orthopaedic vibrometry applications with regards to dental uses, trans-femoral osseointegration (TFOI), and THR.

2.4.2.2.1 Dental

One of the earlier successes of vibration analysis was for assessing implant stability in dentistry. Meredith *et al.* [126] pioneered the technique that instigated resonance frequency analysis (RFA) in the dental field, through finding that implant height and rigidity had a relative relationship to RFA. Further studies were carried by different researchers [126, 127, 129-133], in which they were able to measure the dynamic properties of an implant in order to identify different implant interference changes. Consequently, commercial systems have been introduced, such as Osstell® (Integration Diagnostics AB, Sweden) and Periotest®(Medizintechnik Gulden E.K, Germany) [128].

2.4.2.2.2 Trans-femoral Osseointegration (TFOI)

Trans-femoral implants were introduced two decades ago and had relative success in the orthopaedic field, with the downside of a long rehabilitation phase and the likelihood of infection [128]. These implants were intended to replace an amputee socket with a femoral anchored implant, which was mainly a titanium implant fixed into the femur distal side [134]. Vibration analysis was used in a number of studies to assess TFOI [124, 128, 135-137]. These studies were inspired by the successful use of vibration analysis in the assessment of dental implant osseointegration [127, 131].

The first *in vitro* study was conducted by Xu *et al.* [135], who measured the resonant frequency in an attempt to assess trans-femoral implant osseointegration (TFOI). They showed promising results, relating the successful osseointegration process to the increase in the natural frequency response. Subsequently, Shao *et al.* [124] performed *in vitro* and *in vivo* studies to investigate the natural frequency of the TFOI. The experiments included impact excitation and an accelerometer to measure resonant frequency. Both *in vivo* and *in vitro* confirmed the results of the previous study [135], whereby the higher resonant (natural) frequency correlated with positive progress of osseointegration before reaching a steady equilibrium phase [124].

Cairns *et al.* [128] published a more recent comprehensive study in relation to TFOI assessment by observing earlier studies done by Xu *et al.* [135] and Shao *et al*. [124]. It was found that their methods included certain limitations that could have altered their findings. Thus, Cairns *et al* [128] started by dealing with these limitations in order to obtain more

realistic measurements that could reflect the feasibility of TFOI assessment. First, they used titanium implants similar to those clinically used, instead of stainless steel. Secondly, boundary conditions were given more attention, with two scenarios (free support and cantilevered) used as an alternative to clamping. Thirdly, both the excitation and the response were measured, instead of a single measurement, in order to compare results. Fourthly, the measurement was excited by vibration analysis as a replacement for impact excitation. Lastly, modal analysis was also used to simulate different boundary conditions. The results showed that good osseointegration was correlated to higher resonant frequency values. However, further research was suggested to examine the effects of the boundary conditions on the results.

2.4.2.2.3 Total Hip Replacement (THR)

In 1932, Lippmann pioneered vibration analysis in the field of medical research, utilising a stethoscope to examine bone fracture healing and using his fingers to elicit the input vibration. Lippmann's study examined the free vibration response of three long bones: the femur, humorous, and clavicle. This was done by applying the excitation from one side, causing the signal to travel through the bone shaft, and measuring the response with a stethoscope from the other. The change in pitch and quality response were used as an indication for the fracture healing level. A high response would reflect a good fracture healing process and a reduced pitch would imply poor healing [138]. Due to the lack of technology, further studies were not conducted until the 1970s, when more literature was available in the area of orthopaedics [139]. This will be explored based on the THR examined component femoral stem and acetabular cup.

Table 2-6: The THR vibration analysis literature overview.

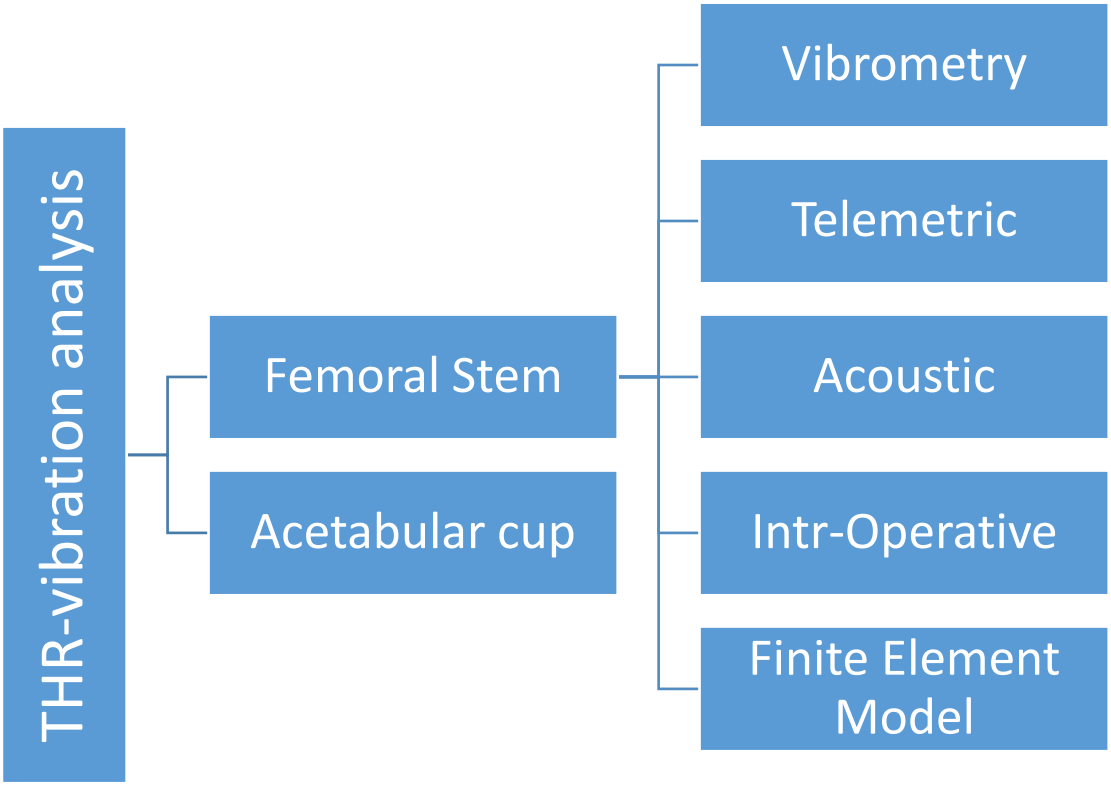

Femoral (Stem) Component

According to Cunningham [140], the first attempt of vibration analysis in the diagnosis of total hip replacement (THR) was promoted by Chung *et al*.[141]and Poss *et al*.[142]. They proposed vibration assessment as a method for monitoring hip prosthesis cement coupling. After being applied, bone acrylic cement starts to harden, causing the implant to be fixed in its desired position. Thus, the hardness process of the cement could be examined using vibration assessment. The study observed the frequency response and noted that, as the cement hardened, the frequency response shifted and intensified. They initially identified the fundamental frequency peaks related to the prosthesis and stem in the frequency response and continued to do so as the acrylic cemented healed. They stated that, as healing took place, the two peaks drifted apart, shifting from their original location. Meanwhile, the signal amplitude intensified and decreased in depth, reaching a steady state after about 30 minutes of stem implantation, as shown in Figure 2-11. In contrast, an in-vitro study by Van der Perre in 1984 examined the dynamic analysis of human bones with loose femoral implants. He stated that stem loosening caused a decrease in the natural frequency of the system and also described the measurement from a loose prostheses as noisy [140, 143].

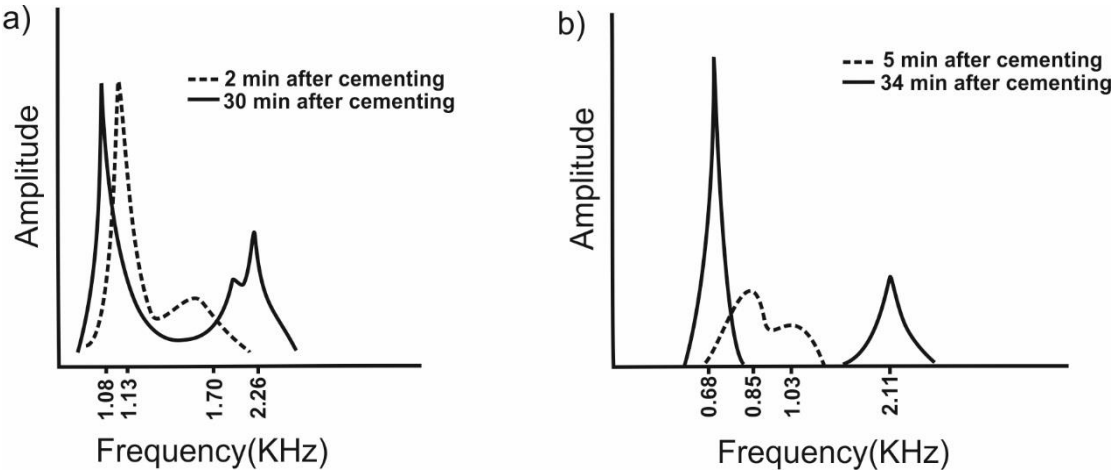

Figure 2-11: The frequency responses reflecting cement healing; a) Chung *et al.* (1979)[141], b) Poss *et al*. (1984)[142]. Illustrations modified by the author.

Rosenstein *et al*. [10] were among the first to utilise vibration analysis in a clinical study, both *in vivo* and *in vitro*, in an attempt to differentiate between loose and secure femoral implants. In the *in vitro* study, ten pathology-free cadaver femurs were used. A mini shaker with a known frequency output was placed on the lateral femoral condyle to generate the excitation, while the output signal was measured with an accelerometer located on the greater trochanter (Figure 2-12). An accelerometer is an electromechanical instrument that converts mechanical vibration into electrical signals, which can then be stored and processed. In an attempt to represent a secure implant, a femoral prosthesis was fixed into each of the femurs and then tested with an input frequency range of 100Hz to 1000Hz. These femoral implants were then loosened by partially detaching some of the proximal cement fixation, in order to represent the loose states. An *in vivo* study was also conducted, using seven in-patients diagnosed with prosthetic loosening, in addition to four who had successful total hip replacements. Patients were placed laterally in a similar fashion to the *in vitro* setup, in order to examine the efficacy of this technique. The four patients with total hip replacements had their implants cemented two weeks before the study. They represented the fixed implant states. The remaining seven patients were examined before their revisions took place, potentially representing the loose state. The vibration analysis was conducted using the Fast Fourier Transform (FFT) algorithm, which can represent any time wave signal using a combination of several sinusoidal signals. Subsequently, it can be seen in the frequency domain as different vertical peaks at the corresponding frequencies, with heights relating to their magnitude [144].This study concluded that vibration analysis was a valid method of distinguishing between a loose and a secure prosthesis. In the secure prosthesis, the bone and implant responded to excitation with a single frequency vibration as one unit. In the loose prosthesis, the bone and implant vibrated at different frequencies, which appeared as different peaks in the frequency spectra, as shown (Figure 2-13). They also showed that soft tissue did not alter the results obtained, and that patients did not experience any discomfort as a result of the experiment's setting. The sensitivity and specificity of this vibration technique were subsequently shown to be 100% [9]. Despite these promising findings for use of vibrometry to diagnose late femoral loosening, early loosening cases were not represented, which led the way for the next couple of studies investigating the potential of vibrometry for early loosening cases.

Figure 2-12: The *in vivo* test setting , source [10] with permission

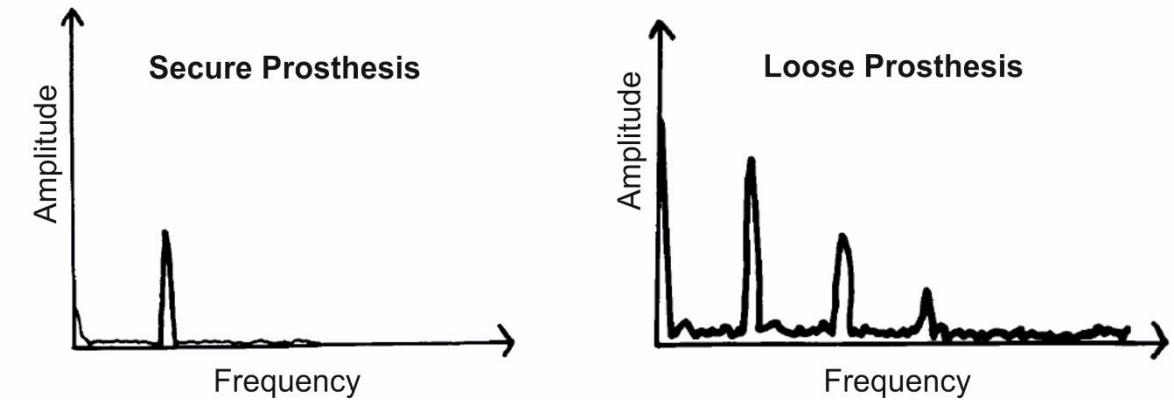

Figure 2-13: The FFT response of the secure and loose prosthesis, source [10] with permission.

Li *et al*.(1995-6) [11, 12] were the next to explore vibration analysis, with the aim of testing its sensitivity in detecting early loosening of THR. They postulated that early loosening was caused by micro-movement between the prosthesis and bone due to a lack of "microlock". This was mimicked for their experiment by stopping the cement from penetrating the trabecular spaces, by adding a Teflon coating to the femoral inner canal. Late loosening was simulated by 2mm macro-movement tolerance at the bone - prosthesis interface. Another late loosening model used silicone rubber to resemble a 2 mm layer of tissue at the cancellous bones – cement interface. The experimental setting included a shaker that was placed on the distal end of the femur and two accelerometers – one attached to the shaker to measure the input magnitude and frequency, and a second to measure the signal from the greater

trochanter. Femoral models (Sawbones; Stratec, Cambridge, UK) were used with an input frequency range between 100Hz to 1200Hz. Signal analysis was conducted using two approaches: frequency response curve and spectral analysis FFT. The frequency response curve examined the overall system feedback to a frequency sweep, whereas the spectral analysis looks at the individual frequencies. They indicated that the spectral analysis had more favourable results, leading to more loosening detecting cases (Figure 2-14 and Figure 2-15).No significant differences were found between the late loose model that had fibrous tissue (2mm silicone) mimicking material and the secure condition. The late loose model with the 2mm micro-movement gap had a high sensitivity of 95% for the frequency response and 100 % for the spectral analysis. Early mimicked loosening was only detected in three cases out of eight using the spectral method, giving a low sensitivity rate of 37.5%, whereas the frequency response was not able to detect the difference. The authors concluded that vibration analysis was a reliable method in the detection of late loosening, but had a low sensitivity (35.5%) for early conditions. They also emphasised that future studies should pay more attention to the importance of boundary conditions and possible mathematical modelling [11, 12].

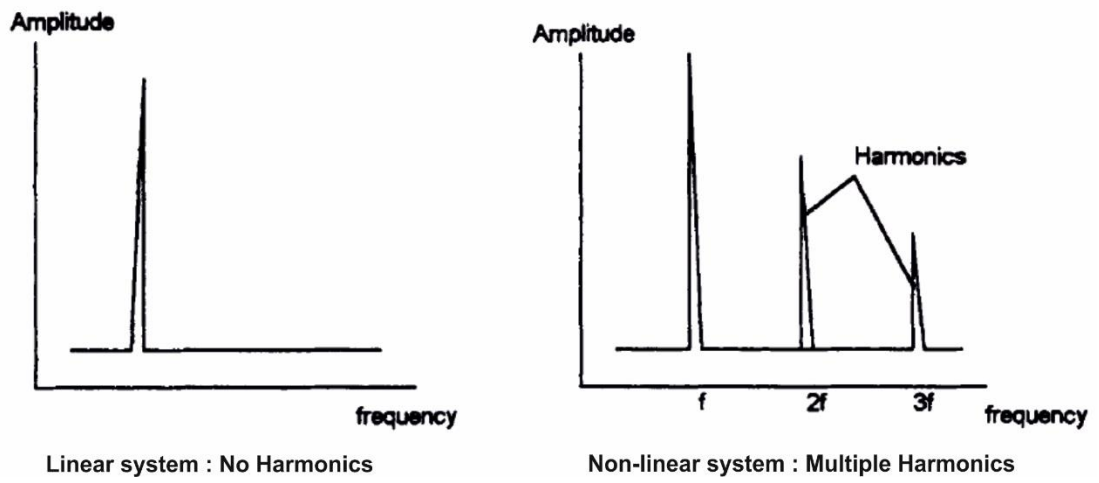

Figure 2-14: Li *et al* (1996) explaining the principle of distinction between secure and loose implants through the (FFT) spectral analysis (not from specimen data just an example), source [12] with permission.

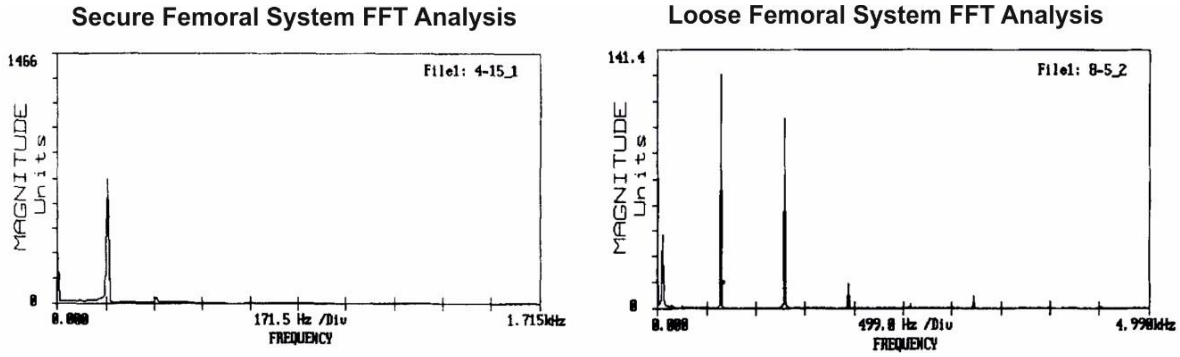

Figure 2-15: Li *et al* (1996) secure and loose femoral component spectral analysis, source [12] with permission.

Georgiou and Cunningham [9] compared vibration analysis with a standard radiology assessment and generated valuable data that was utilised in later publications. The *in vivo* clinical study was conducted on twenty-three patients and a control group provided substantial data. A vibrator, with a 100Hz to 1000Hz input frequency, was placed on the femoral lateral epicondyle and measurements were obtained using an accelerometer on the greater trochanter of the femur. There were two patient groups: one group of twenty-three patients admitted for THR revision and a second group of ten patients (control group) who had a recent THR, giving an assumed secure prosthesis. Vibrometry signal analysis was conducted using two approaches: frequency response curve and spectral analysis; similarly to the work of Li *et al*.(1995-6) [11, 12]. Each approach was given a defined criteria distinguishing between the loose and secure prostheses. For the spectral analysis approach, the criteria was mainly dependent on the fundamental frequency response and the existence of harmonics number and amplitude. When there was no harmonics or the harmonics amplitude was less than 25% of the fundamental frequency, it was considered a secure implant. When there were more than four harmonics or a harmonic that was 50% more in amplitude than that of the fundamental frequency, it was declared as a loosened condition. According to the study, the first harmonic was the most applicable for the harmonic fundamental frequency percentage rate (25%-50%). For the frequency (amplitude) response curve approach, a single response reflected a secure condition while more than a single response represented a loose condition. The results obtained using vibration analysis were compared with results from three clinicians' blinded assessments of the patients' radiographs. Based on the comparison of the vibrometry and radiology results, they concluded that vibration analysis showed more precision in diagnosis of 20%, and was able to detect 13% more cases than radiology. Also, vibration analysis was reported to have a sensitivity and specificity of 81% and 89%, respectively [9].

Rowlands *et al.* [145] was the first to use the Doppler effect in an attempt to diagnose endoprosthetic loosening. Ultrasound was used by different research groups in orthopaedics [146-148], to examine the integrity of bone cement bonding to implant surface [149, 150]; to assess fracture healing, and for osteoporosis diagnosis [151]. Flint *et al*. [146] also implied that ultrasound has the potential to measure prosthetic loosening, but such a study was not realised until 2008, when Rowlands *et al*. conducted their pilot study. Based on the concept of vibration analysis of the total hip implant and the effect of soft tissue on the measured results, they replaced the accelerometer sensor that had been previously used with an ultrasonic probe. The study's aim was to examine the possibility of using ultrasound to measure the output vibration and distinguish between a loose or secure hip prosthesis, and compare it with the accelerometer results. The study included two different types of bone analysis: Sawbones and Tufnol, which are commonly used in laboratory testing, with an input frequency range between 100Hz to 1500Hz. Initially, the Sawbones femur was tested with a fixed and loose hip prostheses through the use of cement fixation. Then, the Tufnol femur was tested for three conditions (fixed, early loose, and loose), by using different solid bar diameters of different fits (tight +0.5mm, sliding -0.2mm and loose -1.2mm). In order to represent a realistic experiment, soft tissue was mimicked by using water for the ultrasound measurement and foam for the accelerometer setting (Figure 2-16). The measurement of both Sawbone and Tufnol femoral bone models revealed the reliability of using ultrasound as a diagnostic tool for loosening through FFT spectral analysis. In fact, the ultrasound was able to measure a greater signal amplitude when compared to the accelerometer (Figure 2-17). The investigators also noticed that, for the Tufnol femoral bone model, the 100Hz to 450Hz frequency range had more sensitive results for both the ultrasound and the accelerometer measuring techniques [145].

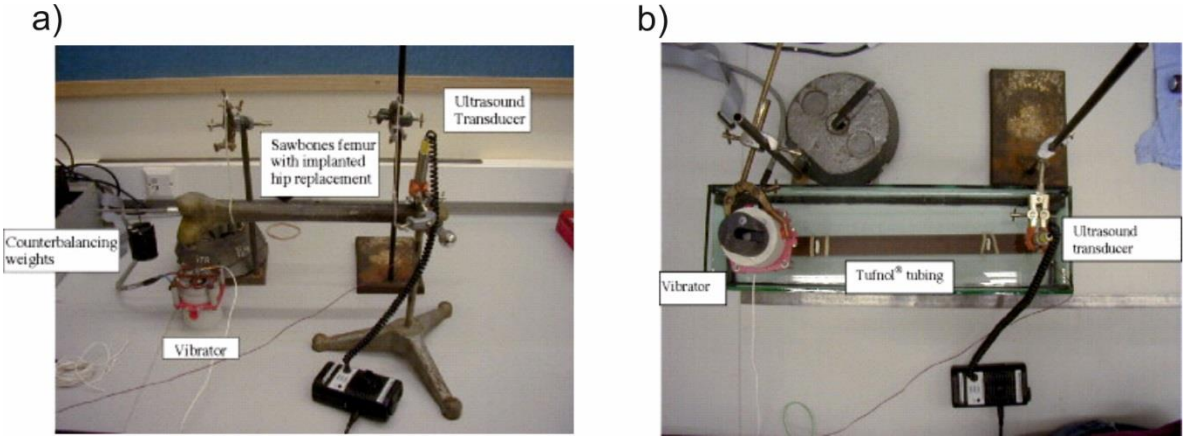

Figure 2-16: The two different types of bone tests; a) Sawbones setup, b) Tufnol setup, source [145] with permission.

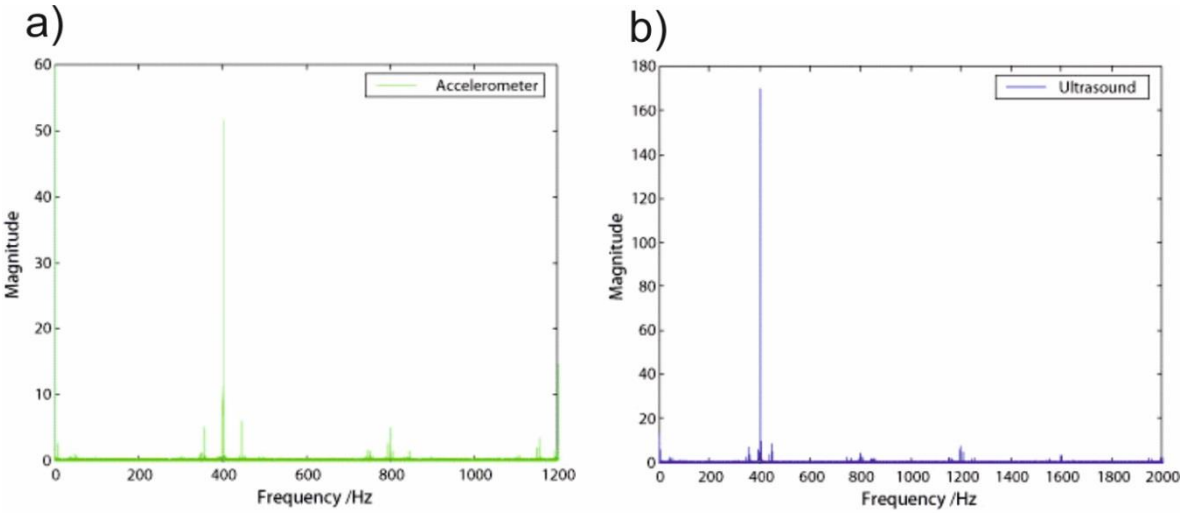

Figure 2-17: The two sensors Sawbones FFT response of the loose prosthesis at driving frequency of 400Hz, showing the higher signal magnitude for the ultrasound (y-axis); a) Accelerometer, b) Ultrasound, source [145] with permission.

Rieger *et al*. [8] were the first to explore the possibility of using vibration analysis as a diagnostic tool for the complete Sawbones hip implant (both the stem and cup). The experiment examined four different scenarios with different stem and cup components using Sawbones models (secure stem and cup / loose stem and cup / secure stem and loose cup / loose stem and secure cup). The method of excitation was an electromagnetic shaker in the frequency range of 100 Hz to 2000 Hz applied at two locations; once at the femoral lateral condyle then at the ilium crest. Measurements were recorded using two methods; optical

laser and accelerometer vibrometry. The optical laser is a highly sensitive industrial technique that can measure surface vibration and was utilised as a reference measurement in this experiment. Three accelerometer sensors were located at different locations: medial condyle, greater trochanter, and the crest of the ilium (Figure 2-18). Six pairs were tested; where stem loosening was realised through utilising two stem sizes (10 for secure and 8 for loose), while the cup loosening was realised by using an abraded cup outer surface, preventing it from anchoring to the Sawbones cavity. Their findings revealed the feasibility of using vibration analysis to distinguish between different loosening components (femoral and acetabular), by observing three different parameters: frequency peak count, integral analysis, and peak shift. Frequency peak count is where the addition peaks to the fundamental and harmonics are counted using a specific thresholds. The integral analysis was based on the trapezoidal numerical integration method, by dividing the spectral into different bands (five for the condyle excitation and six bands for the ilium excitation). Peak shift analysis was realised through observing the frequency and magnitude peaks shift of the response resonance frequency with the secure condition being used as a reference. Based on the peak shift results, the stem and cup loosening could be identified using two sensitive frequency ranges; 200Hz and 450Hz-600Hz respectively (Figure 2-19). Based on their findings, the peak shift was found to be the most reliable in detecting loosening, followed by integral analysis for stem loosening. Meanwhile, the frequency peak count revealed more detail about acetabular loosening. Supplementary studies were suggested for further validation before this technique could be introduced to clinical practise for the diagnosis of loosening [8].

a) b)

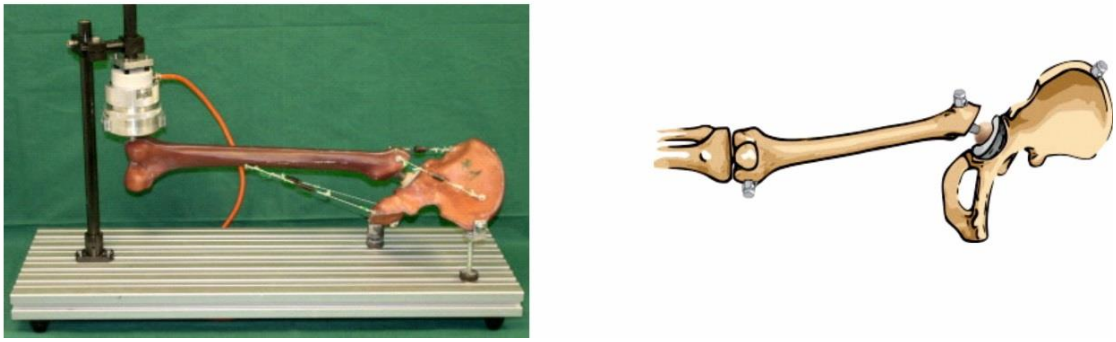

Figure 2-18: The Sawbones model setup for the combined stem cup loosening, a) the model and excitation setup, b) the location of the three used accelerometers, source [8] with permission.

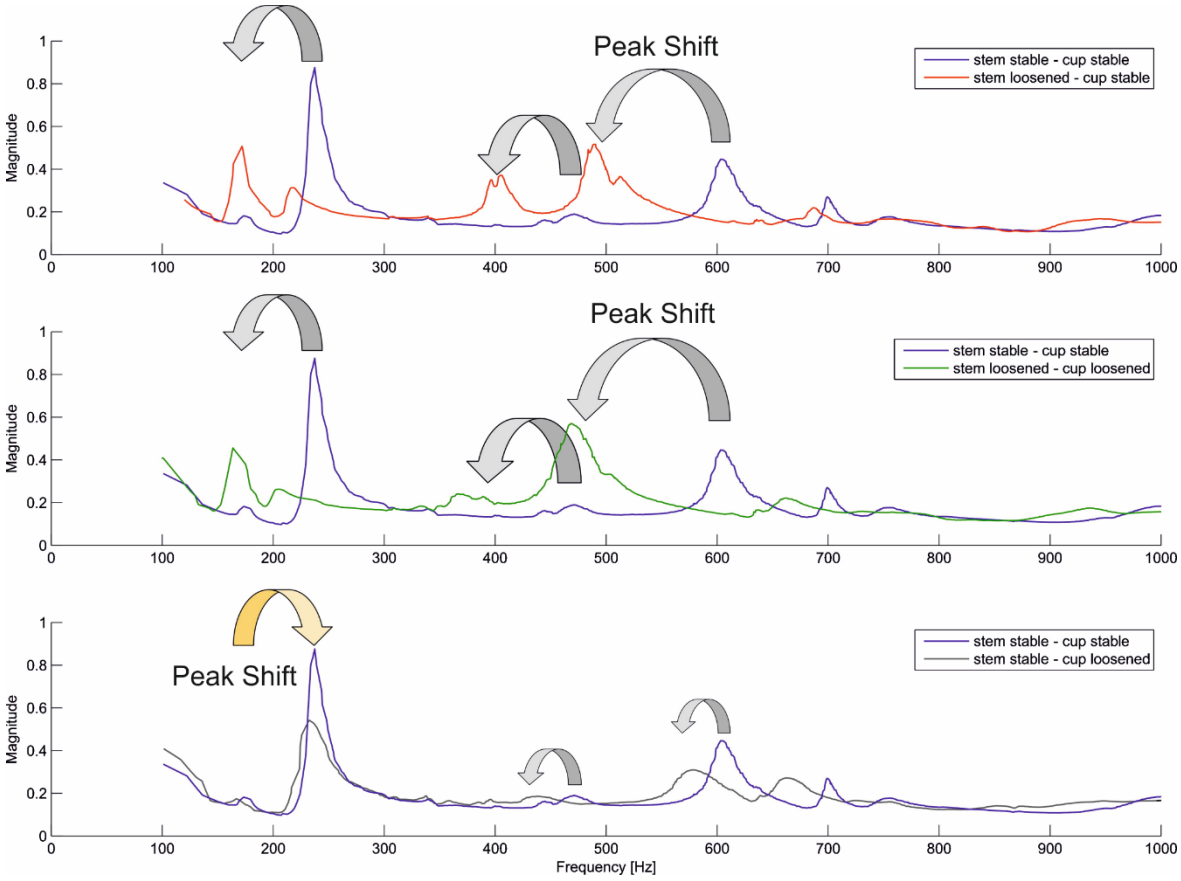

Figure 2-19: The accelerometers average spectral response; clearly illustrating the peak shift with relation to the three simulated conditions, source [8] with permission.

In a more recent study, Rieger *et al*. [5] went one step further by replacing the excitation source with an extracorporeal shockwaves system. The proposed shockwaves system eliminated the need for mechanical excitation, which could cause patients discomfort during the diagnosis process. This new excitation approach was tested on three cadaver specimens (six hip joint, n=6) with four implant loosening simulation (stable stem and cup, loose stem and cup, loose stem and stable cup, loose cup and stable stem) with a frequency range of 100Hz to 5000Hz. Three different excitation locations were tested (lateral condyle, greater trochanter and ilium crest) utilising a variety of gel-pad sizes as a method of controlling the desired tissue penetration depth from 5mm to 40mm, as illustrated in Figure 2-20. Measurements were collected using three accelerometers simultaneously, positioned similarly to the three selected excitation locations. Similarly to the previous study, stem loosening was realised by using a smaller stem size while cup loosening was stimulated with an abraded cup exterior surface. The study had two aims. Firstly, to test the new excitation approach and, secondly, to see if the loose implant would cause the resonance spectral to

shift. A further aim was to investigate the possibility of distinguishing stem loosening from cup loosening. The main resonance of the secure hip prosthesis was about 2000Hz. The lateral condyle excitation resulted in no significance differences between the simulated conditions. Between the trochanter and the ilium locations, the clearest different was shown with the excitation at the ilium crest and accelerometer reading located at the trochanter. This was the case for the isolated stem loosening and the combined stem cup loosening, where a significant response shift was evident in the frequency range between 386Hz and 847Hz. However, isolated acetabular cup loosening did show a resonance shift but was not statistically significant. The authors concluded that distinguishing between individual THR loosening components remained a challenge, even with the use of a novel excitation system. The specimens during the study were suspended rather than lying on their side, which needed to be considered when interpreting the findings, as highlighted by the authors.

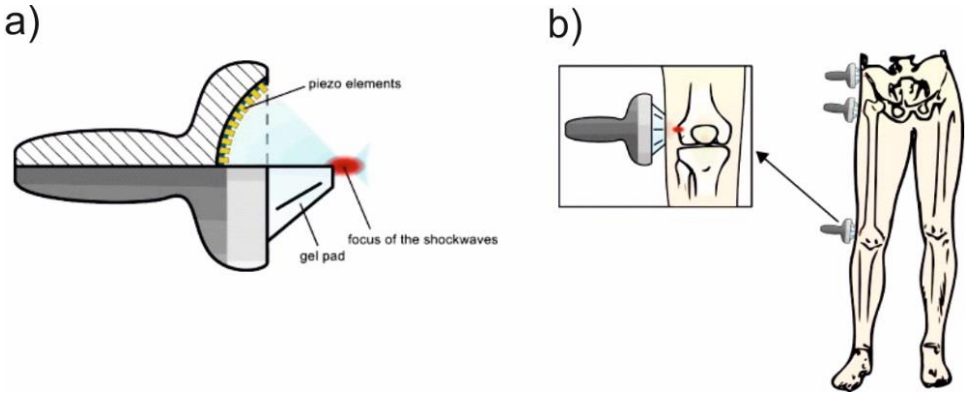

Figure 2-20: The new proposed shockwaves excitation, a) the shockwave source, b) the excitation location used, source [5] with permission.

The visual examination of the frequency response has been the main method of defining the loose condition from the secure implant using it as a reference [6]. Perez *et al* [6] explored different frequency response algorithms, with the aim of reaching the best quantifiable means possible and eliminating the need for visual dependency. A cadaveric femur was utilised to create two stem conditions (loose and secure). Loosening was realised by introducing a bone implant gap that was greater than 150 µm, resulting in an unstable stem condition. Excitation was conducted through 75 N transverse load, which caused the specimen to vibration freely for 5 seconds while two strain gauges were recorded the responses (Figure 2-21a). The most distinctive differences were found using the Thomson's Multi-Taper (MTM) frequency response algorithm with a frequency range 600Hz-900Hz, holding the highest energy for the loose implant over the secure condition (Figure 2-21b).

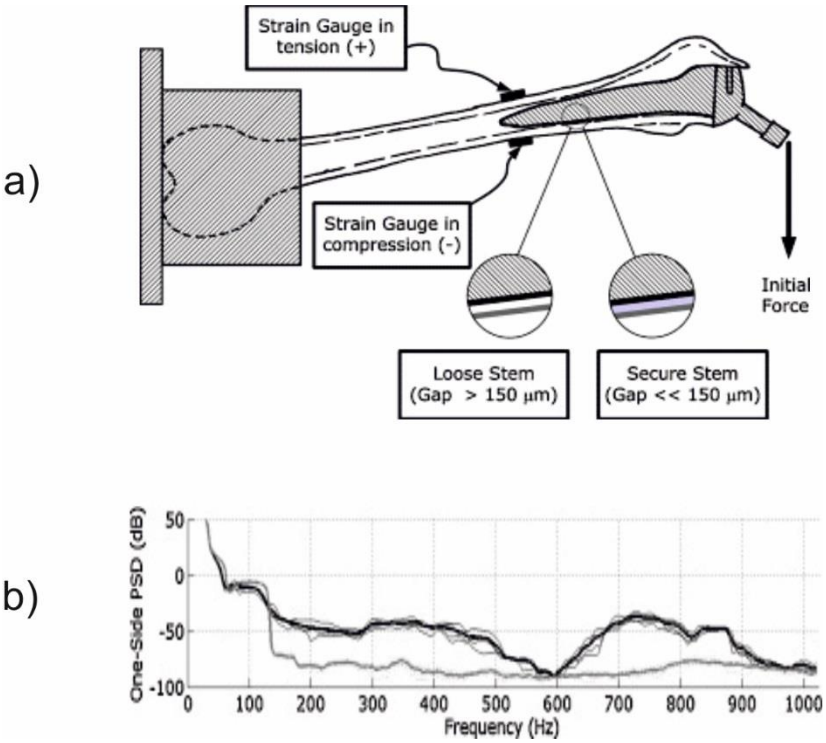

Figure 2-21: Perez *et al.*'s experiment setup and results. a) the setup sketch , b) the frequency response (grey line: average secure stem response, bold line: average loose stem response), source [15] with permission.

Telemetry

To pursue more precise diagnostic tools, some researchers have proposed a telemetry technique, whereby wireless data transmission and integrated sensors are excited externally in an attempt to detect THR loosening [152-155].

Puers *et al*. [152] were the first to explore this field for the purposes of the THR loosening detection. Their study used vibration analysis with the new approach of introducing a monitoring system inside the prosthesis. The imbedded system included a capacitive accelerometer that could transmit measurements wirelessly for analysis (Figure 2-22). In attempt to test the viability of this new approach, a cadaver experiment was carried out with simulated loose and fixed cemented implants and using a vibration excitation range of 100Hz–200 Hz to the lateral condyle. Two different coils were used, one for the power and a second for the data transfers, utilising different frequency bands. Data analysis of the wireless transferred measurement showed a very clear distinction between the loose and fixed prosthesis, as shown in (Figure 2-22c). This study opened up a new field of exploration of the use embedded wireless monitoring systems.

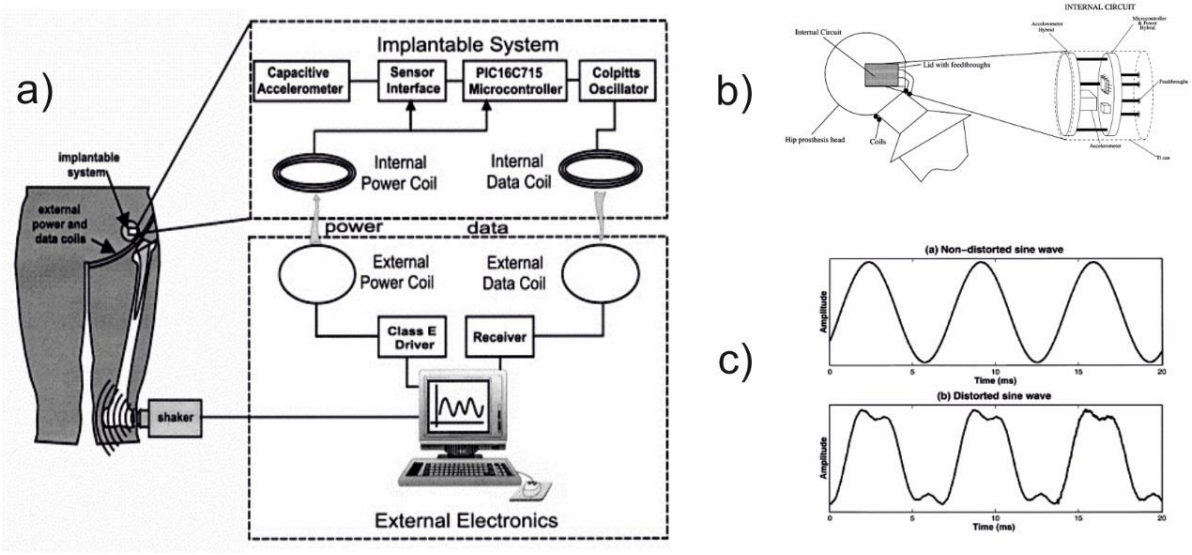

Figure 2-22: The first wireless vibrometry system; a) the system concept, b) the imbedded sensor in the femoral head, c) the time domain response at 150Hz excitation (upper figure for the secure output – lower figure for the loose condition), source [152] with permission.

Clasbrummel *et al*. [153] also assessed endoprosthetic loosening in an attempt to produce a digital system for stem loosening detection. In their experiment, loose and fixed prosthetic conditions were simulated. A 0.5mm silicone layer was used to mimic the loose condition, while cement was used to replicate the secure condition. Alongside two transition conditions from firm to loose were used (1/3 and 2/3 distal femoral loosening with the rest surrounded by a silicone layer). A 100g weight was used as a method of excitation by being dropped from different heights of between 5cm and 25cm. The resulting signal was picked up by five accelerometers (3 embedded on the stem and 2 on the Sawbones femur for reference). Subsequently, the data was processed using the Fast Fourier Transformation method. They were able to identify the loose stem from the secure one. The group's results were promising in detecting loosening. They suggested further developments in this approach and possibly have an intraoperative application.

Further work on telemetry was conducted by Marschner *et al.* [154], who changed the location of the accelerometer to the distal end of the stem. The experiment utilised a digital lock-in amplifier for the pre-processing of the accelerometer data, separating the noise from the measurement signal. They integrated all the elements (accelerometer, lock-in amplifier, and telemetry) together and a single coil was used for the measurement transfer and energy input. They verified the ability of the system to detect femoral loosening experimentally; however, its sensitivity and specificity were not assessed [154].

In another telemetry study, the accelerometer location was proposed to be in the prosthesis head [155]. This approach was advocated by Sauer, who argued that it would be easier to manufacture and sterilise[4]. Moreover, there are fewer head types when compared with other prosthesis components. In addition to the integrated measuring unit, the excitation and the measurement coil were external. Loosening stem scenarios were mimicked by the use of screw fixations; progressively securing screws moving from the loose states to the totally secure condition. The results showed that the more loosening there is, the frequency response tended to shift to the lower values. This was in agreement with previous vibrometry literature [5, 8, 141, 142]. Further studies were suggested to explore other factors that may influence resonance shift, as well as to enhance the data transference quality and biocompatibility of the housing [155].

2 Manufacturing: due to the expensive stem approaches, Sterilising: was not feasible in previous system.

Acoustic

Acoustic emission is another branch of non-destructive testing that is used to observe the integrity of surfaces by measuring the acoustic resonance responses through "listening to the different sounds made by a structure under stress". [125]. One of the first studies that utilised acoustic emission in the area of prostheses assessment was led by Davies *et al.* [147]. Their goal was to study THR cement-bone debonding initiation and propagation under simulated physiological loading. They found that depending propagation led to an increase in acoustic emissions. They hypothesised that such response information (intensity and frequency) could be related to the cement-implant depending (failure) level, but this was not proven [147].

Paech *et al*. [156] was the first study to examine the stem implants acoustic properties (natural frequency) with the aim of determining the reliability of acoustic techniques in the diagnosis of loosening. Initially, the acoustic characteristics of four different stems were examined using a 120g steel ball impact excitation at prosthesis' neck area. The sound was measured via a microphone positioned 10 cm away from the stem midpoint. It was then processed from the time domain to the frequency domain, in order to analyse the frequency resonance response. This process was then repeated for soft tissue simulation using water mixed with 0.9% Natrium-Saline (NaCl), in order to examine the possible signal damping effects. The study's findings showed that acoustic emissions could give a distinctive visual (frequency response) fingerprint for the different stem conditions (air and water surrounding medium), using frequencies up to 20 kHz, based on visual observation. However, this study did not show how the (frequency response) fingerprint could be utilised to distinguish between different implant stability conditions. Thus, another cadaveric study [122] was conducted by the same group, attempting to answer this question. The experiment measured the acoustic frequency resonance response of different stem conditions (secure and loose) and fixation (cemented and cementless), in a 65 year old female cadaver. Measurements were obtained by a microphone attached to the lateral femoral condyle during impact excitation. Then, through spectral analysis, the frequency resonance responses were examined for the different simulated conditions. The general observation was that loose conditions cause an overall resonance amplitude reduction with more reduced frequency peaks when compared with the secure condition. It was concluded that acoustic monitoring of the frequency resonance response may have the potential to be a clinical tool for THA stability assessment [122].

Another series of studies [7, 23, 100, 121, 157-164] examined a new acoustic-mechanical approach, replacing the electromagnetic shaker external excitation with an oscillator integrated in the prosthesis, which could be excited externally. The oscillator was made up of a flat steel spring with a magnetic spherical body attached to its end (Figure 2-23). The oscillator was externally excited through an external coil causing it to strike the prosthesis internally. This caused the implant to vibrate, which was subsequently measured by an external sensor. They experimented with different output parameters, such as oscillation time, velocity after impact, and frequency resonance response. The oscillation time is the period needed for the magnetic body to become stationary, which was shown to be greater for the loose condition than the secure condition [121]. The reflected oscillator velocity (first negative maximum amplitude after the oscillator impacted) also displayed a similar pattern, with the secure condition having the lowest reflected velocity, while the loose implant had the highest [160]. The frequency resonance parameter was found to have positive correlations with the system reducing stiffness (due to loosening) and the overall frequency resonance reduction, through animal experiments and finite element modelling studies [7, 100, 157, 163]. However, altering the implant inner structure could have potential effects on the biomechanical properties. This was not explored by the group, indicating the need for further study in this area [5].

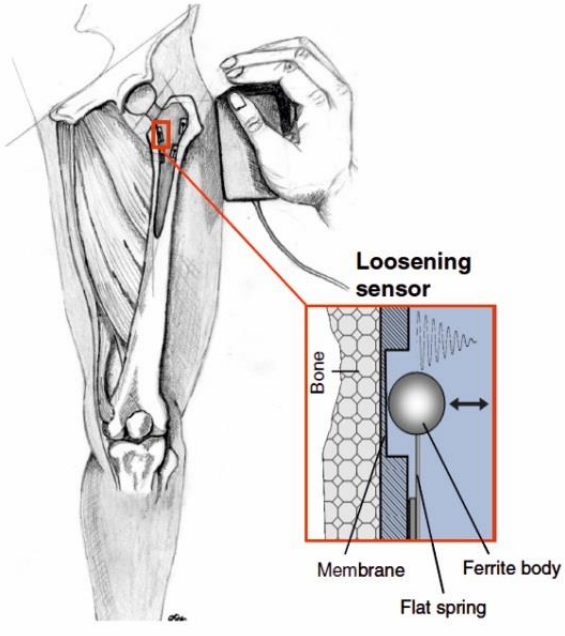

Figure 2-23: The acoustic-mechanical methods concept diagram, source [121].

Intra-Operative

The best osseointegration results go hand in hand with success of the initial implantation of the prosthesis. However, surgeons tend to rely more on their experience than precision instruments in such operations. Press-fitting of implants is a common practise in the insertion of cementless prostheses, which are preferred for young active patients. Yet, the degree of the mechanical stability achieved with a press-fit could determine the operation success rate and long-term outcomes. An insufficient press-fit could lead to loosening and too much could cause bone fracture. Consequently, a number of research groups have investigated the possibility of measuring the initial stability of the implant during the intra-operative stage, in an attempt to provide surgeons with better real-time assessment tool of implant stability. Some of these studies focused on measuring micromotion caused by an applied torque [165, 166] while others used vibration analysis [167-170].

Initial attempts to assess intraoperative implant stability were based on the measurement of the initiated torque applied by the surgeon, relating the applied torque to the results of micromotion [170]. High implant/bone shear micromotion has been shown to be related to high hip torsion movements that are part of usual daily activities, such as chair raising or stair climbing, where the normal torsion range is between 15 and 29 Nm [166, 171]. Osseointegration between the implant and bone surface has a desired micromotion ≤ 40 μm up to 150 μm, but if more soft tissue could be generated, leading to loosening [172, 173]. Harris *et al.* [165] carried out one of the earliest studies of the assessment of intraoperative implant stability. They suggested using a torque wrench micrometre. This would give surgeons a tool at their disposal to quantify their applied torque for the first time, rather than relating it to personal intuition. However, this study lacked crucial information regarding the repeatability and accuracy of the tool [166]. In another study, Cristofolini *et al.* [166] developed a system to measure the intra-operative stability of cementless implants . A lot of attention was given to the design of the system ensuring its accuracy, serialisability, user-friendly nature, size variability, and the ease of saving and retrieving data and programmability. Other studies [167, 170] found this methodology to be relatively complicated for clinical use.

Lannocca *et al.* [167] were the first to validate an intra-operative system based on vibration analysis for the purpose of measuring initial implant stability. The aim was to give the surgeon a tool to guide the optimal press-fit, by use of the resonant frequency measurement. In their *in vitro* test, they measured the resonance frequency at selected frequencies before,

during, and after the external torque was applied. For the loose condition simulation, a torque lower than 15 Nm was applied, while it was applied for an extended period using a handle with a lighting gauge for identifying the secure condition. Excitation was conducted in the range 1200Hz-2000Hz using a piezoelectric vibrator, while simultaneously an accelerometer was utilised to examine the amplitude response and the highest frequency peak shift. Both the excitation and measurement systems were embedded with the torque meter system. The preliminary findings correlated with those of Georgiou and Cunningham [9]; relating the secure implant to a single peak amplitude response while the loose condition has several responses peaks. Also, the unstable implant response displayed a shift of the highest peak towards the lower frequencies, in addition to a reduction in amplitude, as illustrated in Figure 2-24. However, the threshold for discrimination between the conditions was not provided for the torque applied in relation to the micromotion and frequency resonance response; showing the need for more clinical studies. Subsequently, clinical *in vivo* [168-170] and finite element studies (FES) [14, 171] have been conducted, all exploring the preoperative aspect and attempting to answer these threshold questions. They have stated that a protocol based on a change in frequency response measurement could be used to guide surgeons for the optimal end point for stem insertion [168, 169]. They specify that surgeons applying torque leading to <5 Hz resonance frequency shift always lead to micromotion < 150 μm, which could be used as a potential threshold [170]. The relation between the surgeons' applied torque and resulting micromotion was also examined with a finite element study [171] reaching a close experiment and model results, showing the micromotion measurements for the torque range (0-11.4 Nm), as illustrated in Figure 2-25. Also, another FES [14] agreed with the previous studies; showing that, as the implant/bone contact increases, the frequency response shifts positively and the stem proximal contact change has the most effect on the frequency response.

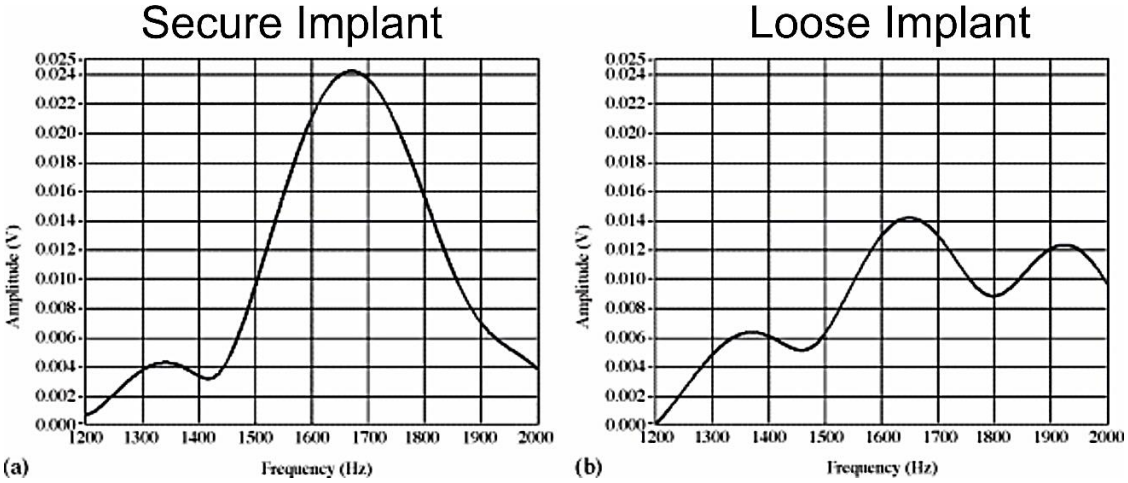

Figure 2-24: The frequency response of two of the simulated conditions, a) stable (with micromotion reading of 20 µm) and, b) unstable implant (with micromotion reading of 200 µm), source [167, 170] with permission.

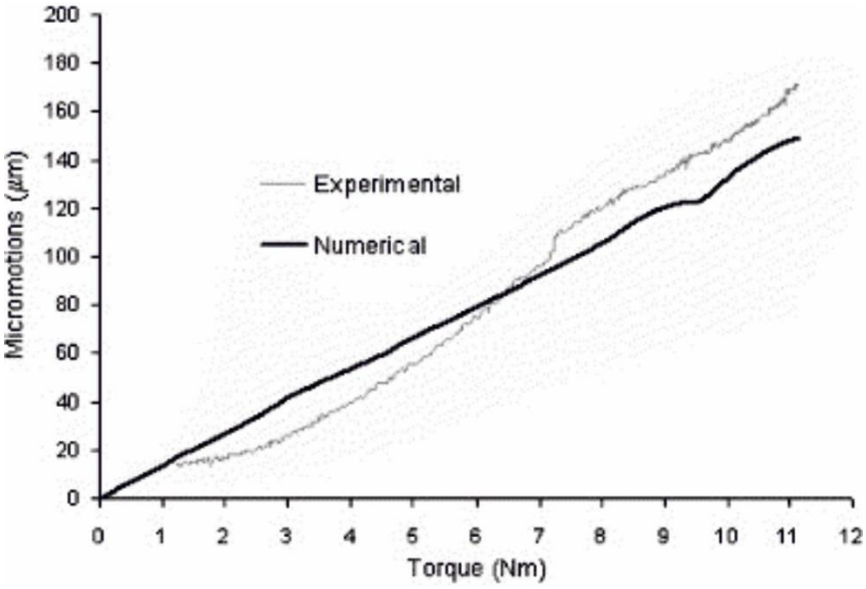

Figure 2-25: The applied torque and micromotion relation for the experimental and finite element model, source [171] with permission.

Other intraoperative studies [174-178] have focused on the acetabular cup initial stability. They have attempted to find a quantifiable variable, such as impact duration[5] [174], impact momentum[6] and pull out force [175-178], which could be correlated to the cup biomechanical primary stability. The impact duration and momentum reached a steady state by the fifth impact (3.5Kg mass drop, 4cm amplitude) [174, 175]. The maximum impact

5- Impact duration: time between the start and end of the applied force (impact) with threshold (30N).

6- Impact momentum: Integral of force with time.

momentum and pull out force reading was obtained for the 1mm interface fit (cavity diameter was 1mm less than the cup diameter) [176-178]. A finite element study aimed at evaluating acetabular cup initial stability was also conducted based on resonance frequency principles [179]. Comparing the model results with six male cadavers' specimens, the frequency range was 500Hz-3000Hz sine wave, while the output was visualised utilising the FFT power spectral. The main finding was that stable cup condition frequency response demonstrated higher density compared to the unstable condition. Concluding, that power spectrum could, therefore, hold valuable information about the absolute stiffness of press-fit implant [179].

Finite Element (modelling)

Several finite element studies (FES) have explored the potential of vibration analysis in the orthopaedic field. Quite a few have focused on the pre-operative aspect [14, 22, 171, 179], which has been elaborated on previously. Others have explored post-operative aspects, either for loosening [13, 180] or osseointegration [15, 142] assessment.

Loosening

Various degrees of stem loosening were simulated in two FE studies [13, 180] with the aim of defining the minimum detectable threshold and testing how much vibration can reveal with regards to the different loosening levels. They observed that, as the implant-bone failure (loosening) takes place, the THR system stiffness decreases. This affects the system's natural frequency and causes a reduction in the resonance frequency response [13, 180]. Reduction in stiffness was hypothesised to be driven by the size and location of the loosening [13]. Qi *et al*. (2003) defined one-fifth of the stem loosening to be the detectable threshold, while stressing the difficulty of detection of central region failure, regardless of the loosening level. Proximal loosening (when ≥ ½ stem length) has shown to be more sensitive than distal failure, due to the greater mass and surface contact for the proximal region. The loosening indicators used were the harmonic shift, phase angle and amplitude in the frequency spectra. Also, different frequency bands were highlighted as follows: dead/blind (<500Hz), less sensitive (500-1500Hz), sensitive (1500-2500Hz), and highly sensitive (>2500Hz) [13]. Despite these findings, further clinical validation data was not carried out, making the results inconclusive.

Osseointegration

The effect of the cementless stem bonding (osseointegration) process on the resonance frequency response has also been explored using a FES [15]. This was possibly due to the phenomenological interface model mimicking the osseointegration mechanical effect. The osseointegration simulation began in week one, whereby the implant-bone was debonded with no loading, followed by 25 weeks of daily healthy activities. The imitated daily activity included four loading conditions; walking, standing, stair climbing and resting, with different load forces and cyclic number configurations. Resonance frequency analysis was conducted at the end of each week for stability assessments. They observed that as the simulation progressed, the implant-bone interface increased, increasing the system stiffness, and increasing the resonance frequency in the form of high frequency mode values, as illustrated in Figure 2-26.

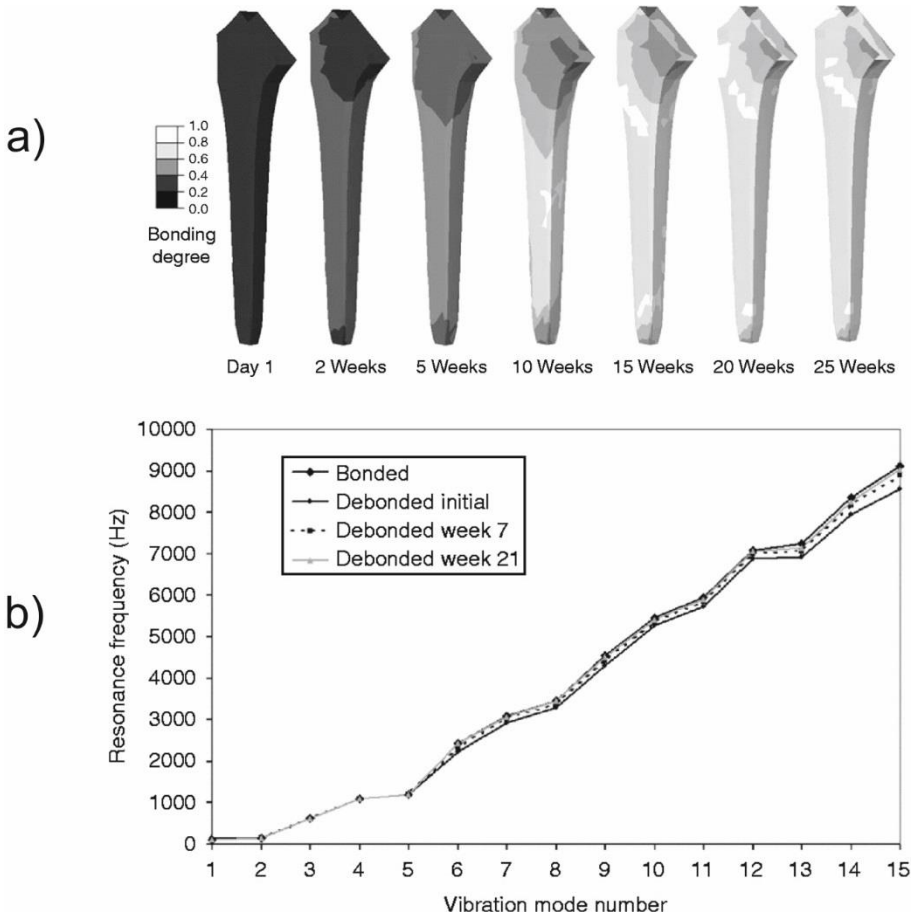

Figure 2-26: The FES cementless stem osseointegration simulation (a) stem-bone bonding process during the 25 weeks, b) the resonance frequency values during the simulation, source [15], with permission.

Acetabular Cup Component

Despite the fact that acetabular cups have a higher revision rate over femoral components, according to various national registries [17-21], the majority of the existing vibrometry loosening diagnostic literature [6, 9-13, 22, 23] is stem related. Others have explored the detection of acetabular cup loosening [5, 8, 9, 16] and were able to distinguish it from the stable condition, but without defining the loosening level detected.

Georgiou and Cunningham [9] were the first to explore the viability of vibrometry in the detection of acetabular cup loosening through an *in vivo* clinical study. The study attempted to characterise the loosening of the different THR components, giving each a specific loosening criteria. The femoral loosening criteria was discussed earlier in the femoral loosening vibrometry studies section. The criteria given for the distinction between the loosening components were as follows: number of resonant frequencies, the amplitude of the first harmonic, the amplitude of the second harmonic, the average amplitude of the remaining harmonics, and the number of the remaining harmonics. These amplitudes were all compared after being related to the fundamental frequency. This vibrometry study was the first to use the harmonic fundamental frequency ratio as a criteria for loosening detection. The study compared the outcomes of the vibrometry diagnosis with the conventional radiology method, reaching the conclusion that vibrometry was a reliable method for the stem component but less favourable for the acetabular component. Only 50% of the loosening cups were detected using vibrometry. They suggest that the unsuccessful acetabular cup loosening could be due to the location being further away from of the source of vibration.

Tudor *et al.* (2008) conducted the first small scale experimental study on acetabular cup loosening [16]. A Sawbones hemi-pelvis was used to create variable loosening conditions (loose, tight fit and intermediate), using three screws holding the cup. The cup was declared to be loose when there was no screw fixation. Two screw fixations resulted in intermediate loosening and all three screws resulted in the tight fit condition. The input excitation sinusoidal signal range was between 200Hz and 800Hz. Doppler ultrasound was used as a measurement method having the specimen in a water bath for soft tissue mimicking purposes. Due the small sample size (three measurements for each condition, n=3), the results were not conclusive. However, they stated that a signal pattern was observed as loosening progressed when compared to the secure condition. This was possible through the

visual examination of the spectral analysis through FFT analysis. The loosening conditions resulted in more harmonics and noisy signal outputs, much more than the secure condition. They also emphasised the need for future studies to pay more attention to the loosening simulation, in order to create a more realistic scenario.

Rieger *et al*. (2013-2015) were the next to explore the reliability of vibrometry in the detection of complete THR (stem and cup) loosening. They aimed to distinguish between the two loose components. Stem loosening was replicated by using a smaller stem size, whereas cup loosening was replicated with an abraded cup exterior surface for both studies [5, 8]. Initially, Rieger *et al*. (2013) tested a complete Sawbones hip model, replicating different stem and cup loosening conditions. The main finding was that loosening of the two components can be distinguished through relating each to a specific frequency detection zone with a specific analysis approach (peak shift, integral analysis, and frequency peak count). The peak shift was found to be the most reliable in detecting loosening, followed by integral analysis for stem loosening. The frequency peak count revealed more detail about acetabular loosening [8]. In a subsequent study, Rieger *et al.* (2015) [5] attempted to refine the vibrometry approach by proposing a shockwaves excitation system, in order to eliminate the need for mechanical excitation, which can cause patients discomfort when used in the diagnosis process. The aim remained the same; replacing the initial sawbone models with cadaver specimens and exploring different excitation locations (lateral condyle, greater trochanter and ilium crest). The lateral condyle excitation resulted in no significant differences. Between the trochanter and the ilium locations, the clearest different was achieved with excitation at the ilium crest and the accelerometer reading located at the trochanter. Isolated stem loosening and the combined stem cup loosening did show a significant response shift in the frequency range 386Hz to 847Hz. Isolated acetabular cup loosening did not show a statistically significant shift; leading to the conclusion that distinguishing between the individual THR loosening component remained a challenge, even with the use of the novel excitation system.

2.4.2.3 Soft Tissue

Soft tissue consists of different layers with their own dynamic properties that need to be examined in order to understand their effects on measurements. Soft tissue comprises arrangements of skin, muscles, tendons, ligaments, fat, nerves, blood vessels, and synovial membranes. Thus, the characteristics of soft tissue will be the combination of all of these various elements. Soft tissue properties are not constant and are vulnerable to different influences that can dramatically change their characteristics. These influences include age, health, state (*in vivo, in vitro*), loading and body location [181]. Therefore, the next sections will consider soft tissue properties, effects, and substitutes.

2.4.2.3.1 Soft Tissue Acoustic Properties

The study of soft tissue properties is important in order to quantify the effect it has on measurements and to produce more realistic substitutes. The main properties to be considered are the speed of sound, acoustic impedance, attenuation coefficient, backscattering coefficient, nonlinearity parameters, longevity, Young's modulus, and temperature [181-183]. Firstly, the speed of sound varies according to the tissue's thickness. Secondly, the acoustic impedance can be calculated from the material density and speed of sound. Thirdly is the signal strength reduction, also known as attenuation coefficient. Fourthly, the backscattering coefficient refers to the reduction caused by scattering. Fifthly, the nonlinearity parameter describes the material's nonlinearity behaviour. Sixthly is the period of time over which materials can sustain a constant acoustic property, known as longevity. Seventhly, the material elasticity, which is usually represented by Young's modulus. Lastly, temperature, whereby acoustic properties are usually stated at normal room temperature (25˚C). These properties are of varying importance depending on the measurement and experiment aims; thus, not all properties are always reported in the literature [184]. Some of the acoustic properties for different human tissue are illustrated in Table 2-7.

Table 2-7: The Acoustic prosperities of some of the soft tissue components, source [181].

Material	Velocity(m/s)	Density (kg/m3)	Attenuation (dB/cm MHz)	Acoustic Impedance (MRayl)
Air	330	1.2	-	0.0004
Blood	1584	1060	0.2	1.68
Cortical Bone	3476	1975	6.9	7.38
Connective Tissue	1613	1120	1.57	1.81
Trabecular bone	1886	1055	9.94	1.45
Muscles	1547	1050	1.09	1.62
Tendon	1670	1100	4.7	1.84
Soft tissue (Average)	1561	1043	0.54	1.63
Water	1480	1000	0.0022	1.48

2.4.2.3.2 Soft Tissue Effect of Vibration Measurement

More significant information about the influence of soft tissue (skin, muscles, ligaments, joints) on natural resonant frequency was found in the literature regarding long bone properties. These studies examine the effect of skin stiffness variation, preload conditions [185-189], muscle, ligament, and joint [190-195] effects on the natural resonance responses of long bones (tibia or ulna). The results revealed that the effect of the skin on obtaining measurements is very low compared to muscles and joints [192-194]. For example, in the case of the tibia bone, the absence of soft tissue (skin, muscles, and ligaments) has the effect of increasing the natural frequency measurement by up to 5-18% [190, 192].

2.4.2.3.3 Soft Tissue Substitutes

Since the early 1960s, tissue mimicking substitutes have been used for ultrasound imaging calibration and training purposes. Generally, most of these mimicking materials have isotropic and homogenous structures and properties, although more complicated structures are commercially available. Substitutes have the advantages of tailored acoustic properties, dimensions, and internal features. Conversely, commercial substitutes are often expensive and designed for specific applications. Thus, customized projects that require more specific features and reduced costs are usually fabricated and designed in labs. Substitute materials can be made into hard tissue or soft tissue. Hard tissue mimicking materials often represent

cortical bone, trabecular bone and dental enamel. Soft tissue substitutes mimic muscles, tendons, ligaments, fat, nerves and blood vessels [181].

Ongoing research has led to the continuous introduction of different soft tissue materials in attempts to achieve ultimate tissue characteristics. Water and water-based substitutes were among the early mimicking materials that are still preferred for their simplicity, transparency, and usability. However, they have some shortcomings, such as lower attenuation coefficient and lower speed of sound compared to soft tissue, and they are strongly temperature dependent. Nevertheless, reports have shown that the speed of sound can be enhanced to 1540m/s when ethanol is added (7.4% by mass) [181], and glass beads or graphite powder can provide the desired characteristic for the attenuation and scattering [183]. Also, other materials have been introduced, such as gelatine, agarose, and silicone, to achieve better soft tissue mimicking structures (more materials and their acoustic properties are shown in Table 2-8) [181, 183].

Table 2-8: The acoustic properties of hard and soft tissue substitutes, source [181].

Hard Tissue			Soft Tissue	
Material	Tissue	Velocity (m/s)	Material	Velocity (m/s)
Acrylic	Cortical Bone	2500	Agarose-based	1498-1600
Carbone Fibre Plastic	Cortical Bone	4400	Gelatine-based	1520-1650
Ebonite	Cortical Bone	2200	Magnesium Silicate-based	1458-1520
Epoxy	Cortical Bone	2740-3168	Oil Gel-based	1480-1580
Perspex	Cortical Bone	2657	Open Cell Foam-based	1540
Epoxy	Trabecular Bone	1844-3118	Polyacrylamide Gel-based	1540
Polyvinyl Chloride	Whole Bone	2300	Tofu	1520
Dental Composite	Dentin	3306	Water-based	1518-1574

2.5 Literature review summary

A detailed review of the literature provides a better understanding of the different development stages and trends that have characterised the history of total hip replacement. Leading to the reasoning of the current stat of the art fixation methods, component types, materials selection, failure factors and diagnostic techniques. Existing literature, along with the annual reports of national joints registries, were utilised to follow these different development stages; placing them in a historical context.

Vibrometry has been proposed as an alternative, more sensitive method for THR loosening diagnosis. Despite the fact that acetabular cups have a higher revision rate over femoral components, most of the existing literature is stem related. Also, the limited acetabular cup studies only examined late loosening scenarios.

Literature review summary in points:

- ✓ THR demand is growing, particularly within a younger and active patient group [53].
- ✓ Aseptic loosening is the primary reason for THR revision [46, 84].
- ✓ Imaging techniques are the primary diagnostic and follow-up method, but shown to be unreliable for early loosening detection [5-7].
- ✓ New diagnostic techniques have been developed and proposed on the basis of non-destructive testing (NDT), such as vibration analysis (vibrometry) [100].
- ✓ Vibrometry can distinguish implant instability (loosening) through the frequency spectrum of the response signal and by referring it to the vibrational response of the secure case [6].
- ✓ Despite the fact that acetabular cups have a higher revision rate over femoral components [17-21], the majority of the existing vibrometry loosening diagnostic literature [6, 9-13, 22, 23] is stem related.
- ✓ Attempts have been made in the literature [5, 8, 9, 16] to examine cup loosening. These studies were able to detect late cup loosening, but did not specify the earliest detectable threshold, which this study is attempting to address.

Chapter 3 – Aim and Objectives

3.1 Aim

Vibrometry has been proposed as an alternative THR implant loosening non-invasive diagnostic technique, which attempts to overcome the current technique's limitations [6, 8]. Vibrometry has been applied in different lower limb orthopaedic related studies; mainly in implant intra-operative assessment [165-170, 174, 175, 196], osseointegration assessment [128, 135, 141, 142] and in loosening diagnoses [8-12, 14, 22]. The acetabular cup component revision rates are higher than the stem component rates in accordance with various national registries [17-19]. Yet, the majority of the existing vibrometry loosening diagnostic studies [6, 9-13, 22, 23] have been stem related and a limited number [5, 8, 9, 16] have examined cup loosening without defining the loosening level detected. Thus, the aim of this project is to investigate the viability of vibrometry for accurately detecting early acetabular component loosening.

3.2 Research questions

- Can THR acetabular component loosening be detected using the vibrational analysis method?
- What is the earliest loosening phase that can be accurately detected?

3.3 Research objectives

The objectives of the study, which help to the answer the research questions, were to develop a series of case studies that varied in complexity. Initially, these case studies involved testing the concept using a simplified set-up with minimum boundary conditions. Thereafter, they increased in complexity. These case studies could be grouped under three objectives, as follows:

Objective -1 Development of acetabular component loosening using Sawbones® blocks.
Objective -2 Development of acetabular component loosening using a Sawbones® Hemi-pelvis.
Objective -3 Development of acetabular component loosening using a Sawbones® Femoral and Hemi-pelvis composite bones.

1. Development of acetabular component loosening using Sawbones® blocks

The first step in the accurate interpretation and understanding of the vibration analysis of the acetabular cup component is to reduce the elements involved, such as muscles and ligaments, in an attempt to reduce the source of measurement errors. Thus, the first stage involves an acetabular cup and simplified controlled Sawbones® polyurethane solid foam, in order to create various loosening scenarios. The case studies that follow under this objective were, as follows:

- First case study - Late spherical (2mm and 4 mm) loosening.
- Second case study - Early spherical (1mm) loosening.
- Third case study - Early zone (1&2, 1&3, and 2) 1mm loosening.

2. Development of acetabular component loosening using a Sawbones® Hemi-pelvis

The second objective was the development of loosening model using a Sawbones hemi-pelvis fitted with an acetabular cup. This attempt to accommodate the complex geometry of the hemi-pelvis bone and observe the effect on the loosening detection using vibrometry. Thus, a Sawbones hemi-pelvis was utilised to house the simulated two loosening situations. They were two spherical loosening levels (1mm and 2mm) that was compared to a secure condition (1mm press-fitted). The 1mm spherical loosening could be attributed to early loosening while the 2mm to the late stage. More clarification of the set-up of this stage and the means of measurement will follow in Chapter 6.

The second objective case study:

- Fourth case study – (Early and late) hemi-pelvis spherical cup loosening

3. Development of acetabular component loosening using a Sawbones® Femoral and Hemi-pelvis composite bones

This stage was an attempt to create a more clinically relevant experiment through the development of acetabular cup loosening using the Sawbones femoral and hemi-pelvis composite bones. The previous four case studies used an excitation position that was much closer to the acetabular cup than would be clinically possible, using the non-invasive approach. Thus, the femoral composite bone was add to reflect a more realistic scenario where the excitation source is placed on the lateral femoral condyle as initially suggested by Rosenstein *et al.* [10]. The simulated loosening condition were; 1mm press-fit (secure), 1mm and 2mm spherical loosening. Further explanation of the set-up and measurement methods will follow in Chapter 7.

The third objective case study:

- Fifth case study – (Early and late) femoral and hemi-pelvis spherical cup loosening.

Chapter 4 – Research Methodology

4.1 Introduction

The hip joint can withstand cyclic loading equivalent to three times the human body-weight [25] which makes it more vulnerable to damage than many other joints. Due to the joint's location and function, in some cases any damage could eventually leave patients with unbearable pain and consequently a constriction in their mobility. Total hip replacement (THR) is a human intervention which has the aim of pain relief and function restoration. THR has come a long way since it was introduced by Charnley in the early 1960s, and was nominated as the operation of the century [1]. The high success rate of the THR procedure has contributed to its rapid increase in use, reaching one million operations annually worldwide [41]. Despite these numbers about 4-10 % of all implants are expected to fail in their first decade [3, 95], mostly due to aseptic loosening, which has been identified as the primary THR failure factor since 1979 [4]. When analysing the THR failure factors, it becomes clear how important diagnostic techniques are in orthopaedics.

Early and accurate diagnosis is of crucial importance for both patients and healthcare providers, because this reduces patient discomfort and disability, while also reducing physicians' misused time and costs. The diagnosis approaches are generally categorised into two groups; conventional imaging and non-imaging approaches. Imaging diagnostic techniques are the mostly widely used due to their availability and cost effectiveness [102]. Also, they are used as one of the main post-operative follow-up procedures [86]. The radiology criteria for THR loosening include component position, alignment and the presence of a radiolucent line. For example, more than 2-mm radiolucent line thickness could indicate a loose or migrated component [101]. Some limitations and shortcomings are evident in the conventional imaging methods of diagnosing prosthesis loosening. Even with a sensitivity and specificity of up to 80%, a revision operation on a perfect hip endoprosthesis may still be possible [121]. Consequently, new techniques have been further developed and proposed on the basis of non-destructive vibration analysis testing which is well established in some industrial fields, such as the aerospace and automobile sectors [122].

This Chapter is intended to explain the methodology of vibration analysis (Vibrometry) in acetabular cup loosening detection. This includes the excitation system, measurement techniques and data analysis methods.

4.2 Vibrometry concept in detecting loosening

Vibrometry has been applied in different lower limb orthopaedic related studies, mainly in implant intra-operative assessment [165-170, 174, 175, 196], osseointegration assessment [128, 135, 141, 142] and in the loosening diagnosis [8-12, 14, 22], as previously explored in Chapter 2. Vibrometry attempts to detect the loosening of orthopaedic implants using a non-invasive vibration analysis technique [9]. Although the acetabular cup component revision rates are higher than the stem component in according to various national registries [17-19]. The majority of the existing vibrometry loosening diagnostic studies [6, 9-13, 22, 23] were stem related and a limited number [5, 8, 9, 16] examined cup loosening without defining the loosening level detected. Thus, the aim of this project is to investigate the viability of vibrometry for accurately detecting early acetabular component loosening.

Vibrometry is best explained using the first two clinical *in vivo* pilot studies [9, 10] that were attempted to differentiate between loose and secure femoral implants using this technique. In these studies patients were placed on their sides (laterally) and were then exposed to an input sinusoidal signal with a frequency sweep range of 100 to 1000Hz. A mini shaker was placed on the lateral femoral condyle to generate the excitation, while the output signal was measured using an accelerometer located on the greater trochanter (Figure 4-1: a and b). In the Georgiou and Cunningham [9] study the mini-shaker was placed at 90° to the femur, while patients were encouraged to relax and avoid any muscle tension that may affect the signal (Figure 4-1b). In both studies frequency analysis of the recorded signal was conducted using a spectrum analyser for both the intact and loosened conditions. Then, by visual observation they pointed out that the frequency spectrum of the loose conditions has higher harmonic numbers and magnitudes than the intact spectrum, as seen in (Figure 4-2 a and b). Also, it was noted by Rosenstein *et al.* [10] in their *in vitro* study that these extra harmonics were more prevalent near the natural frequency of the cadaveric femurs; more details are available in Chapter 2.

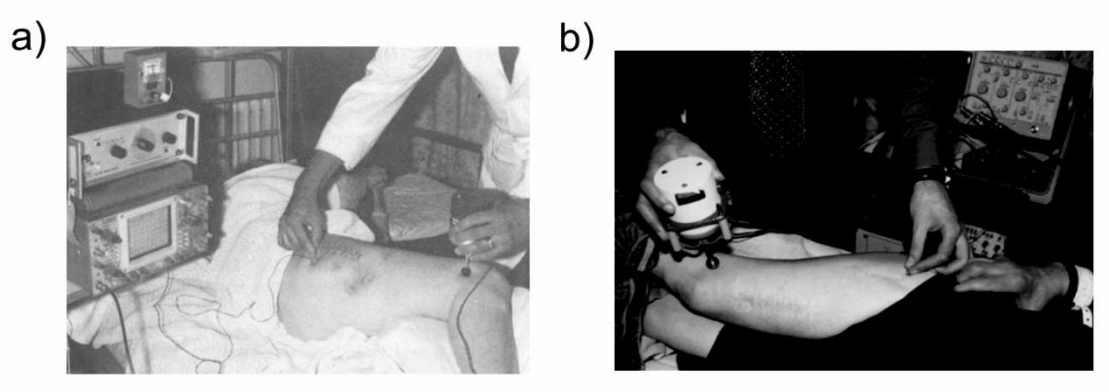

Figure 4-1: The patient setup under vibrometry assessment; A) Rosenstein *et al*. [10] with permission, B) Georgiou and Cunningham [9]with permission.

Vibrometry characteristic of defining THR loosening was defined in the two clinical studies [9, 10]. These studies implied that loosening of the THR affects the mechanical properties of the system, which then is reflected in the presence of an extra number of harmonics. These harmonics can be observed using either the frequency amplitude responses or frequency spectrum analysis [9, 11].

Frequency spectrum analysis was the first reported method for observing the distorted waveforms caused by implant instability [10]. If the implant system was exposed to a sinusoidal wave excitation a secure condition would respond in a linear manner with a single peak in the frequency domain. While the loose condition responds nonlinearly with more peaks in the frequency domain, as observed in previous clinical *in vivo* [9, 10] and *in vitro* [11, 12] studies, as seen in Figure 4-2. The suggested parameters for loosening detection using spectrum analysis were put forward in the Georgiou and Cunningham [9] clinical study as follows: First harmonic amplitude, second harmonic amplitude, remaining harmonics number, remaining harmonics amplitude average and the ratio between harmonics and the primary frequency.

The frequency amplitude responses were the second method described to indicate THR loosening using vibrometry [9, 11]. The amplitude response of any targeted system is plotted against the driving frequency range [197], where each system has a unique response as a vibration signature and can be used as a reference for any future testing. Such a monitoring technique could hold valuable information on any system's mechanical properties and assembly, and give a highly reliable indication of the system unbalance, loosening or misalignment [197]. The method's parameters for loosening were defined by the number of resonance frequencies, where loose implants would have more resonance frequencies than

the secure implant, according to Li *et al* [11] in *in vitro* testing and asserted by the Georgiou and Cunningham [9] in a clinical study; see Figure 4-3. Also, shifting of the resonance frequencies is another method that has been observed in other studies [6, 8, 13]. However, any THR system amplitude response requires a range of excitation frequencies to elicit the response, which can potentially cause patients to experience discomfort [163].

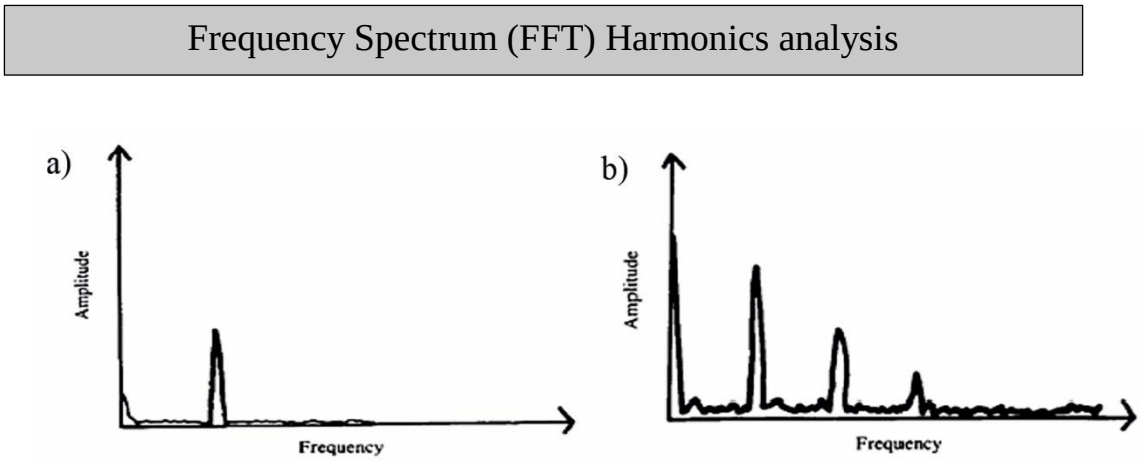

Figure 4-2: Rosenstein *et al*. [10] clinical study results for the secure implant (a) and for the loose condition (b), with permission.

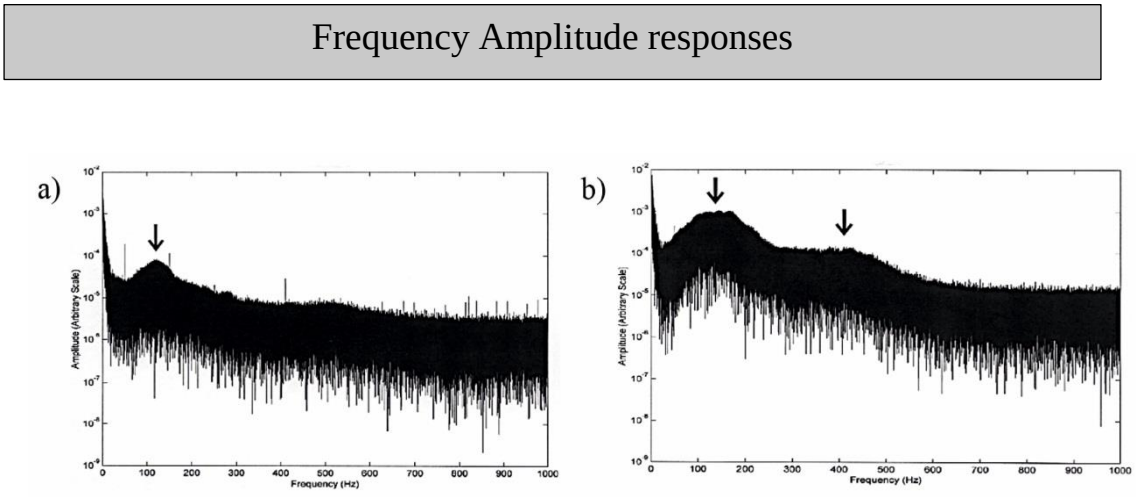

Figure 4-3: Georgiou and Cunningham [9] clinical study results for the secure implant (a) and for the loose condition (b), with permission.

In this study, frequency spectrum analysis was the main method adopted for loosening detection, through the quantification of the harmonics' magnitudes and their ratio to the primary (fundamental) frequency. This was selected over the number of resonance

frequencies parameter because a frequency sweep is not required. Thus, a single frequency excitation and it response should be enough to characterise a loose condition using observation of the primary frequency and related harmonics, as illustrated in Figure 4-4. Still, to be able to define the best excitation frequency a sweep would initially be required to find the optimum frequency for the vibrometry diagnosis. [198]

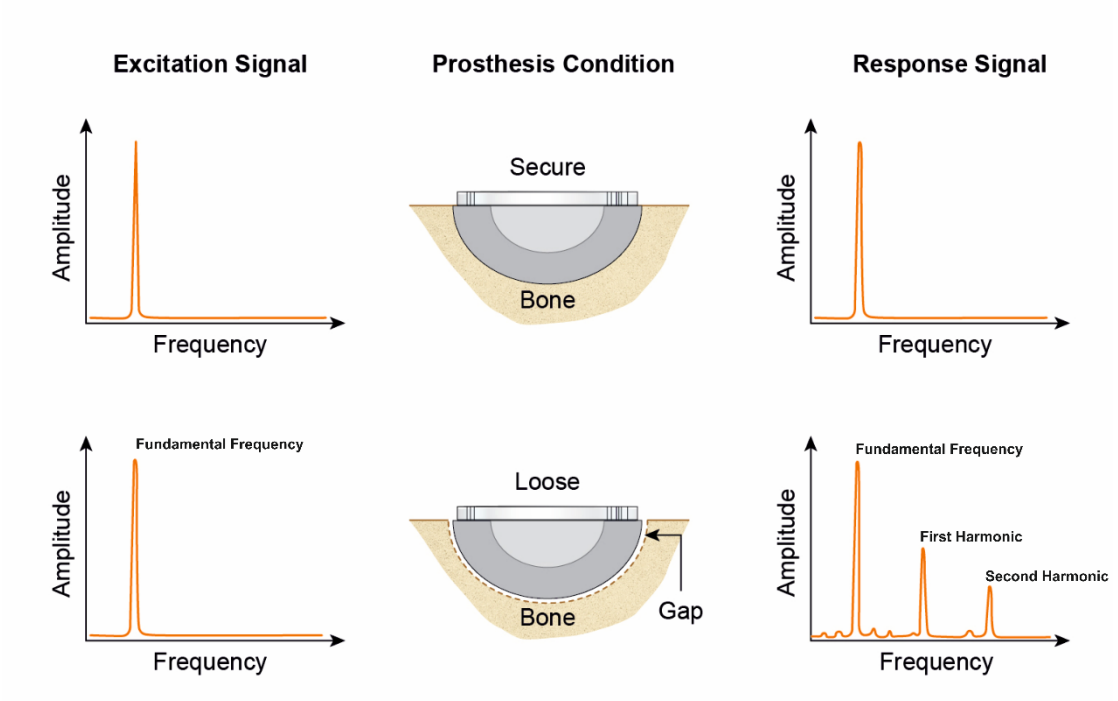

Figure 4-4: Frequency Spectrum Analysis concept in detecting Acetabular cup loosening, source [194], with permission.

4.2.1 Study Design

In order to achieve the study aim of investigating the viability of using vibrometry in the accurate detection of acetabular cup loosening, it was necessary to develop a series of case studies that varied in complexity. Initially, these case studies involved testing the concept using a simplified set-up with minimum boundary conditions. Thereafter, they increased in complexity. These case studies could be grouped under three objectives, as illustrated in Figure 4-5.

The first objective was the detection of acetabular cup loosening utilising a simplified controlled Sawbones® polyurethane solid foam. This objective included three case studies that mimicked radiolucent line loosening at different levels; late and early spherical loosening and early zone loosening. Late spherical loosening was replicated using a 2-mm and 4-mm gap, while the early loosening case had a 1-mm spherical gap. Early zone loosening condition was a 1 mm thickness gap that was zone specific. Further explanation and justification of these scenarios' setups will follow in the next Chapter 5.

The second objective was an attempt to accommodate the complex geometry of the hemi-pelvis bone and observe the effect on the loosening detection of the vibrometry. Thus, a Sawbones hemi-pelvis was utilised to house the simulated two loosening situations. They were two spherical loosening levels (1mm and 2mm) that was compared to a secure condition (1mm press-fit). More clarification of this objective will follow in Chapter 6.

The third objective was the development of a Sawbones femur and hemi-pelvis acetabular cup loosening. The use of the femur reflects a more realistic scenario where the excitation source is placed on the lateral femoral condyle as initially suggested by Rosenstein *et al*.[10]. The simulated loosening condition were; 1mm press-fit (secure), 1mm and 2mm spherical loosening. Further explanation of the set-up and measurement methods will follow in Chapter 7.

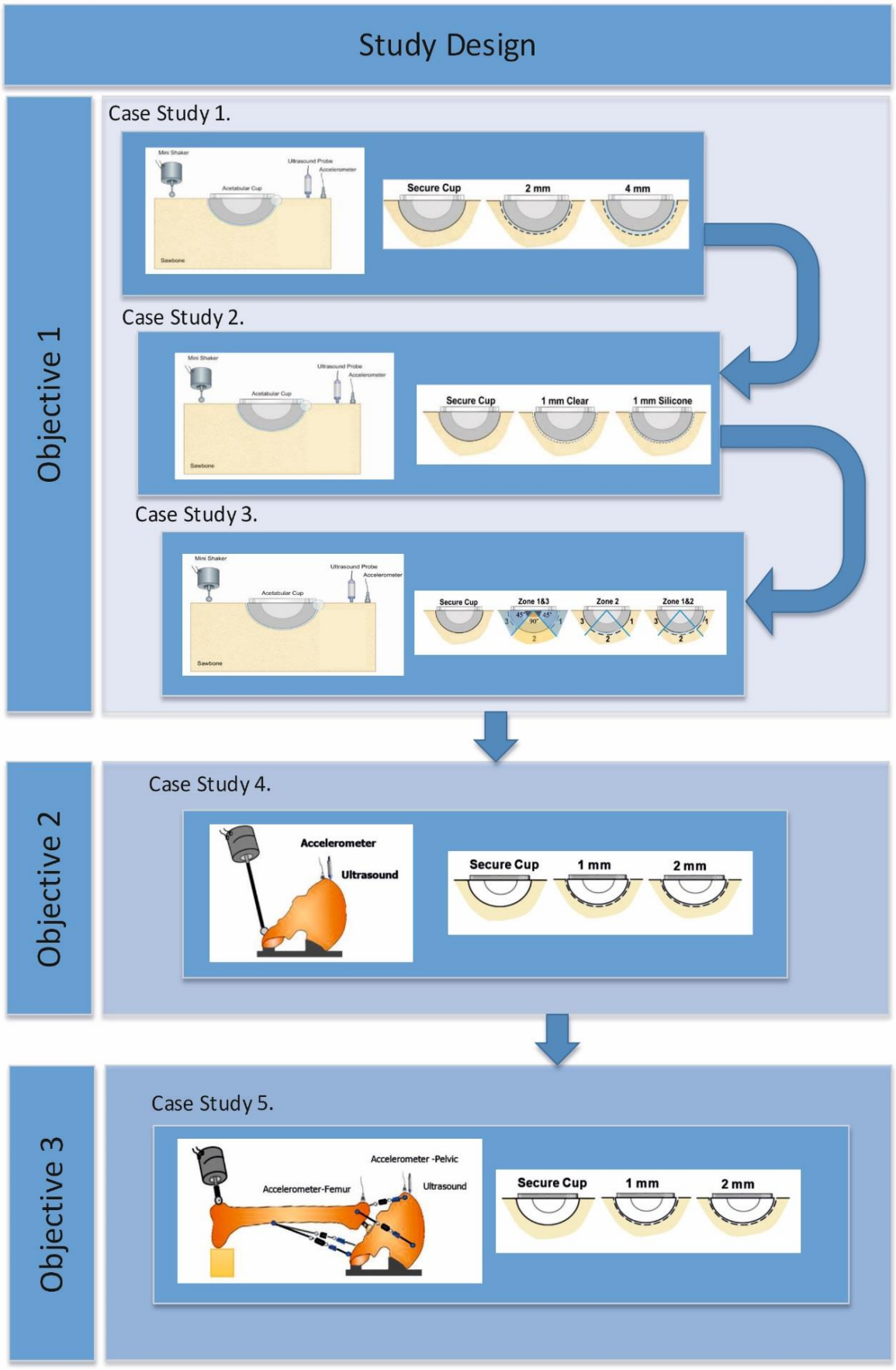

Figure 4-5: The Study three Objectives

4.3 Excitation System

Electromechanical vibrators (mini-shaker) are the most used apparatus in vibrometry studies [8-12] for introducing an input excitation signal to the target system. Characterised as periodical (sinusoidal) deterministic force vibration. Thus, the same method was adopted for the signal excitation for all the different case studies.

This excitation signal is introduced to the targeted system through a 19 mm diameter spherical tip attached to a mini-shaker (V201, Ling Dynamic Systems Ltd, UK). The shaker was driven through a function generator (TG230, Thurlby Thandar Ltd, UK) via a power amplifier (PA25E, LDS Ltd, UK). The excitation signal characteristic was controlled through the function generator options setting, then the signal passes through the power amplifier system with a gain value of one reaching to the mini-shaker system.

The input signal was a sinusoidal wave of constant amplitude, with a defined frequency sweep range for each case study. The selection of each range of excitation frequencies and signal characteristics will be explained and justified accordingly. The input signal to the mini-shaker was verified through the use of a digital oscilloscope (Tektronix TDS 1002) that was connected between the power amplifier and the mini shaker system. This was conducted in order to verify the input signal frequency and amplitude.

The input excitation frequency range was between 100 Hz and 1500 Hz with constant amplitude for the first two case studies, early and late spherical cup loosening. Then was increased to 2500 Hz for the third case study, zone non-uniform cup loosening. Likewise, the fourth (hemi-pelvis) and fifth (femur and hemi-pelvis) case studies had an excitation range between 100 Hz and 1500 Hz. Summary of the case studies' excitation frequency ranges and the signal amplitudes are provided below Table 4-1 .

Table 4-1: The case studies excitation signal

		Frequency Rang	**Signal Amplitude**
Objective 1	First case study	100-1500Hz	3 Volts p-p
	Second case study	100-1500Hz	4 Volts p-p
	Third case study	100-2500 Hz	4 Volts p-p
Objective 2	Fourth case study	100-1500Hz	4 Volts p-p
Objective 3	Fifth case study	100-1500Hz	4 Volts p-p

4.4 Measurement Techniques

The output response signal of the targeted systems was recorded using two measurement methods; an accelerometer transducer and an ultrasound probe. This was achieved using sound and vibration Measurement Labview software. More clarification of the measurement sensors and signal analysis software will follow in the next sections.

4.4.1 Accelerometer

The majority of THR vibrometry studies [5, 10-12, 124, 128, 135] use an accelerometer as a measuring technique due to their availability and reliability. Other studies [8, 145] have used accelerometers as a reference measurement method for proposed new measurement techniques. Thus, to be consistent with other orthopaedic vibrometry studies this study uses an accelerometer as a reference technique to the proposed ultrasound approach. A piezoelectric accelerometer (Model 353B18; PCB Piezotronics Inc, US) sensor was selected for the different case studies, mounting and fixation will be further explained in each case study. In the fifth case study two piezoelectric accelerometers were used for selection of the optimum measurement location. The Piezoelectric accelerometers work on the principle of the piezoelectric effect that when exposed to an acceleration force will generate an electrical output that in proportionate. Great attention was given to the accelerometer coupling, which will be explained in further detail for each case in the set-up section.

4.4.2 Ultrasound

An ultrasound transducer (Mini Dopplex 500 4 MHz, Huntleigh Technology Plc, UK) was used in the measurement of the response signals in addition to the accelerometer measurement method. The ultrasound approach for detecting THR loosening using vibrometry was initially proposed by Rowlands *et al*.[145] in an attempt to overcome the soft tissue attenuating effect. In the two pilot clinical studies [9, 10] the output response signal was measured using an accelerometer firmly pressed onto the greater trochanter. The applied force on the sensor was an attempt to reduce the effect that the soft tissue thickness, overlaying the hip trochanter region, has on the reading and this may also lead to patient discomfort [145]. Thus, the use of Doppler ultrasound allows this issue to be overcome.

The principle of ultrasound in the detection of vibration is realised through the Doppler shift phenomena. The ultrasound probe sends a sound wave with a defined frequency (f_0), which is then reflected from the moving target surface and is received by the same probe with a shifted frequency. The difference between the transmitted and reflected wave frequencies is the Doppler shift (f_D) [199]. The calculation of the Doppler shift (f_D) is conducted through the following equation:

$$f_D = \frac{2 f_0 v}{c} \cdot \cos\theta$$

Where the variables are; V= the speed of the object, C = the speed of the sound in the medium, f_0 = transmitted beam frequency, and θ = the angle between the ultrasound reflected beam and the direction of the object movement [145, 199]. An increased Doppler shift value shows that the system is moving in the direction of the probe and vice versa, like in the example of blood follow. Thus, the ultrasound output signal reading is a voltage which is proportional to the Doppler shift with a sensitivity of 0.5 V/kHz, represented using the frequency unit hertz (Hz). The ultrasound probe is coupled to the target surface using an ultrasonic transmission gel (Aquasonic-100, Huntleigh Technology Plc, UK). This is mainly to prevent any air interference between the probe and the surface, which could cause the reflection of the signal due to the very low air impedance, where 99.9% of the signal would be reflected if air existed [199].

The method of collecting the accelerometer and ultrasound probe data through the different case studies and data analysis method will be further explained in the following sections.

4.4.3 Signal measurement

The output response to the excitation signal was recorded using the dedicated sound and vibration Labview software package (Signal Express, Suite version 11, National Instruments). The signal data was recorded first and then post-processed using the power spectrum analysis tool at a later stage.

The output data from the sensors, accelerometer and ultrasound, was collected using a BNC (Bayonet Neill–Concelman) connector cable to a USB powered data acquisition system (USB-4431, National Instruments). This data acquisition system is the means for the data to be collected and processed by the LabVIEW sound and vibration package. This was realised through the use of a personal computer (Core2Duo 3.16 GHz, CPU 4 GB RAM).

The sampling frequency was selected so that it would overcome the aliasing effect. Thus, the sampling frequency for the first case study was 8 kHz, about five times the highest input frequency, this was then increased to 20 kHz in the following case studies for more sampling accuracy. The case study sample sizes were not less than ten to ensure that the preconditions for the statistical analysis are favourable. The data collection process was done in accordance with a specified protocol for each case study. This included data labelling to reflect the type of experiment done and means of measurement that was crucial for the next analysis stage. This was an attempt to achieve a better testing repeatability for the different samples.

4.5 Signal Analysis Technique (Spectrum Analysis)

The characteristics of diagnosing THR loosening using vibrometry are mainly dependent on the frequency analysis of the targeted system, through the primary frequency and related harmonics magnitudes. This analysis is realised using the spectrum analysis provided by the LabVIEW sound and vibration package. The signal analysis process will be explained followed by further elaboration regarding the parameters for loosening diagnosis in this study.

A code was developed using LabVIEW sound and vibration software, initially to record the data and then to process it. The analysis stage started by recalling the stored data with the aid of the data labelling system used to distinguish between the different testing conditions. The data analysis then went through three different stages; filtering, power spectrum and

peak searching. These stages were carried out using the (process and analysis) tools provided in the sound and analysis package.

Filtering was the first stage of the data analysis using a low pass filter with a cut off frequency of 10 KHz, taking into account the sensors measurement range. This was followed by the power spectrum phase that used the filtered data as an input. The power spectrum stage set-up was as follows; Window (Hanning), Spectrum type (Magnitude), Magnitude scale (Linear), peak conversion (RMS). Window filters are applied to the time waveform data and the Hanning type was selected in accordance with software user guidance for the sine waves. The (magnitude) was selected as a spectrum type over the power, where the power is equivalent to the square the magnitude. Also, the magnitude scale selection was linear units, rather than decibels. The frequency magnitude could be referred to using (peak value, peak to peak value or RMS root mean square). However, RMS is the preferred method for quantifying human vibration exposure [200]. The method of analysis is based on the Fast Fourier transform (FFT) algorithm. This can represent any time wave signal using a combination of several sinusoidal signals, which can be seen in the frequency domain as different vertical peaks at the corresponding frequencies, with heights relating to their magnitude [144], as seen in Figure 4-6. The last stage of the signal analysis was the peak-search stage, which is a specific tool used to identify the different frequency peaks in the frequency domain. These peaks were then exported in the form of a Microsoft excel format file containing the fundamental frequency and related harmonics magnitudes. These peaks readings were the parameters used to compare the different conditions, as will be further explored in the following sections.

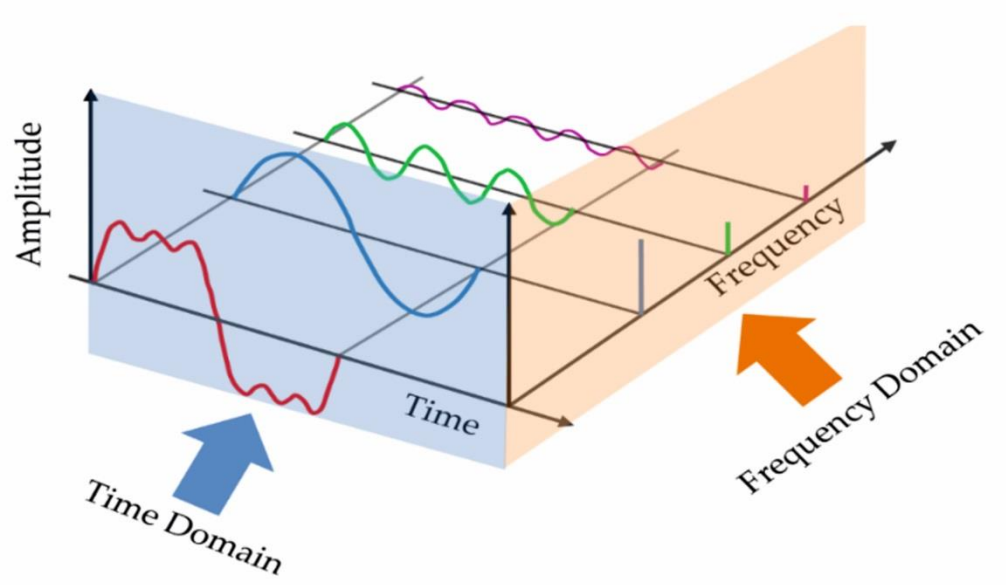

Figure 4-6: The Frequency Spectrum (FFT) analysis.

In summary, the targeted system was elicited using a defined input frequency range and the response was measured using two different methods; ultrasound and accelerometer. The data was then processed using the specified sound and vibration system in the following order; filtering, frequency spectrum and peak search to give the frequency spectrum for each targeted system. The parameters for diagnosing loosening in this study were mainly dependent on the frequency spectrum of the targeted system, through magnitudes of the primary frequency and related harmonics.

4.5.1 Frequency Spectrum Analysis

In 1989, Rosenstein *et al*.[10] was the first to correlate THR loosening to the existence of an extra harmonic compared to the secure condition; other studies followed [9, 11, 12] adopting the same approach and verifying the concept. Thus, this study is an attempt to adopt the same frequency analysis approach in the diagnosis of acetabular cup loosening. The frequency analysis identifies the fundamental frequency and the related harmonics in the form of vertical peaks, with heights relevant to their magnitude, at the corresponding frequencies.

The fundamental frequency is mainly the response to the driving excitation signal. This is followed by harmonics that are relevant to the signal type. In the case of this study the driving signal was a sinusoidal waveform of constant amplitude. The harmonics of the periodical signals come in the following order relative to the fundamental frequency (F); first harmonic (2F), second harmonic (3F), third harmonic (4F) and the remaining harmonics follow the

same pattern [144, 201], as shown in Figure 4-7 Thus, the first harmonic for the periodic sinusoidal signal is twice the fundamental frequency value, followed by the second harmonic that is three times the fundamental frequency, etc. For example, if the driving signal was a 50-Hz sinusoidal wave, in the response frequency analysis the fundamental frequency would be F=50Hz followed by the harmonics; first harmonic =2F=100Hz, second harmonic =3F=150Hz, third harmonic =4F=200Hz, etc.

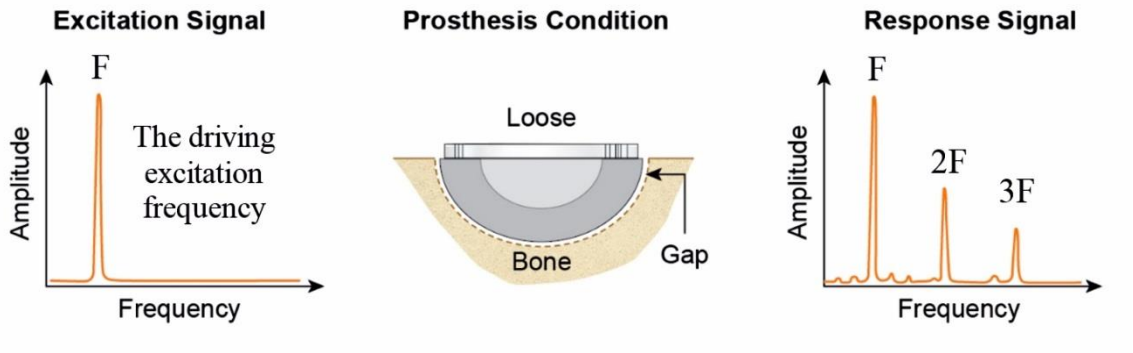

Figure 4-7: The periodical signal spectrum analysis: Fundamental frequency (F), 1st harmonic (2F), 2nd harmonic (3F), etc.

The study's main parameters of comparison between the different loosening conditions are through the fundamental frequency and the harmonic magnitudes. The first parameter is the primary (fundamental) frequency magnitude response, where the secure response is compared to the various loosening levels and the resulting patterns are observed. The same evaluation was conducted for the following harmonics. Each harmonic magnitude was compared with the different simulated loosening conditions and related to the secure state. This forms the first part of the data analysis which is then followed by the harmonic ratio, explained in the subsequent section.

4.5.2 Harmonic Ratio

The harmonic ratio is an attempt to quantify the frequency analysis across the difference driving frequency range, the aim being to define the best optimum excitation range based on the resulting responses. Conducting the frequency spectrum analysis and observing the fundamental and harmonic frequencies can only be realised for one specific frequency at a time. Thus, the harmonic ratio was used as a method to better illustrate the relationship between the harmonics and the fundamental frequency for the whole driving frequency

range. Hence at each frequency response in the horizontal frequency axis the harmonic ratio variables represent the ratio between the harmonic in relation to the fundamental frequency to be observed alone, rather than both frequencies. Where the secure condition harmonic ratio would be used as a reference to distinguish the loosening condition, patients would be observed over time in order to act as their own control.

The harmonic ratio was characterised in accordance with the number of the harmonics used in comparison to the fundamental frequency. Thus, the first harmonic ratio is the relation between the first harmonic and the fundamental frequency magnitude (1st harmonic ratio = 1^{st} harmonic magnitude [F_1] /fundamental magnitude [F]). Similarly for the 2^{nd} and 3^{rd} harmonic ratio, simplifying the number of harmonics that were used to get the related ratio. These different ratios were used to see if the same pattern is reflected throughout or if one ratio type is better at representing loosening than the others.

The concept of finding a relation between the harmonic magnitudes and the primary fundamental frequency was pointed out in different studies [9, 11, 12], and as early as 1989 [10]. As initially noted by Rosenstein *et al.* [10] in their *in vitro* study loosening conditions had higher harmonic magnitudes relative to the fundamental frequency. This was later explored by Li *et al*. [11, 12] who reached the same conclusion, adding that this could only be applied to late loosening. Georgiou and Cunningham [9] then put forward the 25 % - 50 % 1^{st} harmonic amplitude concept, where if the harmonic amplitude is 25% or less than the fundamental amplitude then the implant would be considered secure, whereas more than 50% would be considered a loose condition. Nevertheless, these previous studies were stem related and the relativity of the harmonics to the fundamental frequency was only visually observed [6]. Thus, this study is the first to attempt to apply vibratometry – frequency spectrum analysis in the diagnosis of acetabular cup component and to quantify the harmonic ratio rather than visual observation.

4.5.3 Statistical Analysis

The statistical analysis of the different conditions was conducted using SPSS software (version 20.0; SPSS, Chicago, IL, USA). Initially, the Shapiro-Wilk test was used to observe the normal distribution, as recommended for sample sizes below 50 [202]. Accordingly, due to the non-normal distribution of the data non-parametric analyses were performed. Initially, this involved the use of a Kruskal-Wallis test between the different conditions, followed by

Mann-Whitney U-tests between each two cases. The statistical significance was defined as a p value of <0.05.

4.6 Summary

This Chapter outlined the research methodology behind using vibrometry (vibration) analysis in the detection of the acetabular cup component loosening. Initially, the conventional loosening diagnostic techniques and the justification of the use of the vibrometry approach were briefly explained. Then, the vibrometry concept in the loosening diagnosis and how this study is different from other vibration analysis studies were clarified. The different case studies that were used to achieve the study aims were also explained. This was followed by the specification of the excitation method and measurement techniques that were used. Finally, the data analysis approach used was described highlighting the parameters that were used in the loosening diagnosis. The excitation, measurement and data analysis approach are the same for the different case studies with the exception of the excitation frequency range and sensor coupling, which will be justified accordingly. The following Chapters will explain in detail the different case studies using the same outline structure for ease of comparison.

Chapter 5 –The First Objective (Sawbones blocks Cup Loosening)

5.1 Introduction

The first step towards the accurate interpretation and understanding of vibration analysis of the acetabular cup component is to simplify the set-up with minimum boundary conditions. This should reduce any source of potential measurement errors. Thus, the first stage involves using an acetabular cup and simplified controlled Sawbones foam model to create various loosening scenarios. These were as follows: late spherical, early spherical, and early zone loosening. This was done in order to replicate the radiolucent line gap, which is one of the main criteria for detecting implant loosening when using imaging techniques [101]. In this study, 'late loosening' refers to the loosening gap when it is equal to or more than 2mm. The term 'early loosening' is any loosening gap less than 2mm. The 2mm gap thickness was used as the threshold because imaging techniques use it as the minimum reliable means of confirming the presence of loosening [100]. This criteria was adopted in order to simplify the acetabular cup loosening complexity and test the vibrometry concept. The three case studies presented in this chapter have undergone the same vibration excitations, data collection and analysis processes, in order to ensure a controlled and repeatable environment. Further explanation of the set-up of these scenarios will follow in the next sections.

To answer the research question, whether vibrometry can be used to detect acetabular cup loosening, the first objective included the following case studies:

- First case study – Late spherical loosening
- Second case study – Early spherical loosening
- Third case study – Early zone loosening

5.2 First Case Study: Late Spherical Loosening

The first approach in verifying the ability of vibration analysis to detect acetabular cup loosening was through using the late spherical loosening set-up. Vibration analysis had to demonstrate the same level of ability of detecting loosening as the established radiological techniques, in order to be a valid method of loosening detection. Thus, since the 2mm radiolucent line gap thickness was the minimum reliable detection threshold for imaging techniques, it was essential for the vibrometry to detect the same level of loosening. This stage was labelled as "late" loosening due to the ability of the imaging techniques to reliably detect the loosening level at the radiolucent line where it was equivalent to 2mm and above. This case study included two spherical loosening levels (2mm and 4mm). These were compared to a secure condition (1mm press-fit), in order to see their effect on the frequency analysis responses and whether a pattern could be observed (Figure 5-1).

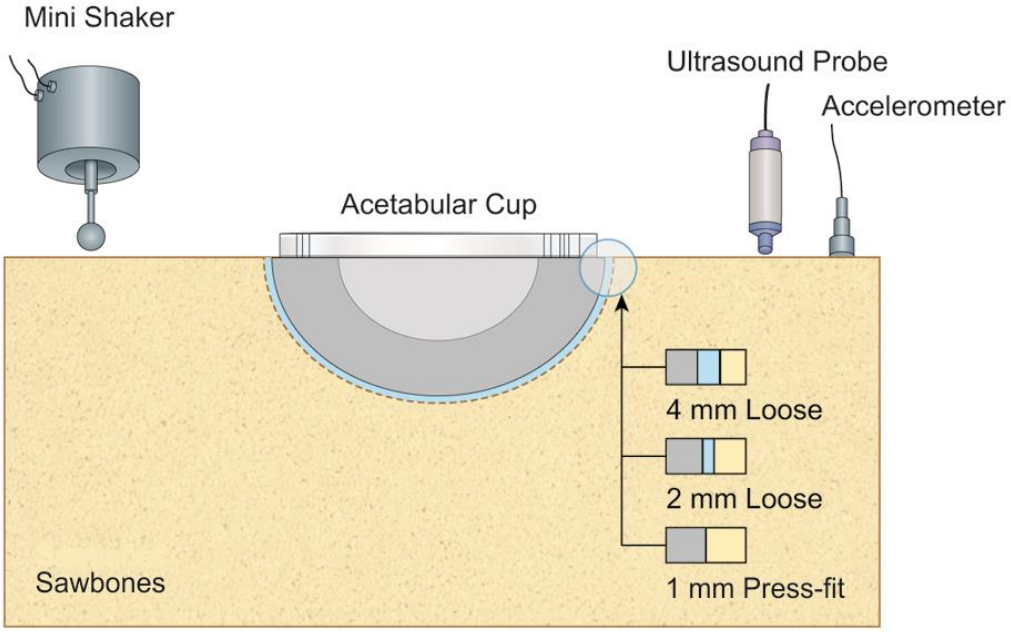

Figure 5-1: The polyurethane solid foam and the excitation and measurement techniques used, source [194], with permission,

5.2.1 Materials and Methods

5.2.1.1 The loosening setup

The acetabular model was replicated in the study with the aid of a polyurethane solid foam material (Sawbones Europe AB, Malmö, Sweden). This material has the same mechanical properties as the human bone and is commonly used in orthopaedic implant studies as an alternative to the cadaver human bone [203]. The Sawbones foam material comes in a block shape with the following characteristics according to the manufacturers data:, density of 30 pcf (0.48g/cm3), compressive strength of 18 MPa, compressive modulus of 445 MPa, tensile strength 12 MPa, tensile modulus of 592 MPa, and size 13 cm x 9 cm x 4 cm. The different loosening conditions were mimicked through the creating hemispherical cavities of different diameters to accommodate the different loosening levels. This was realised by the use of two acetabular cups (Trident® Hemispherical HA Cluster Sheller shell, Titanium (it-6AI-4V) with Arc Deposit Surface, Stryker Orthopaedics, Mahwah, New Jersey, USA), with diameters of 54 and 52 mm and a liner (Trident® x3 polyethylene insert UHMWPE). The three conditions that were mimicked in this case study were: 1mm press-fit acetabular cup, 2mm spherical loose and 4 mm spherical loose, as illustrated in Figure 5-2.

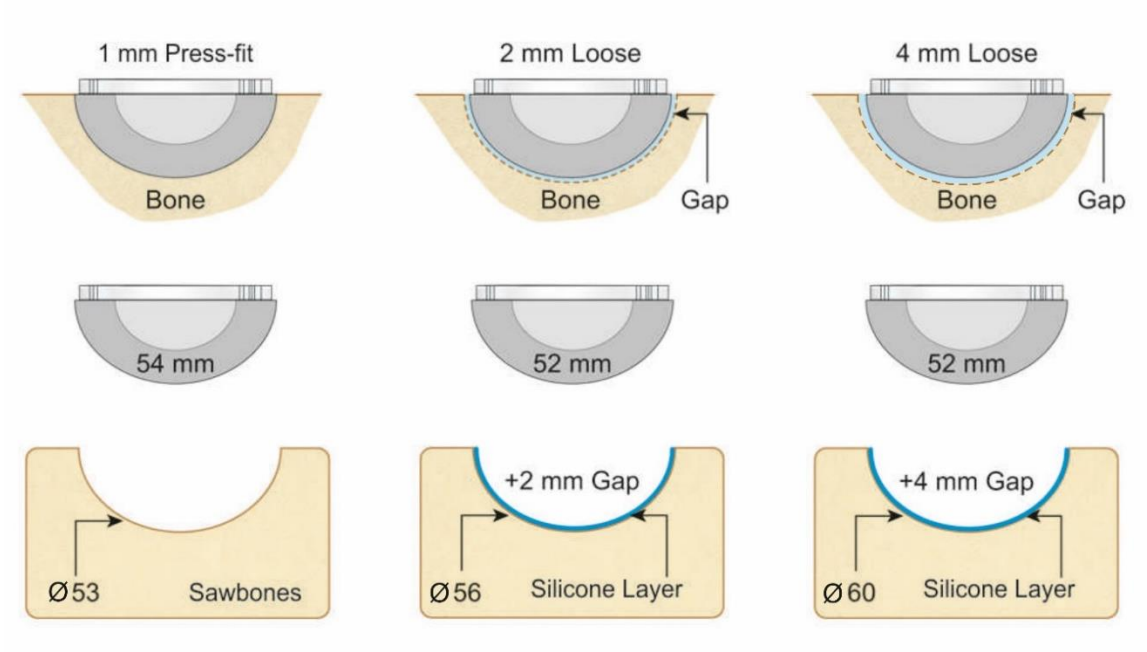

Figure 5-2: Case study three conditions (1mm press-fit, 2mm spherical loose and 4mm spherical loose), source [194], with permission.

The cementless acetabular cup component fixation is primary achieved by press-fit fixation and additional screws can also be used for extra stability [204, 205]. The press-fit technique leaves the acetabular hemispherical cup cavity under-reamed with a 1 mm or 2 mm diameter interface [205, 206]. Thus, the 1mm press-fit was adopted to replicate the secure cup condition. It would be used as a reference for the two loosening conditions. The press-fit cavity was machined by utilizing a computerised numerically controlled (CNC) milling machine to achieve the desired cavity geometry. The secure cup cavity was designed to have a diameter of 53mm and a depth of 27.5mm. The diameter was designed to be 53mm and to have a 1mm diameter interface with the 54mm acetabular cup. The depth of the 27.5mm cavity was used to accommodate the depth of the acetabular cup. The depth was achieved by using a 1mm offset to the cavity, causing it to be 1mm deeper. This allowed it to reach 27.5mm and prevented the cup from bottoming-out, as described in the press-fit stability assessment study by Crosnier *et al.* [173]. Subsequently, the Stryker acetabular cup (54mm diameter) was inserted into the prepared cavity (53mm diameter and 27.5mm depth) through repeated impacting using a soft mallet until it was fully seated, in accordance with the literature [207-209].

The two spherical loosening conditions mimicked, 2mm and 4mm, were mainly to replicate the radiolucent line clinically observed gap width. The 2mm spherical gap thickness was created using a 56mm diameter cavity with a 52mm Stryker cup diameter size. The 4mm loosening was created through the use of a 60mm diameter with the same Stryker cup size of 52mm. These hemispherical cavities, 56mm and 60mm in diameter, were produced using acetabular reamers (Figure 5-3). The soft tissue interface between the acetabular cup outer shell and bone surface was mimicked using a low modulus silicone (EVO-STIK, Bostik Limited, England), in accordance with the literature [11, 124, 135, 153]. The silicone layer interference thickness was controlled by using a surgical assessment measurement tool that is typically used to ensure the acetabular cup cavity size after reaming. It consists of different dome sizes that surgeons can choose from. A 52mm diameter dome was used after being spread with a silicone releasing agent (Ambersil Formula 6, Bridgwater Somerset, UK) to prevent the silicone from sticking to the dome surface. It was held in the cavity using a specific handle that was screw-fixed into the dome, as seen in Figure 5-3. The silicone curing time was 24 hours according to the manufacturer's instructions. The experiment set-up and the application of the excitation and measurement system will be explained in the following section.

Figure 5-3: The instrument used to create the loosening cavity and the silicone layer.

5.2.1.2 Excitation signal

The input excitation signal was a sinusoidal wave with a frequency range between 100 Hz and 1500 Hz, with a step increase of 50Hz and a constant amplitude of 3 Volts (peak – peak). The method of introducing the input signal to the targeted system was through an electromechanical mini shaker (V201, LDS, UK). The shaker generated a signal that was controlled through a power amplifier (PA25E, LDS, UK) that was driven by a function generator (TG230, TT, UK). The excitation system, input signal characteristics and frequency range was adopted in accordance with the following studies [9-12, 145], where the authors highlight the prospect of detecting stem loosening using a sinusoidal frequency sweep excitation range that is below 1500Hz.

5.2.1.3 Testing setup

After the different loosening conditions were created using the polyurethane solid foam block, they were tested within an aluminium frame. The set-up aimed to reduce any elements that may affect the different loosening condition responses. It also aimed to reduce the source of measurement errors. The aluminium frame was composed of twelve aluminium beams (30mm width, KJN Aluminium, UK) that were joined by eight cubic junctions, making the following size: 280mm x 190mm x 500mm. This set-up was attached to a wood base. The aluminium frame had a moveable inner bracket that was used to suspend the sawbone system. The Sawbones block was lightly suspended using a cord (SPECTRA thread, ø 0.3mm) to produce a consistent boundary condition. The cord had a defined length of 25cm where it was used to suspend the block at defined points that were marked. The Sawbones suspension was achieved through screws that were fixed at the Sawbones sides with a

defined depth of 7.5mm inside the block. The suspension wires were not tensioned. It was only the combined weight of the Sawbones block and implanted acetabular cup that contributed to the wire tension (Figure 5-4).

The excitation and measurement location of the targeted system surface were defined for accuracy and repeatability. The excitation signal was introduced using a metallic rod with a spherical head (19mm diameter), attached directly to the sawbone surface on one side. The two measurement sensors (accelerometer and ultrasound) were located on the other side. The mini shaker was held in place using holding clamps to neutralise the effect of the shaker weight on the specimen reading. The ultrasound probe was also clamped in place to ensure a constant height in order to apply the ultrasound gel for coupling with the sawbone surface. The accelerometer was also coupled to the surface using petro-wax material in accordance with the manufacturer's instructions.

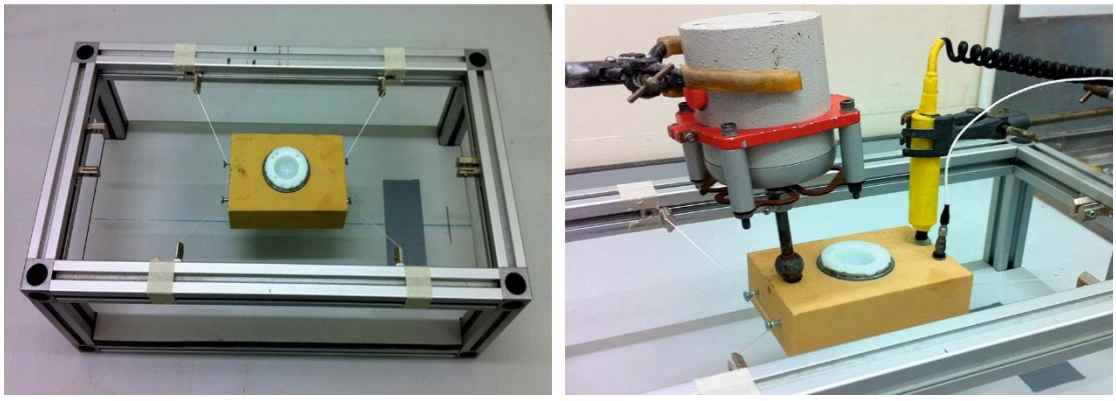

Figure 5-4: The system ste-up ; Sawbones block, excitaion, and measurment method, source [194], with permission.

5.2.1.4 Testing protocol

The different loosening scenarios were tested using the same procedures to ensure accuracy and repeatability. The testing protocol can be divided into three stages: pre-testing, testing, and post-testing. The pre-testing stage involved the preparation of the Sawbones sample, excitation and measurement system. The testing stage measured the response of the system tested due the vibration signal. The post-testing involved verifying the recorded data and disassembling and re-assembling the system; leading to preparation for the second reading phase, as illustrated in Figure 5-5.

The pre-testing stage included three phases of preparation, which were the Sawbones sample, excitation and measurement system. The first phase was the Sawbones sample preparation. This initially required the adjustment of the inner brackets within the titanium frame to hold the wire needed to suspend the Sawbones block. The blocks with the mimicked loosening were then suspended using four screws; two on each side. The next phase was the excitation signal preparation and validating the input signal. The function generator was the method of setting the signal type, amplitude and frequency range. It was connected to the mini shaker through a power amplifier with a master gain value of one. The signal feeding the mini shaker was observed using a digital oscilloscope in order to verify the frequency input amplitude and frequency range. The last phase was the preparation of the measurement instruments, including the coupling of the sensors, sound and vibration code running and data labelling. Initially, the accelerometer was coupled to the Sawbones block surface using a wax, whereas the ultrasound probe was coupled using an ultrasound gel. The sound and vibration LabVIEW code was then prepared, embedding the sensors sensitivities, sampling frequency and data labelling for each reading within the software. Data labelling was used to label the recorded loosening condition, Sawbones density, frequency range, amplitude and the reading number. This was all crucial information for the post processing and analysis stage.

The testing stage was conducted to observe the system tested, while undertaking the frequency sweep excitation. It was necessary to check the sensors' coupling and the shaker's clamping due to presence of the vibration signal which may affect them. The input signal was also observed using the digital oscilloscope to further ensure the accuracy of the input frequency sweep range.

The post-testing stage had three phases incorporated in order to verify the recorded data after each measurement. The first phase of the post-testing was related to the measurement verification. Initially, stop the recoding of the LabVIEW code after the frequency sweep had finished. The frequency sweep could be tracked using either the frequency spectrum reading from the input signal through the oscilloscope or from the response reading on the LabVIEW code in real time. It was then necessary to verify the recorded data set after each reading. This was done through observation of the time domain signal recording and ensuring that the data labelling was correct. This process was followed by the second phase. This phase involved stopping the function generator that was used to drive the mini shaker. The removal of the mini shaker was necessary for changing the Sawbones specimens. The third phase was to disassemble the loosening system set-up by removing the measurement instrument and changing the suspension cord in preparation for the next reading to take place.

In brief, each of the three simulated conditions for the first case study (1mm press fit, 2mm spherical loosening and 4mm spherical loosening) went through the same processes of experiment set-up and data collection, following the testing protocol shown in Figure 5-5.This leads to the next step which is the measurement and analysis, revealing the frequency spectrum for each of the test conditions.

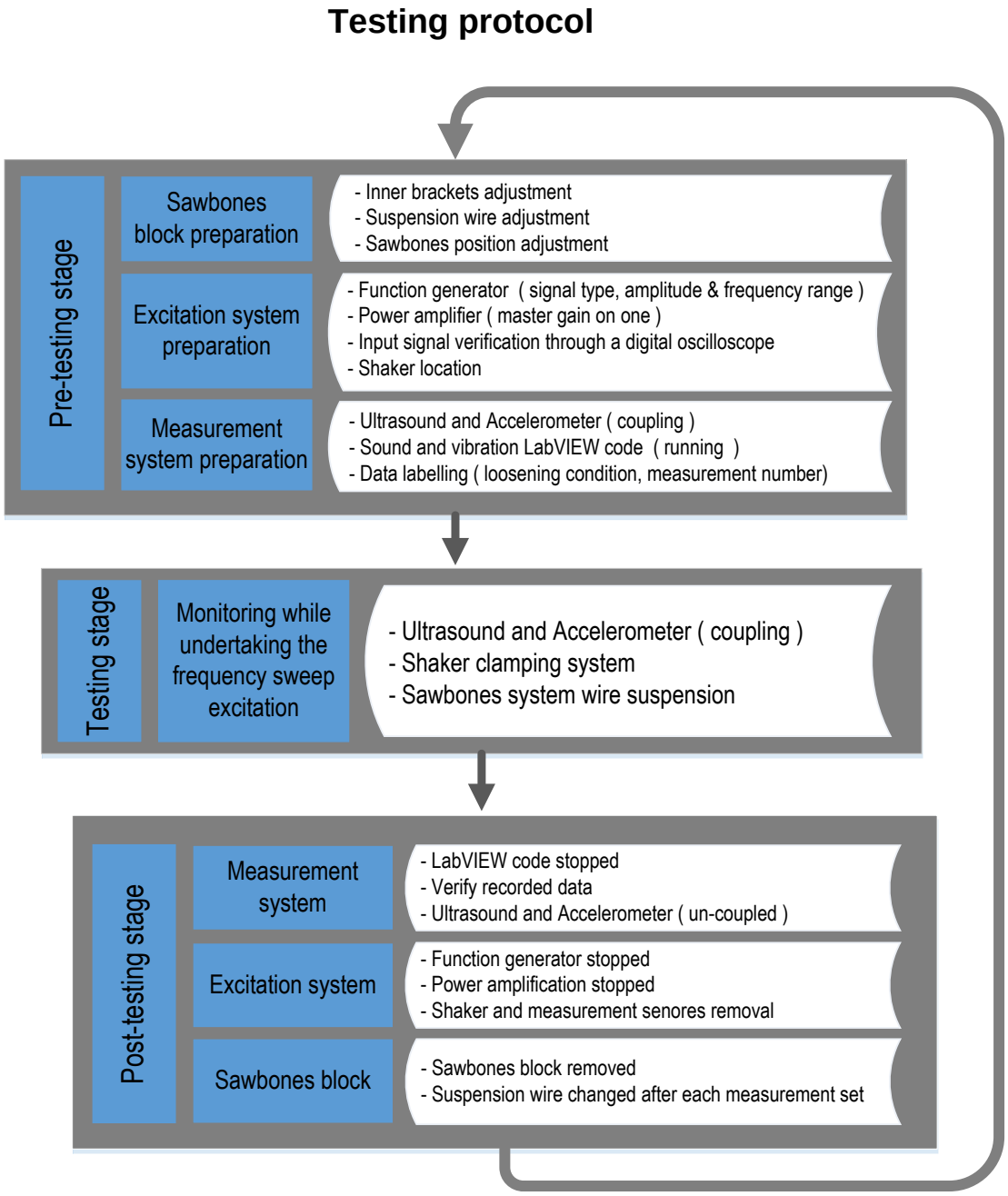

Figure 5-5: The protocol of testing for the spherical late loosening.

5.2.1.5 Sample size

Twelve readings of each of the samples (1mm press-fit, 2mm spherical loose, and 4mm aspherical loose) were obtained similar to the work of Xu *et al*. [135]. After each reading, the sample and measurement system was disassembled and assembled again with the aid of the markings on the aluminium frames, Sawbones block and the suspension wires.

5.2.2 Measurement and Analysis

5.2.2.1 Results

The results will be presented in two ways; spectrum analysis and harmonic ratio. The frequency spectrum analysis is a way of quantifying the system response in the form of fundamental frequency and the related harmonics, which utilises the LabVIEW sound and vibration software (FFT analysis). This was conducted for each of excitation signal frequencies in 50 Hz increments. The harmonic ratio was the second method of analysis whereby the ratio between the harmonics and the primary driving frequency respond was determined and compared for the different simulated conditions.

5.2.2.1.1 Frequency spectrum analysis

The elements of the spectrum analysis were the fundamental frequency (F_0) and the first harmonic (F_1). The fundamental frequency is the direct response to the driving signal and the harmonics are produced in response to the system's nonlinearity.

The fundamental frequency (F_0) was the initial parameter observed for the three conditions (1mm press fit, 2mm spherical loose and 4mm spherical loose). It was noted that, as the acetabular cup loosening level increased, the lower the fundamental frequency magnitude (F_0) became for both measurement methods (accelerometer and ultrasound). Figure 5-6 illustrates the F_0 magnitudes for the output responses of the three conditions at a 200 Hz driving signal. The secure cup (1mm press-fit) had the highest magnitude followed by the two loosening conditions, 2mm and 4mm respectively. The difference in magnitude between the loosening conditions was much higher for the ultrasound reading than for the accelerometer readings.

The first harmonic (F_1) was the second parameter observed using the FFT analysis. This parameter behaved in the opposite manner to the fundamental frequency (F_0). It increased as the simulated acetabular cup loosening level increased. The secure condition (1mm press fit) had the lowest first harmonic peak (magnitude), followed by the 2mm and 4mm loosening conditions respectively, as seen in Figure 5-6. However, the absolute magnitude increase difference between the loosened conditions was higher for the accelerometer reading than the ultrasound probe.

These findings, at the driving frequency of 200 Hz, imply that, as the mimicked cup loosening level increases, the fundamental frequency (F_0) magnitude decreases and the first harmonic (F_1) magnitude increases. To further quantify this signal behaviour across the different driving frequencies, the harmonic ratio was utilised.

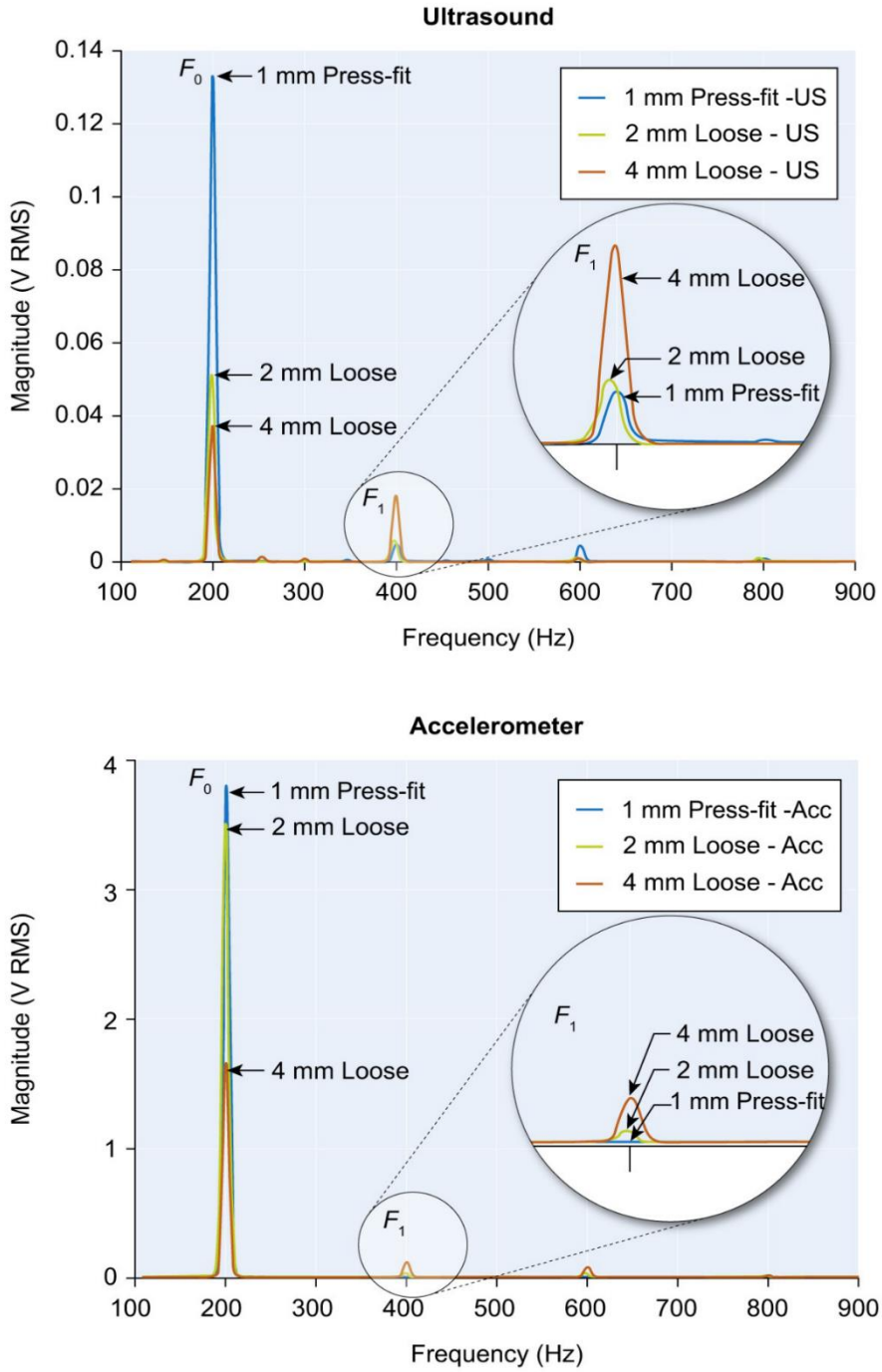

Figure 5-6: FFT spectrum analysis at driving signal 200Hz, source [194], with permission.

5.2.2.1.2 Harmonic Ratio

The harmonic ratio was an attempt to define the optimum frequency range for detecting cup loosening using spectrum analysis. This ratio can be defined as the relationship between the first harmonic magnitude and the fundamental frequency (harmonic ratio = first harmonic magnitude (F_1)/fundamental frequency magnitude (F_0)). When taking into account the previous spectrum analysis – an increase in the fundamental (F_0) magnitude and decrease in the first harmonic (F_1) – we would expect to a have higher harmonic ratio as the loosening increases. Thus, the secure (1mm press fit) condition has the lowest harmonic ratio because it has the lowest first harmonic and the highest fundamental magnitude, while the 4mm loosening condition has the highest harmonic ratio, because it has the highest first harmonic and lowest fundamental magnitude. This is illustrated in Figure 5-7 for the responses at the driving signal of 200 Hz.

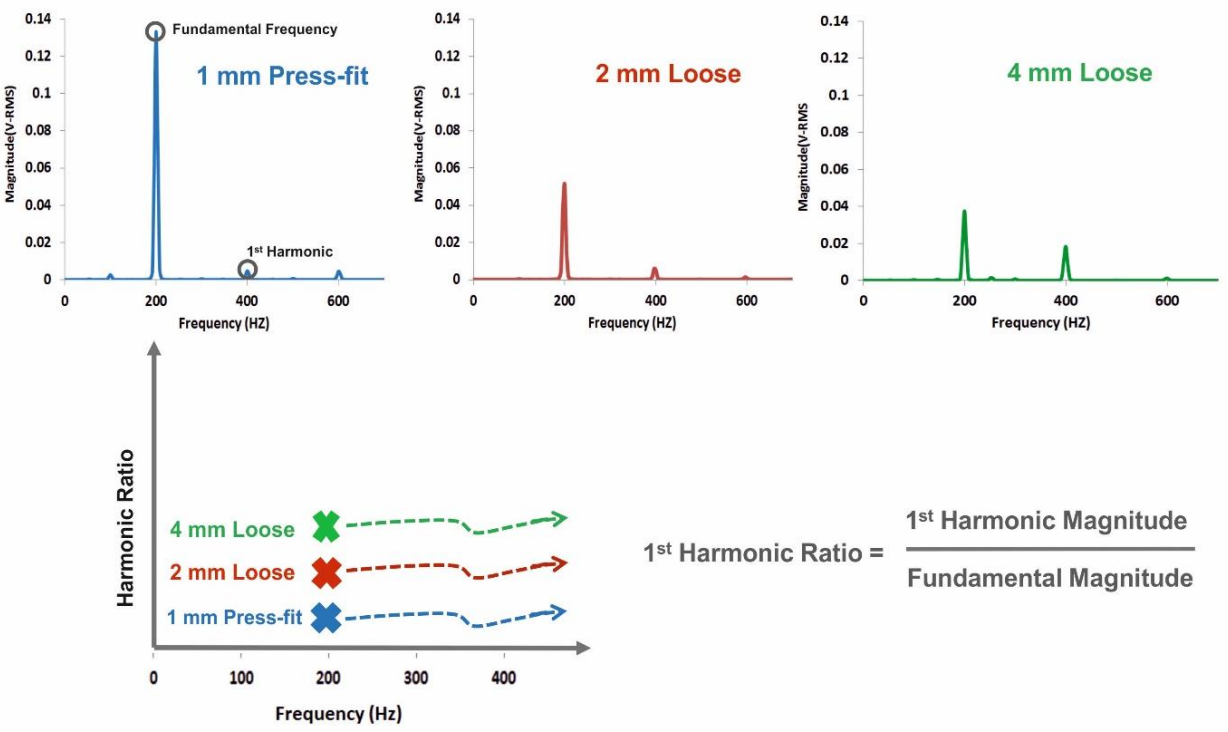

Figure 5-7: The harmonic ratio for the ultrasound signal at 200Hz driving frequency. The ultrasound probe sensitivity was (0.5V/KHz).

The harmonic ratio for the accelerometer reading, showing the different conditions, is shown in Figure 5-8a. There is a clear pattern illustrated that relates to the simulated loosening levels. The greater the radiolucent line mimicked gap gets, the greater the harmonic ratio becomes. This can clearly be seen in Figure 5-8a where the 4mm loose condition has the highest harmonic ratio, followed by the 2mm loose condition, and lastly the secure (1mm press-fit) condition with the least ratio in the frequency range up to 950 Hz. When comparing the 2mm spherical loosening condition to the 1mm press fit condition it was noticed that the 2mm has a greater ($p<0.01$) ratio than the secure state at the driving frequency range 100-1050 Hz. Whereas between 100-1000 Hz the 4mm loose condition has a much greater ($p<0.01$) ratio over the secure condition. However, when comparing the two loosening conditions, 2mm and 4mm, the 4mm harmonic ratio was greater ($p<0.05$) at 11 frequencies in the range between 150-250 Hz and 550-900 Hz. The accelerometer harmonic ratio of the 2mm loose condition was higher than the secure condition at 20 frequencies and with the 4 mm loose condition at 19 frequencies; followed by 11 frequencies for the comparison between the two loosening conditions.

The ultrasound harmonic ratio for the three simulated conditions was plotted alongside the accelerometer reading for ease of comparison, as seen in Figure 5-8b. The same pattern was also observed that could be related to the loosening levels, but at a lower frequency readings than for the accelerometer. The harmonic ratio for the ultrasound was conducted for the driving frequency range 200-1500 Hz, due to an inbuilt cut-off filter affecting measurement below 200 Hz in the ultrasound unit. When comparing the 2mm loosened situation to the secure one, it was found that it had higher ratios ($p<0.01$) for the driving frequency range 850-1050 Hz. whereas between 500-950 Hz, the 4mm loosening condition had a greater ($p<0.01$) ratio over the secure condition. The 4mm loose condition ratio was also higher ($p<0.05$) than the 2mm loose condition at the driving frequencies ranges of 500-700 Hz and 800-850 Hz. Accordingly, the ultrasound harmonic ratio of the 2mm loose was higher than the secure condition at 5 frequencies and with the 4 mm loose condition at 9 frequencies; followed by 7 frequencies for the comparison between the two loosening conditions.

To summarise, the harmonic ratio was able to support the spectrum analysis loosening diagnostic approach through a quantifiable means, thus highlighting a more favourable frequency range for both measurement methods (the accelerometer and ultrasound), as illustrated in Table 5-1 .Generally, the accelerometer method did show better results over the ultrasound method with regards to the harmonic ratio variation and wider detectable frequency range.

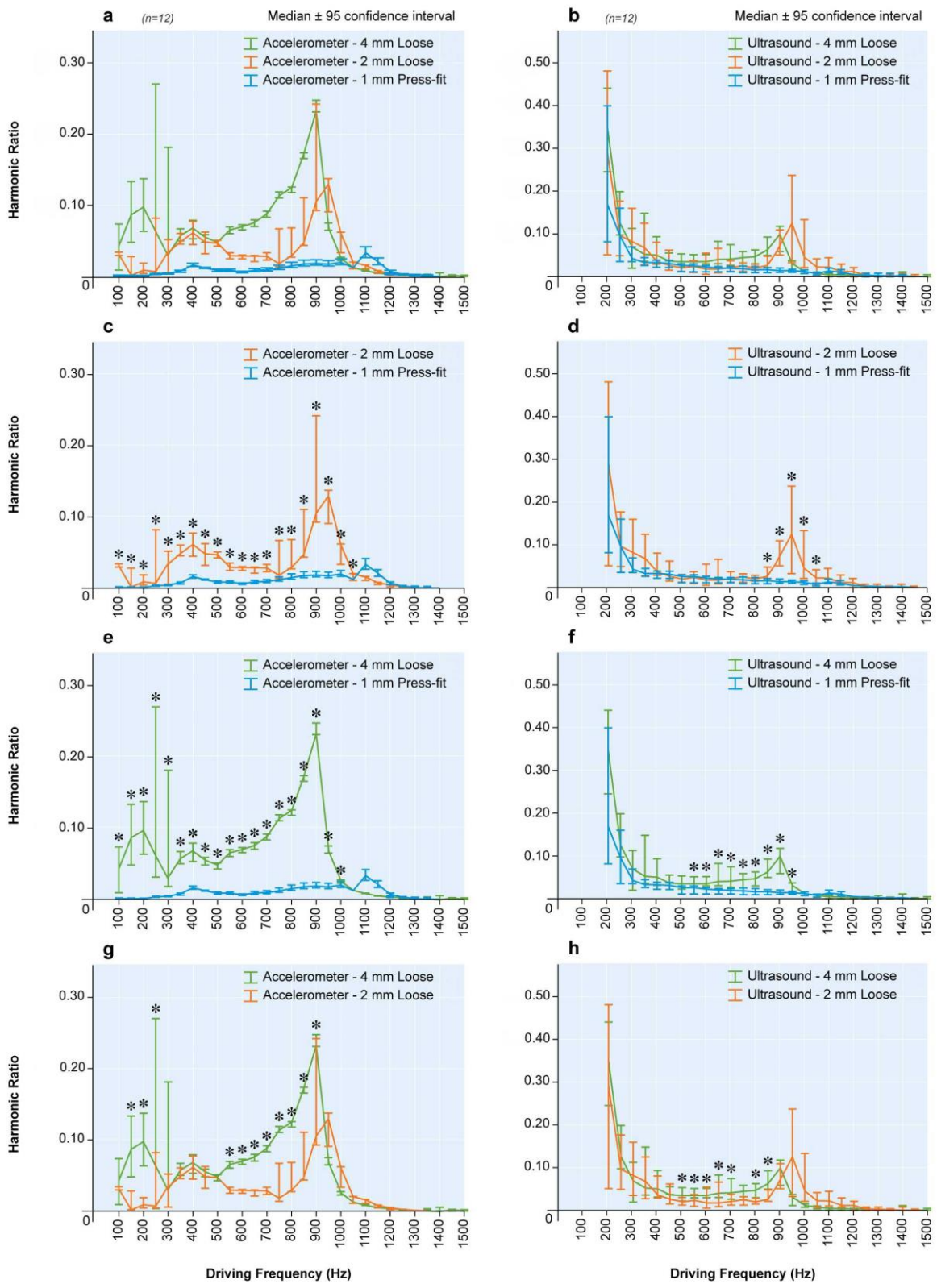

Figure 5-8: The harmonic ratio of the different simulated condition for both measurement techniques. *Graphs a, c, e* and *g* were obtained using the accelerometer sensor for the comparison between the conditions; (secure, 2 and 4 mm loose), (secure and 2mm loose), (secure and 4 mm loose) and (2 and 4mm loose), respectively . *Graphs b, d, f* and *h* show the same sequence of comparisons using the ultrasound probe measurement technique. * Mann-Whitney test $p < 0.05$, n = sample size, source [194], with permission.

Accelerometer - Late Loosening

	Driving Frequency (Hz)	100	150	200	250	300	350	400	450	500	550	600	650	700	750	800	850	900	950	1000	1050	1100	1150	1200	1250	1300	1350	1400	1450	1500	#
1st Harmonic Ratio	Secure Cup - 2 mm	.000[b]	.000[b]	.000[b]	.000[b]	.000[b]	.000[b]	.000[b]	.000[b]	.000[b]	.000[b]	.000[b]	.000[b]	.000[b]	.003[b]	.000[b]	.000[b]	.000[b]	.000[b]	.000[b]	.005[b]	NA	NA	NA	NA	NA	NA	NA	NA	NA	20
	Secure Cup - 4 mm	.000[b]	.000[b]	.000[b]	.000[b]	.000[b]	.000[b]	.000[b]	.000[b]	.000[b]	.000[b]	.000[b]	.000[b]	.000[b]	.000[b]	.000[b]	.000[b]	.000[b]	.000[b]	.010[b]	NA	NA	NA	NA	NA	NA	NA	NA	NA	NA	19
	4 mm - 2mm	NA	.000[b]	.002[b]	.024[b]	NA	NA	NA	NA	NA	.000[b]	.000[b]	.000[b]	.000[b]	.000[b]	.000[b]	.000[b]	.017[b]	NA	NA	NA	NA	NA	NA	NA	NA	NA	NA	NA	NA	11

Ulrasound - Late Loosening

	Driving Frequency (Hz)	100	150	200	250	300	350	400	450	500	550	600	650	700	750	800	850	900	950	1000	1050	1100	1150	1200	1250	1300	1350	1400	1450	1500	#
1st Harmonic Ratio	Secure Cup - 2 mm	NA	NA	NA	NA	NA	NA	NA	NA	NA	NA	NA	NA	NA	NA	NA	.002[b]	.000[b]	.000[b]	.000[b]	.012[b]	NA	NA	NA	NA	NA	NA	NA	NA	NA	5
	Secure Cup - 4 mm	NA	NA	NA	NA	NA	NA	NA	NA	NA	.000[b]	.000[b]	.000[b]	.000[b]	.000[b]	.000[b]	.000[b]	.000[b]	.014[b]	NA	NA	NA	NA	NA	NA	NA	NA	NA	NA	NA	9
	4 mm - 2mm	NA	NA	NA	NA	NA	NA	NA	NA	.045[b]	.010[b]	.017[b]	.014[b]	.039[b]	NA	.002[b]	.002[b]	NA	NA	NA	NA	NA	NA	NA	NA	NA	NA	NA	NA	NA	7

Table 5-1: The first harmonic ratio comparison between the simulated conditions with the significant value being highlighted,

NA = where the signal is not significant or do not support the main finding pattern.

5.2.3 First Case Study Discussion

The first case study, late spherical loosening, was aimed at verifying the ability of the vibration analysis approach to detect acetabular cup loosening. The output response of the loosening conditions was compared to the stable condition over the frequency range 100-1500 Hz. The excitation system was used in accordance to previous vibrometry studies [8-12] alongside the accelerometer as a measurement method [5, 10-12, 124, 128, 135]. Moreover, the ultrasound measurement approach proposed by Rowlands *et al.* [145] was utilised as an alternative measuring technique. The system response was examined using frequency spectrum analysis with the focus on the fundamental frequency and first harmonic as highlighted by Georgiou and Cunningham [9] as a potential indicators for the implant stability assessment.

The findings of this case study were examined using two methods; spectrum analysis and harmonic ratio. Initially, with the spectrum analysis, it was noted that, as the loosening gap became bigger, the fundamental frequency magnitude decreased and the first harmonic increased. This was then quantified using the harmonic ratio approach by dividing the first harmonic by the fundamental frequency magnitude, in order to define the optimum frequency range for detecting cup loosening using spectrum analysis. The harmonic ratio findings for the simulated conditions, using the accelerometer, revealed a distinct pattern. The greater the radiolucent line, the greater the harmonic ratio became. This was clearly observed for the 2mm spherical loosening condition when compared with the 1mm press fit condition, where the 2mm had a greater ($p<0.01$) ratio than the secure state in the driving frequency range 100-1050 Hz. Whereas between 100-1000 Hz, the 4-mm loose condition has an even a much greater ($p<0.01$) harmonic ratio over the secure condition. The ultrasound harmonic ratio also supported the accelerometer signal pattern, but with a less number of significant readings. The frequency range for the ultrasound method was 200-1500 Hz, due to the ultrasound unit having a built in cut-off filter that affected measurements below 200 Hz. When comparing the 2mm loose situation to the secure one, it was found that it had a higher ratio ($p<0.01$) for the driving frequency range 850-1050Hz, whereas between 500-950 Hz the 4mm loosening condition had a greater ($p<0.01$) ratio over the secure condition. Accordingly, both measurement methods were able to distinguish the simulated late loosening acetabular cup condition from the stable condition through a quantifiable

mean. However, the accelerometer method did show better results over the ultrasound reading with regards to the harmonic ratio variation and a wider detectable frequency range.

It should be noted that this case study has some limitations due the simplification of the experimental set-up. The loosening level was within the imaging techniques range of reliable detection [100] . Also, the use of a single density polyurethane foam material is not enough to support the vibrometry diagnosis reliability. The excitation and measurement coupling used the same table surface, which could lead to the shaker base affecting the sensors readings. These limitations were addressed in the next case study, in order to create a more reliable testing set-up and draw more conclusive conclusions.

5.3 Second Case Study: Early Spherical Loosening

The second stage in testing the vibrometry was to create loosening levels that imaging techniques have difficulty detecting. Despite the fact that vibrometry was able to detect late loosening at certain frequency ranges, the detected loosening gap (2-4mm spherical) is still within the range of imaging techniques diagnostic ability. Thus, the second stage was introduced to test the ability of vibrometry to diagnose early loosening scenarios. This was realised by mimicking a loosening that was a 1mm radiolucent line equivalent. The 1mm spherical loosening was mimicked using two methods; once with a silicone layer interface and another where the gap was clear (air gap) (Figure 5-9). This criteria of the early spherical loosening was adopted in an attempt to simplify the acetabular cup loosening complexity and test the vibrometry concept. Further attention was given to the sensors and shaker coupling in order to reduce the source of measurement errors. This will be clarified in the Material and Methods section below.

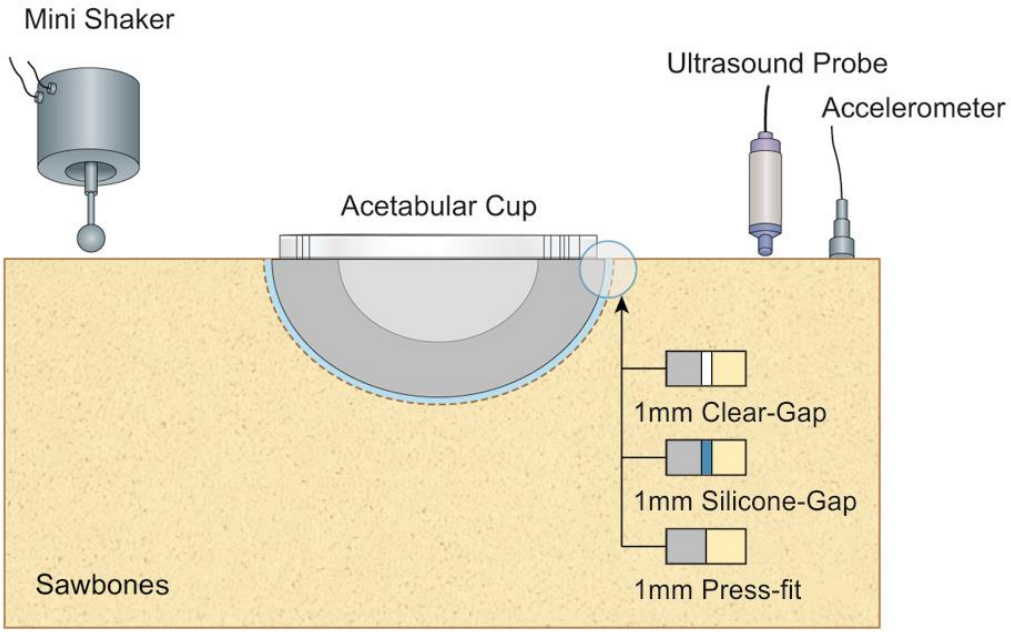

Figure 5-9: The early spherical loosening testing set-up.

5.3.1 Materials and Methods

5.3.1.1 The loosening setup

The acetabular early loosening model was replicated using the same polyurethane solid foam materials (Sawbones Europe AB, Malmö, Sweden). However, the density of the material was reduced (20 pcf -0.32g/cm3) to closely resemble human cancellous bone mechanical properties (young's modulus and yield strength)[210]. The selected polyurethane solid foam characteristics, according to the manufacturer's data were: density of 20 pcf (0.32g/cm3), compressive strength of 8.4 MPa, compressive modulus of 210 MPa, tensile strength 5.6 MPa, tensile modulus of 284 MPa, and size of 13 cm x 9 cm x 4 cm. The early loosening condition was produced through the machining of hemispherical geometry to accommodate a 1mm thickness gap that was spherical and uniform. The polyurethane foam cavity also had a 5mm-width channel that was machined between the bottom of each of the created cavities and the bottom surface of the block. This was used as a method for controlling the silicone thickness and the cup removal for the press-fit condition. A one-size 54mm diameter acetabular cup (Trident® Hemispherical HA Cluster Sheller shell, Titanium (it-6AI-4V) with Arc Deposit Surface, Stryker Orthopaedics, Mahwah, New Jersey, USA) and a liner (Trident® x3 polyethylene insert UHMWPE) was used for the three conditions. They were 1mm press-fit (secure condition), 1mm spherical silicone loose and 1mm spherical clear loose, as illustrated in Figure 5-10.

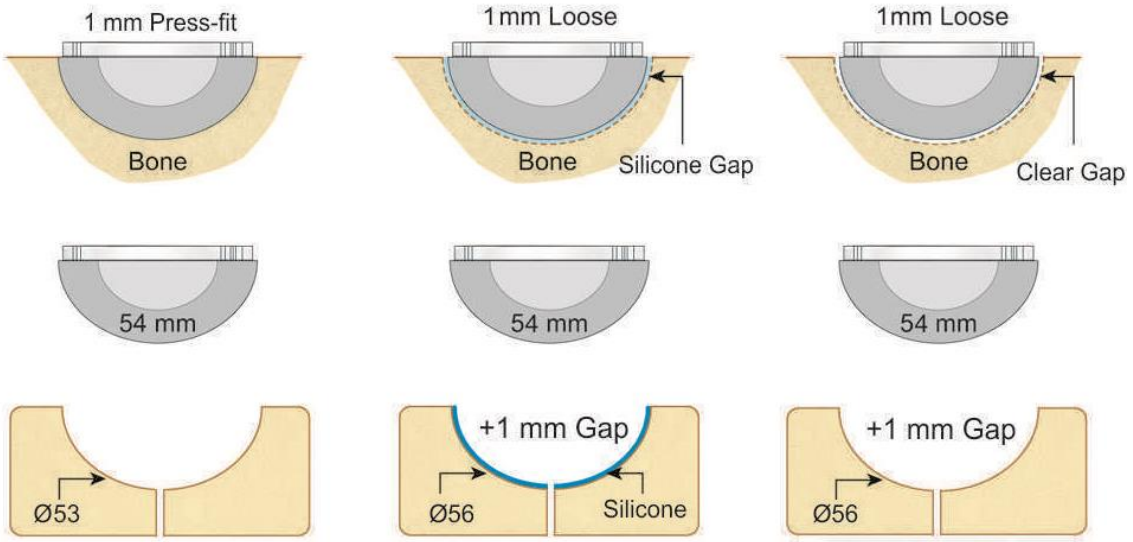

Figure 5-10: Case study two three conditions (1mm press-fit, 1mm spherical silicone loose and 1 mm spherical clear loose).

In this stage, the secure condition (1mm press fit) has the same hemispherical cavity geometry (53mm in diameter) as the first case study. This was CNC (computer numerically controlled) machined with a depth 27.5mm. However, the cup insertion method for the press-fit was different for this stage. It was inserted using a 30KN Instron Universal Testing Machine 5675 (Instron Corp., Canton, MA, USA) with a compression force of 1500N (rate of 10mm/min). This method of cup fixation was adopted in an attempt to provide more accuracy and repeatability in contrast to the impacting fixation method used in the previous case study [211-213]. The 54mm diameter Stryker cup was exposed to a uniformed load of 1500N with a loading rate of 10mm/min until the cup was fully seated into the 53mm diameter cavity. A small 5mm-width channel was also CNC machined between the polyurethane cavity bottom and the block's lower surface, in order to enable easy removal of the cup between the different readings. After each reading, the cup was gently hammered out using a soft mallet before re-inserting another polyurethane cup and this was repeated ten times.

Two early loosening conditions were created: 1mm spherical (clear and silicone) loosening, in an attempt to replicate the radiolucent line clinically observed around loosened implants. The 1mm spherical gap thickness was created using a 56mm-diameter cavity with a 54mm Stryker cup diameter size. The Sawbones block was machined by the computer numerically controlled (CNC) milling machine to achieve the desired cavity geometry. The 1mm radiolucent line equivalent loosening was done into two ways. One set-up was simply a 1mm clear gap interface between the cup shell and Sawbones surface, while the second had a 1mm gap with a silicone layer interface (Figure 5-12). This was done in order to see what effect the soft tissue interface had on the loosening detection. The low modulus silicone layer interface thickness was controlled by using a specific manufactured dome shape that was made from Nylon 66 (RS Ltd. Northants, UK). The dome had the same diameter as the inserted cup (54mm) and an extended stem that was 13mm in length and 5mm diameter. The stem was used as a method of holding the dome in place through the silicone curing time and to guarantee the thickness symmetry. The dome was also spread with a silicone releasing agent (Ambersil Formula 6, Bridgwater Somerset, UK) to prevent the silicone from sticking to the dome surface. It was held in the cavity using a specific handle screw-fixed into the dome, as seen in Figure 5-11.After the silicone layer was produced in the Sawbones cavity using the Nylon dome, it was held in place for twenty-four hours using a clamp system before testing.

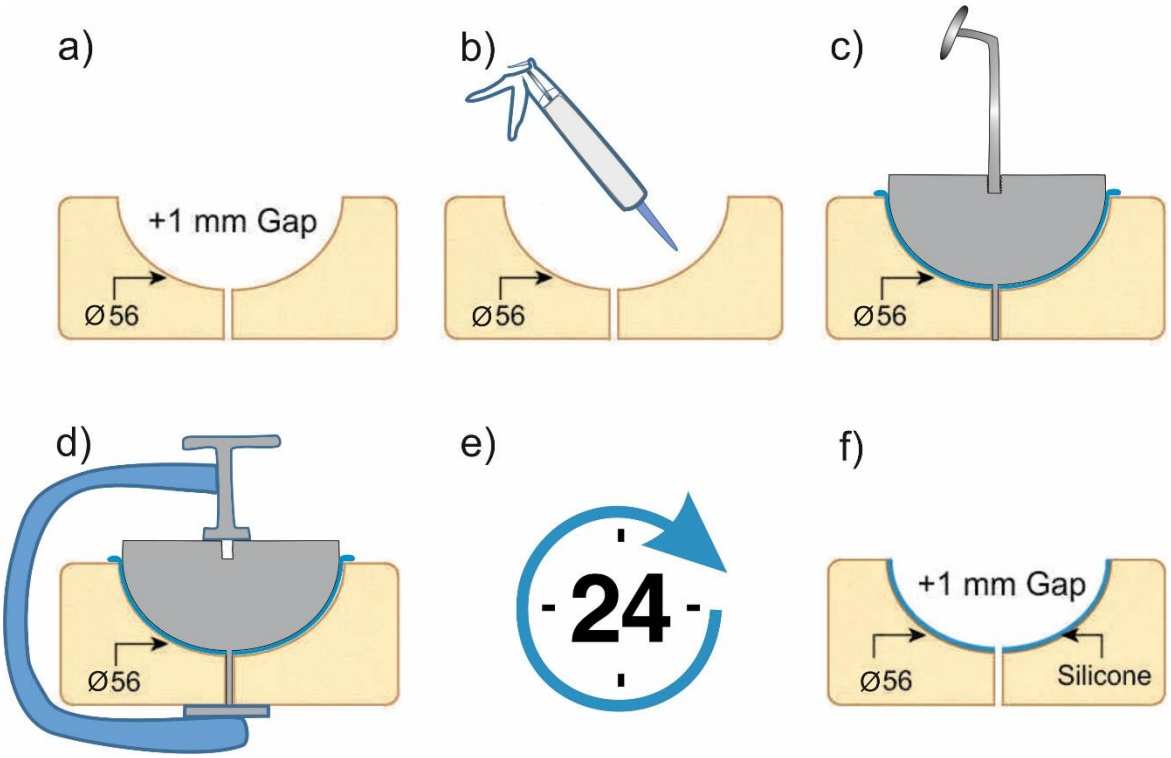

Figure 5-11: Steps taken to mimic loosening that was a 1mm radiolucent line equivalent using the silicone.

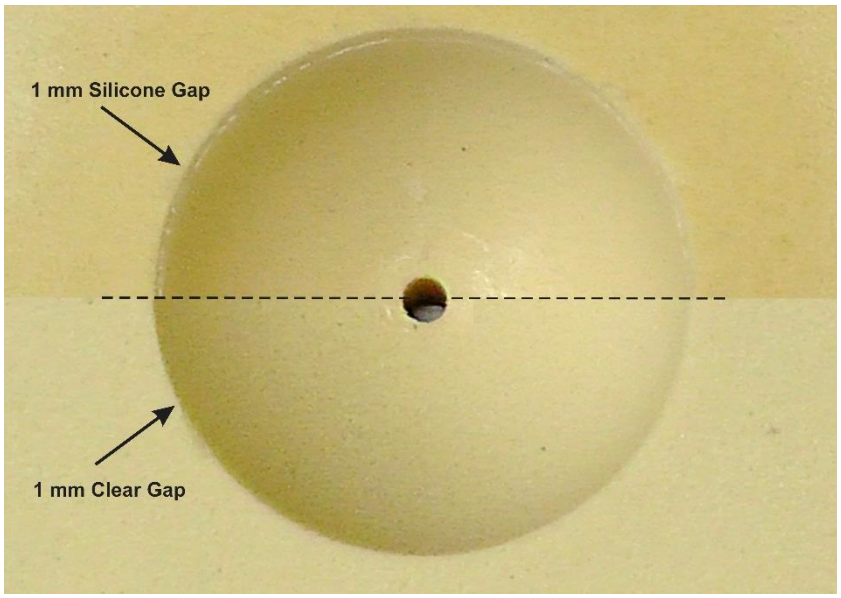

Figure 5-12: The Sawbones block showing the added 1mm silicone layer.

5.3.1.2 Excitation signal

The input excitation signal was a sinusoidal wave with frequency range between 100 Hz and 1500 Hz, with step increase of 25 Hz and a constant amplitude of 4 Volts (peak – peak). The step increment of the frequency sweep was reduced to 25 Hz from 50 Hz used in the late loosening case study, in order to better enhance the frequency sweep accuracy. Moreover, the sinusoidal signal amplitude was increased to 4 Volts (peak-peak) to see what effect it may have on the loosening detection.

5.3.1.3 Testing setup

The different simulated loosening conditions were tested using a similar testing set-up used in the previous case study, with the aim of reducing the source of measurement errors. However, a further aluminium frame was added to provide better coupling of the measurement sensors (Figure 5-13). The aluminium frame was fitted with an adjustable holder that could be easily moved and aligned. The additional frame and holder was fixed to the frame system using four moveable inner brackets that could be adjusted if needed. The Sawbones suspension was conducted under the same conditions as in the first case study. The block measurements and excitation locations were labelled using CNC milling to ensure accuracy.

During this stage, more attention was given to the measurement and excitation system coupling in order to reduce any source of measurement errors. The mini shaker clamp base used to be on the same table as the measurement system, which may cause disturbances to the response readings. Thus, the base was moved and isolated from the measurement system surface to provide more favourable testing conditions. The excitation location on the sawbone surface was the same, but a longer rod was used to prevent the shaker from touching the additional aluminium frame used to hold the sensors. The measurement sensors were also coupled and aligned using the additional frame instead of the clamp system used previously. In addition, the accelerometer sensor was screw-fixed to the Sawbones using threaded steel inserts (PEM® Inserts, UK), providing additional stability (Figure 5-14). Ultrasound gel was used with the ultrasound probe to maximize coupling.

5.3.1.4 Testing Protocol

This case study testing protocol was closely related to the first case study (late loosening). The testing protocol as explained in the previous case study had three stages, which are the pre-testing, testing, and post-testing stages. Due to the addition of the sensors aluminium alignment frame an extra step was add to the pre and post testing stage. This was only at the measurement system set-up phase were the ultrasound probe was coupled using the frame instead of a clamp system.

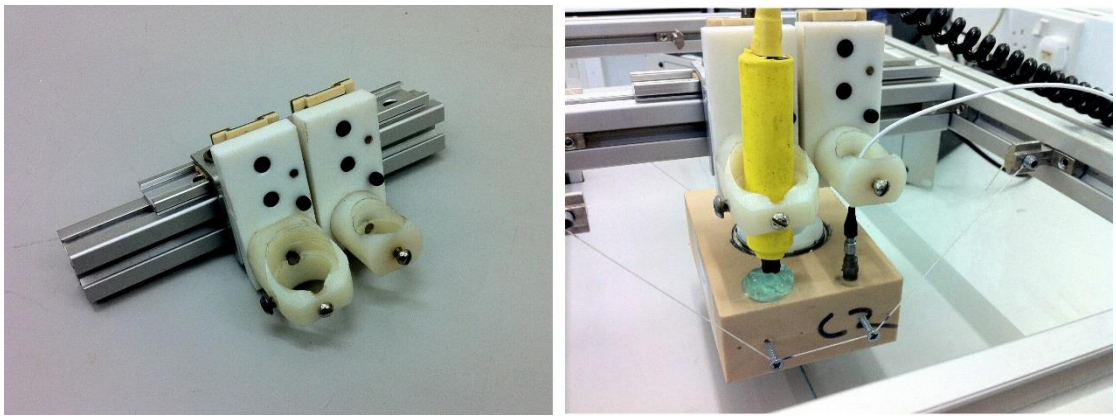

Figure 5-13: Early loosening set-up showing the additional aluminium frame used for the sensors alignment.

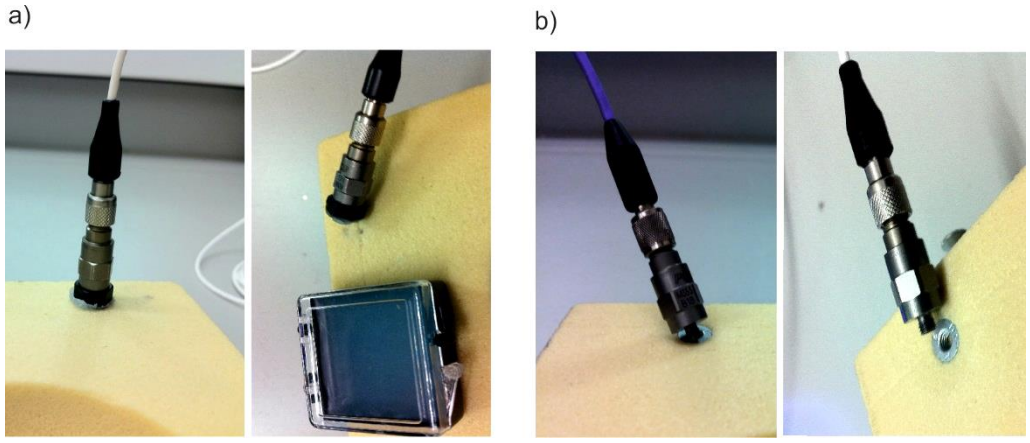

Figure 5-14: The accelerometer coupling to sawbone surface, a) using a petro-wax material for the late loosening case study, b) using the screw-fixation coupling for the early loosening case study

5.3.1.5 Sample size

Ten readings of each of the simulated conditions (1mm press-fit, 1mm spherical clear loose, and 1mm aspherical silicone loose) were obtained using ten different Sawbones samples. After each reading, the targeted system was disassembled and assembled again with the aid of the marking on the aluminium frames, Sawbones block and the suspension wires.

5.3.2 Measurement and analysis

At this stage, data analysis included two parameters more than at the earlier stage. They were the second harmonic magnitude and the second harmonic ratio. These additions were to see if loosening has the same effect pattern on the system spectrum response harmonics.

5.3.2.1 Results

The results will be presented in two ways: spectrum analysis and harmonic ratio. The frequency spectrum analysis includes the fundamental frequency, first and second harmonic. While the harmonic ratio includes the first and second harmonic ratio.

5.3.2.1.1 Frequency spectrum analysis

The analysis of the spectrum analysis examined three parameters for loosening comparisons: fundamental frequency, first and second harmonic. The second harmonic was added to the analysis for this stage to see if it would reveal the same observations as the first harmonic in relation to loosening.

The fundamental frequency (F_0) was the initial parameter observed for the three conditions (1mm-press fit (secure cup) and 1mm spherical (clear and silicone) loosening). When comparing the fundamental frequency magnitude of the three simulated conditions, there was no significant difference. This was the case for the ultrasound and the accelerometer readings across the frequency range 100-1500 Hz.

The first harmonic (F_1) was the second parameter observed using the FFT analysis. The loosening levels did show a significantly higher ($p<0.05$) first harmonic reading with both measurement methods at particular frequencies, 5 for the accelerometer and 3 for the

ultrasound. With the accelerometer reading, when comparing the 1mm spherical clear loosening situation to the secure one, it was found that it had a higher magnitude ($p<0.05$) at the driving frequencies 100 Hz and 800 Hz. Meanwhile, between 1050-1150 Hz, the 1mm spherical silicone loosening had a greater ($p<0.01$) magnitude over the secure condition (Figure 5-15). Accordingly, the ultrasound first harmonic magnitude was higher ($p<0.01$) for the 1mm spherical clear loose situation over the secure one at the driving frequency 650 Hz. It was greater ($p<0.01$) at 950 Hz and 1350Hz for the 1mm spherical silicone loosening condition.

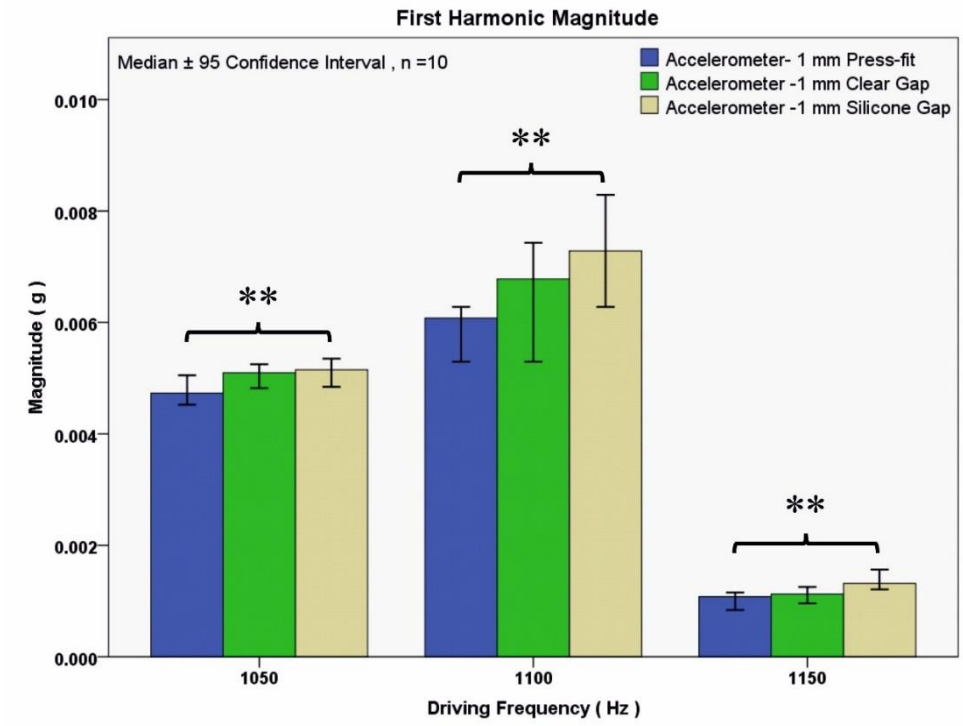

Figure 5-15:The accelerometer first harmonic magnitude response to the three simulated condition at the driving frequencies 1050 Hz, 1100 Hz and 1150 Hz. ** Mann-Whitney test $p < 0.05$, n = sample size .Source (27).

The second harmonic (F_2) was the third parameter examined in the spectrum analysis. Through the comparison of the simulated conditions, significantly higher ($p<0.05$) second harmonics were found for the loose condition over the secure condition for both measurement techniques, at 4 frequencies using the ultrasound and at 3 frequencies for the accelerometer reading. With the ultrasound results, when comparing the 1mm spherical clear loose situation to the secure one, it was found that it had a higher magnitude ($p<0.05$) at driving frequencies of 800 Hz and 1050 Hz. At 950 Hz and 1050 Hz, the 1mm spherical silicone loosening had a greater ($p<0.05$) magnitude over the secure condition (Figure 5-16).

For the accelerometer results, the second harmonic magnitude was higher ($p<0.01$) for the 1mm spherical clear loose situation over the secure one at driving frequencies of 100 Hz and 800 Hz, and greater ($p<0.01$) at 800 Hz for the 1mm spherical silicone loosening over the secure one.

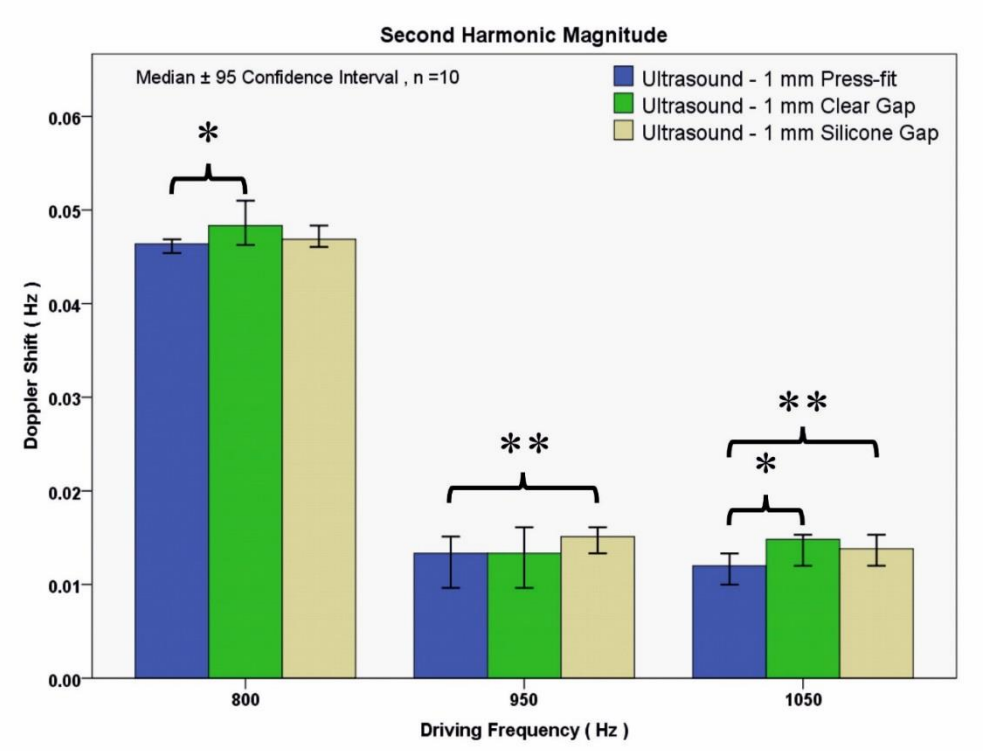

Figure 5-16:The ultrasound second harmonic magnitude response to the three simulated condition at the driving frequencies 800 Hz, 950 Hz and 1050 Hz.* and ** Mann-Whitney test $p < 0.05$, n = sample size. Source (27).

In brief, these spectrum analysis findings in the driving frequency range of 100-1500 Hz, imply that early spherical cup loosening may affect the related magnitudes of the harmonics but not the fundamental frequency. The magnitude of the first and second harmonics did have a significant ($p<0.05$) increase with loosening at 15 discrete readings for both sensors. The first harmonic (F1) had 5 significant readings for the accelerometer and 3 using the ultrasound method, whereas the second harmonic (F2) had 3 significant readings for the accelerometer and 4 for the ultrasound (see Table E-1 and Table E-2).

5.3.2.1.2 Harmonic Ratio

The harmonic ratio was the second method of observing the loosening variation which included the first and the second harmonic ratio. The second ratio was further adopted in this case study to see if the first ratio pattern with loosening variation will be repeated.

The accelerometer harmonic ratios reading did show a significantly ($p<0.05$) higher reading for the loosening conditions over the secure conditions at 6 discrete frequency readings. This was at 2 for the first ratio and 4 for the second harmonic ratio. With the first harmonic ratio, when comparing the 1mm spherical clear loosening with the 1mm press fit (secure) condition, it was noticed that the 1mm loose condition had a greater ($p<0.01$) ratio than the secure state at the driving frequency 800 Hz. Whereas at driving frequency of 1150Hz, the 1mm spherical silicone loosening condition had a greater ($p<0.01$) ratio over the secure condition (Figure 5-17). Consequently, the accelerometer second harmonic ratio was also higher ($p<0.05$) for the 1mm spherical clear loose condition over the secure one at driving frequencies of 100 Hz , 550 Hz and 800 Hz. The second harmonic ratio was greater ($p<0.01$) at 800 Hz for the 1mm spherical silicone loosening over the secure condition.

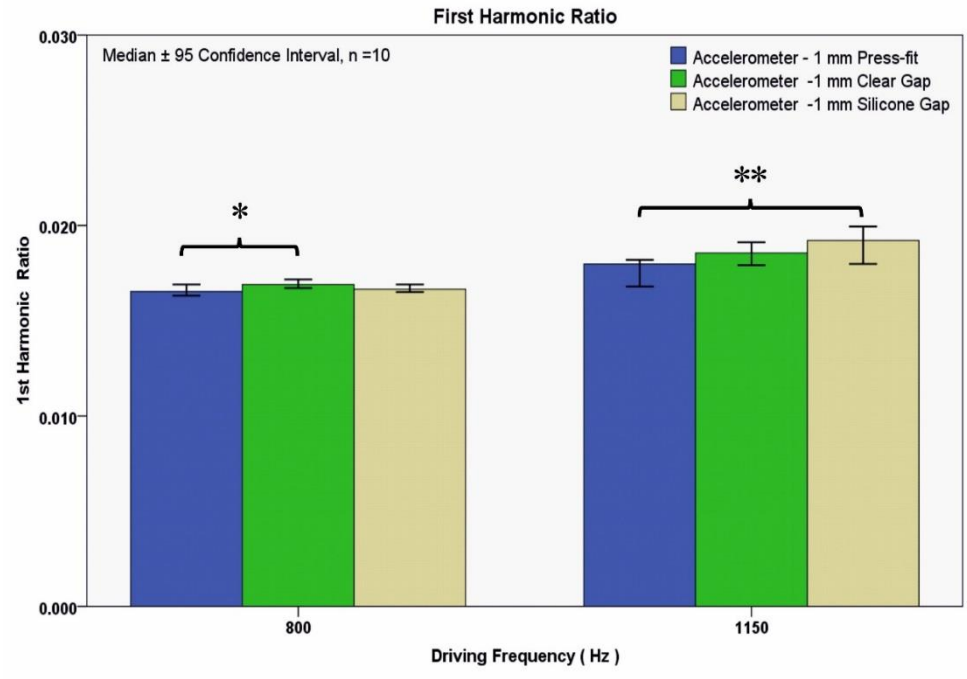

Figure 5-17: The accelerometer first harmonic ratio to the three simulated condition at the driving frequencies 800 Hz and 1150 Hz.* and ** Mann-Whitney test $p < 0.05$, n = sample size.

The ultrasound harmonic ratio readings did show significantly ($p<0.05$) higher readings for the loosening conditions over the secure conditions at 5 discrete frequency readings. This was at 2 frequencies for the first ratio and 3 frequencies for the second harmonic ratio. For the first harmonic ratio, the loosening condition was higher ($p<0.05$) than the secure condition at driving frequencies of 950 Hz and 1350 Hz for the 1mm spherical silicone loose situation. The second harmonic ratio was also higher ($p<0.05$) for the 1mm spherical silicone loose condition over the secure condition at a driving frequency of 950 Hz. It was also greater ($p<0.05$) at 800 Hz and 1000 Hz for the 1mm spherical clear loosening (Figure 5-18).

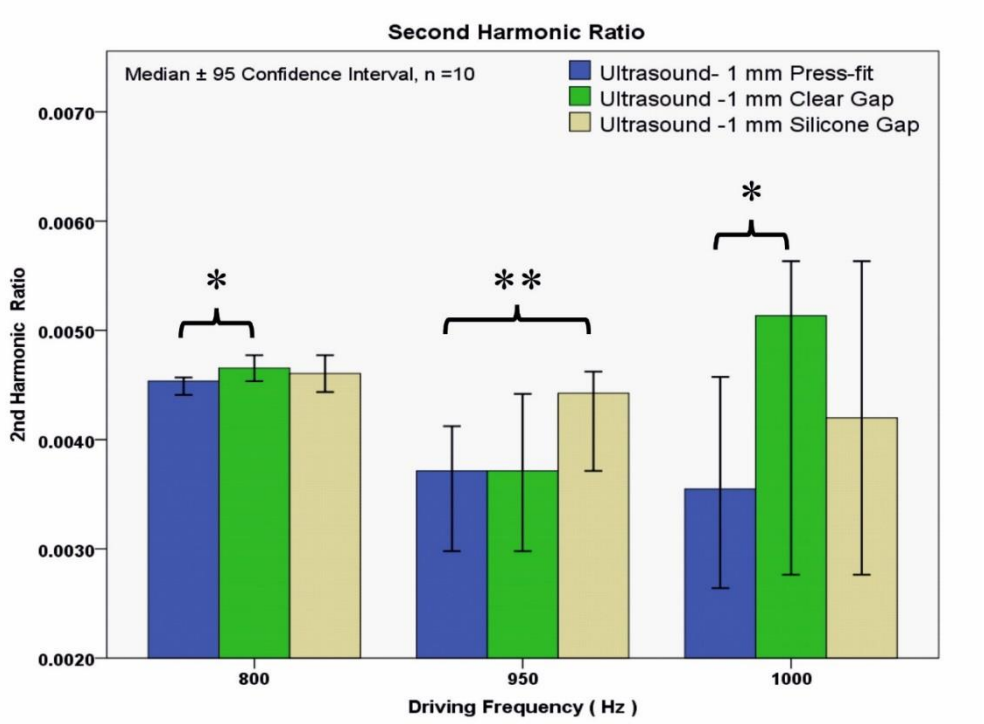

Figure 5-18:The ultrasound second harmonic ratio to the three simulated condition at the driving frequencies 800 Hz ,950 Hz and 1000 Hz.* and ** Mann-Whitney test $p < 0.05$, n = sample size.

In summary, these harmonic ratio results over a frequency range up to 1500 Hz, indicate that early spherical cup loosening can be detected with the two measurement techniques, but at fewer frequencies than for late spherical loosening (2mm and 4mm) as seen in Table E-1 and Table E-2 . The first and second harmonics ratio did have a significant ($p<0.05$) increase with relation to loosening at 11 particular readings for both sensors. The accelerometer reading had a greater ratio at 6 frequencies, whereas with the ultrasound readings this was at 5 frequencies.

5.3.3 Second Case Study Discussion

The second case study, early spherical loosening, was an attempt to further explore the validity of the vibrometry approach in detecting acetabular cup loosening. In this case study, some of the limitations of the first case study (Late spherical loosening) were addressed. Initially, the loosening level was reduced to a 1mm radiolucent line equivalent. The 1mm spherical loosening was mimicked in two ways: once with a silicone layer interface and another where the gap was clear. The Sawbones density was also reduced to 20 pcf ($0.32 g/cm^3$) to closely resemble human cancellous bone mechanical properties [210]. In addition, the measurement sensors were coupled and aligned using an additional frame instead of the clamp system, in an attempt to reduce the source of measurement errors. Further attention was also given to the silicone layer interface by using a specific manufactured dome shaped with an extended stem. This was used as a method of holding the dome in place through the silicone curing time in order to guarantee the thickness symmetry.

In this study the data analysis included the second harmonic in addition to the first and the fundamental frequency. The two harmonic ratio components are obtained as follows; the first ratio is a result of dividing the first harmonic by the fundamental magnitude and the second is obtained by dividing the second harmonic over the fundamental frequency. Initially, when examining the three parameters using spectrum analysis, the fundamental frequency did not show any significant magnitude reduction in relation to the loose conditions. However, the first and second harmonics did demonstrate a significant ($p<0.05$) increase for the loosening conditions, in relation to the simulated secure cup at 15 readings for both sensors. Secondly, the harmonic ratio results also showed that early spherical cup loosening can be detected with the two measurement techniques. The first and second harmonic ratios had a significant ($p<0.05$) increase for the loosening conditions, compared to the secure cup at 11 readings for both sensors. In summary, the findings of this case study imply that early spherical cup loosening may affect the harmonics magnitude but not the fundamental frequency. The harmonic ratio results indicate that early spherical cup loosening can be detected, but with a less significant number of readings than for late spherical loosening conditions with 2mm and 4mm spherical gaps. Parallel findings were also noted in the existing literature [11, 12] for the stem component, which demonstrated

that vibrometry was reliable for detecting late stem loosening but less favourable for demonstrating early loosening.

In terms of the limitations of this case study, the simulated loosening condition was a 1mm radiolucent line equivalent to a uniformed spherical gap between the acetabular cup outer shell and the polyurethane surface. However, this is not how early cup loosening is characterised clinically [96, 97]. Therefore another case study (zone loosening) was conducted in order to create a more clinically relevant loosening condition, to help further verify the vibrometry diagnosis approach.

5.4 Third Case Study: Early Zone Loosening

The reliability of the vibrometry approach in detecting acetabular cup loosening has been supported by the findings of the first two case studies presented. However, spherical uniform loosening is not how early cup loosening is characterised clinically. Acetabular cup loosening is classified according to the zones in which the loosening is located and the degree of associated gap between the bone and cup outer surface [96, 97]. Thus, this third case study will attempt to accommodate a more clinically relevant loosening scenario through mimicking acetabular cup zone loosening (Figure 5-19). The same Sawbones foam (density of 20 pcf, 0.32g/cm3), will be used under the same boundary conditions in the second case study, to see if similar patterns are observed or not. The simulated loosening condition was a 1mm non-uniform zone cup loosening and was assessed using an excitation range 100-2500Hz. The frequency range was increased in this study to accommodate the natural frequency of the polyurethane solid foam (1826Hz) and observe its effect on the loosening detection.

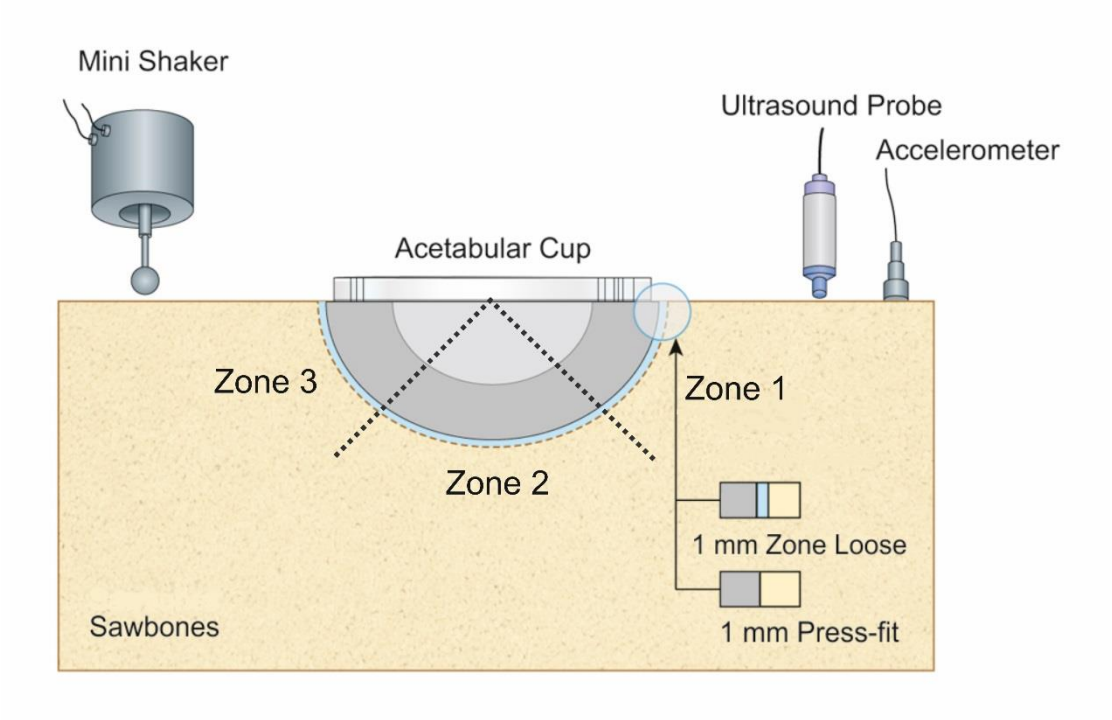

Figure 5-19: The Sawbones testing set-up for the zone loosening case study.

5.4.1 Materials and Methods

5.4.1.1 Loosening setup

The acetabular early zone loosening condition was modelled through the machining of the hemispherical geometry to accommodate a 1mm thickness gap that was zone specific. The foam cavity also had a 5mm diameter channel that was used as a method for better controlling the silicone thickness and the cup removal for the press-fit condition. The polyurethane foam material properties were according to the manufacturer's data, a density of 20 pcf (0.32g/cm3), compressive strength of 8.4 MPa, compressive modulus of 210 MPa, tensile strength 5.6 MPa, and a tensile modulus of 284 MPa. A 54mm diameter acetabular cup (Trident® Hemispherical HA Cluster Sheller shell, Titanium (it-6AI-4V) with Arc Deposit Surface, Stryker Orthopaedics, Mahwah, New Jersey, USA) and a liner (Trident® x3 polyethylene insert UHMWPE) was used for the four loosening conditions replicated in this stage. These were a 1mm press-fit (secure condition), 1mm zone (1 and 3) loose, 1mm zone (2) loose and 1mm zone (1 and 2) loose, as shown in Figure 5-20.

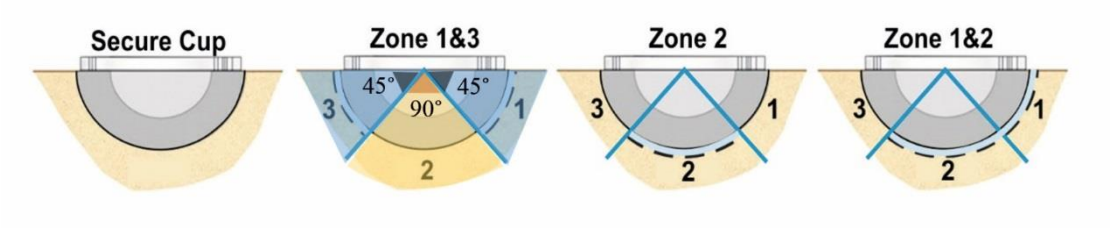

Figure 5-20: The acetabular cup early zone loosening conditions.

The 1mm press fit (secure) cup condition was realised using a 54mm diameter Stryker cup that had a uniformed load of 1500 N applied (30KN Instron, rate of 10mm/min) until the cup was fully seated into the polyurethane cavity of 53mm diameter. This cup fixation approach was conducted in accordance with other acetabular cup pre-operative stability studies [173, 211-213] that used the same cup insertion techniques. The cavity was CNC (computer numerically controlled) machined to the desired diameter with a depth of 27.5mm to accommodate the Stryker cup depth of 27mm. A 5mm diameter channel was also machined between the cavity bottom surface and the block lower surface to enable easy removal of the cup between readings. Ten sample readings were conducted, and after each reading the cup was gently hammered out using a soft mallet before re-inserting it in another Sawbones block.

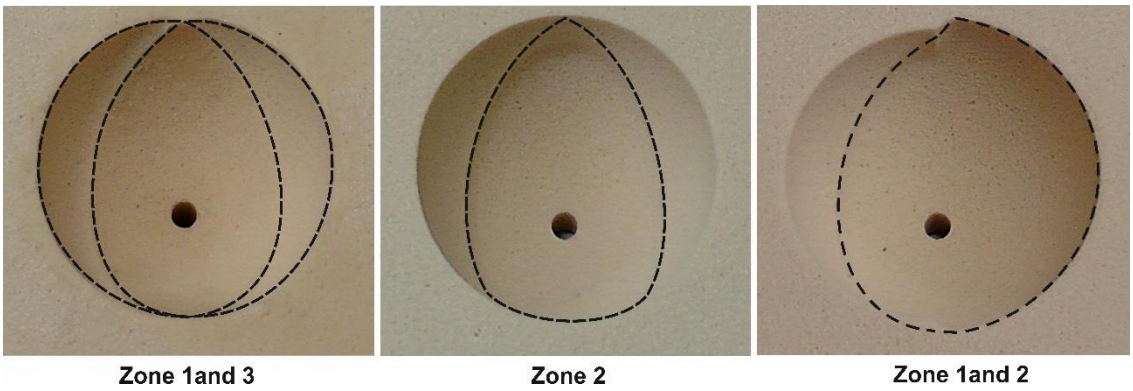

Figure 5-21: The simulated acetabular cup zone loosening conditions.

The three zone loosening conditions were all simulated with a 1mm radiolucent line thickness gap, with the location of the loosening area being the only difference. The conditions were labelled according to the location of the loosening as follows: 1mm zone (1 and 3) loose, 1mm zone (2) loose and 1mm- zone (1 and 2) loose. The approach of diagnosing THR component loosening is not universally agreed upon and different criteria are proposed in the orthopaedic literature [25]. However, the three zone classifications proposed by DeLee and Charnley [96] were adopted due to their convenience and wide use. Zone 1 was used for super-lateral loosening only, zone 2 for the superomedial quadrant and zone 3 for the inferomedial aspect. These zones were mainly intended for cemented cups but are also generally adopted to cement-less sockets with the addition of migration criteria [97]. The three zones were treated as different regions for ease of comparison. The Sawbones cavity was machined to a 56mm diameter and a 5mm channel. The zones were then CNC machined with a 45 degree angle from the Sawbones upper surface to create the 1mm thickness gap, as shown in Figure 5-21. In the case of the zone 2, the CNC machining was extended to the Sawbone cavity periphery. This zone gap was then filled by a low modulus silicone (EVO-STIK, Bostik Limited, England), replicating the soft tissue interface using a specifically manufactured dome that was made from Nylon 66 (RS Ltd. Northants, UK). The dome had the same diameter as the inserted cup (54mm) and an extended stem that is 13mm in length and 5mm in diameter. The dome was spread with a silicone releasing agent (Ambersil Formula 6, Bridgwater Somerset, UK) to prevent the silicone from sticking to the dome surface. It was held in the cavity using a specific handle that was screw-fixed into the dome. After the silicone layer was introduced to the cavity using the Nylon dome, it was held in place for 24 hours using a clamp system for a curing time according to the manufacturer's instructions.

5.4.1.2 Excitation signal

The excitation input signal was a sinusoidal wave with a frequency range between 100 Hz and 2500 Hz with a step increase of 25Hz and constant amplitude of 4 Volts (peak – peak). In this particular study, the frequency range was increased to 2500 Hz with the aim to including the natural frequency of the Sawbones system, in order to observe if this has an effect on the loosening detection. The natural frequency measured for the polyurethane solid foam (density of 20 pcf, 0.32g/cm3), with acetabular cup press fitted into it was at 1826Hz.

5.4.1.3 Testing setup

The different simulated zone loosening conditions were tested using a similar testing set-up for the second case study, with the aim of reducing the source of measurement errors. This was the case for the Sawbones block suspension using the aluminium frame set-up and measurement sensors coupling, which was screw-fixed for the accelerometer and using ultrasound gel for the ultrasound transducer. The ultrasound transducer was fixed and aligned utilising the aluminium frame to provide a constant space between the Sawbones surface and the transducer to accommodate the gel. The excitation approach was similar to that used previously with the use of a longer mini shaker rod to avoid the additional aluminium frame used to hold the sensors.

5.4.1.4 Testing protocol

The testing protocol for the zone loosening conditions was identical to the second case study (early spherical loosening). This was used for the three stages; pre-testing, testing, and post-testing. Each of the tested conditions (1mm press-fit, 1mm zone 2 loose, 1mm zone 1 and 2 loose, and 1mm zone 1 and 3 loose) went through the same processes of experimental set-up, data collection and analysis in order to ensure accuracy and repeatability.

5.4.1.5 Sample size

For each of the tested conditions (1mm press-fit, 1mm zone 2 loose, 1mm zone 1 and 2 loose, and 1mm zone 1 and 3 loose), ten readings were obtained using ten different Sawbones samples. After each reading, the sample and measurement system was disassembled and assembled again with the aid of the markings on the aluminium frames, Sawbones block and the suspension wires.

5.4.2 Measurement and analysis

5.4.2.1 Results

The results will be presented in two ways in terms of spectrum analysis and harmonic ratio. The frequency spectrum analysis includes the fundamental frequency, first and second harmonics. The harmonic ratio includes the first and second harmonic ratios.

5.4.2.1.1 Frequency spectrum analysis

The frequency spectrum parameters for the zone loosening case study were the fundamental frequency (F0), first harmonic (F1) and second harmonic (F2). This was for the frequency range up to 2500 Hz with the aim of observing the effect of the Sawbones system's natural frequency on the loosening detection.

The fundamental frequency (F0) magnitude was the initial parameter observed for the four conditions. The fundamental frequency, in accordance with the findings of the first case study (late spherical loosening), reduced as the loosening levels increased. This was also observed in this case study at particular driving frequencies that will be highlighted. When comparing the secure condition with the 1mm zone (2) loosening condition, it was found that fundamental frequency of the loose condition had a lower magnitude at 26 driving frequencies ($P<0.01$) for the accelerometer reading and at 23 frequencies ($P<0.05$) for the ultrasound. Whereas the 1mm zone (1 and 2) loose condition had a lower ($P<0.01$) fundamental magnitude than the secure condition at 25 frequencies for the accelerometer reading and at 17 frequencies ($P<0.01$) for the ultrasound reading. The 1mm zone (1 and 3) loosening condition also had a lower fundamental magnitude for the ultrasound reading at 13 driving frequencies (1850-1950 Hz and 2050-2500 Hz) ($P<0.05$) and for the accelerometer at 41 driving frequencies ($P<0.01$). It was noticed that the accelerometer sensor had the highest number of significant readings for the fundamental frequency over the ultrasound probe, especially with the two loosening conditions1mm zone (1 and 2 - 1 and 3).

Using spectrum analysis, the second parameter examined was the first harmonic (F1), which behaved in an opposite manner to the fundamental frequency (F0), the magnitude increased as the loosening level increased. This was in line with the findings of the previous two case study. When comparing the two conditions, secure and 1mm zone (2) loose, the 1mm

condition had a higher ($P<0.05$) fist harmonic magnitude at 16 driving frequencies for the accelerometer reading and 24 for the ultrasound. For the secure 1mm zone (1 and 2) loosening conditions, the same pattern can also be observed, with the 1mm loose condition giving the highest ($P<0.05$) magnitude at 18 and 23 driving frequencies for the two sensors, accelerometer and ultrasound, respectively. This was also the case for the 1mm zone (1 and 3) loose condition at 26 driving frequencies ($P<0.05$) for both measurement techniques. The highest number of significant readings for the first harmonic was for the ultrasound transducer over the accelerometer reading, predominantly with the two loosening conditions; 1mm-zone (2- 1 and 2).

The second harmonic (F2) magnitude behaved consistently similarly to the first (F1) harmonic. When comparing the secure and 1mm zone (2) loosening scenario it was found that the 1mm condition had a higher second harmonic magnitude ($P<0.05$) at 26 driving frequencies for the accelerometer reading and at 22 frequencies for the ultrasound reading. The 1mm zone (1 and 2) loosening condition had a higher magnitude ($P<0.05$) when compared with the secure situation at 27 and 26 driving frequencies for the sensor readings, accelerometer and ultrasound, respectively. In the case of the two conditions, secure and 1mm zone (1 and 3) loose, the 1mm had a higher magnitude ($P<0.05$) over the simulated secure condition at 29 driving frequencies for the accelerometer reading and 36 frequencies for the ultrasound.

To summarise, the spectrum analysis findings in the driving frequency range between 100 Hz and 2500 Hz implies that early zone acetabular cup loosening can be distinguished from the secure situation using the vibrometry approach. The fundamental frequency decreases in magnitude with loosening while the harmonic magnitude increases at particular frequencies (Table E-3 and Table E-4).To further quantify this signal behaviour across the different driving frequencies, the results obtained using the harmonic ratio will be discussed next.

5.4.2.1.2 Harmonic Ratio

The harmonic ratio was the second method of observing the loosening variation with the aim of defining the optimum frequency range for detecting cup loosening using spectrum analysis. This includes the first and second harmonic ratio for the two measurement techniques. In accordance with the findings of the first case study (late spherical loosening) the harmonic ratio increases as the loosening level increases. This was also observed in this case study at particular driving frequencies.

Accelerometer

The harmonic ratio for the accelerometer reading, showing the different loosening conditions, can be seen in Figure 5-22a. With the first harmonic ratio, when comparing the 1mm zone (2) loosening with the 1mm press fit (secure) condition it was noticed that the 1mm loosening had a greater ($p<0.05$) harmonic ratio than the secure state at 26 driving frequencies (250-550 Hz , 650-1000 Hz, 1250-1400 Hz, 2000-2200 Hz and 2300-2350 Hz). The 1mm zone (1 and 2) loosening condition had a higher ($P<0.05$) first harmonic ratio than the secure state at 26 driving frequencies. This was at a higher frequency bandwidth than that of the 1mm zone (2) condition as seen in Figure 5-22c. The 1mm zone (1 and 3) loosening condition showed the greatest significant difference ($P<0.05$) in first harmonic ratio over the secure condition at 34 driving frequencies.

For the second harmonic ratio, the accelerometer readings did obtain a greater number of significant differences over the first harmonic ratio for the three simulated zone loosening conditions. The second harmonic ratio of the 1mm zone (2) loose condition in the frequency range 100-2500 Hz did show higher ratios ($P <0.05$) over the 1mm press-fit (secure cup) condition at 32 driving frequencies, 6 more significant readings than for the first harmonic ratio. The 1mm zone (1 and 2) loose condition also had a higher ($P<0.01$) second harmonic ratio for the accelerometer reading at 31 driving frequencies, 5 more significant readings over the first ratio. For the two conditions, secure and 1mm zone (1 and 3) loose, the 1mm loose had a higher harmonic ratio ($P<0.01$) over the simulated secure condition at 38 driving frequencies.

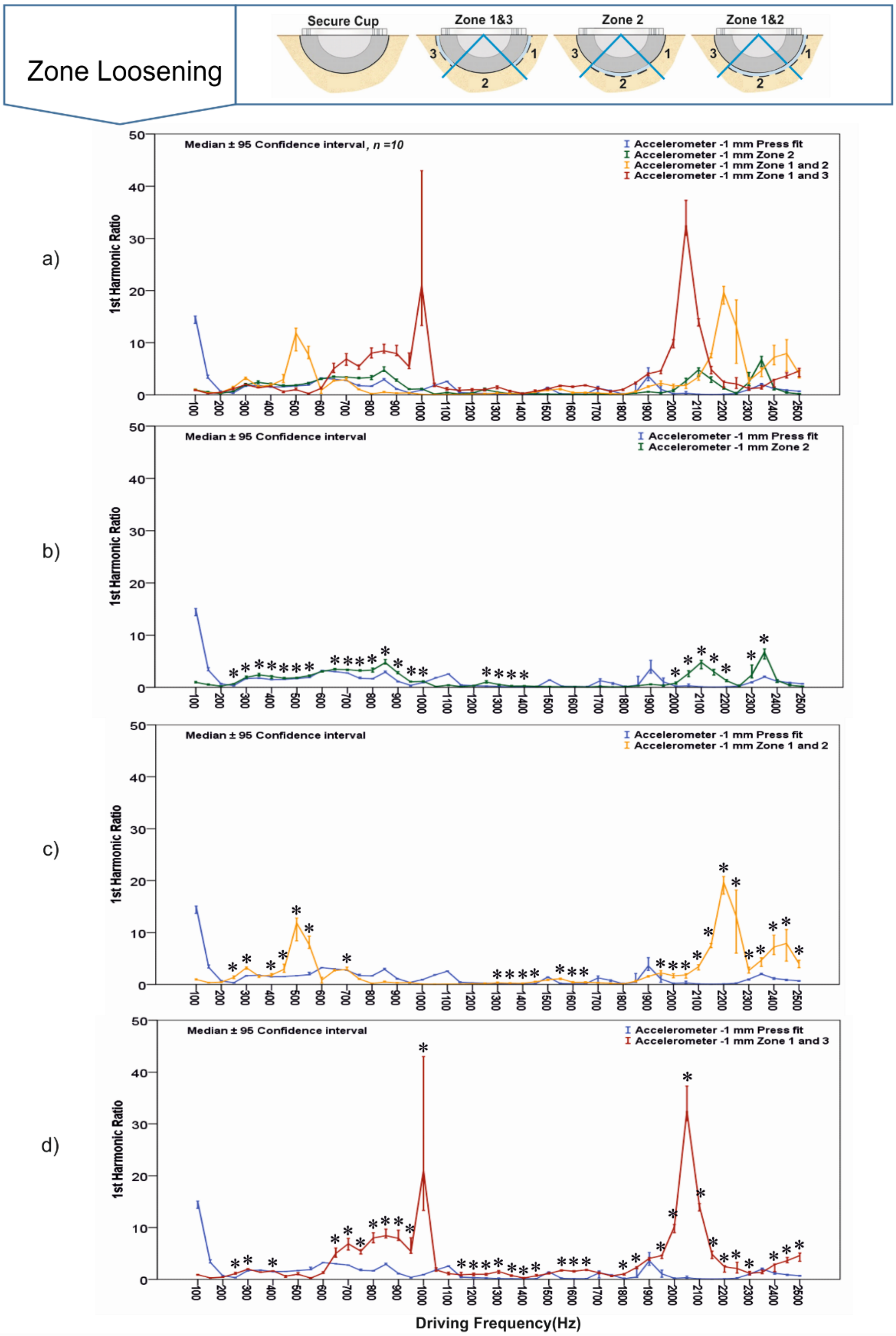

1st Harmonic Ratio	Driving Frequency (Hz)	100	150	200	250	300	350	400	450	500	550	600	650	700	750	800	850	900	950	1000	1050	1100	1150	1200	1250
	Secure Cup - 1 m (zone 2)	NA	NA	NA	.000b	.002b	.000b	.002b	.000b	.002b	$.019^b$	NA	.002b	.000b	.000b	.000b	.000b	.000b	.000b	.000b	NA	NA	NA	NA	$.000^b$
	Secure Cup - 1 m (zone 1 and 2)	NA	NA	NA	$.000^b$	$.000^b$	NA	$.000^b$	$.000^b$	$.000^b$	$.000^b$	NA	NA	$.000^b$	NA	NA	NA	NA	NA	NA	NA	NA	NA	NA	NA
	Secure Cup - 1 m (zone 1 and 3)	NA	NA	NA	$.000^b$	$.000^b$	NA	$.000^b$	NA	NA	NA	NA	$.000^b$	$.000^b$	$.000^b$	$.000^b$	$.000^b$	$.000^b$	$.000^b$	$.000^b$	NA	NA	$.000^b$	$.000^b$	$.000^b$

1st Harmonic Ratio	Driving Frequency (Hz)	1300	1350	1400	1450	1500	1550	1600	1650	1700	1750	1800	1850	1900	1950	2000	2050	2100	2150	2200	2250	2300	2350	2400	2450	2500	#
	Secure Cup - 1 m (zone 2)	$.000^b$	$.000^b$	$.000^b$	NA	NA	NA	NA	NA	NA	NA	NA	NA	NA	NA	$.000^b$	$.000^b$	$.000^b$	$.000^b$	$.000^b$	NA	$.000^b$	$.000^b$	NA	NA	NA	26
	Secure Cup - 1 m (zone 1 and 2)	$.015^b$	$.000^b$	$.002^b$	$.000^b$	NA	$.000^b$	$.000^b$	$.000^b$	NA	NA	NA	NA	NA	$.000^b$	$.000^b$	$.000^b$	$.000^b$	$.000^b$	$.000^b$	$.000^b$	$.000^b$	$.000^b$	$.000^b$	$.000^b$	$.000^b$	26
	Secure Cup - 1 m (zone 1 and 3)	$.000^b$	$.000^b$	$.001^b$	$.000^b$	NA	$.000^b$	$.000^b$	$.000^b$	NA	NA	$.000^b$	$.000^b$	NA	$.000^b$	$.000^b$	$.000^b$	$.000^b$	$.000^b$	$.000^b$	$.000^b$	$.011^b$	NA	$.000^b$	$.000^b$	$.000^b$	34

Table title: Accelerometer - Zone Loosening

Figure 5-22: The accelerometer first harmonic ratio comparison for the different simulated conditions. * Mann-Whitney test $p < 0.05$, n = sample size.

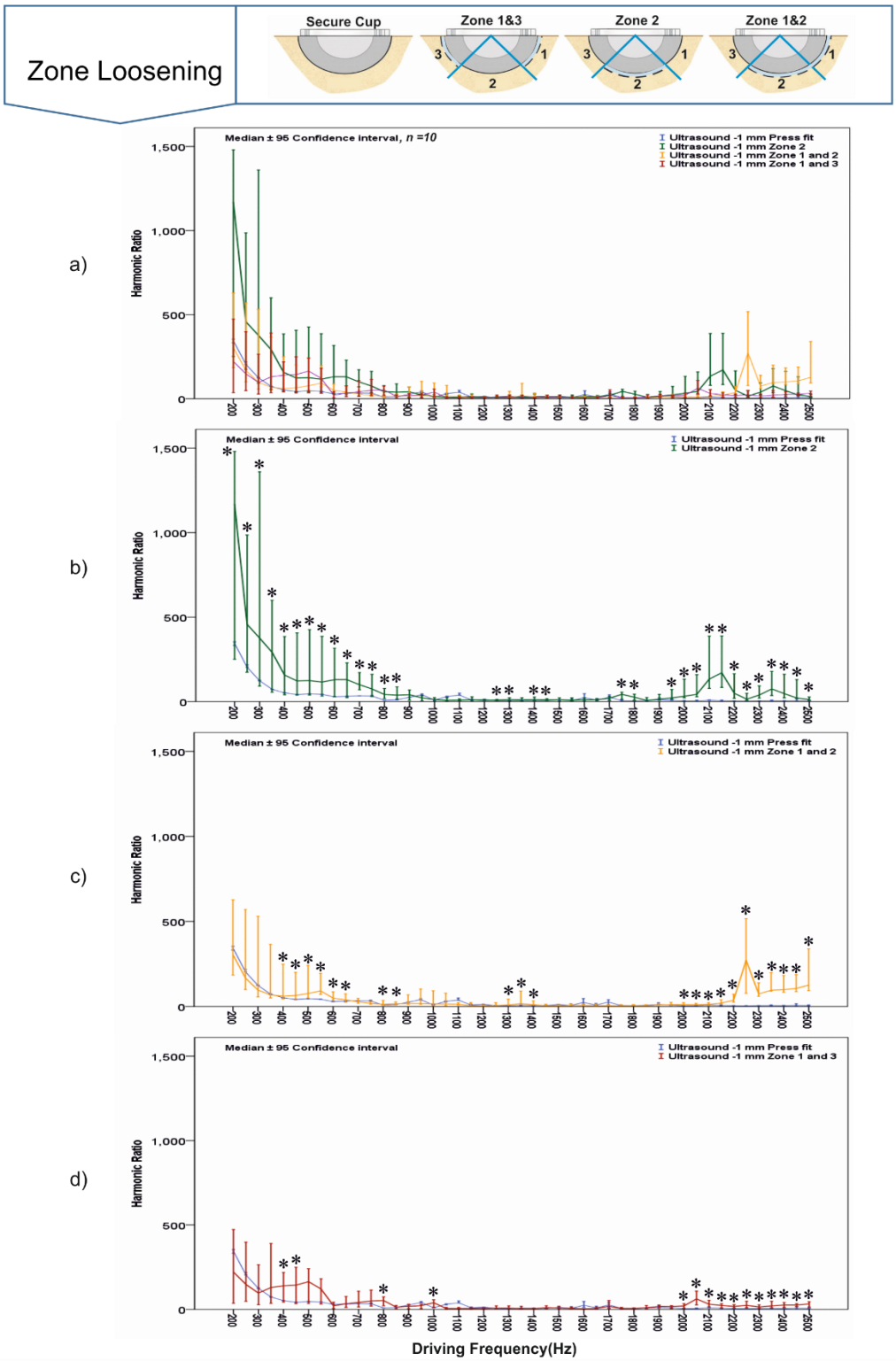

Ultrasound - Zone Loosening

1st Harmonic Ratio	Driving Frequency (Hz)	100	150	200	250	300	350	400	450	500	550	600	650	700	750	800	850	900	950	1000	1050	1100	1150	1200	1250	1300	1350	1400	1450	1500	1550	1600	1650	1700	1750	1800	1850	1900	1950	2000	2050	2100	2150	2200	2250	2300	2350	2400	2450	2500	#
	Secure Cup - 1 m (zone 2)	NA	NA	.023[a]	.019[a]	.023[a]	.023[a]	.023[a]	.023[a]	.023[a]	.023[a]	.002[a]	.023[a]	.002[a]	.023[a]	.000[a]	.000[a]	NA	NA	NA	NA	NA	NA	NA	.002[a]	.023[a]	NA	.005[a]	.000[a]	NA	NA	NA	NA	NA	.000[a]	.000[a]	NA	NA	.000[a]	.000[a]	.000[a]	.000[a]	.000[a]	.000[a]	.000[a]	.000[a]	.000[a]	.000[a]	.007[a]	32
	Secure Cup - 1 m (zone 1 and 2)	NA	NA	NA	NA	NA	NA	.029[a]	.023[a]	.000[a]	.000[a]	.000[a]	.019[a]	NA	NA	.002[a]	.002[a]	NA	NA	NA	NA	NA	NA	NA	NA	.009[a]	.000[a]	.000[a]	NA	NA	NA	NA	NA	NA	NA	NA	NA	NA	.000[a]	.002[a]	.000[a]	.000[a]	.001[a]	.000[a]	.000[a]	.000[a]	.000[a]	.000[a]	.000[a]	.000[a]	22
	Secure Cup - 1 m (zone 1 and 3)	NA	NA	NA	NA	NA	NA	.023[a]	.023[a]	NA	NA	NA	NA	NA	NA	.000[a]	NA	NA	NA	.004[a]	NA	NA	NA	NA	NA	NA	NA	NA	NA	NA	NA	NA	NA	NA	NA	NA	NA	NA	.003[a]	.000[a]	.000[a]	.000[a]	.000[a]	.000[a]	.000[a]	.000[a]	.000[a]	.000[a]	.000[a]	.000[a]	15

Figure 5-23: The ultrasound first harmonic ratio comparison for the different simulated conditions.

* Mann-Whitney test $p < 0.05$, n = sample size.

Ultrasound

The findings of the harmonic ratios results for the ultrasound demonstrate a similar pattern to the accelerometer results. Most of the consistently significant readings occurred at driving frequencies above 1900 Hz (Figure 5-23). With the first harmonic ratio for the ultrasound, when comparing the 1mm zone (2) loosening with the 1mm press fit (secure) conditions it was noticed that the 1mm loose cup had a greater ($p<0.05$) ratio than the secure cup at 32 driving frequencies (200-850 Hz ,1250-1300 Hz, 1400-1450 Hz, 1750-1800 Hz and 1950-2500 Hz)(Figure 5-23b). The 1mm zone (1 and 2) loose condition had a higher ($P<0.05$) first harmonic ratio than the secure state at 22 driving frequencies (Figure 5-23c). In the case of the secure and 1mm zone (1 and 3) loose condition, the 1mm loose condition had a higher ratio ($P<0.05$) over the secure condition at 15 driving frequencies, see Figure 5-23d. The greatest number of ultrasound first harmonic ratio significant differences were for the 1mm zone (2) loose at 32 driving frequencies, followed by the 1mm zone (1 and 2) at 22 frequencies, and finally the zone (1 and 3) loose condition at 15 driving frequencies.

The second harmonic ratio of the ultrasound reading also supported the accelerometer findings, in that the second harmonic ratio echoed the first harmonic ratio results with even more significant readings, especially with the two loosening conditions; 1mm-zone (1 and 2- 1 and 3). The 1mm zone (2) loosening had a higher harmonic ratio ($P<0.05$) over the secure condition at 26 driving frequencies. The 1mm zone (1 and 2) had a second harmonic ratio that was greater ($P<0.05$) than the secure ratio at 27 driving frequencies, with 5 more significant readings than the first harmonic ratio. Also, with 13 more significant readings than the first harmonic, the 1mm zone (1 and 3) condition had a greater second harmonic ratio ($P<0.05$) than the secure condition at 28 driving frequencies. With the ultrasound reading, the second harmonic ratio had the highest significant reading for the 1mm zone (1 and 3) loose condition at 28 driving frequencies, followed by 27 frequencies for the 1mm zone (1 and 2), and finally the zone (2) loose condition with 26 driving frequencies.

In summary, the harmonic ratio method was able to support the spectrum analysis approach through a quantifiable means (the ratio between the fundamental frequency and related harmonics magnitudes). Likewise, it has also supported the findings of the first case study (late spherical loosening), where the highest ratio value was correlated to the greatest loosening at particular frequencies (Table E-3 and Table E-4). Also, the results of the second

harmonic ratio echoed those of the first harmonic ratio, but with more significantly different readings.

5.4.3 Third Case Study Discussion

The third case study, early zone loosening, aimed to create a more clinically relevant acetabular cup loosening simulation. This was to simulate the clinical situation in classifying early acetabular cup loosening in the form of zones, where it is related to the location and degree of associated bone loosening [96, 97]. The simulated loosening condition was created with a 1mm non-uniform zone cup loosening tested within an excitation range of 100-2500Hz. The conditions were 1mm zone (2) loose, 1mm zone (1 and 2) loose and 1mm zone (1 and 3) loose. The excitation range was increased in this case study to accommodate the natural frequency of the polyurethane solid foam and observe its effect on the loosening detection.

The findings of this case study were examined through the spectrum analysis and harmonic ratio methods. The spectrum analysis findings supported the first case study (late spherical loosening). Namely, it was found that the fundamental frequency decreased in magnitude with loosening while the harmonic magnitude increased. Similarly, for the harmonic ratio, the highest ratio value was correlated to the condition of greatest loosening. The simulated zone loosening conditions were distinguished from the secure condition by having more overall significant readings than the early spherical loosening condition. This was probably due to the wider excitation range, especially around the natural frequency of the system. Similar observations had been made for the stem loosening detection, highlighting that frequencies near the natural frequency of the system are more favourable for the vibrometry loosening detection approach [10].

Despite the ability of vibrometry to distinguish the simulated loosening condition from the secure one, the three case studies did not account for the complex hemi pelvis bone geometry. Using the polyurethane foam material was the first step towards the verification of the vibrometry concept using very controlled boundary conditions. The next objective will be to take into account the complex geometry of the hemi pelvis bone and further examine the capability of vibrometry of detecting acetabular cup loosening.

5.5 Overall Discussion

Simulated acetabular cup loosening using a polyurethane Sawbones foam material was used as the first step in testing the feasibility of the vibrometry concept in detection of cup loosening. Vibrometry has been proposed as alternative, more sensitive method for THR loosening diagnosis over the conventional imaging techniques that have historically been used [9]. Pilot clinical studies [9, 10], *in-vitro* [11, 12] and finite element studies [13-15] have all supported the vibrometry approach with positive findings that were mainly focused on the stem component. Others have explored the detection of acetabular cup loosening [8, 9, 16] and were able to distinguish it from the stable condition, but without defining the loosening level detected. Thus, this study is the first to attempt to apply vibrometry in the diagnosis of controlled simulated acetabular cup loosening. The excitation system was adopted in accordance with the existing vibrometry literature [8-12], alongside use of the accelerometer as a measurement method [5, 10-12, 124, 128, 135]. Moreover , the ultrasound measurement approach proposed by Rowlands *et al.* [145] was utilised as an alternative measuring technique. This first objective consisted of three case studies: late spherical loosening, early spherical loosening, and early zone loosening. Each subsequent case study was an attempt to overcome the limitations of the previous studies and create a more clinically relevant set-up.

The first case study was the comparison of late spherical loosening (2mm and 4mm) with the 1mm press fit (simulated secure) condition. For vibrometry to be a valid method of loosening detection it needs to demonstrate the same level of diagnostic ability as radiological techniques. Thus, since the 2mm radiolucent line gap thickness was the minimum reliable detection threshold for imaging techniques, it was essential for the vibrometry to detect the same level of loosening. This stage was therefore labelled as “late” loosening, due to the ability of imaging techniques to detect loosening level at a 2mm radiolucent line equivalent and above. The system response was examined using frequency spectrum analysis with the focus on the fundamental frequency and first harmonic, as highlighted by Georgiou and Cunningham [9] as potential indicators for the implant stability assessment. Initially, the spectrum analysis demonstrated that as the loosening gap became bigger, the magnitude of the fundamental frequency decreased and that of the first harmonic increased. This was then quantified with the harmonic ratio approach, whereby the first harmonic was divided by the fundamental frequency magnitude, with the aim of defining the optimum frequency range for detecting cup loosening using spectrum analysis. The

harmonic ratio findings for the simulated conditions revealed a pattern, in which the greater the radiolucent line simulated gap, the greater the harmonic ratio became. Both measurement methods (accelerometer and ultrasound) were able to quantifiably distinguish between the simulated late loosening from the stable condition. However, the accelerometer method did show better results with regards to the harmonic ratio variation and wider detectable frequency range.

The second case study was the examination of the early spherical loosening scenario. This consisted of two conditions (1mm clear loose and 1mm silicone loose) that were compared to the simulated secure condition (1mm press fit). Through this case study, some of the limitations of the first case study (late spherical loosening) were addressed. Initially, the loosening level was reduced to a 1mm radiolucent line equivalent. The Sawbones density was also reduced to 20 pcf (0.32g/cm3) to closely resemble human cancellous bone mechanical properties. In addition, the measurement sensors were coupled and aligned using an extra frame instead of the clamp system. This was in an attempt to reduce some of the potential measurement errors. Further attention was given to the silicone layer interface by using a specifically manufactured dome shaped with an extended stem. This ensured a better method of holding the dome in place through the silicone curing time and also to guarantee the thickness symmetry of the silicone layer. The analysis of the data of this case study included the second harmonic in addition to the first and the fundamental frequency, these allowing two harmonic ratios to be determined. Initially, when examining these three parameters, the fundamental frequency did not show any significant magnitude reduction in relation to the loose conditions. However, the first and second harmonics did have a significant ($p<0.05$) increase in magnitude for the loosening conditions compared to the simulated secure cup at 15 frequency readings for both sensors. The harmonic ratio results therefore showed that early spherical cup loosening can be detected with the two measurement techniques. The first and second harmonic ratios did significantly ($p<0.05$) increase for the loosening conditions in relation to the simulated secure cup at 11 significant readings for both sensors. In summary, this case study of early spherical cup loosening spectrum analysis findings implies that early loosening may affect the harmonic magnitudes but not the fundamental frequency. The harmonic ratio results indicate that early spherical cup loosening can be detected, but at lower driving frequencies than for the late spherical loosening conditions (2mm and 4mm); parallel findings were also noted in the existing literature [11, 12] for the stem component.

The third case study was to examine early zone loosening which simulated a more clinically relevant loosening. The simulated loosening condition was a 1mm non-uniform zone cup loosening with an excitation range 100-2500 Hz. The conditions were 1mm zone (2) loose, 1mm zone (1 and 2) loose and 1mm zone (1 and 3) loose. The excitation range was increased in this study to accommodate the natural frequency of the Sawbones solid foam and observe its effect on the loosening detection. The spectrum analysis findings supported the results of the first case study (late spherical loosening). The fundamental frequency decreased in magnitude with loosening while the harmonic magnitude increased. Likewise the harmonic ratio, correlated to the greatest loosening. The simulated zone loosening was distinguished from the secure condition at significantly more readings than the early spherical loosening condition. This was probably due to the wider excitation range, especially around the natural frequency of the system. Similar observations have been made for the detection of stem loosening, indicating that frequencies near the system's natural frequency are more favourable for the vibrometry loosening detection [10].

In summary, the findings of this work demonstrated that the vibrometry approach can be utilised to distinguish simulated cup loosening from the secure condition. These findings have confirmed the previous literature [8, 9, 16], which states that the acetabular cup loosening can be observed thought the presence of extra harmonic magnitudes in the frequency spectrum response. Different Sawbones densities were also explored reflecting osteoporosis condition. The alternative ultrasound measurement approach [145] also showed good potential but with less overall significant readings than for the accelerometer. This study differed from previous vibrometry studies in the simulation of the controlled acetabular cup loosening and in the quantitation of the relationship between the harmonic and primary (fundamental) frequency in the form of the harmonic ratio. Moreover, this study defined the minimum loosening levels that can be reliably detected (1mm zone (2) loose) and also the favourable frequency detection range (2000-2500Hz).

5.6 Conclusion

This Chapter has addressed the feasibility of using the vibrometry approach in the detection of acetabular cup loosening. Although spherical and zone simulated cup loosening was distinguished from the secure condition, this study has some limitations that need to be addressed. The use of the polyurethane Sawbones block was an attempt to simplify the set-up complexity and allow the machining of the different simulated acetabular cup loosening.

Initially, the findings of the two case studies, late and early spherical loosening, revealed that vibrometry approach is more reliable at detecting late acetabular cup loosening than early loosening. These findings agree with that of Georgiou and Cunningham [9] and Li *et al.* work who examined late and early stem loosening [11, 12]. However, when more realistic early cup loosening scenarios were simulated in the form of zone loosening the results demonstrated favourable findings in terms of loosening detection, especially around the system's natural frequency. Similar observations were made for the stem loosening detection; highlighting that frequencies near the system's natural frequency are more favourable for the vibrometry loosening detection approach [10].

These preliminary findings support the validity of the vibrometry approach in detecting acetabular cup loosening. However, these initial studies have not taken into account the complex geometry of the hemi-pelvis bone. Also, the excitation and measurement location were closer to the acetabular cup cavity than would clinically be possible for the non-invasive method. Thus, the next two objectives will attempt to tackle these limitations; initially by accounting for the hemi pelvis bone geometry and then by positioning the excitation and measurement system in a more realistic clinical set-up.

Chapter 6 – The Second Objective (Sawbones Hemi-Pelvis Acetabular Cup Loosening)

6.1 Introduction

This Chapter will examine the reliability of vibrometry loosening detection of the cup component, taking into account the bone geometry. The findings for spherical and zone loosening testing (First Objective) supported the vibrometry approach, which was shown to be reliable in detecting acetabular cup loosening. However, the results obtained did not take into account the complex geometry of the hemi-pelvis. Therefore, this next stage will examine cup loosening using a fourth generation hemi-pelvis Sawbones composite bone (Sawbones Europe AB, Malmö, Sweden) with two aims. The first aim is to validate the first objective's findings and the second is to provide a more realistic environment to examine the possible effects on loosening detection (Figure 6-1). The simulated loosening conditions were 1mm and 2mm spherical cup loosening that attempted to replicate the radiolucent line gap. Further explanation of the case study set-up and means of measurement will follow.

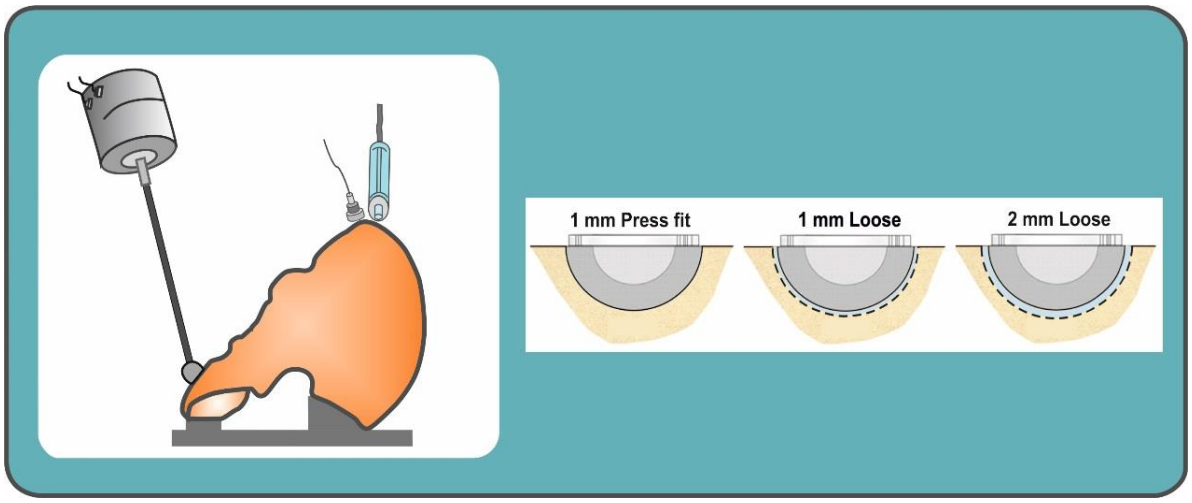

Figure 6-1: The hemi-pelvis three simulated conditions

6.2 Fourth Case Study: Hemi-pelvis acetabular cup loosening

The approach used to account for the bone geometry was to simulate the cup loosening using a Sawbones hemi-pelvis. Vibration analysis had to demonstrate the same level of ability of loosening detection using the hemi-pelvis composite bone compared to the polyurethane block. The previous case studies used Sawbones blocks to accommodate a variety of loosening scenarios as a simplified approach in testing the vibrometry concept. A Sawbones hemi-pelvis was therefore utilised to simulate two loosening situations (Figure 6-1). There were two spherical loosening levels (gap sizes of 1mm and 2mm) that were compared to a secure condition (1mm press-fit), in order to see the effects on the frequency analysis responses and whether a pattern could be observed. The 1mm spherical loosening gap could be attributed to early loosening, while the 2mm gap could be attributed to the late stage. The late and early loosening classification was in relation to what imaging techniques could reliably detect. A 2mm radiolucent line gap thickness is the reliable detecting threshold for imaging techniques [100] and therefore was labelled as late loosening, whereas the 1mm gap is not so easily detected and was therefore labelled as early loosening. This criteria of the early spherical loosening was adopted in an attempt to simplify the acetabular cup loosening complexity and test the vibrometry concept. This loosening model was conducted using two mediums; one in a water bath and another without. The water bath was used as a soft tissue mimicking material for the ultrasound measurement approach in a accordance with the work of Rowlands *et al.* [145].

6.2.1 Materials and Methods

6.2.1.1 The loosening set-up:

The experimental condition for the hemi-pelvis was realised using a fourth-generation composite bone (Hemi-pelvis 3405, Sawbones Europe AB, Malmö, Sweden). The Sawbones pelvis characteristics, according to the manufacturer data, were for the cortical layer; a density of (1.64g/cm3), a compressive strength of 157 MPa, and a compressive modulus of 16.7 GPa. The Sawbones cancellous bone layer had a density of (0.32g/cm3), a compressive strength of 5.4 MPa, and a compressive modulus of 137 MPa. The pelvis was CNC machined to accommodate the desired cup hemispherical geometry diameter. An angle plate and a holding clamp system were utilised, taking into account the recommended favourable cup fixation angle of 40 degrees abduction and 20 degrees of anteversion [214] allowing the cup cavity to be approximately horizontal to enable the ease of machining, as shown in Figure 6-3. A one size 56mm diameter acetabular cup (Trident® Hemispherical HA Solid back shell, Titanium (it-6AI-4V) with Arc Deposit Surface, Stryker Orthopaedics, Mahwah, New Jersey, USA) and a liner (Trident® x3 polyethylene insert UHMWPE) was used for the three conditions replicated in this stage. They were a 1mm press-fit (secure condition), 1mm spherical loosening, and 2mm spherical loosening, as shown in Figure 6-2.

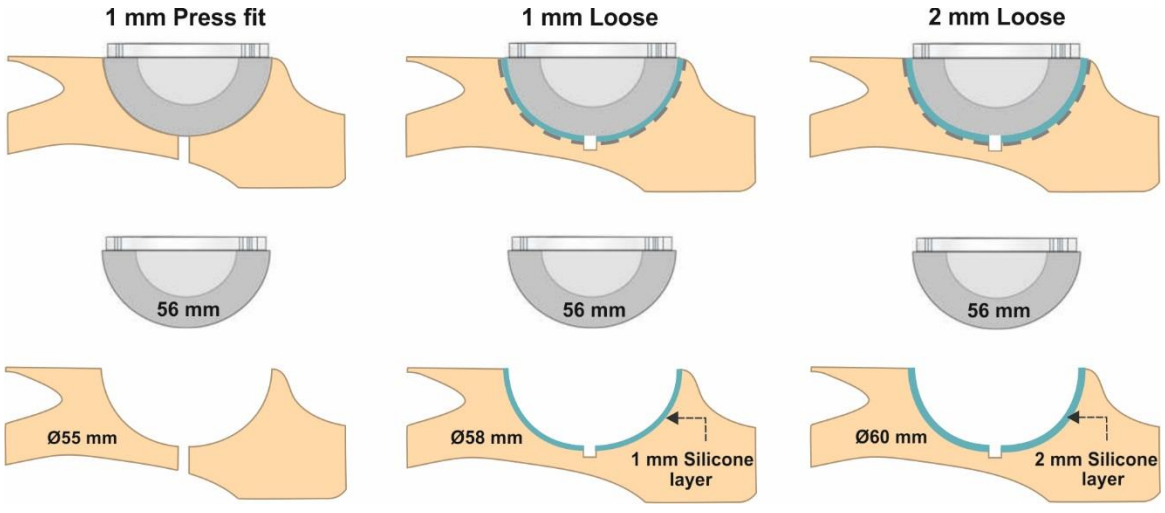

Figure 6-2: The Hemi-pelvis case study three conditions (1mm press-fit, 1mm and 2mm spherical loose)

The secure (1mm press-fit) condition has a hemispherical cavity geometry of 55mm diameter, which was CNC machined to a depth of 28.5mm. The diameter was chosen to be 55mm in order to have a 1mm diameter interface with the used 56mm diameter acetabular cup. The depth of 28.5mm was used to accommodate the depth of the acetabular cup. The depth was realised by using 1mm offset to the cavity, causing it to be 1mm deeper; reaching the 28.5mm depth and preventing the cup from bottoming out. This is as conducted by Crosnier *et al.* [173], in a study of the assessment of press-fit stability. Subsequently, the Stryker acetabular cup (56mm diameter) was inserted into the pelvis prepared cavity (55mm diameter and 28.5mm depth) through repeated impaction using a soft mallet until it was fully seated, in accordance with the existing literature [207-209] utilising the angle plate fixation system (Figure 6-3e). The cavity geometry also had a 5mm diameter width channel that was CNC machined, from the cavity bottom surface through to the opposite bone surface. This was utilised to enable cup removal between the different readings. After each reading, the cup was gently hammered out using a soft mallet in preparation for the system to be disassembled and assembled again with the aid of the markings on the composite bone and the holding table.

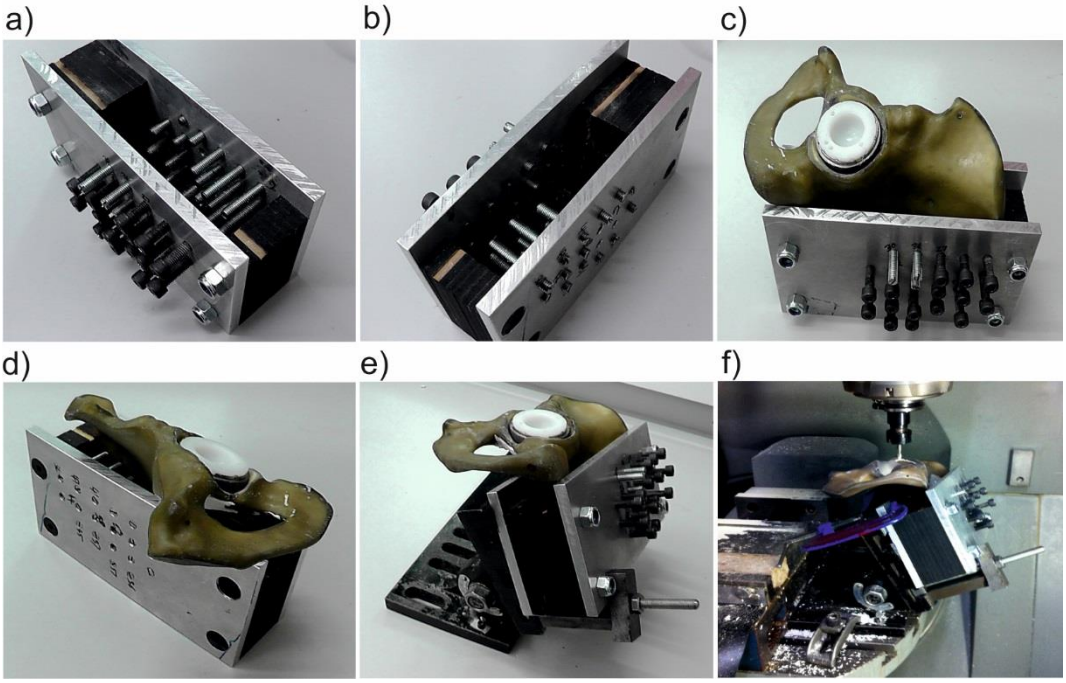

Figure 6-3: The hemi-pelvis acetabular cup cavity CNC machining process, *Graphs a*, *b*, *c* and *d* show the holding base and the screw formation. *Graphs e* and *f* show the same base being held by angle plate in preparation for the machining.

The two spherical loosening conditions mimicked, 1mm and 2mm, were mainly to replicate the radiolucent line clinically observed gap width. The 1mm spherical gap thickness was created using a 58mm cavity diameter with a 56mm Stryker cup diameter size, while the 2mm loosening condition was simulated using a 60mm diameter cavity. These hemispherical cavities, 58mm and 60mm diameters, were produced by CNC machining. The cavity geometry for both cases also included a 5mm diameter channel with a 3mm depth at the lower cavity surface, to control the silicone thickness (Figure 6-4a). A low modulus silicone (EVO-STIK, Bostik Limited, England) was inserted into the loosening gap, in accordance with the existing literature [11, 124, 135] with the intention to replicate the soft fiber interface between the cup and bone surface. A dome shape was manufactured from Nylon 66 (RS Ltd. Northants, UK) and was utilised to control the silicone layer thickness. Two domes were made, both having the same diameter as the inserted cup (56mm diameter) and a 5mm diameter extended stem. However, each had different stem lengths (4mm and 5mm). The difference between the stem lengths (4mm and 5mm) and the cavity channel length (3mm) is to control the silicone thickness (Figure 6-4). A silicone releasing agent (Ambersil Formula 6, Bridgwater Somerset, UK) was spread on the dome surface to prevent the silicone from sticking while being held onto the cavity using a specific handle that was screw-fixed into the dome. After the silicone layer was introduced to the cup cavity, the Nylon dome was held in place for twenty-four hours before testing (Figure 6-5).

The three simulated conditions (1mm press-fit, 1mm and 2mm spherical loosening) were tested using two mediums. One testing set-up was conducted in water in a glass tank while the second was conducted in air, foam supported. The water was intended to replicate the work of Rowlands *et al.* [145] to simulate the soft tissues, in order to see its effect on the ultrasound readings. There was no accelerometer reading when the pelvis was placed in the water bath to eliminate the possibility of water induced damage to the accelerometer. The experiment set-up and how the excitation and measurement system was applied will be explained in the following section.

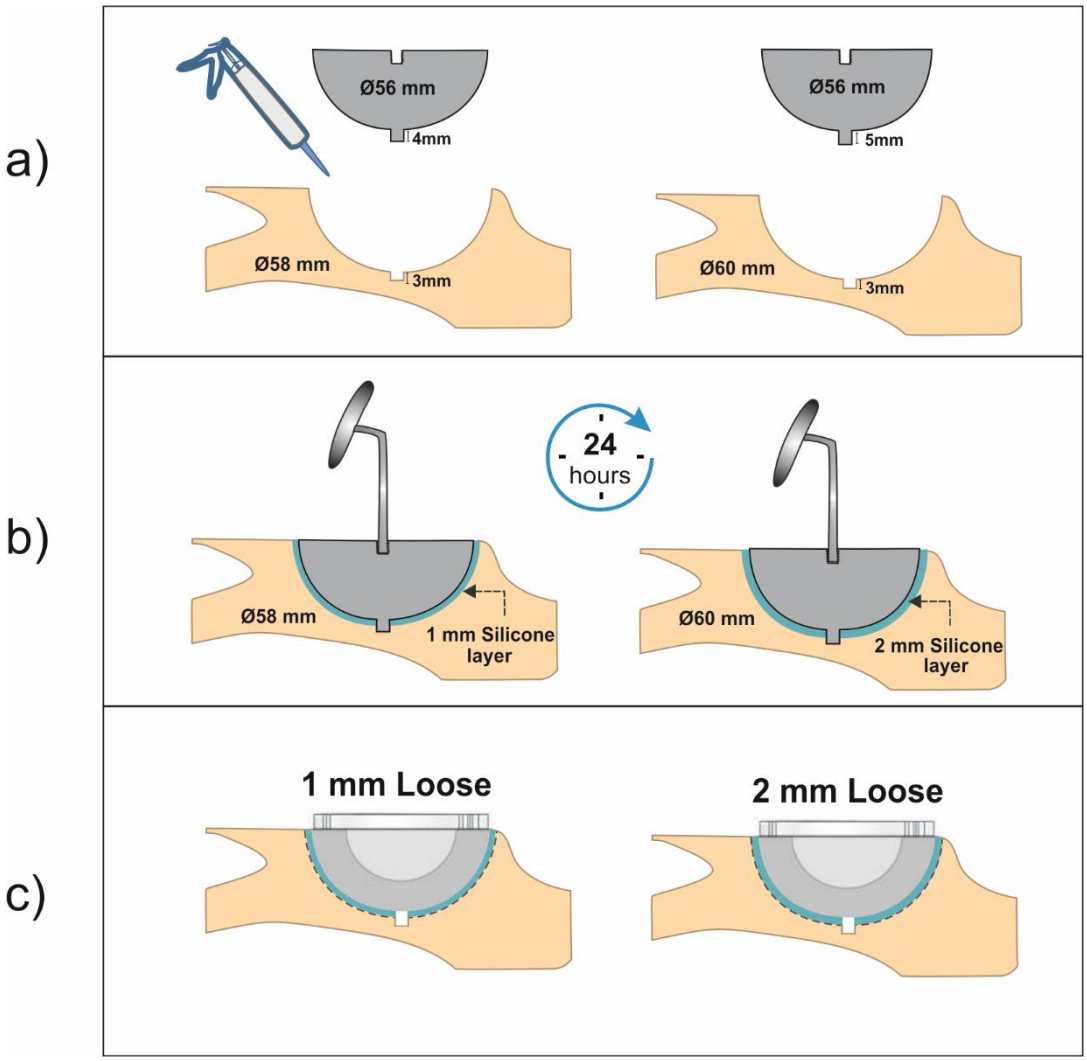

Figure 6-4: Steps taken to mimic loosening that was 1mm and 2mm spherical.

Figure 6-5: The silicone layer set-up, the preparation stage to left and on the right the silicone curing stage

6.2.1.2 Excitation signal

The input excitation signal was sinusoidal wave with a frequency range between 100Hz and 1500Hz, with a step increase of 25Hz and a constant amplitude of 4 Volts (peak – peak). The method of excitation system, input signal characteristics and frequency range was adopted in accordance with the literature [9-12, 145], where researchers have highlighted the prospect of detecting implant loosening using a frequency sweep range below 1500Hz. The mini shaker introduced the input signal at the inferior pubic ramus region of the hemi-pelvis composite bone.

6.2.1.3 Testing set-up

After the different loosening conditions were created using the composite generation hemi-pelvises, they were tested using a foam support set-up. The pelvis in each of the conditions was held in place using a foam material (Neoprene Foam, durometer value 15A-20A) that was coupled together using Velcro (VELCRO® brand heavy duty strip). This coupling approach was adopted over the screw fixation [8] to prevent measurement errors. Preliminary tests of both methods revealed that the screw fixation gave additional unexplained harmonics in the frequency spectrum, as seen in Appendix C (Figure C-1).

The location of the excitation and measurement were defined on the targeted system for accuracy and repeatability. The mini-shaker system introduced the input signal to the hemi-pelvis composite at the inferior pubic ramus region, where the two sensor (accelerator and ultrasound) measurements were taken at the iliac crest. The mini-shaker rod was 25cm long with a spherical tip that was covered with a rubber layer. The length of the rod was to account for both medium conditions and avoid the water affecting the shaker system. The mini-shaker was held in place using holding clamps to neutralise the effect of the shaker weight on the specimen reading. The base of the shaker holding system was also isolated from the targeted system to reduce any involved elements that may have affected the condition responses and reduce the source of measurement errors. The ultrasound probe was also clamped to hold the probe at a constant height in order to apply the ultrasound gel for coupling with the iliac crest of the pelvis. The accelerometer sensor was fixed to the pelvis using threaded steel inserts (PEM® Inserts, UK), providing additional stability (Figure 6-6a).

During testing in water, only the ultrasound probe was used. This was realised using a glass tank (20cm x 20cm x 30cm) that was filled with water at room temperature in a similar way to the work conducted by Rowlands *et al.* [145], who used the ultrasound measurement approach (Figure 6-6b). For the air medium two measurement techniques were applied (accelerometer and ultrasound).

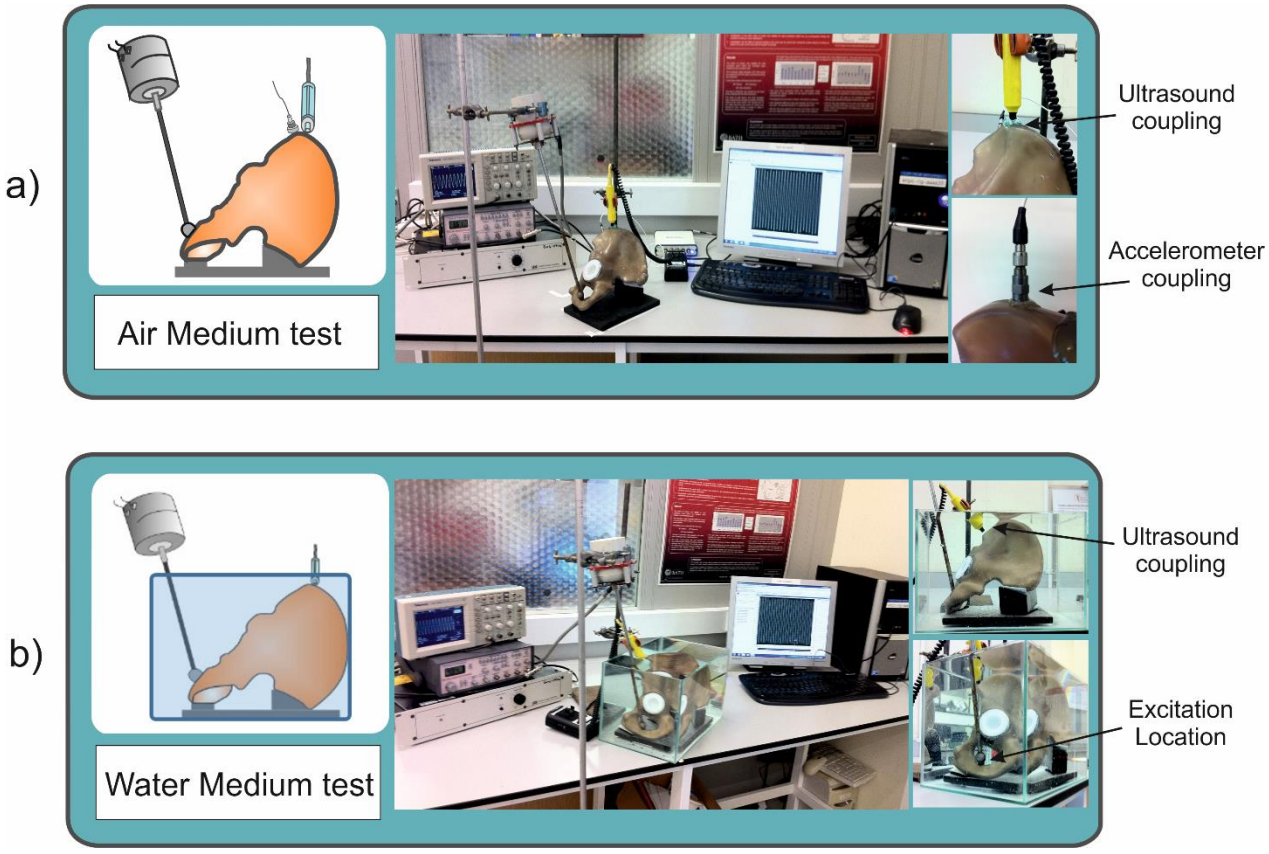

Figure 6-6: The hemi-pelvis set-up (with the two mediums)

6.2.1.4 Testing protocol

After the hemi-pelvises were machined to house the desired simulated loosening conditions, they were tested under the same procedure for repeatability and accuracy. The testing protocol consisted of three stages: pre-testing, testing, and post-testing. The first stage (pre-testing) would involve the preparation of the targeted sample, excitation and measurement system. The second stage (testing) would involve conducting the measurement of the targeted sample. Finally, the third stage (post-testing), involved verifying the collected data and disassembling the set-up in preparation for the second reading phase.

The pre-testing stage comprised three phases of preparation: hemi-pelvis sample, excitation and measurement. The first phase was the preparation of the hemi-pelvis composite bone in the testing set-up. This included the adjustment of the foam support to accommodate the pelvis using Velcro tape. The foam support was coupled to the table using the three Velcro tapes that were 15cm long and 5cm wide. The pelvis was then coupled to the supporting foam at two regions; one at the articular surface of pubis and the second at the articular surface of the iliac crest. In the case of the water medium, the foam base was then secured inside a glass tank (20cm x 20cm x 30cm) using the same approach (Figure 6-7) .The next phase was the preparation of the excitation system that included the verification of the input signal. The signal frequency range and amplitude set-up was verified at each reading using a digital oscilloscope connected between the power amplifier driven by a function generator and the mini-shaker system. The excitation system applied to the target condition was similar for both medium conditions (with water and without). The last phase before testing was the measurement instrument preparation. This was different for the two medium testing set-ups. This required the coupling of the sensors and the operating of the sound and vibration LabVIEW code and data labelling. The measurement sensors for the air medium condition were placed on the iliac crest. The accelerometer was screw-fixed using threaded steel inserts (PEM® Inserts, UK) while the ultrasound was clamped in place in order to hold the probe at a constant height in order to apply ultrasound gel between the sensor and the pelvis for coupling. The water medium was tested only with the ultrasound measurement method and was positioned facing the anterior superior iliac spine. The operation of the sound and vibration code was the next step, which included checking the sensors' sensitivities, sampling frequency and data labelling for each reading. Labelling was used to reflect the

loosening condition, medium (water or air), frequency range, amplitude and the number of the sample reading. This was vital information for the post-processing and analysis stage.

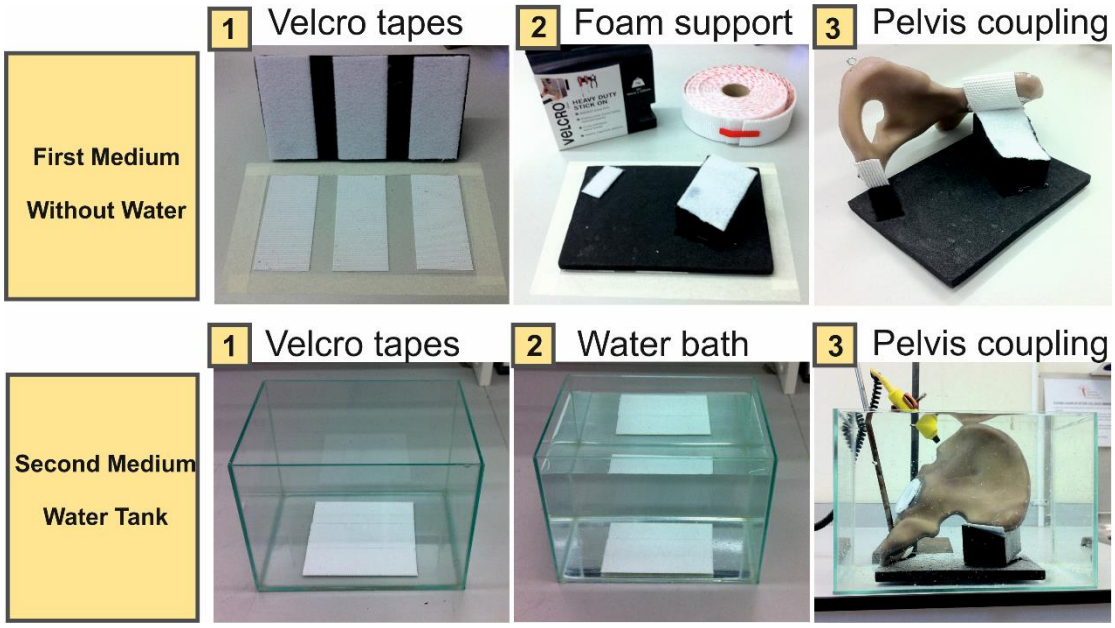

Figure 6-7: The two medium set-up testing

During the testing stage the targeted system was monitored throughout the frequency sweep excitation range. The sensors' coupling and the mini-shaker holding units were closely observed to avert any source of measurement errors. The input signal was also constantly observed to validate the frequency sweep range utilising the digital oscilloscope. This stage was identical for both medium testing set-ups.

The third stage in the testing protocol was post-testing. This stage involved three phases to verify the recorded data after each measurement. The first step was to end the data recoding after the end of the frequency sweep. This was possible through tracking the frequency signal using either the input signal, via the digital oscilloscope, or the response signal through the sound and vibration code in real time. Next, it was necessary to check the recoded data through observing that the time domain signal recording and data labelling were correct. The function generator that was used to drive the mini-shaker was then stopped, in order for the removal of the shaker leading to the change of the hemi-pelvis sample. Finally, the system set-up was taken apart by removing the measurement instrument and changing the Velcro fixation in preparation for the second reading to be conducted.

Each of the three simulated conditions (1mm press-fit, 1mm and 2mm spherical loosening) went through the same processes of experiment set-up and data collection, following the testing protocol. This was followed by the next step, which was measurement and analysis to reveal the frequency spectrum and harmonic ratio for each of the conditions.

6.2.1.5 Sample size

Ten readings of each of the simulated conditions (1mm press-fit, 1mm spherical loose, and 2mm spherical loose) were obtained utilising three hemi-pelvises. Each condition was simulated using a pelvis where, after each reading, the targeted system was disassembled and assembled again with the aid of the markings on the composite bone and the holding table.

6.2.2 Measurement and analysis

6.2.2.1 Result

The hemi-pelvis results are presented using frequency spectrum analysis and the harmonic ratio to display the differences in regards to the measurement methods (accelerometer and ultrasound) and testing mediums (water and air).

6.2.2.1.1 Frequency spectrum analysis

In the first objective, case studies the frequency spectrum analysis were initially examined using the fundamental frequency and the first harmonic magnitude for the late loosening (first case study) and with the addition of the second harmonic with the latter two case studies (early loosening, spherical and zone). In this fourth case study (hemi-pelvis loosening) the third harmonic (F3) was examined in addition to the fundamental and first two harmonics (F2 and F3) used in the earlier case studies. This will allow us to examine if the same pattern of signal behaver in relation to loosening will be reflected in this third harmonic. The analysis will be explained based on the measurement techniques and medium set-up; starting with the hemi-pelvis set-up accelerometer and ultrasound reading, then elaborating on the ultrasound reading with the water medium.

The first parameter for the frequency spectrum analysis was the fundamental frequency (F0) magnitude for the three simulated conditions: 1mm press-fit (secure), 1mm and 2mm spherical loosening. The Sawbones hemi-pelvis set-up testing with the air medium had two measurement methods: accelerometer and ultrasound. The fundamental magnitude, in accordance with earlier work (first objective), reduces as the loosening level increases. When comparing the secure condition with the 1mm loose condition, it was found that the fundamental frequency of the loose condition had a lower magnitude at 6 driving frequencies ($P<0.05$) for the accelerometer reading and at one frequency (200Hz) ($P<0.01$) for the ultrasound reading . Whereas for the 2mm loose condition, the fundamental frequency had a lower fundamental magnitude than the secure condition at 7 frequencies ($P<0.01$) for the accelerometer (Figure 6-8). For the ultrasound, there was no significant magnitude reduction in the reading. The highest significant fundamental reading was for the accelerometer reading in the case of the comparison between the two loosening conditions, 1mm and 2mm, where the 2mm had a lower fundamental magnitude at 20 driving frequencies ($P<0.01$) and at 4 frequencies ($P<0.05$) for the ultrasound reading.

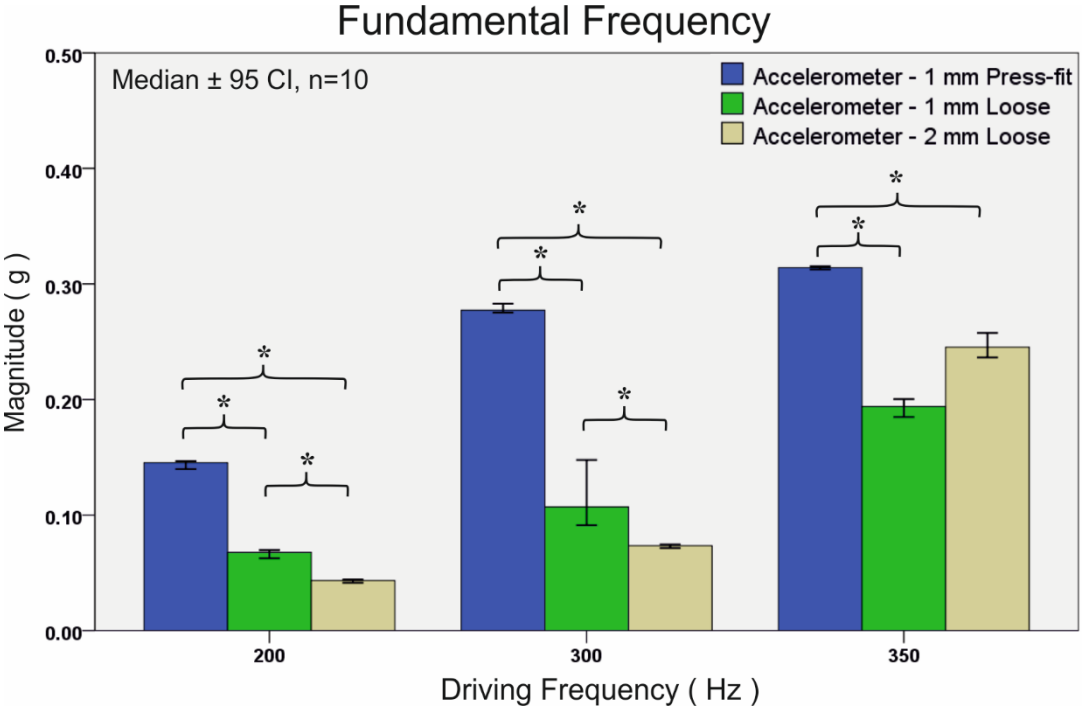

Figure 6-8: The accelerometer fundamental frequency magnitude response to the three simulated condition at the driving frequencies 200 Hz, 300 Hz and 350 Hz. * Mann-Whitney test $p < 0.05$, n = sample size.

The next parameter examined was the first harmonic (F1) magnitude that increased in response to the system nonlinearity (loosening), as noticed in the previous objective's findings. This was the case for the comparison between the 1mm press-fit and the 1mm spherical loose condition. The 1mm loose condition had a higher ($P<0.05$) first harmonic magnitude over the secure condition at 19 driving frequencies for the accelerometer reading and at 22 frequencies for the ultrasound reading. The reading with the highest significant for the first harmonic was for the ultrasound reading for the comparison between the secure and 2mm loose conditions, as shown in Figure 6-9. The 2mm condition had a higher harmonic magnitude at 27 driving frequencies ($P<0.01$) for the ultrasound and at 20 frequencies ($P<0.05$) for the accelerometer. In the case of the two loosening conditions, 1mm and 2mm, the 2mm first harmonic magnitude was higher ($P<0.05$) than the 1mm condition at 8 driving frequencies for the ultrasound reading and at 7 frequencies for accelerometer sensor.

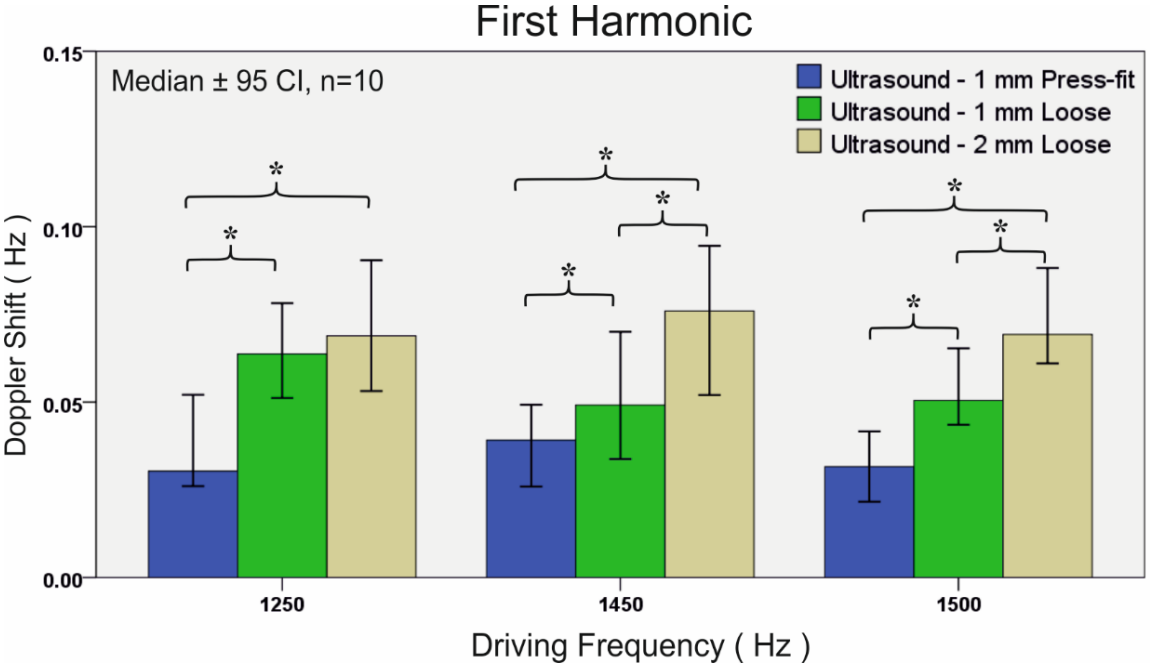

Figure 6-9: The ultrasound first harmonic magnitude response to the three simulated condition at the driving frequencies 1250 Hz, 1450 Hz and 1500 Hz. * Mann-Whitney test $p < 0.05$, n = sample size.

The second harmonic (F2) magnitude also behaved in a similar pattern to the first harmonic (F1), increasing as the loosening level increased. This was observed when comparing the two spherical loosening conditions, 1mm and 2mm. The 2mm condition had a significantly higher ($P<0.05$) second harmonic magnitude at 10 driving frequencies with the accelerometer reading and at 6 frequencies for the ultrasound. The highest significant reading with the second harmonic was for the ultrasound measurements for the comparison between the secure and 2mm loose conditions. The 2mm condition had a higher ($P<0.05$) harmonic magnitude at 27 driving frequencies while for the accelerometer it was at 20 frequencies (Figure 6-10). In the case of the two conditions, secure and 1mm loose, the 1mm second harmonic magnitude was higher than the secure condition at 26 driving frequencies ($P<0.01$) for the ultrasound reading and at 21 frequencies ($P<0.05$) for accelerometer sensor.

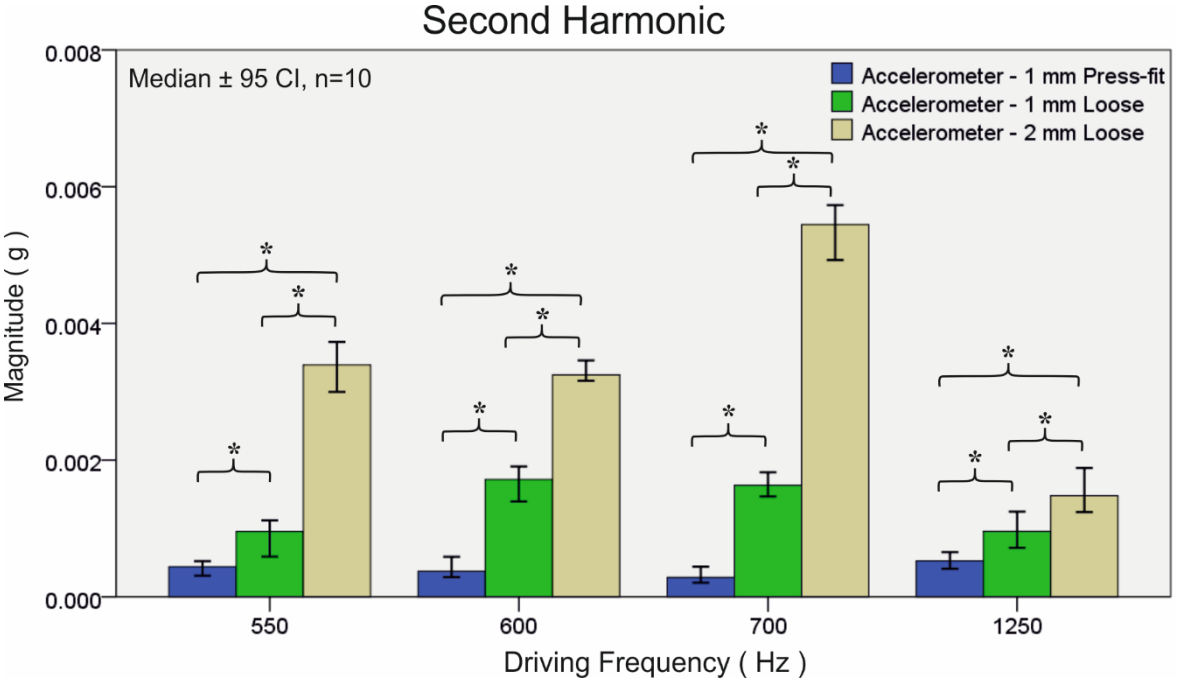

Figure 6-10: The accelerometer second harmonic magnitude response to the three simulated condition at the driving frequencies 550 Hz, 600 Hz, 700 Hz and 1250 Hz. * Mann-Whitney test $p < 0.05$, n = sample size.

The third harmonic (F3) was the last spectrum analysis parameter that behaved consistently with the first (F1) and second (F2) harmonic patterns at certain driving frequencies that are highlighted in Table E-5and Table E-6. When comparing the 1mm press-fit to 1mm loose condition, it was found that the loose condition had a higher ($P<0.05$) third harmonic magnitude at 26 driving frequencies with the ultrasound reading and at 15 frequencies with the accelerometer. For the 2mm spherical loose condition it had a higher magnitude over the secure condition at 27 driving frequencies (200-1500Hz) ($P<0.01$) for the ultrasound reading and 22 frequencies ($P<0.05$) for the accelerometer reading. Likewise, the 2mm loose condition's third harmonic magnitude was greater ($P<0.05$) than that of the 1mm loose condition for the accelerometer reading at 11 driving frequencies and for the ultrasound reading at 4 frequencies, as shown in Figure 6-11.

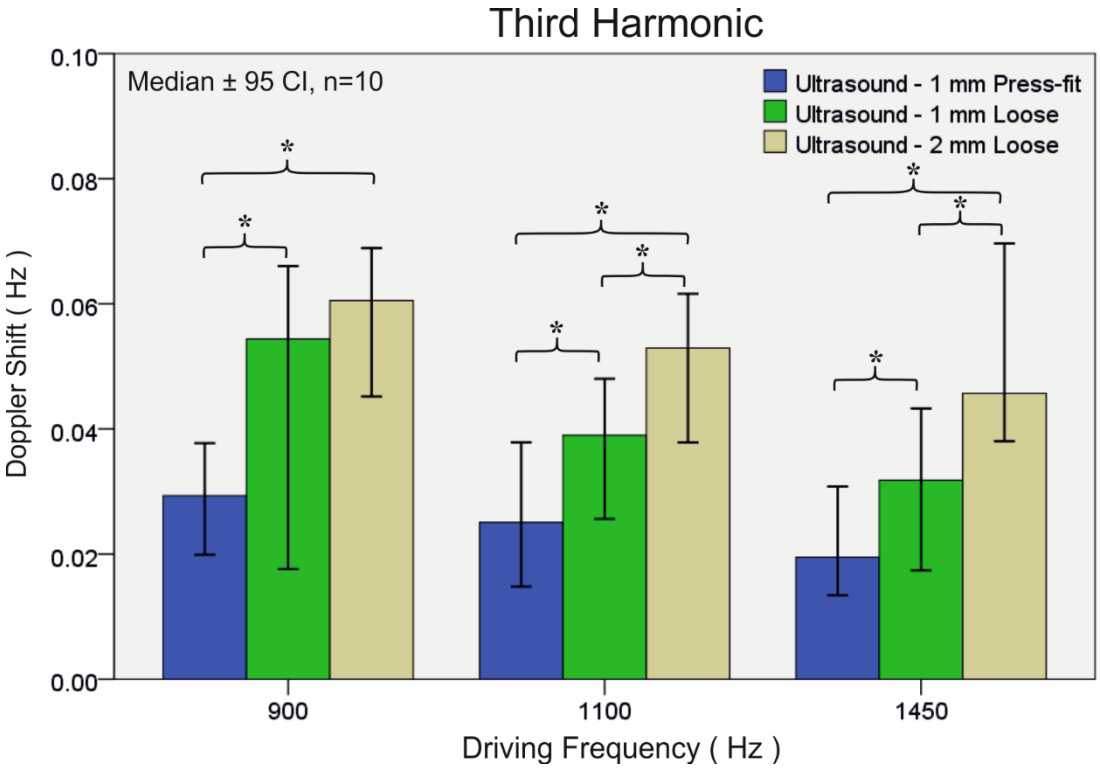

Figure 6-11: The ultrasound third harmonic magnitude response to the three simulated condition at the driving frequencies 900 Hz, 1100 Hz and 1450 Hz. * Mann-Whitney test $p < 0.05$, n = sample size.

In summary, in the spectrum analysis of the Sawbones hemi-pelvis three simulated conditions (1mm press-fit, 1mm and 2mm spherical loosening) were tested using two measurement methods (accelerometer and ultrasound) and the results revealed that even with more a complex bone geometry set-up, cup loosening can be detected via vibrometry. Clearly there are some frequency ranges that are more favourable than others for each spectrum parameter and measurement technique used. When looking at the fundamental frequency parameter, distinguishing between the conditions was possible at 33 significant readings with the accelerometer sensor while at only 5 readings for the ultrasound probe. For the first harmonic magnitude parameter it was possible to distinguish between the conditions at 46 and 57 readings for the accelerometer and ultrasound sensors, respectively. With the second harmonic, a significant distinction between the conditions was possible at 51 reading for the accelerometer and at 59 readings for the ultrasound measurement. The third harmonic gave 48 significantly readings for the accelerometer and 57 for the ultrasound. It should be noted that, the highest significant readings for the fundamental frequency were obtained by the accelerometer, while the ultrasound had the greatest number of significant readings with the magnitudes of the first and second harmonic, as shown in Table E-5and Table E-6 .

Water Medium

The simulated hemi-pelvis conditions were tested under two medium conditions: with water and air. Initially, the hemi-pelvis were tested in air using foam support only followed the water medium. The ultrasound measurement with the water medium will be elaborated on in the following section.

The first parameter examined was the fundamental frequency magnitude, which was lower for the 1mm loose condition than the secure cup at 19 driving frequencies ($P<0.05$). The 2mm condition had a lower ($P<0.01$) magnitude at two frequencies (900 and 950Hz). When comparing the two loosening conditions, 1mm and 2mm, the 2mm loose fundamental frequency did not show a significantly lower magnitude than the 1mm condition.

The second parameter examined the first harmonic (F1) magnitude, which increased as the loosing gap increased. The 1mm loose condition had a higher ($P<0.05$) first harmonic magnitude over the simulated secure cup at 15 driving frequencies, whereas the 2mm condition had a greater ($P<0.05$) first harmonic at 17 driving frequencies. For the two loosening conditions (1mm and 2mm), the 2mm condition had the greatest ($P<0.05$) magnitude over the 1mm condition at 9 driving frequencies.

The second harmonic (F2) magnitude had less significant reading with the water medium but this was still consistent with the air medium in regards to the higher frequency range above 450Hz. The 1mm spherical loose condition had a greater ($P<0.01$) second harmonic magnitude over the simulated secure cup at 19 driving frequencies. Likewise, the 2mm loose second harmonic magnitude was greater ($P<0.01$) at 20 frequencies (500Hz-700Hz and 800Hz-1500Hz). In the case of the two loosening conditions, 1mm and 2mm, the 2mm second harmonic magnitude was higher ($P<0.05$) than the 1mm condition at 5 driving frequencies.

The third harmonic (F3) magnitude for the water medium testing was consistent with the air medium readings, when comparing the two loosening conditions to the secure condition, at driving frequencies above 300Hz. When comparing the two loosening conditions, 1mm and 2mm, to the secure 1mm press-fit condition, it was found that at 25 driving frequencies (300Hz-1500Hz) both of the loosening conditions had a higher ($P<0.05$) third harmonic magnitude over the simulated secure condition. Also, at the driving frequencies 800Hz and

1300Hz, the 2mm loose condition demonstrated a greater ($P<0.05$) third harmonic magnitude over the 1mm simulated condition.

To summarise, the ultrasound spectrum analysis in the water medium did show more significant readings for the fundamental frequency, particularly when comparing the two loosening conditions with the secure condition. For the other spectrum parameters, the significance values were less, such as in the case of the first and second harmonic magnitudes. In the case of the third harmonic, the significant readings were consistent in the frequency range 300Hz-1500Hz. Most of the ultrasound readings were significant and consistent for the two testing mediums at driving frequencies above 900Hz for the first harmonic, above 450Hz for the second harmonic and above 250Hz for the third harmonic magnitude, as shown in Table E-7.

6.2.2.1.2 Harmonic Ratio

The harmonic ratio was the second method of observing the hemi-pelvis acetabular cup loosening variation and included the first, second and third harmonic ratios. The third ratio was adopted in this case study to see if the first two ratio patterns with loosening variations will be echoed. The harmonic ratio findings will be discussed based on the medium set-up and the measurement technique. Initially, the harmonic ratios of the air medium (foam supported) measurements with the two sensors (accelerometer and ultrasound) will be discussed, followed by the water medium harmonic ratios (with the ultrasound sensor only).

With the first harmonic ratio, when comparing the 1mm spherical loose with the 1mm press fit (secure) condition, we noticed that the 1mm loose had a greater ($p<0.05$) ratio than the secure state at 7 driving frequencies for the accelerometer sensor and 4 driving frequencies for the ultrasound ($P<0.01$). Likewise, the 2mm spherical loosening condition had a greater ($p<0.05$) first harmonic ratio over the secure condition at 10 driving frequencies with the accelerometer and at 6 frequencies ($P<0.01$) for the ultrasound. With the two loosening conditions, the 2mm loose had a higher ($P<0.05$) harmonic ratio than the 1mm loose condition at 4 driving frequencies for the ultrasound and at 10 driving frequencies for the accelerometer (Figure 6-12 and Figure 6-13).

For the second harmonic ratio, the 1mm spherical loose condition ratio were higher ($p<0.01$) than the secure condition at 10 driving frequencies (100-400Hz and 850-950Hz) for the

accelerometer readings and at 6 driving frequencies (200-400Hz and 950Hz) for the ultrasound readings. The simulated 2mm loosening condition also had a greater ($P<0.01$) second harmonic ratio over the 1mm press fit condition at 13 driving frequencies for the accelerometer readings and only 5 frequencies for the ultrasound readings ($P<0.05$). Likewise, with the two simulated loosening conditions, the 2mm loose condition had a higher ($P<0.05$) second harmonic ratio over the 1mm loose condition, at 14 driving frequencies for the accelerometer readings and at 5 frequencies for the ultrasound readings.

With the third harmonic ratio, the 1 mm spherical loose condition showed a significantly higher ($p<0.01$) ratio over the secure condition with both measurement methods at particular driving frequencies; 7 for the accelerometer and 5 for the ultrasound. With the ratios obtained using the accelerometer, when comparing the 2mm spherical loose condition to the secure one, it was found that it had a higher ratio ($p<0.01$) at 5 driving frequencies (200-300Hz and 1450-1500Hz) . For the ultrasound this occurred at 7 frequencies (200-400Hz and 1450-1500Hz) ($p<0.05$). In the case of the two loosening conditions, 1mm and 2mm, it was found that the 2mm condition had a higher ($P<0.05$) harmonic ratio for the accelerometer readings at 16 driving frequencies while the ultrasound readings this was at 6 frequencies (500-700Hz and 1300Hz).

In summary, these harmonic ratio results, over a frequency range up to 1500Hz, indicate that acetabular cup simulated loosening can be detected even with a significantly more complex bone geometry using both measurement techniques, accelerometer and ultrasound. This is, however, evident at lower number of readings for the ultrasound method than for the accelerometer. The driving frequency range in which both sensors had the highest consistently significant readings was predominantly between the frequencies of 200-700Hz.

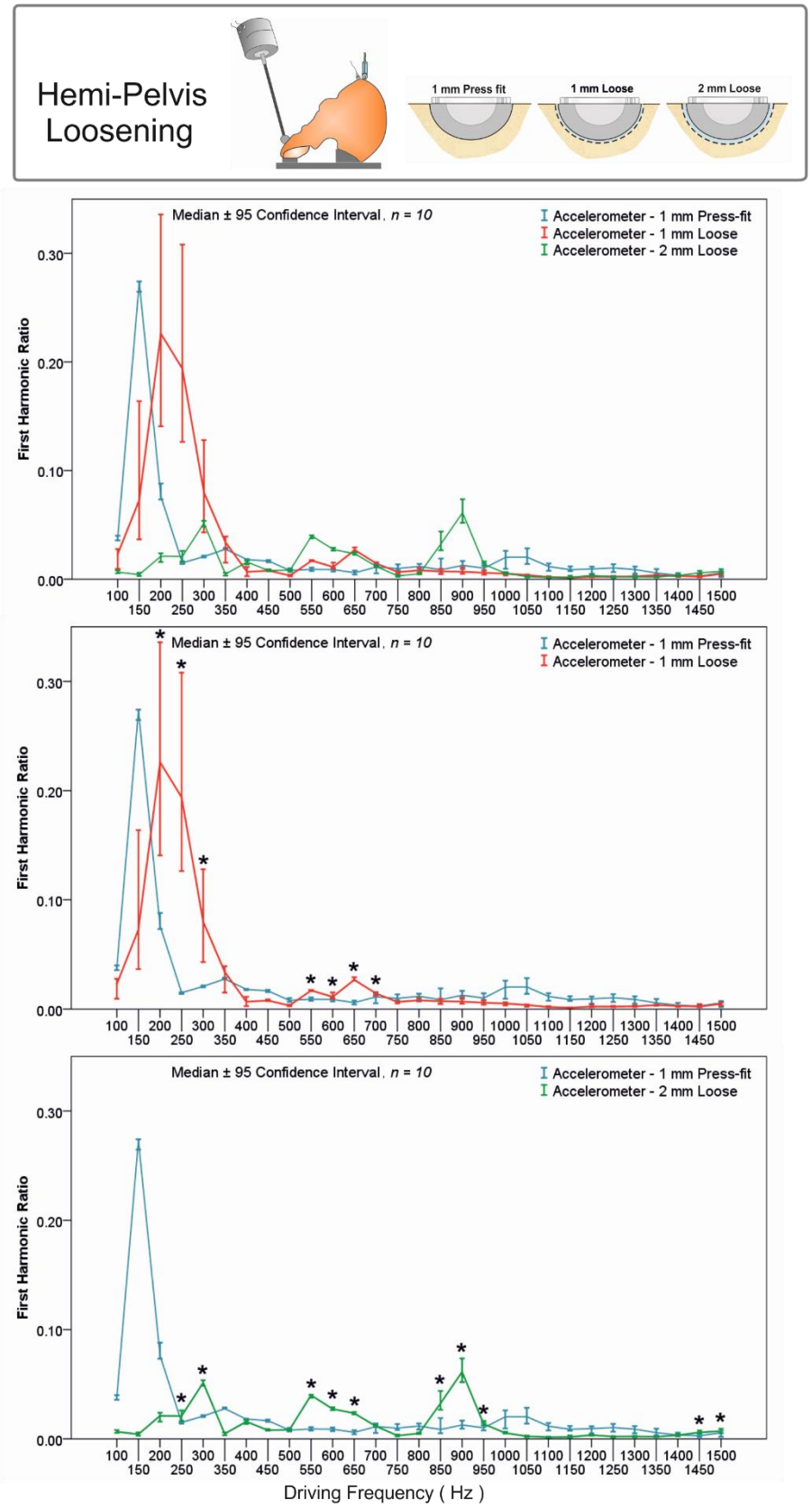

		Accelerometer- Hemi-Pelvis																														
	Driving Frequency (Hz)	100	150	200	250	300	350	400	450	500	550	600	650	700	750	800	850	900	950	1000	1050	1100	1150	1200	1250	1300	1350	1400	1450	1500	#
1st Harmonic Ratio	Secure Cup - 1 mm Loose	NA	NA	.000b	.000b	.000b	NA	NA	NA	NA	.000b	.002b	.000b	.019b	NA	NA	NA	NA	NA	NA	NA	NA	NA	NA	NA	NA	NA	NA	NA	NA	7
	Secure Cup - 2 mm Loose	NA	NA	NA	.002b	.000b	NA	NA	NA	NA	.000b	.000b	.000b	NA	NA	NA	.000b	.000b	.043b	NA	NA	NA	NA	NA	NA	NA	NA	NA	.000b	.043b	10
	1 mm - 2 mm	NA	NA	NA	NA	NA	NA	.000b	NA	.000b	.000b	.000b	NA	NA	NA	NA	.000b	.000b	.000b	NA	NA	NA	.011b	NA	NA	NA	NA	NA	.000b	.005b	10

Figure 6-12: The Accelerometer first harmonic ratio comparison for the different simulated conditions with air medium. * Mann-Whitney test $p < 0.05$, n = sample size.

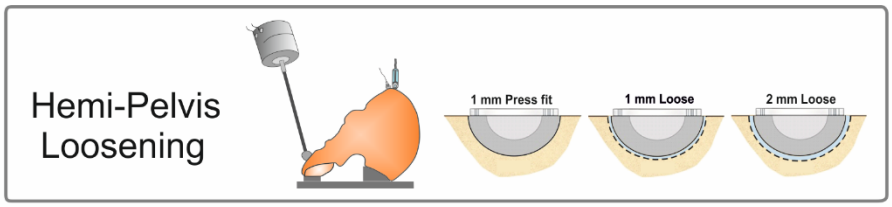

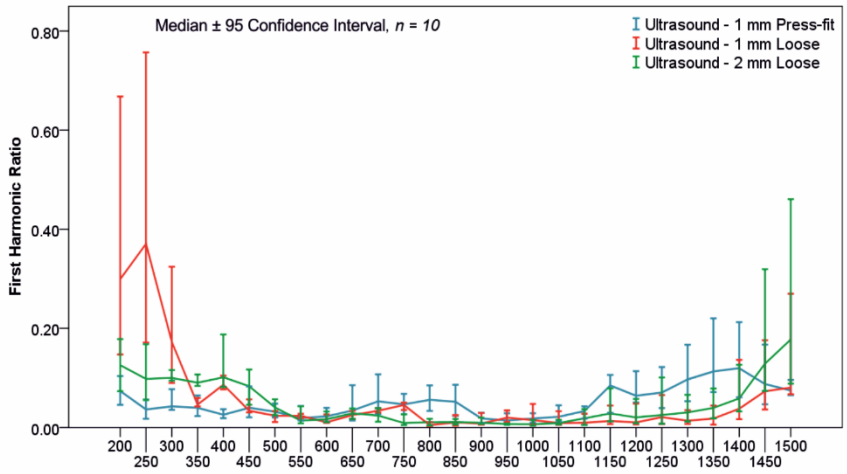

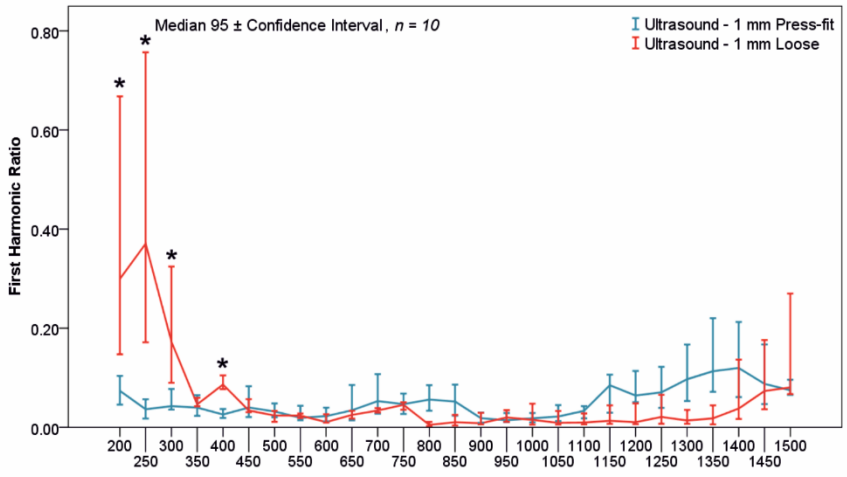

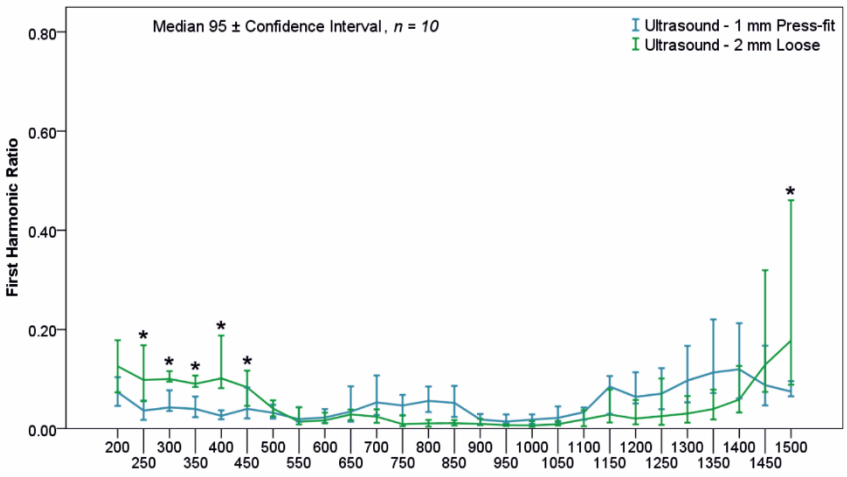

		Ultraound- Hemi-Pelvis																																
	Driving Frequency (Hz)	100	150	200	250	300	350	400	450	500	550	600	650	700	750	800	850	900	950	1000	1050	1100	1150	1200	1250	1300	1350	1400	1450	1500	#
1st Harmonic Ratio	Secure Cup - 1 mm Loose	NA	NA	.000b	.000b	.000b	NA	.000b	NA	NA	NA	NA	NA	NA	NA	NA	NA	NA	NA	NA	NA	NA	NA	NA	NA	NA	NA	NA	NA	NA	4
	Secure Cup - 2 mm Loose	NA	NA	NA	.000b	.000b	.000b	.000b	.009b	NA	NA	NA	NA	NA	NA	NA	NA	NA	NA	NA	NA	NA	NA	NA	NA	NA	NA	NA	NA	.002b	6
	1 mm - 2 mm	NA	NA	NA	NA	NA	.000b	NA	.000b	.015b	NA	NA	NA	NA	NA	.035b	NA	NA	NA	NA	NA	NA	NA	NA	NA	NA	NA	NA	NA	NA	4

Figure 6-13: The ultrasound first harmonic ratio comparison for the different simulated conditions with air medium. * Mann-Whitney test $p < 0.05$, n = sample size.

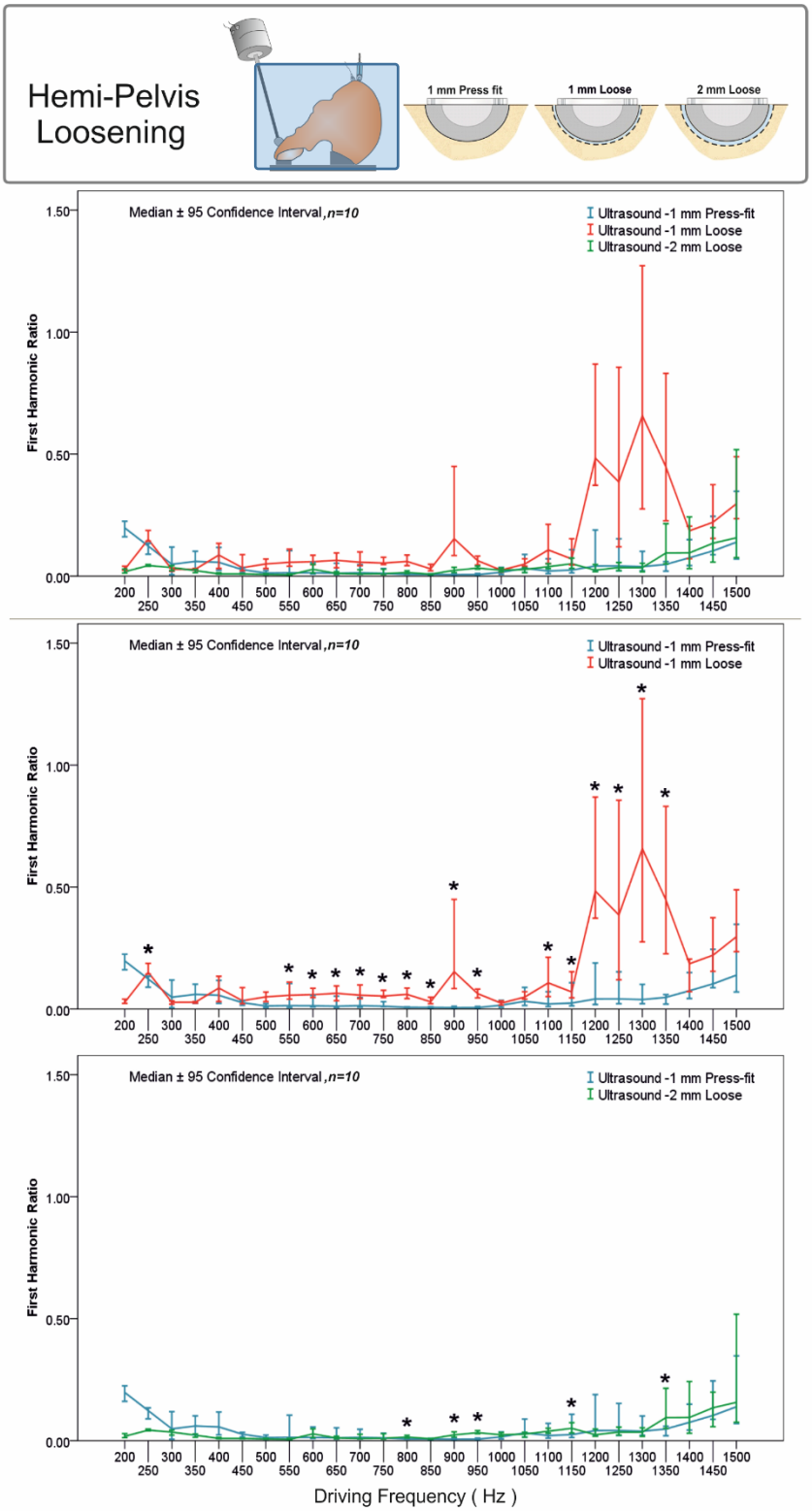

1st Harmonic Ratio	Driving Frequency (Hz)	100	150	200	250	300	350	400	450	500	550	600	650	700	750	800	850	900	950	1000	1050	1100	1150	1200	1250	1300	1350	1400	1450	1500	#
		Ultraound- Hemi-Pelvis (Water medium)																													
	Secure Cup - 1 mm Loose	NA	NA	NA	.000b	NA	NA	NA	NA	.000b	.013b	.002b	.001b	.005b	.000b	.000b	.000b	.000b	.000b	.000b	NA	NA	.009b	.009b	.000b	.000b	.000b	.000b	NA	NA	NA	17
	Secure Cup - 2 mm Loose	NA	NA	NA	NA	NA	NA	NA	NA	NA	NA	NA	NA	NA	NA	.000b	NA	.000b	.000b	NA	NA	NA	.035b	NA	NA	NA	.007b	NA	NA	NA	5
	1 mm - 2 mm	NA	NA	NA	NA	NA	NA	NA	NA	NA	NA	NA	NA	NA	NA	NA	NA	NA	NA	NA	NA	NA	NA	NA	NA	NA	NA	NA	NA	NA	NA

Figure 6-14: The water medium ultrasound first harmonic ratio comparison for the different simulated conditions. * Mann-Whitney test $p < 0.05$, n = sample size.

Water Medium

With testing in the water medium, the first harmonic ratio did show a more significant readings in the case of the comparison between the simulated secure and 1mm loose conditions. The 1mm loose had a higher ($P<0.05$) first harmonic ratio at 17 driving frequencies rather than at 4 frequencies for the air medium. In the case of the 2mm loose condition, the first harmonic ratio was higher ($P<0.05$) than that of the secure condition at 5 driving frequencies, which was one less in significance reading than that of the air medium at 6 frequencies. When comparing the two loosening conditions, 1mm and 2mm, there was no significant difference, as illustrated in Figure 6-14.

The second harmonic ratio of the ultrasound result in the water medium also gave more significant readings for the comparison between the secure and 1mm loose conditions, at 20 driving frequencies while at 6 frequencies for the air medium, where the 1mm loose second harmonic ratio was greater ($P<0.05$) than that of the secure condition. The comparison between the secure and the 2mm loose conditions had 5 significant readings for both medium readings but they were at a higher frequency range for the water medium. The simulated 2mm loose condition had a higher ($P<0.01$) ratio over the secure cup at driving frequencies between 800-950Hz and at 1350Hz. For the comparison between the two loose conditions, there was no significant difference.

The third harmonic ratio, did show an increase in the significant readings of up to four times that of the air medium findings, when comparing the 1mm spherical loose condition to the simulated secure cup. The 1mm loose condition had a greater ($P<0.05$) third harmonic ratio over the secure condition at 24 driving frequencies (200-1000Hz, 1100-1350Hz and 1500Hz). In the case of the 2mm loose condition, the third harmonic ratio was higher ($P<0.01$) than that of the secure condition at 5 driving frequencies (300Hz and 800-950Hz), compared to that of the air medium at 7 frequencies. The 2mm loose condition did show a significantly higher third harmonic ratio over the secure condition at particular driving frequencies, but this was not the case when compared with the 1mm loose condition.

To summarise, the ultrasound harmonic ratio findings for the water medium support the vibrometry approach for the comparison between the conditions (secure, 1mm and 2mm loosening). There was a clear increase in the number of significant readings for the secure vs. 1mm loose comparison for all three harmonic ratios. For the secure vs. 2mm loose conditions, significant readings were closely related (with only three more significant

readings for the air medium) but with a clear shift to higher frequency ranges (for example the second harmonic ratio detection range was between 200-400Hz with air medium and was in the 800-950Hz range for the water medium). However, results obtained for the comparison between the two loosening conditions in the water medium did not follow the previously observed results pattern by having the highest harmonic ratio for the greatest loosening level.

6.2.3 Discussion

Simulated acetabular cup loosening using a composite hemi pelvis bone was the second step in testing the feasibility of the vibrometry concept in detection of cup loosening, taking into account the complex geometry of the pelvis. Initially, the first three case studies supported previous [8, 9, 16] findings and further defined the minimum loosening level that can be reliably detected, along with the favourable frequency detection ranges, utilising a polyurethane Sawbones blocks. This current work had two aims, the first to validate the first objective finding in relation to loosening detection, and the second to provide a more realistic anatomical environment and examine its possible effect on loosening detection. In this case study the frequency analysis was further expanded to cover the third harmonic, to determine if the signal pattern observed in the first two harmonics is mirrored in the third harmonic.

Initial testing was conducted using the air medium (foam supported), in which the spectrum analysis of hemi-pelvis Sawbones had three simulated conditions (secure cup, 1mm and 2mm spherical loosening) using the two measurement techniques (accelerometer and ultrasound). This revealed that even with a more significantly complex bone geometry set-up, cup loosening can be detected via vibrometry. The frequency spectrum had four parameters: the fundamental frequency, first harmonic, second harmonic, and the third harmonic. In agreement with the previous case study, it was noted that as the loosening gap became bigger the magnitude of the fundamental frequency became lower, and the harmonic magnitudes became higher at certain frequencies. This was the case for the fundamental frequency which was able to significantly distinguish between the loosening conditions at 33 readings with the accelerometer, and at 5 readings for the ultrasound. In the case of the first harmonic, 46 significant readings for the accelerometer and 57 for the ultrasound probe were found. Similarly, the second harmonic was significant different at 51 readings for the accelerometer and at 59 readings for the ultrasound measurement. The third harmonic gave 48 significantly different readings for the accelerometer and 57 for the ultrasound probe. The highest number of significant readings for the fundamental frequency were obtained by the accelerometer, while the ultrasound probe had the greatest in terms of harmonic magnitudes. The harmonic ratio findings also agreed with the earlier case study's results, so that the greater the simulated radiolucent line gap became, the greater the harmonic ratio became. However, this was at a smaller number of significant readings for the ultrasound probe than for the accelerometer.

The spectrum analysis obtained with the water medium did show more significant readings for the fundamental frequency, particularly when comparing the two loosening conditions, with the secure condition. Compared to the other spectrum parameters, the number of significant readings were less in the case of the first and second harmonic magnitudes. In the case of the third harmonic, significant readings were consistent in the frequency range between 300 Hz -1500 Hz. Most of the ultrasound readings were consistent for the two testing mediums at driving frequencies above 900 Hz for the first harmonic, above 450 Hz for the second harmonic and above 250 Hz for the third harmonic. The harmonic ratio findings for the water medium set-up support the vibrometry approach for the comparison between the loosening conditions (secure – 1mm and 2mm loosening). There was a clear increase in the number of significant readings for the secure – 1mm loose comparison for all three harmonic ratios. For the secure - 2mm loose conditions, significant readings were closely related (with three more significant readings for the air medium) but with a clear shift to higher frequency ranges. However, results obtained for the comparison between the two loosening conditions in the water did not follow the previously observed results pattern by having the highest harmonic ratio for the greatest loosening level.

In summary, the second objective findings supports the vibrometry approach in the acetabular cup loosening detection. The minimum detected simulated loosening was the 1mm spherical loosening. However, the responses were not consistent across the frequency range for the different parameters, or even for the measurement methods. This may highlight that there are more favourable frequency ranges for each parameter and measurement technique used. The next objective will try to further explore this aspect using different measurement locations and testing mediums.

6.2.4 Conclusion

The second objective aimed to address the previous case study's limitation, to further test the feasibility of the vibrometry approach in the detection of acetabular cup loosening. Despite the fact that the findings of the preliminary work in Sawbones blocks supported the vibrometry approach, it did not take into account the complex geometry of the hemi-pelvis. Thus, a Sawbones hemi-pelvis composite bone was used instead of the polyurethane Sawbones blocks, providing a more realistic anatomical representation of the bone geometry.

The accelerometer frequency spectrum and harmonic ratio results support the previous Sawbones blocks case study findings in correlation to the loosening detection, revealing that even with a significantly more complex bone geometry, loosening can still be detected. However, the detectable frequency ranges were not consistent, possibly due to a difference in the systems natural frequency. The ultrasound approach also demonstrated the same pattern, but with less significant readings for the fundamental frequency and harmonic ratios compared to the accelerometer. However, with the water medium, the number of significant readings for the ultrasound measurement increased for the fundamental frequency and the harmonic ratio, but was unable to show any significant difference between the two loosening conditions. The early loosening condition (1mm spherical loose) had more significantly different readings over the late loosening condition (2mm spherical loose), especially for the fundamental frequency and the harmonic ratios. Clearly there are some frequency ranges that are more favourable in detecting loosening than others both for each spectrum parameter and measurement technique used.

These preliminary findings again support the feasibility of the vibrometry approach of detecting acetabular cup loosening, but are far from conclusive. Because the femoral bone component was not present, the input excitation was not at the previously reported location which was used clinically [9, 10]. Therefore, the femoral bone was added to reflect a more realistic anatomical scenario in the next objective, with the excitation source placed on the lateral femoral condyle.

Chapter 7 – The Third Objective (Sawbones Femur and Hemi-Pelvis Cup Loosening)

7.1 Introduction

The third objective was an attempt to create a more realistic clinical set-up, whereby the excitation source is placed on the lateral femoral condyle, as previously used by Rosenstein *et al.* [10]. The findings of the previous two objectives, using the Sawbones blocks and hemi pelvis, supported the vibrometry approach in detecting controlled acetabular cup loosening. However, the excitation input was not realistically represented, location wise. Thus, this objective will examine acetabular cup loosening using the addition of a femoral composite Sawbones (Sawbones Europe AB, Malmö, Sweden).

This work had two aims. The first was to validate the outcomes of the two previous objectives in relation to loosening detection, while the second aim was to provide a more realistic clinical set-up (Figure 7-1). Hence, the same simulated loosening conditions for the Sawbones hemi-pelvis case study will be adopted for ease of comparison. The simulated conditions were: 1mm press-fit (secure), 1mm and 2mm spherical loosening. Further explanation of the case study set-up and means of measurement will follow.

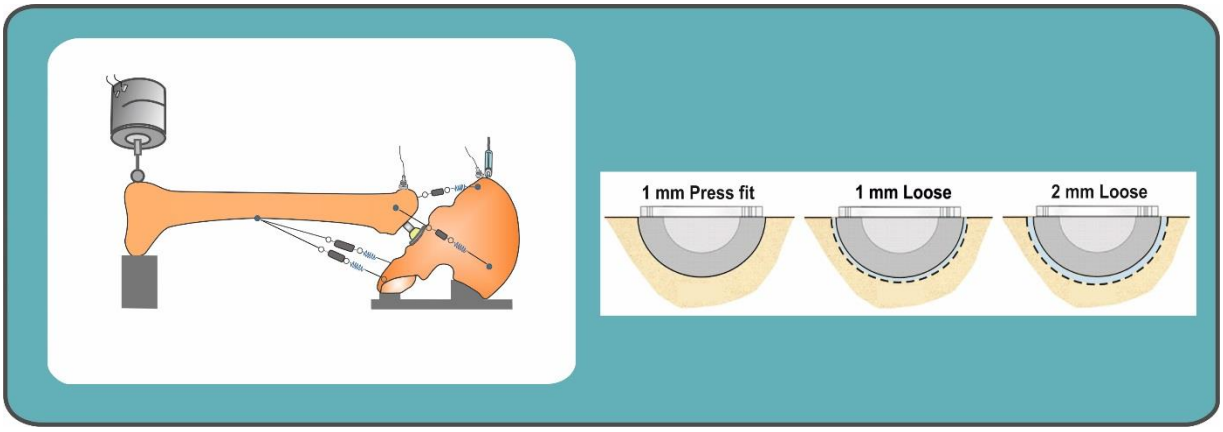

Figure 7-1: The femur and hemi-pelvis Sawbones three simulated conditions.

7.2 Fifth Case Study: Femur and Hemi-pelvis Cup Loosening

The approach in allowing for a more realistic clinical set-up was to add the femoral bone with a fixed femoral component attached. The previous case studies (first, second, third and fourth) used an excitation position that was much closer to the acetabular cup than might be clinically possible. Hence, the femoral composite bone was added in this case study to reflect a more realistic scenario; whereby the excitation source is placed on the lateral femoral condyle as was used *in-vivo* by Rosenstein *et al* [10]. The femoral bone was fixed in position with springs which attempted to replicate the muscle attachments to the hemi-pelvis in accordance with the work of Rieger *et al*.[8]. The femoral bone was also fitted with a cemented stem (Exeter ™ V40 ™ 44mm, 28mm standard head) to replicate a secure femoral component. The simulated conditions were similar to the fourth case study for ease of comparison; 1mm press-fit (secure cup), 1mm and 2mm spherical loosening. A low modulus silicone gel (EVO-STIK, Bostik Limited, England) was also utilised to fill the loosening gap and to replicate the soft tissue interface between the acetabular cup outer shell and bone surface .Similarly, the two medium conditions (with water and air) were applied using an acrylic tank for the ultrasound measuring techniques.

7.2.1 Materials and Methods

7.2.1.1 The loosening set-up:

The femur and hemi-pelvis simulated loosening conditions were realised through the use of a femoral and a hemi-pelvis composite bone (Femur 3406, Hemi-pelvis 3405, Sawbones Europe AB, Malmö, Sweden), a 44mm size stem (Exeter ™ V40 ™, 28mm standard head, Stryker Orthopaedics, USA) and a 56 mm size cup (Trident® Hemispherical HA Solid back shell, Titanium (it-6AI-4V) with Arc Deposit Surface, Stryker Orthopaedics, USA) and a liner (Trident® x3 polyethylene insert UHMWPE). The composite bone characteristics, according to the manufacturer's data, were for the cortical layer a density of (1.64g/cm3), a compressive strength of 157 MPa, and a compressive modulus of 16.7 GPa. For the simulated cancellous bone layer a density of (0.32g/cm3), a compressive strength of 5.4 MPa, and a compressive modulus of 137 MPa. The fourth-generation composite femur was coupled with the hemi-pelvis that accommodated the loosening conditions. The conditions simulated in this case study were identical to the fourth case study (hemi-pelvis) for ease of

comparison; 1mm press-fit (secure condition), 1mm spherical loosening, and 2mm spherical loosening, as shown in Figure 7-1.

The 1mm press-fit condition had a CNC machined cup cavity of 55mm diameter and a depth of 28.5mm. A Stryker cup of 56mm diameter was inserted through repeated impacting using a soft mallet until it was fully seated, in accordance with the existing literature [207-209], utilising the angle plate fixation system. The two spherical loosening conditions, 1mm and 2mm, were simulated using machined hemispherical cavities of 58mm and 60mm diameters, including a 5mm diameter wide channel with a 3mm depth at the lower cavity surface that was utilised to control the silicone thickness. The loosening gaps were filled by a silicone layer (EVO-STIK, Bostik Limited, England) in accordance with the existing literature [11, 124, 135] in order to replicate the soft fibre interface between the cup and bone surface, using a 56mm Nylon 66 dome (RS Ltd. Northants, UK). The silicone thickness was controlled through two Nylon domes with two different extended stem lengths (4mm and 5mm), that were fixed into the cup cavity channel (length 3mm) for a twenty-four hour period to allow silicone healing time, in according with the manufacturer's instructions.

The Exeter stem was cemented into the fourth-generation femoral composite, in accordance with the manufactures surgical protocol. Subsequently, the femoral bone was attached to the pelvis using springs, in an attempt to replicate the attachment muscles in accordance with the work of Rieger *et al.* [8]. They simulated the adductor magnus and adductor longus utilising two springs with a spring constant of 2.26N/mm, while the gluteus medius muscle was replicated using two springs of spring constant = 4.17N/mm. This muscle simulation approach was adopted with the addition of a turnbuckle to control the spring tension through the adjustment of the spring length. The gluteus medius muscle springs had an average tension of 18.6 N (14.39 N for the spring attached close to the iliac crust and 22.88N for the spring attached near the ASIS). The adductor magnus and adductor longus had a tension of 13.2N for both springs. The springs and turnbuckles were held to the composite bone surface through six screw hooks attached with a cord (Braided nylon cord, 0.5mm diameter). The screw hooks were also glued to the composite bone surface for additional bonding. The spring tension was constantly checked throughout the different readings for accuracy and repeatability.

The two medium approaches were also adopted in this case study. Three simulated conditions (1mm press-fit, 1mm and 2mm spherical loosening) were tested using two

mediums. One testing was conducted in water (acrylic tank) while the second was conducted with foam support (air medium). The water medium was to replicate the work of Rowlands *et al*.[145], in order to see its effect on the ultrasound reading. While in the air medium, two accelerometers were used to examine the optimum response measurement location. The experiment set-up and the application of the excitation and measurement system will be explained in the following section.

7.2.1.2 Excitation signal

The excitation signal was introduced at the femoral lateral condyle region with a frequency range between 100Hz and 1500Hz with step increase of 25Hz and a constant amplitude of 4 Volts (peak–peak). The frequency range was adopted for ease of comparison with the results of the fourth case study and location in accordance with the literature [8, 10].

7.2.1.3 Testing set-up

Once the simulated loosening conditions were created, using the composite femur and hemi-pelvis, they were tested using a foam support set-up. The hemi-pelvis was Velcro coupled (VELCRO® brand heavy duty, Polyamide) with a foam support material (Neoprene Foam, durometer value 15A-20A) at two regions the articular surface of pubis and the articular surface of the iliac crest. The Sawbones femur medial epicondyle was also foam supported rather than using clamping [11, 12] or counterbalancing weights [145]. This was in an attempt to prevent the femur bone from the excessive movements observed at lower driving frequencies. The muscle attachment between the pelvis and femur was also put in place before each reading. This was done using a spring constant of 2.26N/mm (for the adductor magnus and adductor longus muscles) and another spring with a constant of 4.17N/mm (for the gluteus medius) as seen in Figure 7-2.

The excitation and measurement locations were fixed for reliability and accuracy. The mini-shaker excitation signal was introduced at the lateral femoral condyle region. The shaker was held in place through a clamping system to isolate the effect of the shaker weight on the specimen reading. The excitation approach was the same for the two mediums (with water and air) with the exception of the use of a longer shaker rod (25cm) for the water medium, in order to ensure the shaker stayed clear of the water. The measurement instruments adopted were different according to the testing medium. During the water medium testing, only the ultrasound probe was used. It was positioned facing the anterior superior iliac spine (Figure

7-2b). While with the air medium (foam support), two accelerometers and an ultrasound probe were used (Figure 7-2a). The ultrasound probe and one accelerometer were coupled at the iliac crest whereas the second accelerometer was located at the greater trochanter of the femur. The use of two accelerometers was intended to determine the optimum location for measuring the response. They were coupled to the Sawbones surface using screw fixation, utilising threaded steel inserts (PEM® Inserts, UK) in order to provide additional stability. The ultrasound was coupled with an ultrasound gel. With the water medium, no gel was needed.

The water medium testing set-up was possible through use of an acrylic tank (70cm x 25cm x 20cm). This tank was filled with water at room temperature until the Sawbones specimens were totally under water. The water was changed between each testing condition, 1mm press-fit, 1mm and 2mm spherical loosening, but not between subsequent readings (for the ten sample readings of each condition).

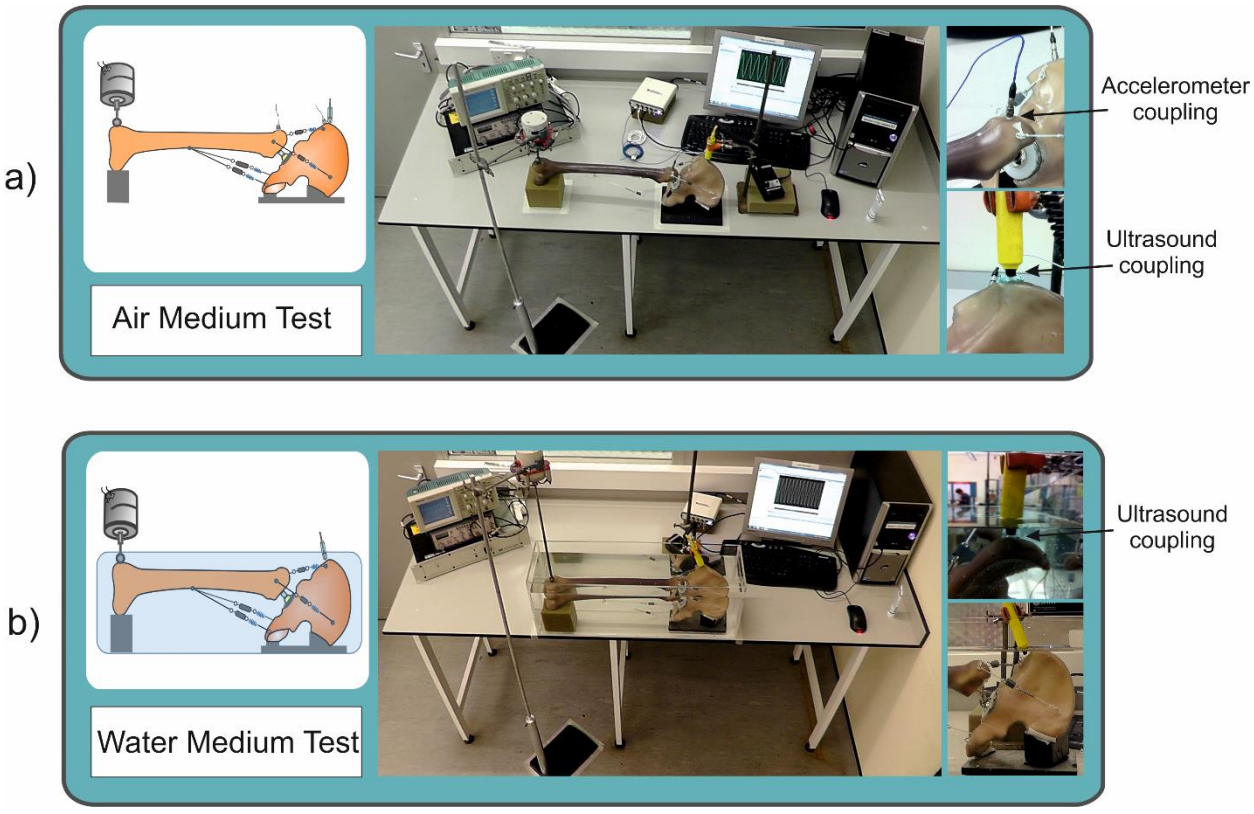

Figure 7-2: The testing set-up for both mediums; a) foam support air medium, b) water medium set-up.

7.2.1.4 Testing protocol

The three simulated conditions were tested following the same pattern for repeatability and accuracy. The testing protocol included three stages: pre-testing, testing, and post-testing. The second and third stags were identical to the hemi-pelvis case study, thus we will only elaborate on the first stage here. The pre testing stage included the preparation of the sample, excitation and measurement system, which was different in accordance with the testing set-up medium (water or air).

The air medium set-up included no water where the femur and hemi-pelvis were only foam supported. In this medium, the preparation of the sample started by initially marking the foam support boundaries so that the subsequent readings would be made in the same location, Figure 7-3. The foam support base was then fixed to the table with three Velcro tapes that were 15cm long and 5cm wide. This was followed by the pelvis being coupled to the foam using the same Velcro tapes. Next, the 28mm stem diameter head was positioned into the acetabular cup liner inner dome utilising the spring attachment. The spring tension was controlled using a turnbuckle placed on the same core, holding the pelvis to the femur. The next phase was the preparation of the excitation system, initially by placing the mini-shaker holder base in the marked location isolating it from the target surface (Figure 7-2). The mini-shaker was then clamped in place to neutralise its weight. It was placed at a right-angle to the femoral condyle, in accordance with the literature [8-10, 145]. This was followed by verifying the input signal amplitude and frequency range via a digital oscilloscope connected between a power amplifier (driven by a function generator) and the mini shaker system. The last phase in the pre-testing stage was the preparation of the measurement instrument. This phase include coupling the sensors and the operating the sound and vibration LabVIEW code and data labelling. The first step was to couple the sensors, where the two accelerometers were screw-fixed onto the Sawbones surface in a defined location using threaded steel inserts (PEM® Inserts, UK). The ultrasound probe was coupled using ultrasound gel. Then, comes the operation of the sound and vibration code that included checking the sensors' sensitivities, sampling frequency and data labelling for each reading. This would be vital information for the post-processing and data analysis stages.

In the water medium set-up, the system was placed under water in an acrylic tank. Initially, the tank was placed in a pre-marked position and Velcro tapes were used for the hemi-pelvis foam support coupling. Then the femur and hemi-pelvis were joined, in a similar way to the previous air medium set-up, and coupled in the acrylic tank. The tank was then filled with water at room temperature until the Sawbones specimens were totally submerged. The excitation system preparation approach was also similar to the previous set-up, with the exception of using a longer rod. This led to the shaker to be clamped at a higher position than in the air medium (Figure 7-3). For this set up (water medium) the measurement system preparation was different as the ultrasound probe was the only measurement method used. The probe was clamped facing the anterior superior iliac spine of the hemi-pelvis and the tip of the probe was totally immersed in water, as shown in Figure 7-3.

In summary, each of the three replicated conditions (1mm press fit, 1mm and 2mm spherical loosening) went through the same protocol of experiment set-up and data collection, following the explained testing protocol. This leads us to the next step, which was the measurement and analysis, revealing the frequency spectrum and harmonic ratio for each of the conditions.

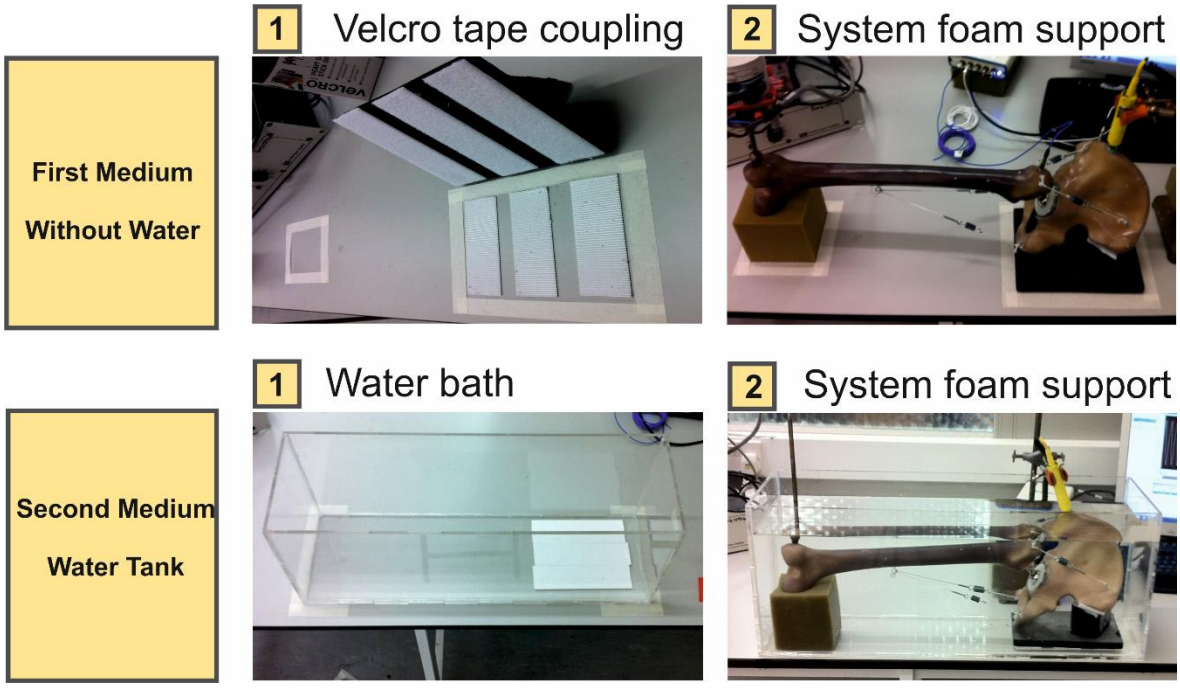

Figure 7-3: The two medium support approaches.

7.2.1.5 Sample size

Three hemi-pelvises and a femoral Sawbones composite bone were utilised to obtain ten sample readings for each simulated condition (1mm press fit, 1mm spherical loose, and 2mm spherical loose). After each reading, the system was disassembled and assembled again with the aid of the marks on the composite bone and the holding table.

7.2.2 Measurement and analysis

7.2.2.1 Results

The responses of the frequency sweep on the femur and hemi-pelvis system will be presented using the spectrum analysis and harmonic ratio approaches. The differences in regards to the medium used (air and water) and the sensor used (accelerometer and ultrasound) will be highlighted.

7.2.2.2 Frequency spectrum analysis

The spectrum analysis consisted of the fundamental frequency (F0), first harmonic (F1), second harmonic (F2) and third harmonic (F3). Initially, the results of the two accelerometers will be compared. The accelerometers were located at the iliac crest of the pelvis and the greater trochanter of the femur (Table E-8 and Table E-9). Then the two ultrasound readings will be compared for the two different mediums (air and water) (Table E-10 and Table E-11). The ultrasound probe was facing the anterior superior iliac spine of the hemi-pelvis for the water medium and facing the iliac crest for the air medium.

Accelerometer

The fundamental frequency (F0) magnitude was the first parameter observed for the 1mm press-fit (secure), 1mm and 2mm spherical loosening conditions. The fundamental magnitude, in accordance with the findings of the previous case studies, reduced as the loosening level increased. This was also observed in this case study at particular driving frequencies that will be highlighted, with the majority being above 500Hz. When comparing the secure condition with the 1mm loose, it was found that fundamental frequency of the 1mm loose condition had a lower magnitude at 8 driving frequencies ($P<0.01$) for the femoral accelerometer reading and at 14 frequencies ($P<0.01$) for the pelvis accelerometer. For the 2mm loose condition, it had a lower fundamental magnitude than the secure

condition at 12 frequencies (P<0.05) for the pelvis accelerometer and at 8 frequencies (P<0.01) for the femoral accelerometer. For the comparison between the 1mm and 2mm loose conditions, the 2mm loose had a lower fundamental magnitude at 16 driving frequencies (P<0.05) for the pelvis accelerometer reading and at 10 frequencies (P<0.01) for the femoral accelerometer reading (Figure 7-4). Hence, the highest significant differences for the fundamental frequency were obtained with the accelerometer located on the iliac crest of the pelvis.

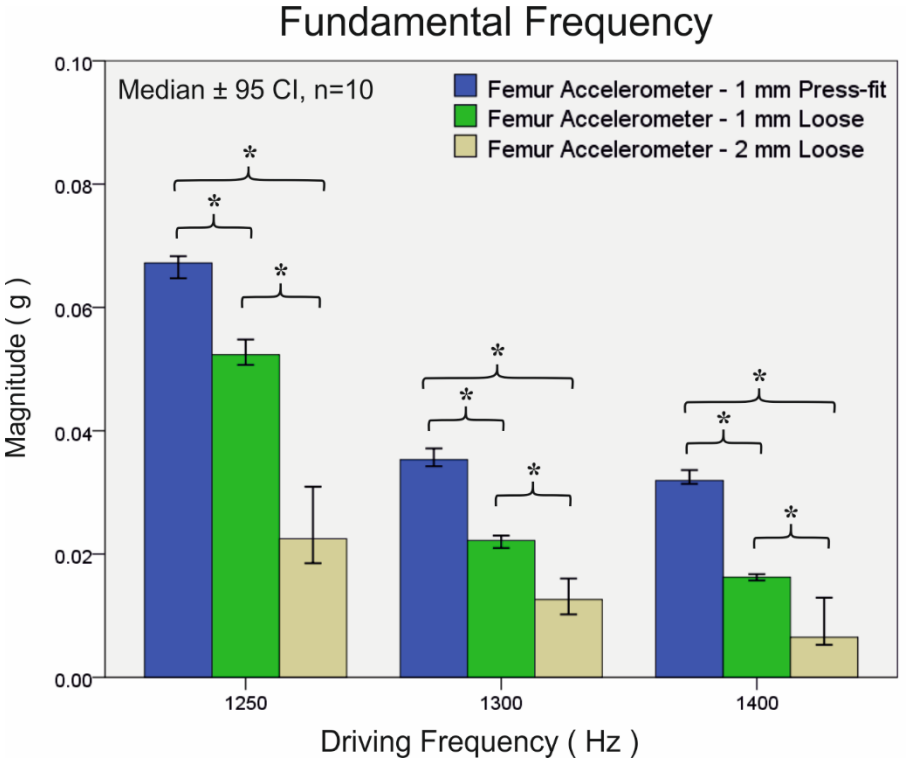

Figure 7-4: The femur accelerometer fundamental frequency magnitude response to the three simulated condition at the driving frequencies 1250 Hz, 1300 Hz and 1400 Hz. * Mann-Whitney test $p < 0.05$, n = sample size.

The second parameter examined was the first harmonic (F1). This behaved in the opposite manner to the fundamental frequency (F0), where the magnitude increased as the loosening level increased. When comparing the two conditions, secure and 1mm loose, the 1mm loose condition had a higher fist harmonic magnitude (P<0.05) at 23 driving frequencies for the femoral accelerometer reading and at 17 frequencies for the pelvis accelerometer reading. The 2mm loose condition also had a higher magnitude (P<0.05) over the 1mm press fit condition, at 20 frequencies for the femoral accelerometer reading and at 15 frequencies for the pelvis reading. However, the comparison between the 1mm and 2mm loose conditions

indicated that only the accelerometer on the pelvis crest was able to detect significant differences at 5 driving frequencies, where the magnitude of 2mm first harmonic was higher than the 1mm condition. The femoral accelerometer had the highest number of significant reading with regards to comparing the two loosening scenarios with the secure condition, as shown in Figure 7-5. However, we were unable to distinguish between the two loosening conditions using the pelvis accelerometer reading.

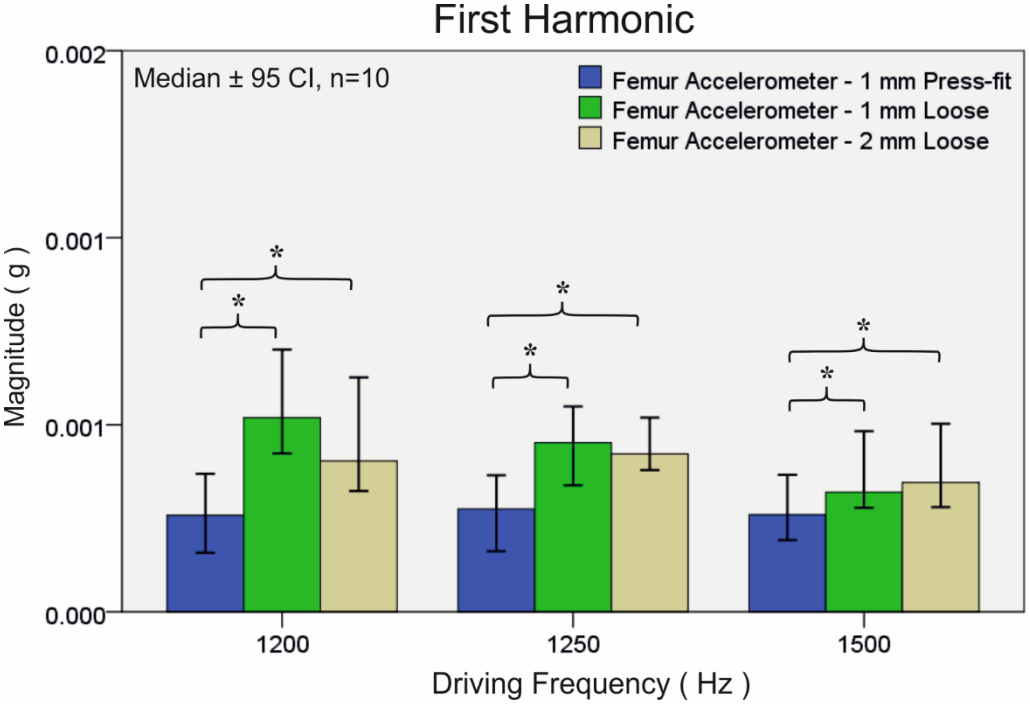

Figure 7-5: The femur accelerometer first harmonic magnitude response to the three simulated condition at the driving frequencies 1200 Hz, 1250 Hz and 1500 Hz. * Mann-Whitney test $p < 0.05$, n = sample size.

The second harmonic (F2) acted in similar manner to the first harmonic (F1), namely, increasing as the loosening level increased. This was the case for the comparison between the 1mm press fit and 1mm loose conditions, where the 1mm loose had a higher second harmonic magnitude ($P<0.05$) at 20 driving frequencies for the femoral accelerometer reading and at 11 frequencies for the pelvis accelerometer reading, as shown in Figure 7-6 . Similarly, the 2mm loose condition had a higher magnitude over the secure condition at 17 frequencies ($P<0.01$) for the femoral accelerometer reading and at 9 driving frequencies ($P<0.05$) for the pelvis accelerometer reading. However, when comparing the 1mm and 2mm loose conditions, the 2mm second harmonic magnitude was only higher ($P<0.05$) with the

femoral accelerometer reading at 2 driving frequencies, there were no significant differences between the magnitudes of the two loose conditions with the pelvis accelerometer readings.

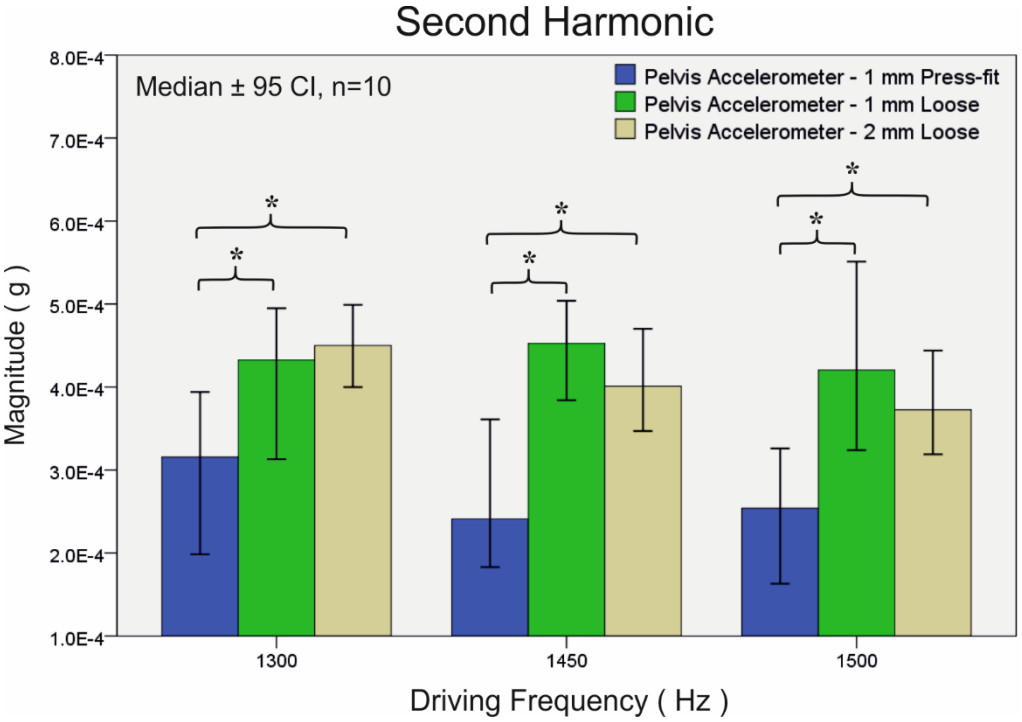

Figure 7-6: The pelvis accelerometer second harmonic magnitude response to the three simulated condition at the driving frequencies 1300 Hz, 1450 Hz and 1500 Hz. * Mann-Whitney test $p < 0.05$, n = sample size.

The third harmonic (F3) was the last FFT parameter examined and to behaved consistently similarly to the first (F1) and second (F2) harmonics. When comparing the secure and 1mm loose conditions, it was found that the 1mm loose condition had a higher third harmonic magnitude ($P<0.05$) at 20 driving frequencies with the femoral accelerometer reading and at 18 frequencies for the pelvis accelerometer reading (Figure 7-7). Also, the 2mm loose condition had a higher magnitude ($P<0.05$) when compared with the secure condition at 18 driving frequencies for the pelvis accelerometer reading and at 16 frequencies for femoral accelerometer reading. In the case of the two loosening conditions, 1mm and 2mm, the 2mm had a higher magnitude ($P<0.01$) over the 1mm condition at a single frequency of 250Hz for the pelvis accelerometer reading.

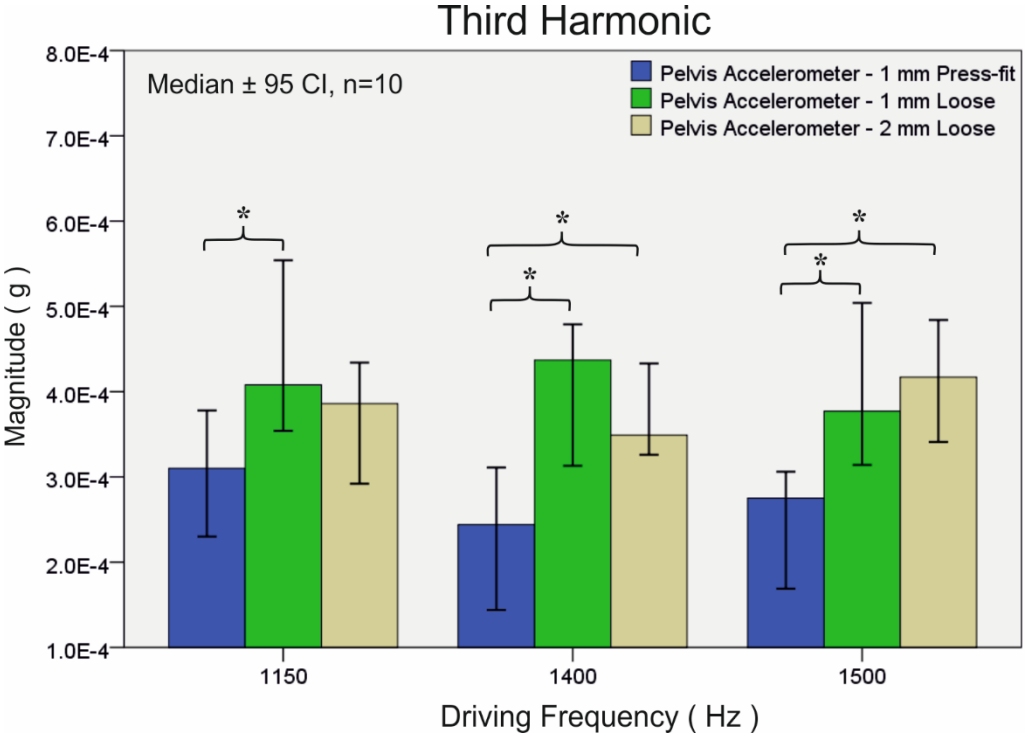

Figure 7-7: The pelvis accelerometer third harmonic magnitude response to the three simulated condition at the driving frequencies 1150 Hz, 1400 Hz and 1500 Hz. * Mann-Whitney test $p < 0.05$, n = sample size.

In summary, analysis of the spectrum analysis of the accelerometer reading over the frequency range up to 1500Hz, show that 1mm and 2mm of spherical cup loosening can be distinguished from the secure condition using the Sawbones femur pelvis set-up. This finding supports the preliminary findings of this study. This also highlighted the favourable frequency ranges for both accelerometer measurement locations (Table E-8 and Table E-9). Distinguishing between the three conditions (secure vs. 1mm loose; secure vs. 2mm loose and 1mm loose vs. 2mm loose) with fundamental frequency readings was possible at 26 significant readings for the femoral accelerometer and 42 readings for the pelvis accelerometer. Similarly, the first harmonic showed 43 significant readings with the femoral accelerometer and 37 for the pelvis accelerometer reading. The second harmonic was also able to distinguish between the conditions at 20 readings for the pelvis accelerometer sensor and at 39 for the femoral accelerometer. Finally, the third harmonic showed 39 and 37 significant readings for both accelerometer sensors, located on the femur and pelvis, respectively. Next, we will compare the ultrasound probe readings for both of the mediums used: with water and air (foam support).

Ultrasound

The fundamental frequency (F0) magnitude was obtained using the ultrasound approach for the different simulated conditions: 1mm press fit (secure), 1mm and 2mm spherical loosening. This was done in the two mediums, with water and air. When the reading is stated without referring directly to the medium, then this refers to the air medium testing. When comparing the secure condition with the 1mm spherical loose cup, it was found that the fundamental frequency of the 1mm condition had a lower magnitude ($P<0.05$) at 8 driving frequencies for the water medium while at 4 frequencies for the air medium (Figure 7-8) . For the 2mm loose condition, it had a lower fundamental magnitude than the secure condition at 22 frequencies ($P<0.05$) for the water medium and at 18 frequencies ($P<0.01$) air water. However, for the comparison between the 1mm and 2mm loose conditions, the 2mm loose had a lower fundamental magnitude at 23 driving frequencies ($P<0.01$) for the air medium and 17 frequencies ($P<0.05$) for the water medium.

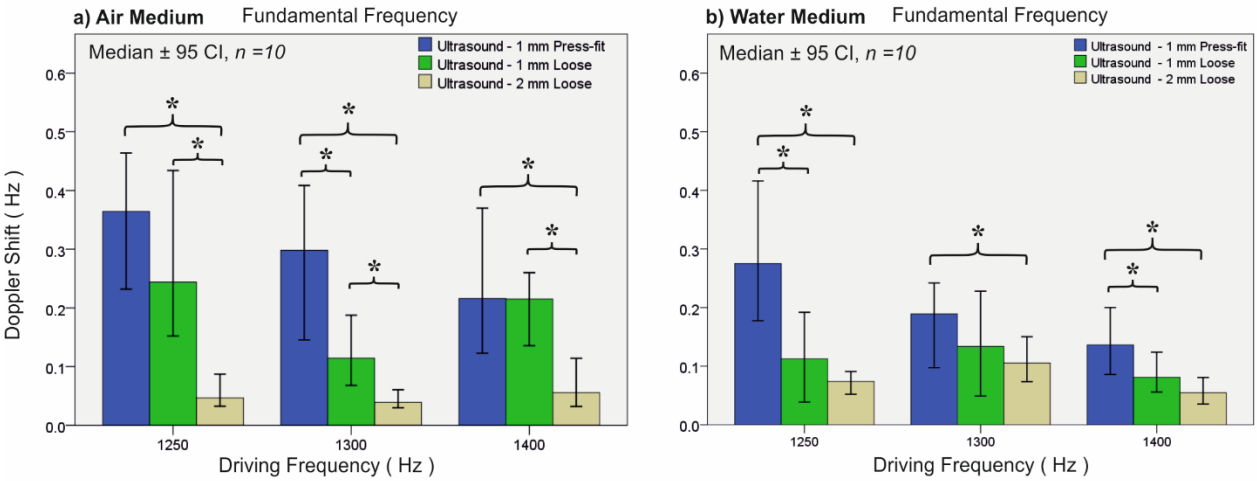

Figure 7-8: The ultrasound fundamental frequency magnitude response to the three simulated condition at the driving frequencies 1250 Hz, 1300 Hz and 1400 Hz with the two mediums a) air medium, b) water medium. * Mann-Whitney test $p < 0.05$, n = sample size.

The first harmonic (F1) ultrasound reading was also able to distinguish between the secure and 1mm loose condition at 25 driving frequencies ($P<0.05$) for the air medium ; with the 1mm loose condition having a higher magnitude at 10 frequencies ($P<0.05$) with the water medium. The 2mm loose condition had a higher first harmonic magnitude than the secure condition at 12 frequencies ($P<0.05$) and at 2 frequencies (200Hz and 250Hz) ($P<0.01$) for the water medium. When comparing the 1mm and 2mm loose conditions, the 2mm loose had a higher first harmonic magnitude only at 1 driving frequency (250Hz) ($P<0.01$) with the water medium.

The second harmonic (F2) magnitude was the next FFT analysis parameter examined. When comparing the secure and 1mm loose conditions, the 1mm loose had a higher second harmonic magnitude ($P<0.05$) at 8 and 19 driving frequencies with the two mediums, water and air, respectively. In the case of the secure and 2mm loose comparison, the 2mm loose condition had a higher magnitude ($P<0.05$) at 12 frequencies and at 3 driving frequencies with the water medium. For the two loosening conditions, 1mm and 2mm, comparison within the water medium allowed us to distinguish the differences at two driving frequencies (200Hz and 250Hz) ($P<0.01$); where the 2mm condition had a higher magnitude than the 1mm loose condition. For the air medium distinguishing between the two loosening condition were not possible.

The third harmonic (F3) was the last spectrum analysis parameter used for the comparison between the simulated conditions. Initially, when looking at the comparison between the secure and 1mm spherical loosening conditions, it was found that the 1mm loose condition had a higher third harmonic magnitude ($P<0.05$) at 17 driving frequencies and at 6 frequencies for the water medium. Accordingly, the 2mm loose condition also had a higher third harmonic magnitude ($P<0.05$) than the secure cup at 3 driving frequencies for the water medium and 14 driving frequencies for the air medium. In the case of the two spherical loosening conditions, 1mm and 2mm, the 2mm condition had a higher third harmonic magnitude ($P<0.01$) over the 1mm condition at two driving frequencies (200Hz and 250Hz) with the water medium only .

In summary, the ultrasound spectrum analysis of the three simulated conditions (1mm press fit, 1mm and 2mm spherical loosening) using the two mediums (water and air), revealed that even with a more complex Sawbones femur-pelvis set-up, cup loosening can be detected. There are evidently some frequency ranges that are more favourable than others for each medium (Table E-10 and Table E-11). When looking at the water medium, distinguishing between the conditions was possible at 47 significant readings for the fundamental frequency (F0), which were all located above the 300Hz range. This was followed by the first (F1) and second (F2) harmonics, at 13 significant readings, and finally the third harmonic (F3) at 11 readings. Testing with the air medium (foam support), distinguishing between the conditions was significant at 45 readings for the fundamental frequency, 37 readings for the first (F1) harmonic and 31 readings for both the second (F2) and third (F3) harmonics. The harmonic ratio will be discussed in the next section, with the aim of quantifying the harmonic magnitude variation with relation to the fundamental frequency.

7.2.2.3 Harmonic Ratio

The harmonic ratio results of the Sawbones femur hemi-pelvis system is presented up until the third harmonic. The ratios (first, second and third) will be given based on the measurement techniques. The harmonic ratio, in accordance with the findings of the previous case studies, increased as the loosening level increased. This was also observed in this work at particular driving frequencies that will be highlighted. Accordingly, the location effect for the accelerometer measurements and the water medium on the ultrasound ratio will be examined in the following sections.

Accelerometer

The accelerometer harmonic ratio was quantified for the first three harmonics in relation to the primary fundamental frequency magnitude. At each driving frequency response, the resultant harmonics were divided by the main fundamental frequency responding to the driving signal. The harmonic ratios were numbered based on the number of the harmonic used (Table E-8 and Table E-9).

The first harmonic ratio was the first parameter for the harmonic ratio where the first harmonic (F1) magnitude was divided by the fundamental frequency magnitude for the simulated conditions: 1mm press fit (secure), 1mm and 2mm spherical loosening. When comparing the secure condition with the 1mm loose, it was found that first harmonic of the 1mm condition had a higher ratio at 18 driving frequencies ($P<0.05$) for the femoral accelerometer reading and at 17 frequencies ($P<0.01$) for the pelvis accelerometer reading. The 2mm loose condition had a higher harmonic ratio than the secure condition at 16 frequencies ($P<0.01$) for both the pelvis and femoral accelerometer readings. When comparing the two loosening conditions, 1mm and 2mm, the first harmonic ratio of the 2mm condition was higher than the 1mm condition at 12 driving frequencies ($P<0.01$) for the pelvis accelerometer reading and at 7 frequencies ($P<0.05$) for the femoral accelerometer reading, as shown in Figure 7-9 and Figure 7-10.

The second harmonic ratio was the second parameter examined. This was to see if the first harmonic ratio pattern, in relation to loosening, was also observed with the second harmonic ratio. This was the case indeed but at slightly lower driving frequencies for the second harmonic ratio. Initially, when comparing the secure and the 1mm spherical loosening conditions, it was found that the loose condition had higher second harmonic ratios at 16

driving frequencies ($P<0.05$) for the accelerometer femoral reading and at 11 frequencies ($P<0.01$) for the accelerometer pelvis reading. This was also true for the 2mm loosening condition, which had a higher second harmonic ratio ($P<0.05$) compared to the secure condition at 14 driving frequencies for the femoral accelerometer and at 13 frequencies for the pelvis accelerometer. Whereas for the two loosening conditions, the 2mm had a higher ratio over the 1mm at 12 and 15 driving frequencies for both accelerometer readings, femoral and pelvis, respectively.

The accelerometer third harmonic ratio also had the same pattern as the first and second ratios. This was evident when comparing the 1mm loose condition with the 1mm secure condition, whereby the loose condition showed a higher third harmonic ratio at 16 driving frequencies ($P<0.05$) for the femoral accelerometer and 14 frequencies ($P<0.01$) for the pelvis accelerometer. The 2mm loose condition had a higher third harmonic ratio at 17 driving frequencies ($P<0.05$) for the pelvis accelerometer and 10 frequencies ($P<0.01$) for the femoral accelerometer. For the two loosening scenarios, the 2mm condition also showed a higher third ratio over the 1mm condition, at 6 driving frequencies ($P<0.01$) for the femoral accelerometer and twice that for the pelvis reading at 13 frequencies ($P<0.05$).

In summary, the two accelerometer (femoral and pelvis) harmonic ratios for the three simulated conditions (1mm press fit, 1mm and 2mm spherical loosening), imply that, even with the more complex Sawbones femur pelvis set-up, cup loosening can still be detected reliably. This supports the findings in the previous case studies in relation to loosening, where it has been shown that as loosening increases the harmonic ratio also increases. When comparing the two loosening conditions to the 1mm press fit secure condition, the femoral accelerometer readings showed slightly more significant readings over the pelvis accelerometer readings. Whereas with the two loosening conditions, 1mm and 2mm, the pelvis accelerometer had the highest number of significant harmonic ratios, even reaching twice the values obtained from the femoral accelerometer readings for the third harmonic ratio.

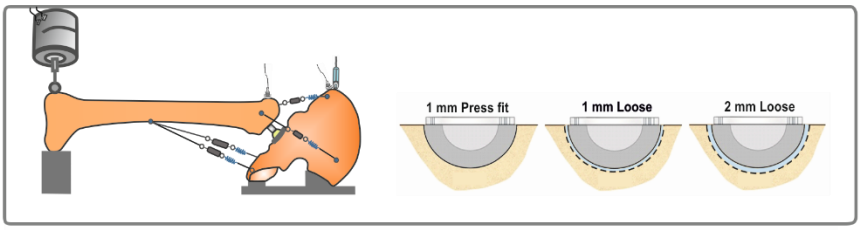

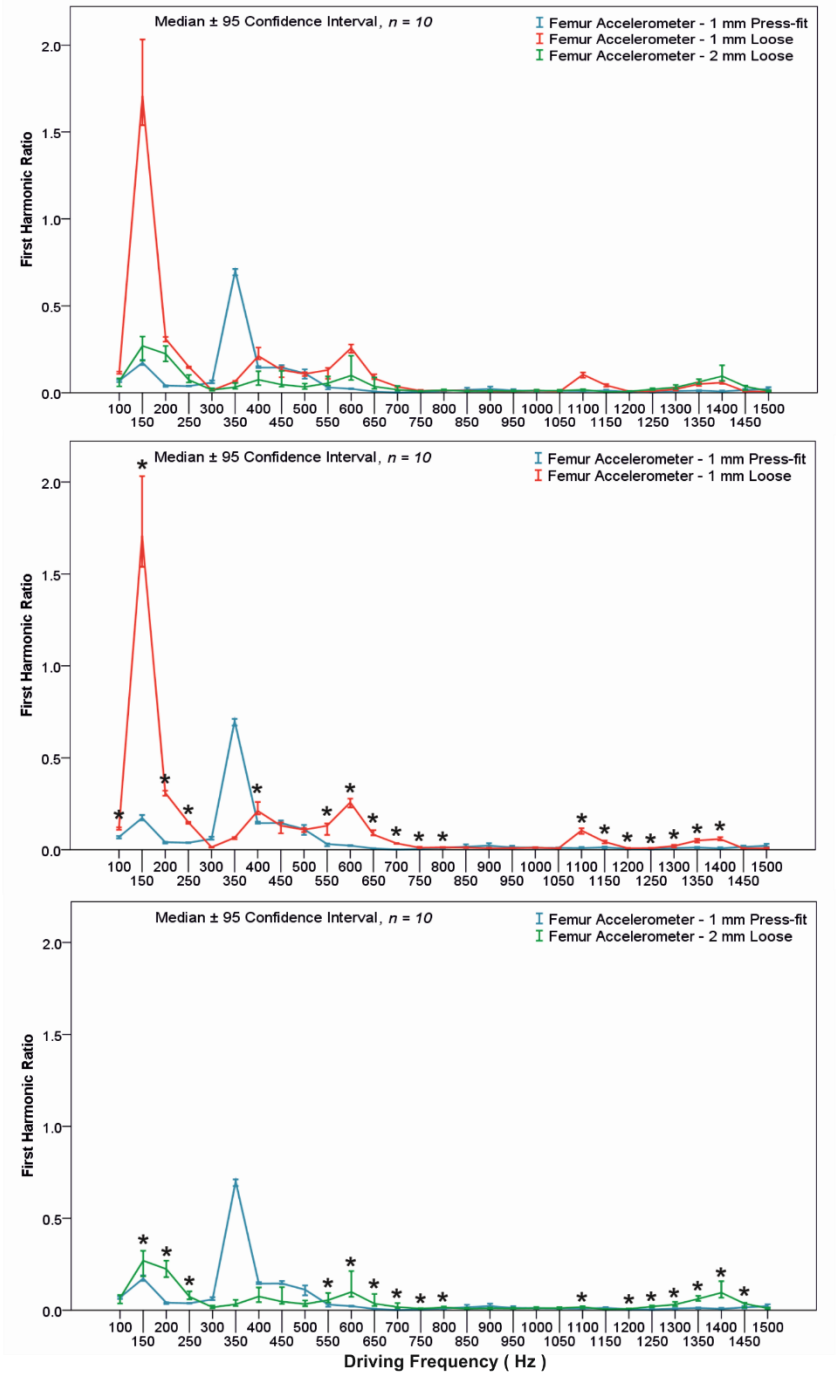

1st Harmonic Ratio	Driving Frequency (Hz)	100	150	200	250	300	350	400	450	500	550	600	650	700	750	800	850	900	950	1000	1050	1100	1150	1200	1250	1300	1350	1400	1450	1500	#
		Accelerometer - Femur																													
	Secure Cup - 1 mm Loose	.000b	.000b	.000b	.000b	NA	NA	.000b	NA	NA	.000b	.000b	.000b	.000b	.000b	.011b	NA	NA	NA	NA	NA	.000b	.000b	.002b	.000b	.000b	.000b	.000b	NA	NA	18
	Secure Cup - 2 mm Loose	NA	.000b	.000b	.000b	NA	NA	NA	NA	NA	.000b	.000b	.000b	.000b	.001b	.000b	NA	NA	NA	NA	NA	.009b	NA	.011b	.000b	.000b	.000b	.000b	.000b	.023b	NA	16
	1 mm - 2 mm	NA	NA	NA	NA	NA	NA	NA	NA	NA	NA	NA	NA	NA	NA	.019b	.000b	NA	NA	NA	NA	.023b	NA	NA	NA	.000b	.099b	.023b	.000b	.000b	.023b	NA	7

Figure 7-9: The femur accelerometer first harmonic ratio comparison for the different simulated conditions with air medium. * Mann-Whitney test $p < 0.05$, n = sample size.

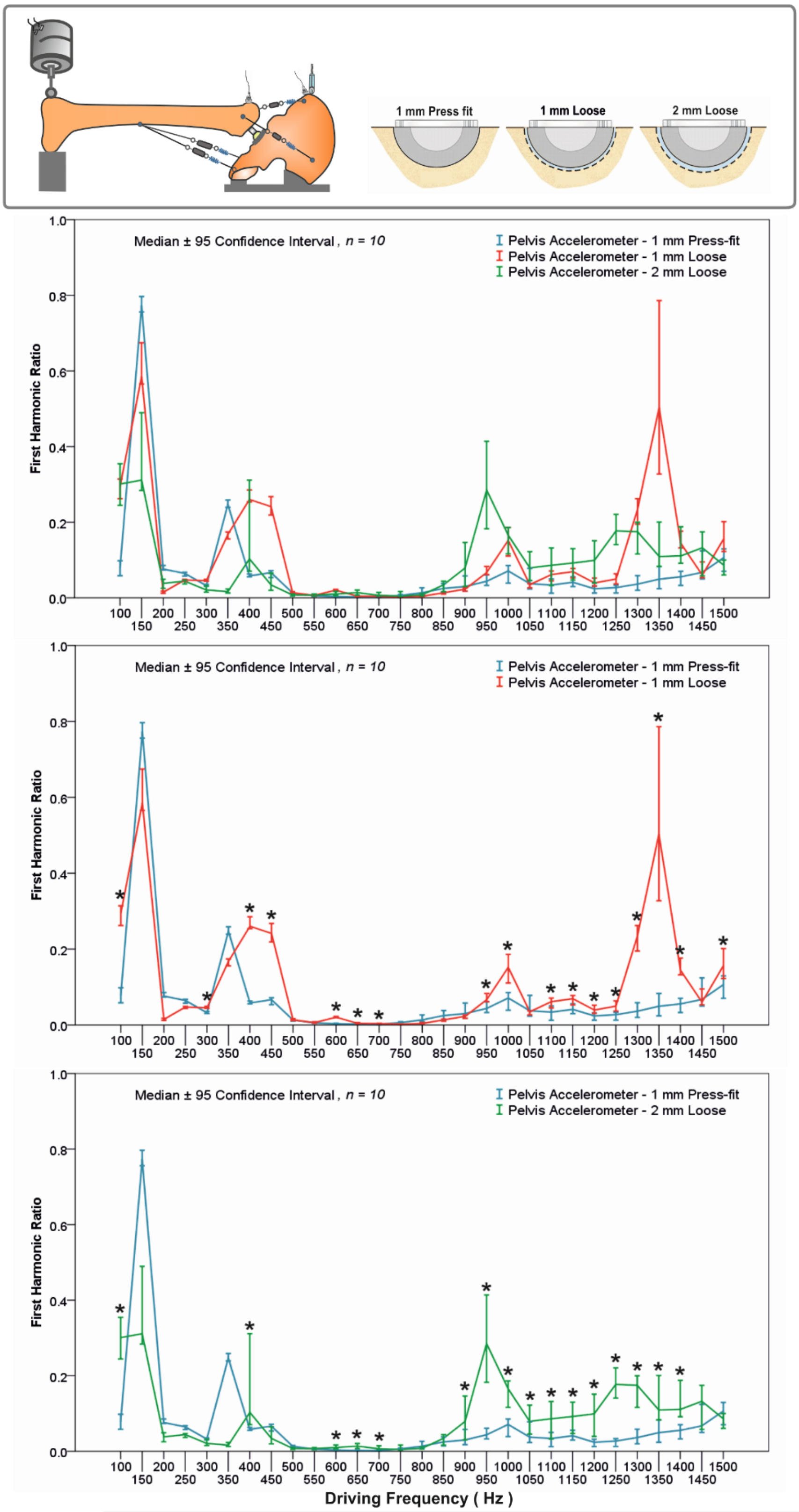

	Accelerometer - Pelvic																													
1st Harmonic Ratio	Driving Frequency (Hz)	100	150	200	250	300	350	400	450	500	550	600	650	700	750	800	850	900	950	1000	1050	1100	1150	1200	1250	1300	1350	1400	1450	1500	#
	Secure Cup - 1 mm Loose	.000b	NA	NA	NA	.001b	NA	.000b	.000b	NA	NA	.000b	.000b	.000b	NA	NA	NA	NA	.002b	.001b	NA	.004b	.000b	.000b	.000b	.000b	.000b	.000b	NA	.002b	17
	Secure Cup - 2 mm Loose	.000b	NA	NA	NA	NA	NA	.000b	NA	NA	NA	.000b	.000b	.000b	NA	NA	NA	.004b	.000b	.000b	.009b	.007b	.003b	.000b	.000b	.000b	.000b	.000b	NA	NA	16
	1 mm - 2 mm	NA	NA	.000b	NA	NA	NA	NA	NA	NA	NA	NA	.000b	.000b	.000b	.001b	.000b	.000b	.000b	NA	.000b	NA	NA	.007b	.000b	NA	NA	NA	.009b	NA	12

Figure 7-10: The pelvis accelerometer first harmonic ratio comparison for the different simulated conditions with air medium. * Mann-Whitney test $p < 0.05$, n = sample size.

Ultrasound

The ultrasound harmonic ratio was also quantified for the two tested mediums, water and air. Most of the consistently significant findings were in the frequency range 500Hz – 1500Hz and sporadically between the 200Hz-450Hz range. The significant readings will be highlighted for each harmonic ratio that correlated with the previous pattern of findings (Table E-10 and Table E-11).

The first harmonic ratio for the ultrasound measurements showed the same pattern in relation to the loosening conditions; whereby as loosening levels increase, the harmonic ratio also increase. Initially, when comparing the secure and 1mm spherical loosening conditions, it was found that the loose condition had a higher first harmonic ratio ($P<0.01$) at 8 driving frequencies for the air medium and 16 frequencies ($P<0.05$) for the water medium. The 2mm loose condition had a higher first harmonic ratio at 20 frequencies ($P<0.05$) for the water medium and at 16 frequencies ($P<0.01$) for the air medium. In the case of the two spherical loosening conditions, 1mm and 2mm, the 2mm condition had a higher harmonic ratio over the 1mm condition at 19 driving frequencies ($P<0.05$) for the air medium and at 12 frequencies ($P<0.01$) with water medium, as shown in Figure 7-11 and Figure 7-12.

The second harmonic ratio was equally able to distinguish between the conditions at significant readings that were closely related to the first harmonic ratio frequency ranges. When comparing the secure and 1mm loose conditions, it was found that the 1mm loose condition had a higher second harmonic ratio ($P<0.05$) at 7 driving frequencies for the air medium and at 12 frequencies with the water medium. The 2mm loose condition had a higher ratio ($P<0.05$) when compared with the secure condition at 19 driving frequencies for both mediums. Of the two loosening conditions, the 2mm had a higher ($P<0.01$) harmonic ratio over the 1mm condition at 20 driving frequencies for the air medium and 13 frequencies with the water medium.

The third harmonic ratio had the ability to distinguish between the simulated condition in both mediums, air and water. When comparing the secure and 1mm spherical loosening conditions, the 1mm loose condition had a higher third harmonic ratio ($P<0.05$) at 7 driving frequencies and 11 frequencies ($P<0.05$) for the water medium. The 2mm loose condition had a higher harmonic ratio at 21 frequencies ($P<0.01$) for the water medium and at 19 frequencies ($P<0.01$) for the air medium. The third harmonic ratio for the 2mm loose

condition also had a greater ratio over the 1mm loose condition at 20 driving frequencies ($P<0.01$) for the air medium and at 16 driving frequencies ($P<0.05$) for the water medium.

In summary, the results from the ultrasound harmonic ratio was able to support the spectrum analysis loosening diagnostic approach. It has highlighted a favourable frequency range (500-1500Hz) for both testing mediums, air and water. Generally, with the water medium, there were a larger number of significant differences with the two loosening conditions compared to the secure condition. For the two loosening conditions however, the highest number of significantly differences reading were for the air medium.

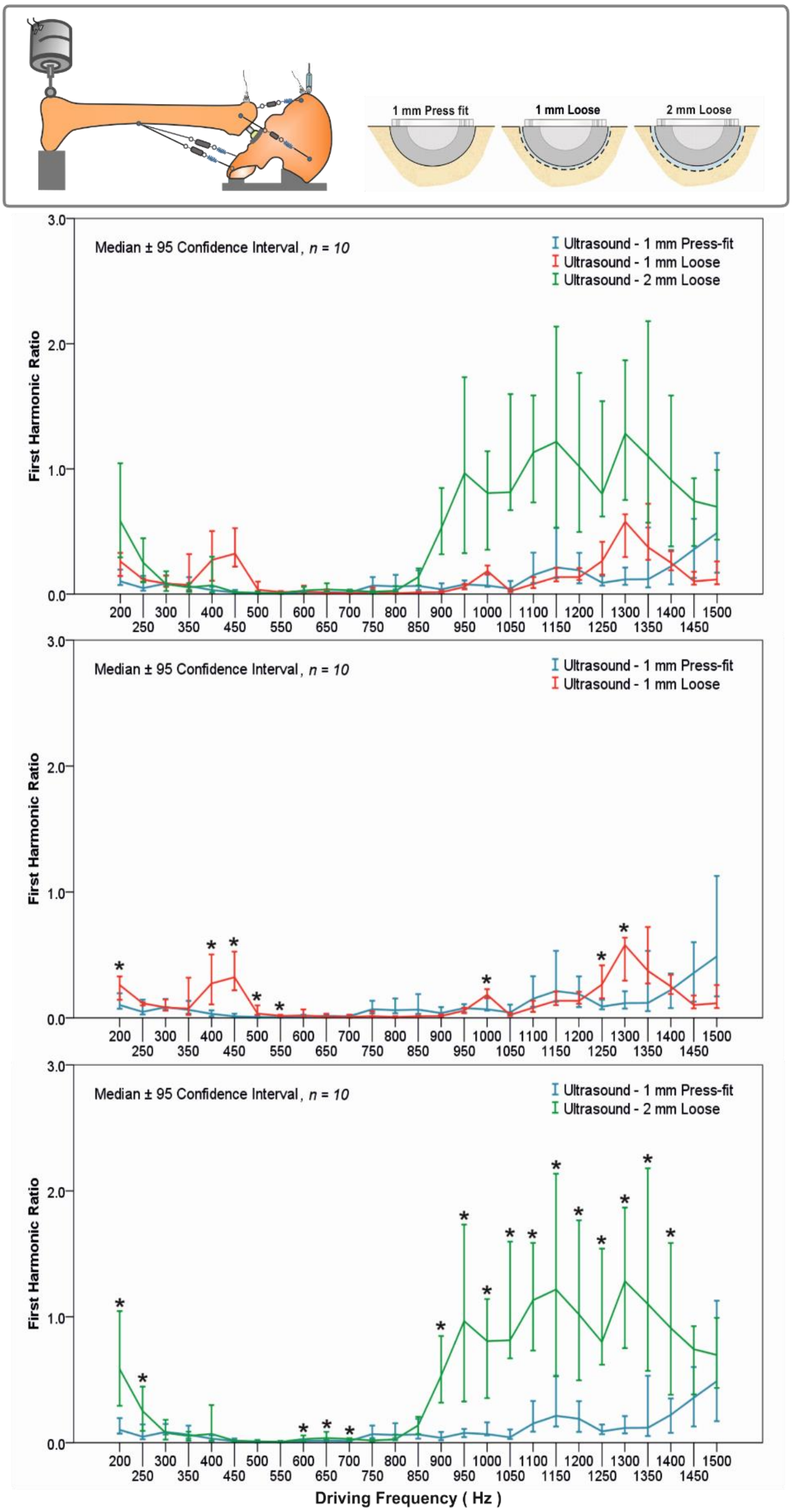

1st Harmonic Ratio	Ultrasound																													
Driving Frequency (Hz)	100	150	200	250	300	350	400	450	500	550	600	650	700	750	800	850	900	950	1000	1050	1100	1150	1200	1250	1300	1350	1400	1450	1500	#
Secure Cup - 1 mm Loose	NA	NA	.001b	NA	NA	NA	.000b	.000b	.001b	.004b	NA	NA	NA	NA	NA	NA	NA	NA	.007b	NA	NA	NA	NA	.000b	.000b	NA	NA	NA	NA	8
Secure Cup - 2 mm Loose	NA	NA	.000b	.002b	NA	NA	NA	NA	NA	NA	.007b	.002b	.000b	NA	NA	NA	.000b	.000b	.000b	.000b	.000b	.000b	.000b	.000b	.000b	.000b	.000b	NA	NA	16
1 mm - 2 mm	NA	NA	.002b	.035b	NA	NA	NA	NA	NA	NA	NA	.001b	.001b	NA	.000b	.000b	.000b	.000b	.000b	.000b	.000b	.000b	.000b	.000b	.000b	.001b	.001b	.000b	.000b	19

Figure 7-11: The ultrasound first harmonic ratio comparison for the different simulated conditions with air medium. * Mann-Whitney test $p < 0.05$, n = sample size.

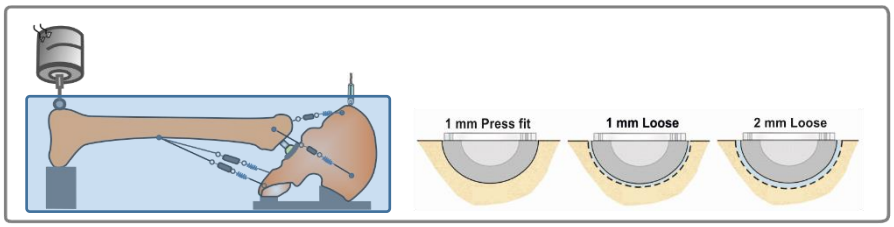

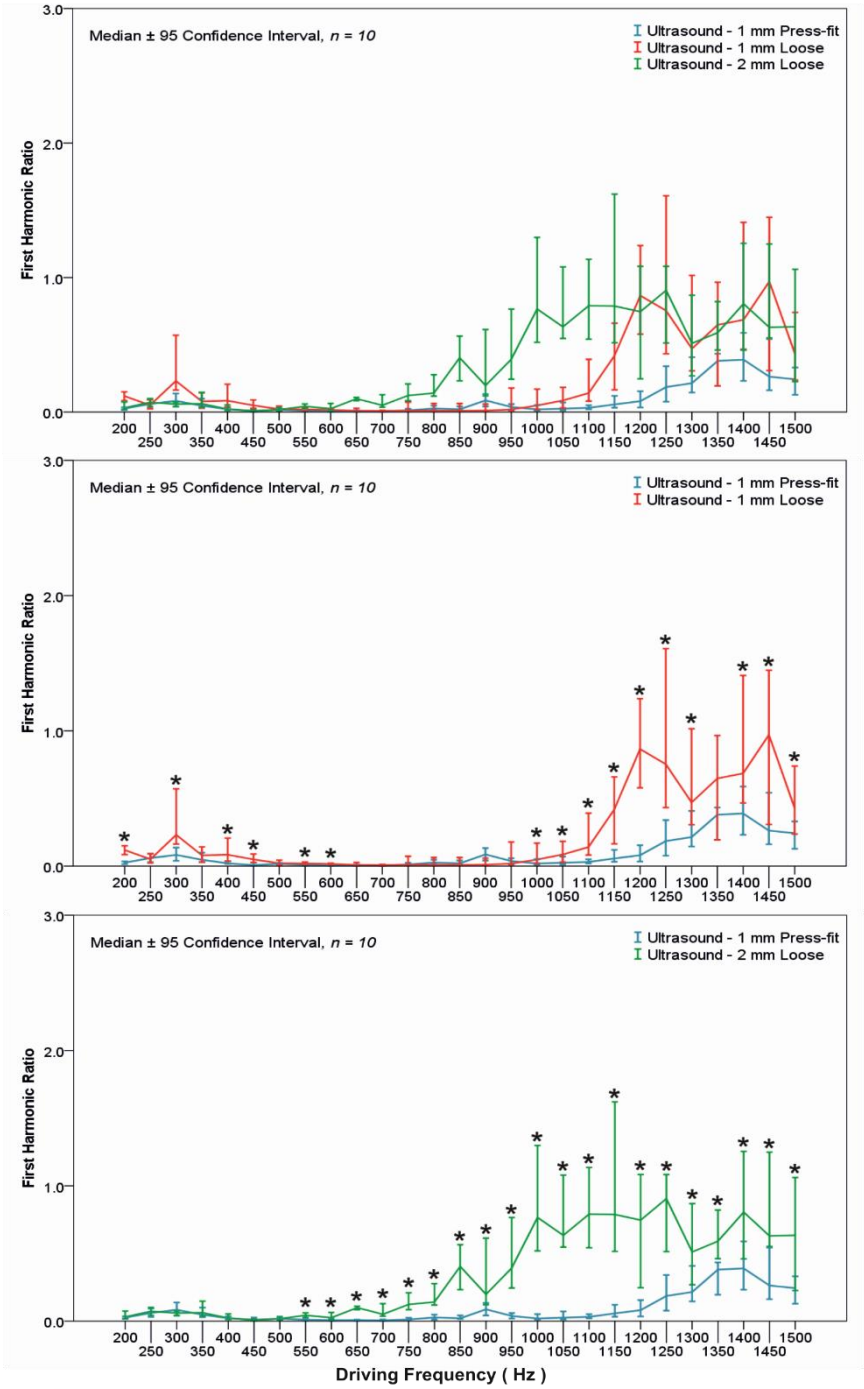

1st Harmonic Ratio	Ultrasound - (Water medium)																																						
	Driving Frequency (Hz)	100	150	200	250	300	350	400	450	500	550	600	650	700	750	800	850	900	950	1000	1050	1100	1150	1200	1250	1300	1350	1400	1450	1500	#
	Secure Cup - 1 mm Loose	NA	NA	.000b	NA	.001b	NA	.000b	.000b	NA	.000b	.009b	NA	NA	NA	NA	NA	NA	NA	.043b	.011b	.000b	.000b	.000b	.002b	.007b	NA	.001b	.002b	.023b	16
	Secure Cup - 2 mm Loose	NA	NA	NA	NA	NA	NA	NA	NA	NA	.000b	.001b	.000b	.000b	.000b	.000b	.000b	.000b	.000b	.000b	.000b	.000b	.000b	.000b	.000b	.007b	.043b	.001b	.001b	.023b	20
	1 mm - 2 mm	NA	NA	NA	NA	NA	NA	NA	NA	NA	.000b	NA	.000b	.000b	.002b	.000b	.000b	.000b	.000b	.000b	.000b	.000b	.001b	NA	NA	NA	NA	NA	NA	NA	12

Figure 7-12: The water medium ultrasound first harmonic ratio comparison for the different simulated conditions. * Mann-Whitney test $p < 0.05$, n = sample size.

7.2.3 Discussion

Simulation of the acetabular cup loosening using a Sawbones femur and hemi-pelvis composite bones was an attempt to account for a more realistic anatomical set-up. The femoral bone was fixed in position with springs replicating the muscle attachment to the hemi-pelvis in accordance with Rieger *et al.* [8] work. This allowed the positioning the excitation source on the lateral femoral condyle to be as initially suggested by Rosenstein *et al* [10]. The femoral Sawbones was also foam supported rather than clamped [11, 12] or counterbalancing weights [145]. This was an attempt to prevent the femoral bone from exhibiting excessive movement that was observed, at lower driving frequencies. The same simulated loosening condition for the Sawbones hemi-pelvis case study was adopted for ease of comparison. These were: 1mm press-fit (secure), 1mm and 2mm spherical loosening. The aim was to, first validate the previous objectives outcomes, and the second to provide more realistic anatomical set-up. Two medium conditions (water and air) were also applied using an acrylic tank for the ultrasound probe measuring techniques.

The initial testing was conducted using the air medium (foam support), whereby two accelerometers and an ultrasound probe were utilised to measure the output vibration. The use of two accelerometers was to determine the optimum location for measuring the frequency response, one at the greater trochanter of the femur and another at the iliac crest of the pelvis. Initially, the two accelerometers' spectrum analysis over the frequency range up to 1500 Hz, suggested that 1mm and 2mm spherical cup loosening can be distinguished from the secure cup supporting the previous work findings. The accelerometer located at iliac crest of the pelvis gave more significant readings over the sensor located at the greater trochanter for the fundamental frequency results. Whereas, more significant readings for the first and second harmonic results were obtained with the greater trochanter accelerometer sensors, especially when comparing the two loosening scenarios with the secure condition. The third harmonic significant readings number were closely related for both accelerometer locations. The most challenging conditions were when comparing the two loosening conditions, 1mm and 2mm; this gave the least number of significantly different readings with the frequency spectrum parameters. When looking at the harmonic ratio results, they support the previous case studies pattern in relation to loosening, as the loosening gap increases the harmonic ratio increases, and most of the significant readings were in the frequency range 500-1500Hz. When comparing the two loosening conditions to the secure

condition, the femoral accelerometer reading did show a slightly more significantly different readings compared to the pelvis accelerometer. With the two loosening conditions, 1mm and 2mm, the pelvis sensor gave the most significant number of harmonic ratio readings, even reaching twice the femoral readings for the third harmonic ratio.

Through the water medium testing, only the ultrasound probe was used and was positioned facing the anterior superior iliac spine. The ultrasound measurement approach was used for both testing mediums (water and air). The water bath was used to mimic the soft tissue as suggested by Rowlands *et al.* [145] work .The ultrasound spectrum analysis of the three simulated conditions (1mm press-fit, 1mm and 2mm spherical loosening) using the two mediums (water and air), revealed that even with the more complex Sawbones femur pelvis set-up, cup loosening can be detected. When looking at the water medium testing, distinguishing between the conditions was possible at 47 significant readings which were all located above 300 Hz for the fundamental frequency. This was followed by first and second harmonic at 13 significant readings and 11 readings, respectively. Testing with the foam support (air medium) saw 45 significant readings for the fundamental frequency, 37 readings for the first harmonic, and 31 readings for the second and third harmonic. The ultrasound harmonic ratio highlighted a favourable frequency range between 500-1500 Hz for both testing mediums (water and air). Generally with the water medium, there were more significant differences with the two loosening conditions compared to the secure states. This suggests that use the water medium enhanced ultrasound probe measurements leading to more significant different readings numbers. However, in the comparison between the two loosening conditions, the highest significant reading was for the air medium testing set-up. This could be attributed to the fact that both loosening conditions had a relatively higher harmonic ratio compared to the secure condition but still closely related making it hard to have a significant different between themselves.

In Summary, the findings of this objective support the earlier case studies with regards to acetabular cup loosening using vibrometry. When the cup loosening gap became bigger (i.e. 1mm to 2mm), the lower the fundamental frequency magnitude became, and the higher the magnitude of the harmonics became at certain frequencies. For the harmonic ratio, an increase was consistently seen as the loosening level increases. These findings support the previous literature [8, 9, 16] in which it was stated that acetabular cup loosening can be detected using the vibrometry approach. This study differed from these by defining the

minimum loosening level that can be reliably detected, 1mm-sperical loose, and a favourable frequency detection range between 500Hz and 1500Hz. The use of the spherical loosening is however a simplification of acetabular cup loosening, which could account as a limitation of this study. Also, the experiment did show the ability of vibrometry to distinguish the cup loosening using the cementless component, but did not consider a cemented one. However, this was a first step towards testing the feasibility of the vibrometry approach for the acetabular cup loosening detection, and therefore demanded simplification. Further clarification of how these limitations could be overcome will be discussed later.

7.2.4 Conclusion

This part of the thesis (third objective) was performed to overcome the previous case study limitations (simplified geometry and isolated testing on the hemi-pelvis) and further validate the vibrometry approach accounting for a more realistic excitation location. This was done through the addition of the femoral component that was attached to the pelvis by springs in an attempt to replicate the muscle attachments.

Both simulated conditions, 1mm and 2mm of spherical loosening, were distinguished from the secure states using both measuring techniques, whereby the 1mm spherical gap was the minimum detected loosening level with a favourable frequency detection range between 500Hz and 1500Hz. With regards to the accelerometer measurements, the greater trochanter of the femur location did gave the most significantly different harmonic ratio readings when comparing the two loosening conditions to the secure condition, while the measurement location at the iliac crest of the pelvis had the most significantly different harmonic ratio readings when comparing the two conditions, 1mm and 2mm loosening. The ultrasound harmonic ratios obtained with the two mediums (air and water) also showed the same pattern with regards to loosening detection. The greater the thickness of the radiolucent line, the greater was the harmonic ratio. The water medium had the most significantly different harmonic ratio readings with the two loosening conditions compared to the secure states. This suggests that that ultrasound probe can compete with the accelerometer in the vibrometry signal measurement.

Chapter 8 – Discussion

8.1 Discussion

The literature review highlighted the important of THR loosening diagnosis techniques and how they are vital for after surgery follow-up assessment. This becomes even more prevalent with the increasing THR procedures that take place daily around the world, reaching over one million operations annually [1, 41, 215, 216]. Also, surgeons are taking on younger and more active patients, who are likely to outlive the implant's life expectancy, and with more mobility and quality of life demands [217, 218]. According to the Swedish, British and Australian national registries, implant failure rates are in the range of 4 to 10 % at ten years [2, 3]. Aseptic loosening has been recognised as the primary cause of THR failure since early 1979 by the Swedish Hip Arthroplasty Register [4]. Currently, imaging techniques are the primary diagnostic and follow-up method, but have been shown to be unreliable for early loosening detection [5-7], especially of the acetabular cup [8].This challenge has led to the proposal of new and novel techniques, such as vibrometry, by several research groups at Universities of Rostock [23, 121, 157-164], Leicester [11, 12], Leuven [14, 22, 169, 196] and Bath [9, 140, 145].

Vibrometry can distinguish implant instability (loosening) through the frequency spectrum of the response signal and by referring it to the vibrational response of the secure case [6]. Despite the commercial success that the vibrometry approach has gained in dentistry in the assessment of dental implant stability [219], it has not gained much acceptance in the orthopaedics field. This can be attributed to the small size of dental implants in relation to THR implants, as well as the surrounding tissue layer that acts as a buffer, that has led to the adoption of wireless technology[152, 154, 155] and ultrasonic measuring techniques [145] to overcome this issue. This is in addition to the tendency for the orthopaedic surgeons to rely heavily on the radiology imaging assessment for musculoskeletal system disorders. This is mainly attributed to availability, cost-effectiveness [102] and being the main method that junior surgeons are trained in during their training and, therefore, the technique they are most familiar with. Vibrometry has been applied in different lower limb orthopaedic related studies, mainly in implant intra-operative assessments [165-170, 174, 175, 196], osseointegration assessments [128, 135, 141, 142] and in loosening diagnoses [8-12, 14, 22]. Although the acetabular cup component revision rates are higher than the stem component [17-20], the majority of the existing vibrometry loosening diagnostic studies [6, 9-13, 22, 23] are stem related. A limited number of studies [5, 8, 9, 16] have examined cup loosening without defining the loosening level detected. Thus, the aim of this project has been to

investigate the viability of vibrometry for accurately detecting early acetabular component loosening.

Since the early introduction of the vibration analysis concept of fracture healing assessment by Lippmann [138] in the 1930s, further vibrometry studies did not follow until the early 1970s, due the lack of technology [139]. Subsequently, when sensory technology improved, the vibrometry literature reached a point where THR loosening detection became a possibility for stem loosening [6, 9-12, 22, 23], with a critical detectable threshold of one-fifth of the stem length interface failure [13]. Then there was the challenge of distinguishing stem loosening from cup loosening, which was achieved by the work of Georgiou and Cunningham [9] and Rieger *et al.* [5, 8] , but with the emphasis that acetabular cup loosening detection was shown to be challenging [5]. Only half of the cup loosening cases were correctly identified during Georgiou and Cunningham [9] clinical study. Also, a Sawbones experiment [8] revealed that cup loosening can be significantly identified using a frequency resonance shift at only two frequencies, 450Hz and 600Hz. However, when this method was replicated on cadaver specimens [5], cup loosening resulted in a non-significant shift. In these three studies [5, 8, 9], an acetabular cup loosening level was not defined. Thus, a critical detectable threshold for acetabular component loosening using vibrometry is not yet realised. The aim of this study has been to address this gap in the literature by investigating the viability of detecting acetabular component loosening using vibrometry, and to define the earliest loosening phase that can be accurately detected. This has been achieved through a series of case studies that varied in complexity, which can be grouped under three objectives, as follows:

1- Development of acetabular cup loosening using Sawbones blocks.

2- Development of acetabular cup loosening using a Sawbones hemi-pelvis.

3- Development of acetabular cup loosening using a Sawbones femur and hemi-pelvis.

The first objective consisted of three case studies that were aimed at testing the feasibility of the vibrometry approach in acetabular cup loosening detection. A Sawbones polyurethane solid foam was used in order to create various loosening scenarios. These were as follows: late spherical, early spherical, and early zone loosening. The term 'early loosening' in the orthopaedic field correlates to loosening that occurs in the first ten years, especially for hip replacements [220-223]. During this study, 'early loosening' was used to refer to a mimicked gap of 1mm radiolucent line equivalent. This criteria was adopted in order to simplify the acetabular cup loosening complexity and test the vibrometry concept. In accordance with the previous vibration analysis literature [8-12], the same excitation system was adopted with the use of an accelerometer as a measurement method [5, 10-12, 124, 128, 135] alongside the use of ultrasound transduces [145, 224]. The soft tissue interface between the acetabular cup outer shell and bone surface was mimicked using a low modulus silicone gel, also in accordance with the existing literature [11, 124, 135, 153]. The first two case studies, early and late loosening, used an excitation driving frequency range of 100-1500 Hz in accordance with the previous studies [9-12, 145], where the authors highlighted the prospect of detecting stem loosening using a sinusoidal frequency sweep excitation range below 1500Hz. The findings revealed that the vibrometry approach is more reliable at detecting late acetabular cup loosening than early loosening. Parallel findings were also noted in the existing literature [11, 12] for the stem component; whereby it has been shown that vibrometry is reliable for detecting late stem loosening but has less favourable findings for early loosening cases. Loosening was demonstrated by a reduction in the fundamental frequency and the increase in the magnitude of the related harmonics, especially the first, as originally highlighted by Georgiou and Cunningham [9]. This was then quantified in the form of harmonic ratios. The first harmonic was divided by the fundamental frequency magnitude at each driving frequency, with the aim to define the optimum frequency range for detecting cup loosening using spectrum analysis. The harmonic ratio findings for the simulated conditions revealed a pattern, whereby the greater the radiolucent line simulated gap, the greater the harmonic ratio. This suggested a possible way of differentiating between various loosening levels. The accelerometer method gave better results over the ultrasound readings with regards to the harmonic ratio variation and a wider detectable frequency range. The third case study was the early zone loosening scenario that accommodated a more clinically relevant loosening set-up [96, 97]. The conditions were 1mm zone (2) loose, 1mm zone (1 and 2) loose and 1mm zone (1 and 3) loose. Also, the excitation range was increased to accommodate the natural frequency of the polyurethane solid foam block and observe its effect on the

loosening detection. The spectrum analysis findings supported the results pattern of the first case study (late spherical loosening). However, the simulated zone loosening conditions were distinguished from the secure condition at more significant readings overall than the early spherical loosening condition. This was due to the wider excitation range, especially around the natural frequency of the system. In summary, the findings of the first two case studies, late and early spherical loosening, revealed that the vibrometry approach is more reliable at detecting late acetabular cup loosening than early loosening. This finding is in agreement with the existing stem loosening literature [11, 12]. When more realistic early cup loosening scenarios were simulated, in the form of zone loosening, results revealed favourable findings, especially around the system's natural frequency. Similar observations were made for stem loosening detection, highlighting that frequencies near the system's natural frequency are more favourable for the detection of loosening using vibrometry [10]. For the three Sawbones block case studies, the minimum detected simulated loosening was 1mm zone (2) loose, with the frequency range 2000-2500Hz producing the most consistent results for the two measurement techniques.

The second objective was the development of a Sawbone hemi-pelvis acetabular cup loosening model. This was done in an attempt to accommodate the complex geometry of the hemi-pelvis and observe the effect on the loosening detection of the vibrometry. There were two aims. The first was to validate the first objective's findings in relation to loosening detection, and the second was to provide a more realistic anatomical environment and examine its possible effects on loosening detection. This objective consisted of one case study with the simulated conditions of 1mm and 2mm spherical cup loosening. Two testing mediums were adopted; one set-up was conducted under water in a glass water tank while the second was conducted in air (foam support). The water medium was intended to replicate the work of Rowlands *et al.* [145] in which water was used to simulate soft tissue. The loosening gap interface was filled with low modulus silicone in accordance with the existing literature [11, 124, 135]. Two measurement techniques (accelerometer and ultrasound) were used for the air medium, while for the water medium only the ultrasound method was used. The frequency spectrum had four parameters: the fundamental frequency, first harmonic, second harmonic, and the third harmonic. In agreement with the findings of the previous case study, as the loosening gap became bigger the lower the fundamental frequency magnitude became, and the higher the harmonic magnitudes became at certain frequencies. The harmonic ratio was the second method of observing the hemi-pelvis acetabular cup

loosening variation, which included the first, second and third harmonic ratio. The harmonic ratio findings also agreed with the earlier case study's signal pattern, whereby the greater the simulated loosening gap became, the greater the harmonic ratio became at certain frequencies. The spectrum analysis with the water medium showed more significant readings for the fundamental frequency, particularly when comparing the two loosening conditions with the secure condition. However for the other spectrum parameters, the significant readings number were less in the case of the first and second harmonic magnitudes. As such, the harmonic ratio findings of the ultrasound water medium set-up support the vibrometry approach for the comparison between the conditions (secure, 1mm and 2mm loosening). There was a clear increase in the significant readings for the secure – 1mm loose comparison over the three harmonic ratios; in fact, over three times more. For the secure – 2mm loose condition, the number of significant readings were closely related, but with a clear shift to the higher frequency ranges. However, the results were not consistent across the frequency range for the different parameters, or even for the measurement methods. This suggest that there are more favourable frequency ranges for each parameter and measurement technique used. In summary, the minimum detected loosening condition was 1mm spherical acetabular cup loosening. This supports the feasibility of the vibrometry approach in detecting loosening, but the results are far from conclusive, as the femoral bone was not present and, therefore, the input excitation was not at the optimum location as previously clinically proposed [9, 10].

The third objective aimed to create a more clinically relevant experiment through the development of acetabular cup loosening model using the Sawbones femur and hemi-pelvis composite bones. The previous four case studies used an excitation position that was much closer to the acetabular cup than would be clinically possible. Thus, the femur bone was added to reflect a more clinically realistic scenario, in which the excitation source was placed on the lateral femoral condyle as initially suggested by Rosenstein *et al.* [10]. The simulated loosening conditions were similar to the fourth case study for ease of comparison; 1mm press-fit (secure cup), 1mm and 2mm spherical loosening. The two medium approaches (water and air) were also adopted in this case study. With the water medium, only the ultrasound probe was used, while for the air medium (foam support), the measurements were taken through two accelerometers and an ultrasound probe. The accelerometers were located at the iliac crest of the pelvis and another at the greater trochanter of the femur. This was done to determine the optimum location for measuring the frequency response in similar

approach to that of Rieger *et al.*[8]. The two accelerometers' spectrum analysis over the frequency range up to 1500 Hz, suggested that 1mm and 2mm spherical cup loosening can be distinguished from the secure cup supporting the previous work's findings. The accelerometer located at iliac crest of the pelvis gave more significant readings over the sensor located at the greater trochanter for the fundamental frequency results. Whereas, more significant readings for the first and second harmonic results were obtained with the accelerometer sensor on the greater trochanter, especially when comparing the two loosening scenarios with the secure condition. The significant readings for the third harmonic were closely related for both accelerometer locations. The most challenging conditions were when comparing the two loosening conditions, 1mm and 2mm, gave the least number of significantly different readings with the frequency spectrum parameters. The harmonic ratio findings also support the findings of the previous case studies in relation to loosening, as it increases as the loosening increases. Most of the significant readings were in the frequency range 500-1500 Hz. When comparing the two loosening conditions to the secure, the femoral accelerometer reading did show slightly more significantly different readings compared to the readings from the pelvis accelerometer. With the two loosening conditions, 1mm and 2mm, the pelvis sensor had the most significant ratio readings, even reaching twice that was found for the femoral readings for the third harmonic ratio. The ultrasound measurement approach was used for both testing mediums (with water and air). The ultrasound spectrum analysis of the three simulated conditions (secure cup, 1mm and 2mm spherical loosening) using the two mediums, revealed that, even with a more complex Sawbones femur pelvis set-up, cup loosening can still be detected. The ultrasound harmonic ratio highlighted a favourable frequency range (500-1500Hz) for testing in both mediums. Generally, with the water medium, there were more significant differences with the two loosening conditions compared to the secure states. Nevertheless, in the particular case of the comparison between the two loosening conditions, the highest significant readings were for the air medium testing set-up. This could be attributed to the fact that both loosening conditions had a relatively higher harmonic ratio compared to the secure condition but were still closely related making it hard to have a significant different. In summary, the earliest loosening phase that was accurately detected was 1mm spherical acetabular cup loosening with a frequency range between 500-1500 Hz. The pelvis iliac crest was shown to be the optimum measurement location due to its ability to differentiate between the two loosening cases much better than the greater trochanter of the femur location. This is in agreement with the work of Rieger *et al.* [8], who stated that trochanter measurements were less distinct.

In attempting to answer the main research question, certain limitations were present that need to be considered when interpreting the results obtained. The use of the spherical loosening at this stage was a simplification of acetabular cup loosening. Also, while the experiments did show the ability of vibrometry to distinguish cup loosening using the cementless component, this study has not examined the cemented component. Moreover, this study has not looked at the ability to distinguish cup loosening from stem component loosening. The effect of different mimicked muscle tensions was not also evaluated, even though it has been stressed in clinical work [9] that the muscles need to be relaxed. The soft tissue interface simulation was in accordance with the existing literature [11, 124, 135, 153], but still far from the real soft tissue properties. The boundary condition such as the hemi pelvis bone fixation method is another limitation. Different boundary conditions could therefore have been used in order to make the results more conclusive. The use of mini-shaker as excitation source in two vibrometry clinical studies [9, 10] did not raise any issue but it could potentially be a source of patient discomfort [160]. However, this was the first step towards testing the feasibility of the vibrometry approach in acetabular cup loosening detection, and therefore it demanded a degree of simplification. Further clarification of how these limitations could be overcome will be touched upon in an upcoming section.

In summary:

- The aim of this project was to investigate the feasibility of detecting acetabular cup loosening using vibrometry, and to define the earliest loosening phase that can be accurately detected. This was attempted through a series of case studies, which can be grouped under three objectives.

- Loosening was demonstrated by a reduction in the fundamental frequency and an increase in the magnitude of the related harmonics. By quantifying the magnitude of the harmonics in relation to the fundamental frequency, it was found that the harmonic ratio would increase, corresponding to the degree of loosening.

- In the first objective Sawbones blocks case studies, the minimum detected simulated loosening was 1mm zone 2 loosening, with the frequency range 2000-2500Hz.

- For the second (hemi-pelvis) and third (femur and hemi-pelvis) objective findings, the earliest loosening phase detected was 1mm of spherical acetabular cup loosening within the frequency range 500-1500Hz.

- The finding of this study therefore supports the existing vibrometry literature by emphasising that acetabular cup loosening can be detected using vibrometry. Taking the study limitations into account.

Chapter 9 – Conclusion and future work

9.1 Conclusion

The overall study aim was to investigate the feasibility of the vibrometry approach in detecting acetabular cup loosening and, if feasible, define the earliest accurate detectable threshold. Three objectives were devised to address this aim, taking into account common practices established in the existing vibrometry-related literature, the need to overcome limitations, and attempting to create a more clinically relevant set-up. Initially, these involved testing the concept using a simplified set-up with minimal boundary conditions by the development of acetabular cup loosening model using Sawbones blocks. The second objective attempted to accommodate more complex bone geometry through utilising a Sawbones hemi-pelvis. The third objective aimed to create even a more clinically relevant experiment by using a Sawbones femur and hemi-pelvis composite bones.

The findings revealed that, as the cup loosening gap becomes bigger, the fundamental frequency magnitude decreases and the related harmonic magnitude increases compared to the secure condition. By quantifying the harmonic magnitude relevant to the fundamental frequency in the form of harmonic ratio, it was found that the harmonic ratio would increase corresponding to the degree of loosening. The first objective involved three cases studies; late, early spherical loosening and early zonal loosening. Initially, the late and early loosening case studies revealed that the vibrometry approach is more reliable at detecting late acetabular cup loosening than early loosening. Nevertheless, when more realistic early cup loosening scenarios were simulated, in the form of zone loosening, results revealed favourable findings, especially around the system's natural frequency. In the first objective three case studies, the minimum detected simulated loosening was 1mm zone 2 loosening, within the frequency range 2000-2500Hz, for both measurement methods (accelerometer and ultrasound). When examining the second and third objective findings, the earliest loosening phase that was accurately detected was 1mm spherical acetabular cup loosening within the frequency range 500-1500Hz; This frequency range obtained most of the significant readings for both sensors used (accelerometer and ultrasound). The findings of the third objective also highlighted the pelvis side to be the optimum measurement location, due to its ability to differentiate between the two loosening cases much better than the measurement location on the greater trochanter of the femur. Likewise, it was shown that ultrasound can compete with the accelerometer measurements, with the advantage of overcoming the attenuating (damping) effect of the soft tissue.

The finding of this study therefore supports the existing vibrometry literature by emphasising that acetabular cup loosening can be detected using vibrometry. This study was novel because it defined the minimum acetabular cup loosening level that was reliably detected using vibrometry alongside the favourable frequency range. These results are not conclusive, due the current study limitations, but are a step forward in showing the potential reliability of vibrometry in THR loosening detection. Further studies that combine stem and cup loosening will enhance our understanding of the vibrometry approach, by seeking to distinguish component loosening and the degree of loosening, either through the signal response pattern or the frequency range sensitivity.

9.2 Future work

Further work suggestions can be divided into three general aspects; the excitation approach, the experiment setup and mathematical analysis.

The excitation system used was consistent with the existing vibrometry literature. However, the frequency range could be expanded and attempts could be made to explore different signal energy levels through changing the signal amplitude. This may lead to the identification of the lowest signal energy level needed for loosening detection, which a patient with a painful hip could tolerate. A recent pilot study [5] has used new excitation methods that utilise shockwaves, replacing the need to expose patients to external mechanical vibration. This technique, when combined with wireless sensors, could reduce the levels of energy need to elicit an implant response and thus reduce patient discomfort.

The experiment set-up needs to take into account more considerations in order to reflect clinical reality. This could be through the creation of more complicated acetabular cup zone loosening combinations, alongside stems with different levels of loosening. Different boundary conditions should also be considered through the use of different muscle tension simulations (different spring rates) and soft tissue thickness (using different substitutes), in order to examine the potential effect of these factors on the vibrometry approach in loosening detection.

Mathematical analysis could also be utilised to reduce data analysis time and even in the assessment of more complicated loosening conditions that otherwise would consume considerable time and cost. Finite element analysis could be used to define the minimum reliable acetabular cup loosening detection threshold, and even to examine the effect of combined loosening with the stem component. The spectrum analysis and the harmonic ratio calculation could be automated with defined parameters and a threshold set that is clinically related.

Reference

1. Michaelsson, K., *Surgeon volume and early complications after primary total hip arthroplasty.* BMJ, 2014. **348**: p. g3433.

2. Clarke, A., R. Pulikottil-Jacob, A. Grove, K. Freeman, H. Mistry, A. Tsertsvadze, M. Connock, R. Court, N.-B. Kandala, and M. Costa, *Total hip replacement and surface replacement for the treatment of pain and disability resulting from end-stage arthritis of the hip (review of technology appraisal guidance 2 and 44): systematic review and economic evaluation.* 2015. **19**(3).

3. Kandala, N.B., M. Connock, R. Pulikottil-Jacob, P. Sutcliffe, M.J. Crowther, A. Grove, H. Mistry, and A. Clarke, *Setting benchmark revision rates for total hip replacement: analysis of registry evidence.* BMJ, 2015. **350**: p. h756.

4. Garellick, G., J. Kärrholm, H. Lindahl, H. Malchau, C. Rogmark, and O. Rolfson, *Swedish Hip Arthroplasty Register Annual Report 2013*, 2014.

5. Rieger, J.S., S. Jaeger, J.P. Kretzer, R. Rupp, and R.G. Bitsch, *Loosening detection of the femoral component of hip prostheses with extracorporeal shockwaves: A pilot study.* Med Eng Phys, 2015. **37**(2): p. 157-64.

6. Diaz-Perez, F., E. Garcia-Nieto, A. Ros, and R. Claramunt, *Best estimation of spectrum profiles for diagnosing femoral prostheses loosening.* Med Eng Phys, 2014. **36**(2): p. 233-8.

7. Ruther, C., C. Schulze, A. Boehme, H. Nierath, H. Ewald, W. Mittelmeier, R. Bader, and D. Kluess, *Investigation of a passive sensor array for diagnosis of loosening of endoprosthetic implants.* Sensors (Basel), 2012. **13**(1): p. 1-20.

8. Rieger, J.S., S. Jaeger, C. Schuld, J.P. Kretzer, and R.G. Bitsch, *A vibrational technique for diagnosing loosened total hip endoprostheses: an experimental sawbone study.* Med Eng Phys, 2013. **35**(3): p. 329-37.

9. Georgiou, A.P. and J.L. Cunningham, *Accurate diagnosis of hip prosthesis loosening using a vibrational technique.* Clinical Biomechanics, 2001. **16**(4): p. 315-323.

10. Rosenstein, A.D., G.F. McCoy, C.J. Bulstrode, P.D. McLardy-Smith, J.L. Cunningham, and A.R. Turner-Smith, *The differentiation of loose and secure femoral implants in total hip replacement using a vibrational technique: an anatomical and pilot clinical study.* Proceedings of the Institution of Mechanical Engineers. Part H, Journal of engineering in medicine, 1989. **203**(2): p. 77-81.

11. Li, P.L., N.B. Jones, and P.J. Gregg, *Loosening of total hip arthroplasty. Diagnosis by vibration analysis.* J Bone Joint Surg Br, 1995. **77**(4): p. 640-4.

12. Li, P.L., N.B. Jones, and P.J. Gregg, *Vibration analysis in the detection of total hip prosthetic loosening.* Med Eng Phys, 1996. **18**(7): p. 596-600.

13. Qi, G., W.P. Mouchon, and T.E. Tan, *How much can a vibrational diagnostic tool reveal in total hip arthroplasty loosening?* Clin Biomech, 2003. **18**(5): p. 444-58.

14. Pastrav, L.C., J. Devos, G. Van der Perre, and S.V.N. Jaecques, *A finite element analysis of the vibrational behaviour of the intra-operatively manufactured prosthesis–femur system.* Medical Engineering & Physics, 2009. **31**(4): p. 489-494.

15. Perez, M.A. and B. Seral-Garcia, *A finite element analysis of the vibration behaviour of a cementless hip system.* Comput Methods Biomech Biomed Engin, 2013. **16**(9): p. 1022-31.

16. Tudor, J., *Can Acetabular Component Loosening be Determined using a Vibration Based Technique?* , 2008, University Of Bath - final year report.

17. Smith, M.A. and W.T. Smith, *The American Joint Replacement Registry.* Orthopaedic Nursing, 2012. **31**(5): p. 296-299.

18. Sakellariou, V.I. and T. Sculco, *Acetabular options: Notes from the other side.* Seminars in Arthroplasty, 2013. **24**(2): p. 76-82.

19. NJR, *National Joint Registry for England, Wales and Northern Ireland 11th Annual Report 2014*, in *ISSN 2054-183X (Online)*2014.

20. NJR, *National Joint Registry for England, Wales and Northern Ireland 10th Annual Report 2013*, in *ISSN 1745-1450 (Online)*2013.

21. Forster-Horvath, C., C. Egloff, V. Valderrabano, and A.M. Nowakowski, *The painful primary hip replacement–review of the literature.* Swiss medical weekly, 2014. **144**: p. 1-12.

22. Jaecques, S., C. Pastrav, A. Zahariuc, and G. Van der Perre. *Analysis of the fixation quality of cementless hip prostheses using a vibrational technique*. in *International Conference on Noise and Vibration Engineering*. 2004.

23. Ruther, C., J.L. Cunningham, U. Timm, H. Ewald, R. Bader, and D. Kluess, *Comparison of Different Excitation Methods for Vibrometry Diagnosis of the Total Hip Stem*, in *18th Congress of the European Society of Biomechanics*2012.

24. Gray, H., S. Standring, H. Ellis, P. Collins, B.K.B. Berkovitz, and C. Wigley, *Gray's Anatomy Edition: The Anatomical Basis of Clinical Practice*. 39 ed. 2005: Elsevier Science Health Science Division.

25. Harkess, J.W. and J.R. Crockarell, *Arthroplasty Of The Hip*, in *Campbell's Operative Orthopaedics*, S.T. Canale and J.H. Beaty, Editors. 2013, Elsevier Health Sciences. p. 158-310.

26. Bergmann, G., F. Graichen, and A. Rohlmann, *Hip joint contact forces during stumbling.* Langenbecks Arch Surg, 2004. **389**(1): p. 53-9.

27. Caillet, R., *Functional Anatomy of the Hip Joint*, in *The Illustrated Guide to Functional Anatomy of the Musculoskeletal System*. 2004 p. 237-250.

28. Hewitt, J.D., R.R. Glisson, F. Guilak, and T.P. Vail, *The mechanical properties of the human hip capsule ligaments.* The Journal of Arthroplasty, 2002. **17**(1): p. 82-89.

29. Farlex. *Muscles of the hip [online]*. Muscles of the hip [cited 2016 24 March]; Available from: http://encyclopedia.thefreedictionary.com/.

30. Whittle, M., *Gait analysis: an introduction*. 2007: Butterworth-Heinemann.

31. Palastanga, N., D. Field, and R. Soames, *Anatomy and human movement: structure and function*. 1998: Butterworth-Heinemann.

32. NJR, *National Joint Registry for England, Wales and Northern Ireland 12th Annual Report 2015*, in *ISSN 2054-183X (Online)*2015.

33. Association., A.O., *National Joint Replacement Registry annual report 2015*, I. 1445-3657, Editor 2015.

34. Zhu, Y., M. Yuan, H.Y. Meng, A.Y. Wang, Q.Y. Guo, Y. Wang, and J. Peng, *Basic science and clinical application of platelet-rich plasma for cartilage defects and osteoarthritis: a review.* Osteoarthritis and Cartilage, 2013. **21**(11): p. 1627-1637.

35. Metcalfe, S., H. Ji, K. Molodianovitsh, P. Sidhom, L. Faye, and G. Webster, *Hip and Knee Replacements in Canada; Canadian Joint Replacement Registry (CJRR) 2015 Annual Report*, 2015, The Canadian Institute for Health Information (CIHI).

36. Griffiths, R., J. Alper, A. Beckingsale, D. Goldhill, G. Heyburn, J. Holloway, E. Leaper, M. Parker, S. Ridgway, and S. White, *Management of proximal femoral fractures 2011.* Anaesthesia, 2012. **67**(1): p. 85-98.

37. NHS. *Hip fracture*. 2014 [cited 2016 17 March]; Available from: http://www.nhs.uk/conditions/hip-fracture/Pages/introduction.aspx.

38. Malizos, K.N., A.H. Karantanas, S.E. Varitimidis, Z.H. Dailiana, K. Bargiotas, and T. Maris, *Osteonecrosis of the femoral head: Etiology, imaging and treatment.* European Journal of Radiology, 2007. **63**(1): p. 16-28.

39. Jackson, J.C., M.M. Runge, and N.S. Nye, *Common questions about developmental dysplasia of the hip.* Am Fam Physician, 2014. **90**(12): p. 843-50.

40. AAOS. *Rheumatoid Arthritis* 2016 [cited 2016 17 March]; Available from: http://orthoinfo.aaos.org/topic.cfm?topic=A00211.

41. Pivec, R., A.J. Johnson, S.C. Mears, and M.A. Mont, *Hip arthroplasty.* The Lancet, 2012. **380**(9855): p. 1768-1777.

42. Pramanik, S., A.K. Agarwal, and K. Rai, *Chronology of total hip joint replacement and materials development.* Trends Biomater. Artif. Organs, 2005. **19**(1): p. 15-26.

43. Gomez, P.F. and J.A. Morcuende, *Early attempts at hip arthroplasty-1700s to 1950s.* Iowa Orthop J, 2005. **25**: p. 25-9.

44. Kolundzic, R., V. Trkulja, and D. Orlic, *History and factors of survival of total hip arthroplasty.* Med Glas Ljek komore Zenicko-doboj kantona, 2012. **9**(1): p. 136-42.

45. Wiles, P., *The surgery of the osteoarthritic hip.* Br J Surg, 1958. **45**(193): p. 488-97.

46. Holzwarth, U. and G. Cotogno, *Total hip arthroplasty : State of the art, prospects and challenges.* 2012.

47. Charnley, J., *Surgery of the Hip-joint.* BMJ, 1960. **1**(5176): p. 821-826.

48. Wroblewski, B.M., P.D. Siney, and P.A. Fleming, *The Charnley hip replacement - 43 years of clinical success.* Acta Chir Orthop Traumatol Cech, 2006. **73**(1): p. 6-9.

49. Yamada, H., Y. Yoshihara, O. Henmi, M. Morita, Y. Shiromoto, T. Kawano, A. Kanaji, K. Ando, M. Nakagawa, N. Kosaki, and E. Fukaya, *Cementless total hip replacement: past, present, and future.* J Orthop Sci, 2009. **14**(2): p. 228-41.

50. Lewis, G., *Properties of crosslinked ultra-high-molecular-weight polyethylene.* Biomaterials, 2001. **22**(4): p. 371-401.

51. Cooper, R.A., C.M. McAllister, L.S. Borden, and T.W. Bauer, *Polyethylene debris-induced osteolysis and loosening in uncemented total hip arthroplasty. A cause of late failure.* J Arthroplasty, 1992. **7**(3): p. 285-90.

52. Harris, W.H., *Conquest of a worldwide human disease: particle-induced periprosthetic osteolysis.* Clin Orthop Relat Res, 2004(429): p. 39-42.

53. Quesada, M.J., D.R. Marker, and M.A. Mont, *Metal-on-Metal Hip Resurfacing: Advantages and Disadvantages.* The Journal of Arthroplasty, 2008. **23**(7, Supplement): p. 69-73.

54. Fowble, V.A., M.A. dela Rosa, and T.P. Schmalzried, *A comparison of total hip resurfacing and total hip arthroplasty - patients and outcomes.* Bull NYU Hosp Jt Dis, 2009. **67**(2): p. 108-12.

55. Mont, M.A., P.S. Ragland, G. Etienne, T.M. Seyler, and T.P. Schmalzried, *Hip resurfacing arthroplasty.* Journal of the American Academy of Orthopaedic Surgeons, 2006. **14**(8): p. 454-463.

56. Stulberg, B.N., S.M. Fitts, J.D. Zadzilka, and K. Trier, *Resurfacing arthroplasty for patients with osteonecrosis.* Bulletin of the NYU Hospital for Joint Diseases, 2009. **67**(2): p. 138-41.

57. Lachiewicz, P.F., *Metal-on-metal hip resurfacing: a skeptic's view.* Clin Orthop Relat Res, 2007. **465**: p. 86-91.

58. Dorr, L.D., *Editorial Comment: Why do MIS THR?* Seminars in Arthroplasty, 2007. **18**(4): p. 222-225.

59. Pagnano, M.W. and M. Ali, *CHAPTER 65 - Minimally Invasive Total Hip Arthroplasty*, in *Surgical Treatment of Hip Arthritis*, J.H. William, Md, P. Javad, Md, Frcs, and M.D. Benjamin Bender, Editors. 2009, W.B. Saunders: Philadelphia. p. 493-501.

60. Ciminiello, M., J. Parvizi, P.F. Sharkey, A. Eslampour, and R.H. Rothman, *Total Hip Arthroplasty: Is Small Incision Better?* The Journal of Arthroplasty, 2006. **21**(4): p. 484-488.

61. Bal, B.S., *Introduction.* Seminars in Arthroplasty, 2005. **16**(3): p. 171.

62. Parithimarkalaignan, S. and T.V. Padmanabhan, *Osseointegration: An Update.* The Journal of the Indian Prosthodontic Society, 2013. **13**(1): p. 2-6.

63. Chandler, M., R. Z Kowalski, N. Watkins, A. Briscoe, and A. R New, *Cementing techniques in hip resurfacing.* Proceedings of the Institution of Mechanical Engineers, Part H: Journal of Engineering in Medicine, 2006. **220**(2): p. 321-331.

64. Scales, J.T. and W. Herschell, *Perspex in Orthopaedics.* Br Med J, 1945. **2**(4421): p. 423-4.

65. Judet, J. and R. Judet, *The use of an artificial femoral head for arthroplasty of the hip joint.* J Bone Joint Surg Br, 1950. **32-B**(2): p. 166-73.

66. Haboush, E.J., *A new operation for arthroplasty of the hip based on biomechanics, photoelasticity, fast-setting dental acrylic, and other considerations.* Bull Hosp Joint Dis, 1953. **14**(2): p. 242-77.

67. Webb, J.C. and R.F. Spencer, *The role of polymethylmethacrylate bone cement in modern orthopaedic surgery.* J Bone Joint Surg Br, 2007. **89**(7): p. 851-7.

68. Charnley, J., *The Bonding of Prostheses to Bone by Cement.* J Bone Joint Surg Br, 1964. **46**: p. 518-29.

69. Santin, M., A. Motta, A. Borzachiello, L. Nicolais, and L. Ambrosio, *Effect of PMMA cement radical polymerisation on the inflammatory response.* Journal of Materials Science: Materials in Medicine, 2004. **15**(11): p. 1175-1180.

70. Hailer, N.P., G. Garellick, and J. Kärrholm, *Uncemented and cemented primary total hip arthroplasty in the Swedish Hip Arthroplasty Register.* Acta orthopaedica, 2010. **81**(1): p. 34-41.

71. Refior, H.J., R. Parhofer, M. Ungethum, and W. Blomer, *Special problems of cementless fixation of total hip-joint endoprostheses with reference to the PM type.* Arch Orthop Trauma Surg, 1988. **107**(3): p. 158-71.

72. Clement, N.D., L.C. Biant, and S.J. Breusch, *Total hip arthroplasty: to cement or not to cement the acetabular socket? A critical review of the literature.* Arch Orthop Trauma Surg, 2012. **132**(3): p. 411-27.

73. Horne, G., N. Culliford, K. Adams, and P. Devane, *Hybrid total hip replacement: outcome after a mean follow up of 10 years.* ANZ J Surg, 2007. **77**(8): p. 638-41.

74. Diehl, P., M. Haenle, P. Bergschmidt, H. Gollwitzer, J. Schauwecker, R. Bader, and W. Mittelmeier, *[Cementless total hip arthroplasty: a review].* Biomed Tech (Berl), 2010. **55**(5): p. 251-64.

75. Morlock, M., N. Bishop, and G. Huber, *Biomechanics of Hip Arthroplasty*, in *Tribology in Total Hip Arthroplasty*, K. Knahr, Editor. 2011, Springer Berlin Heidelberg. p. 11-24.

76. Cross, M.B., D. Nam, and D.J. Mayman, *Ideal Femoral Head Size in Total Hip Arthroplasty Balances Stability and Volumetric Wear.* HSS Journal, 2012. **8**(3): p. 270-274.

77. Manley, M.T. and K. Sutton, *Bearings of the Future for Total Hip Arthroplasty.* The Journal of Arthroplasty, 2008. **23**(7, Supplement): p. 47-50.

78. Pachore, J.A., S.V. Vaidya, C.J. Thakkar, H.K.P. Bhalodia, and H.M. Wakankar, *ISHKS joint registry: A preliminary report.* Indian journal of orthopaedics, 2013. **47**(5): p. 505-9.

79. Shemesh, S., Y. Kosashvili, S. Heller, E. Sidon, L. Yaari, N. Cohen, and S. Velkes, *Hip arthroplasty with the articular surface replacement (ASR) system: survivorship analysis and functional outcomes.* Eur J Orthop Surg Traumatol, 2014. **24**(6): p. 925-30.

80. Silverman, E.J., B. Ashley, and N.P. Sheth, *Metal-on-metal total hip arthroplasty: is there still a role in 2016?* Current Reviews in Musculoskeletal Medicine, 2016: p. 1-4.

81. Ulrich, S.D., T.M. Seyler, D. Bennett, R.E. Delanois, K.J. Saleh, I. Thongtrangan, M. Kuskowski, E.Y. Cheng, P.F. Sharkey, J. Parvizi, J.B. Stiehl, and M.A. Mont, *Total hip arthroplasties: What are the reasons for revision?* International Orthopaedics, 2008. **32**(5): p. 597-604.

82. Abu-Amer, Y., I. Darwech, and J.C. Clohisy, *Aseptic loosening of total joint replacements: mechanisms underlying osteolysis and potential therapies.* Arthritis Research and Therapy, 2007. **9**(1): p. S1-6.

83. Bergin, P.F., J.B. Noveau, J.S. Jelinek, and R.M. Henshaw, *Aseptic loosening rates in distal femoral endoprostheses: does stem size matter?* Clin Orthop Relat Res, 2012. **470**(3): p. 743-50.

84. Ollivere, B., J. Wimhurst, I. Clark, and S. Donell, *Current concepts in osteolysis.* Journal of Bone & Joint Surgery, British Volume, 2012. **94**(1): p. 10-15.

85. Abraham, R. and A.L. Malkani, *Instability after Total Hip Replacement.* Seminars in Arthroplasty, 2005. **16**(2): p. 132-141.

86. Werner, B.C. and T.E. Brown, *Instability after total hip arthroplasty.* World J Orthop, 2012. **3**(8): p. 122-30.

87. Parvizi, J., D.-H. Suh, S.M. Jafari, A. Mullan, and J. Purtill, *Aseptic Loosening of Total Hip Arthroplasty: Infection Always Should be Ruled Out.* Clinical Orthopaedics and Related Research®, 2011. **469**(5): p. 1401-1405.

88. Senthi, S., J.T. Munro, and R.P. Pitto, *Infection in total hip replacement: meta-analysis.* International orthopaedics, 2011. **35**(2): p. 253-260.

89. Park, S.K., Y.G. Kim, and S.Y. Kim, *Treatment of periprosthetic femoral fractures in hip arthroplasty.* Clinics in Orthopedic Surgery, 2011. **3**(2): p. 101-106.

90. Gogulescu, B.A. and N. Gogulescu, *Periprosthetic Femoral Fractures around Hip Arthroplasties.* Research & Science Today, 2015: p. 10-11.

91. Hou, Z., T.R. Bowen, and W.R. Smith, *Periprosthetic Femoral Fractures Associated With Hip Arthroplasty.* Orthopedics, 2010. **33**(12): p. 908-16.

92. Pierannunzii, L., *Thigh Pain After Total Hip Replacement: A Pathophysiological Review and a Comprehensive Classification.* Orthopedics, 2008. **31**(7): p. 691-9.

93. Ferrata, P., S. Carta, M. Fortina, D. Scipio, A. Riva, and S. Di Giacinto, *Painful hip arthroplasty: definition.* Clinical Cases in Mineral and Bone Metabolism, 2011. **8**(2): p. 19–22.

94. Reinartz, P., T. Mumme, B. Hermanns, U. Cremerius, D.C. Wirtz, W.M. Schaefer, F. Niethard, and U. Buell, *Radionuclide imaging of the painful hip arthroplasty: positron-emission tomography versus triple-phase bone scanning.* J Bone Joint Surg Br, 2005. **87**(4): p. 465-70.

95. Temmerman, O.P., P.G. Raijmakers, W.L. Deville, J. Berkhof, L. Hooft, and I.C. Heyligers, *The use of plain radiography, subtraction arthrography, nuclear arthrography, and bone scintigraphy in the diagnosis of a loose acetabular component of a total hip prosthesis: a systematic review.* J Arthroplasty, 2007. **22**(6): p. 818-27.

96. DeLee, J.G. and J. Charnley, *Radiological demarcation of cemented sockets in total hip replacement.* Clin Orthop Relat Res, 1976(121): p. 20-32.

97. Chiu, K., W. Yau, W. Tang, and T. Ng, *Reading Radiographs after Total Hip Arthroplasty.* 2006. **10**(1): p. 1-9.

98. Miller, T., *Imaging of hip arthroplasty*, in *Seminars in musculoskeletal radiology*2006. p. 30-46.

99. Hatton, A., J.E. Nevelos, J.B. Matthews, J. Fisher, and E. Ingham, *Effects of clinically relevant alumina ceramic wear particles on TNF-alpha production by human peripheral blood mononuclear phagocytes.* Biomaterials, 2003. **24**(7): p. 1193-204.

100. Ruther, C., U. Timm, H. Ewald, W. Mittelmeier, R. Bader, R. Schmelter, Armin, L. and, and D. Kluess, *Current Possibilities for Detection of Loosening of Total Hip Replacements and How Intelligent Implants Could Improve Diagnostic Accuracy, Recent Advances in Arthroplasty , Dr. Samo Fokter (Ed.)*, in *InTech*2012. p. 363-86.

101. McBride, T.J. and D. Prakash, *How to read a postoperative total hip replacement radiograph.* Postgraduate medical journal, 2011. **87**(1024): p. 101-109.

102. Desai, A.U., N. Sriskanadan, and D.C. Howlett, *Imaging of the musculoskeletal system.* Surgery (Medicine Publishing), 2010. **28**(10): p. 518-522.

103. Wong, L.C.Y., W.K. Chiu, M. Russ, and S. Liew, *Review of techniques for monitoring the healing fracture of bones for implementation in an internally fixated pelvis.* Medical Engineering & Physics, 2012. **34**(2): p. 140-152.

104. Temmerman, O.P., P.G. Raijmakers, J. Berkhof, O.S. Hoekstra, G.J. Teule, and I.C. Heyligers, *Accuracy of diagnostic imaging techniques in the diagnosis of aseptic loosening of the femoral component of a hip prosthesis: a meta-analysis.* J Bone Joint Surg Br, 2005. **87**(6): p. 781-5.

105. Nikpoor, N., *Chapter 2 - Scintigraphy of the Musculoskeletal System*, in *Imaging of Arthritis and Metabolic Bone Disease*. 2009, W.B. Saunders: Philadelphia. p. 17-33.

106. Chryssikos, T., J. Parvizi, E. Ghanem, A. Newberg, H. Zhuang, and A. Alavi, *FDG-PET imaging can diagnose periprosthetic infection of the hip.* Clinical Orthopaedics and Related Research®, 2008. **466**(6): p. 1338-1342.

107. Bauer, T.W., J. Parvizi, N. Kobayashi, and V. Krebs, *Diagnosis of periprosthetic infection.* J Bone Joint Surg Am, 2006. **88**(4): p. 869-82.

108. Reinartz, P., *FDG-PET in patients with painful hip and knee arthroplasty: technical breakthrough or just more of the same.* Q J Nucl Med Mol Imaging, 2009. **53**(1): p. 41-50.

109. Gill, H.S., S. Mellon, E. Pegg, S. Ostlere, H. Pandit, and D. Murray, *The role of imaging in follow-up of newly introduced implants.* Orthopaedics and Trauma, 2012. **26**(4): p. 237-241.

110. Pijls, B.G., M.J. Nieuwenhuijse, M. Fiocco, J.W. Plevier, S. Middeldorp, R.G. Nelissen, and E.R. Valstar, *Early proximal migration of cups is associated with late revision in THA: a systematic review and meta-analysis of 26 RSA studies and 49 survivalstudies.* Acta Orthop, 2012. **83**(6): p. 583-91.

111. Nieuwenhuijse, M.J., E.R. Valstar, B.L. Kaptein, and R.G.H.H. Nelissen, *Good Diagnostic Performance of Early Migration as a Predictor of Late Aseptic Loosening of Acetabular CupsResults from Ten Years of Follow-up with Roentgen Stereophotogrammetric Analysis (RSA).* The Journal of Bone & Joint Surgery, 2012. **94**(10): p. 874-880.

112. Ilchmann, T., B. Mjöberg, and H. Wingstrand, *Measurement accuracy in acetabular cup wear: three retrospective methods compared with Roentgen stereophotogrammetry.* The Journal of arthroplasty, 1995. **10**(5): p. 636-642.

113. Stilling, M., S. Kold, S. de Raedt, N. Andersen, O. Rahbek, and K. Søballe, *Superior accuracy of model-based radiostereometric analysis for measurement of polyethylene wear A phantom study.* Bone and Joint Research, 2012. **1**(8): p. 180-191.

114. Lanting, B. and S. MacDonald, *The painful total hip replacement diagnosis and deliverance.* Bone & Joint Journal, 2013. **95**(11 Supple A): p. 70-73.

115. Keogh, C.F., P.L. Munk, R. Gee, L.P. Chan, and L.O. Marchinkow, *Imaging of the painful hip arthroplasty.* American Journal of Roentgenology, 2003. **180**(1): p. 115-120.

116. Ovesen, O., P. Riegels-Nielsen, S. Lindequist, I. Jensen, T. Munkner, T. Torfing, and J. Marving, *The diagnostic value of digital subtraction arthrography and radionuclide bone scan in revision hip arthroplasty.* J Arthroplasty, 2003. **18**(6): p. 735-40.

117. Love, C., A.S. Din, M.B. Tomas, T.P. Kalapparambath, and C.J. Palestro, *Radionuclide Bone Imaging: An Illustrative Review1.* Radiographics, 2003. **23**(2): p. 341-358.

118. Zajonz, D., L. Wuthe, S. Tiepolt, P. Brandmeier, T. Prietzel, G.F. von Salis-Soglio, A. Roth, C. Josten, C.E. Heyde, and M. Ghanem, *Diagnostic work-up strategy for periprosthetic joint infections after total hip and knee arthroplasty: a 12-year experience on 320 consecutive cases.* Patient Saf Surg, 2015. **9**(1): p. 20.

119. Selvik, G., P. Alberius, and A.S. Aronson, *A roentgen stereophotogrammetric system. Construction, calibration and technical accuracy.* Acta Radiol Diagn (Stockh), 1983. **24**(4): p. 343-52.

120. Klerken, T., M. Mohaddes, S. Nemes, and J. Karrholm, *High early migration of the revised acetabular component is a predictor of late cup loosening: 312 cup revisions followed with radiostereometric analysis for 2-20 years.* Hip Int, 2015. **25**(5): p. 471-6.

121. Ruther, C., H. Ewald, W. Mittelmeier, R. Bader, and D. Kluess. *Localization of uncemented hip stem loosening with a novel in-vivo sensor system based on vibration analysis*. in *International Federation for Medical and Biological Engineering*. 2010. Singapore.

122. Unger, A.C., H. Cabrera-Palacios, A.P. Schulz, C. Jurgens, and A. Paech, *Acoustic monitoring (RFM) of total hip arthroplasty - Results of a cadaver study.* Eur J Med Res, 2009. **14**(6): p. 264-71.

123. Bedair, H., N. Ting, C. Jacovides, A. Saxena, M. Moric, J. Parvizi, and C.J. Della Valle, *The Mark Coventry Award: Diagnosis of Early Postoperative TKA Infection Using Synovial Fluid Analysis.* Clinical Orthopaedics and Related Research, 2011. **469**(1): p. 34-40.

124. Shao, F., W. Xu, A. Crocombe, and D. Ewins, *Natural frequency analysis of osseointegration for trans-femoral implant.* Ann Biomed Eng, 2007. **35**(5): p. 817-24.

125. Handbook, M., *Nondestructive Active Testing Technique for Structural Composites.* MIL-HDBK-793, 1989: p. 2-6.

126. Meredith, N., D. Alleyne, and P. Cawley, *Quantitative determination of the stability of the implant-tissue interface using resonance frequency analysis.* Clin Oral Implants Res, 1996. **7**(3): p. 261-7.

127. Meredith, N., K. Books, B. Fribergs, T. Jemt, and L. Sennerby, *Resonance frequency measurements of implant stability in viva. A cross-sectional and longitudinal study of resonance frequency measurements on implants in the edentulous and partially dentate maxilla.* Clinical Oral Implants Research, 1997. **8**(3): p. 226-233.

128. Cairns, N.J., M.J. Pearcy, J. Smeathers, and C.J. Adam, *Ability of modal analysis to detect osseointegration of implants in transfemoral amputees: a physical model study.* Med Biol Eng Comput, 2013. **51**(1-2): p. 39-47.

129. Elias, J.J., J.B. Brunski, and H.A. Scarton, *A dynamic modal testing technique for noninvasive assessment of bone-dental implant interfaces.* Int J Oral Maxillofac Implants, 1996. **11**(6): p. 728-34.

130. Huang, H.M., C.L. Chiu, C.Y. Yeh, C.T. Lin, L.H. Lin, and S.Y. Lee, *Early detection of implant healing process using resonance frequency analysis.* Clin Oral Implants Res, 2003. **14**(4): p. 437-43.

131. Huang, H.M., K.Y. Cheng, C.F. Chen, K.L. Ou, C.T. Li, and S.Y. Lee, *Design of a stability-detecting device for dental implants.* Proc Inst Mech Eng H, 2005. **219**(3): p. 203-11.

132. Lachmann, S., B. Jager, D. Axmann, G. Gomez-Roman, M. Groten, and H. Weber, *Resonance frequency analysis and damping capacity assessment. Part I: an in vitro study on measurement reliability and a method of comparison in the determination of primary dental implant stability.* Clin Oral Implants Res, 2006a. **17**(1): p. 75-9.

133. Lachmann, S., J.Y. Laval, B. Jager, D. Axmann, G. Gomez-Roman, M. Groten, and H. Weber, *Resonance frequency analysis and damping capacity assessment. Part 2: peri-implant bone loss follow-up. An in vitro study with the Periotest and Osstell instruments.* Clin Oral Implants Res, 2006b. **17**(1): p. 80-4.

134. Hagberg, K., *One hundred patients treated with osseointegrated transfemoral amputation prostheses–rehabilitation perspective.* Journal of Rehabilitation Research & Development, 2009. **24**(3): p. 331–344.

135. Xu, W., F. Shao, and D. Ewins, *A resonant frequency measurement system for osseointegration trans-femoral implant.* Key Engineering Materials, 2005. **295**: p. 139-144.

136. Cairns, N.J., C.J. Adam, M.J. Pearcy, and J. Smeathers, *Evaluation of modal analysis techniques using physical models to detect osseointegration of implants in transfemoral amputees*, in *Engineering in Medicine and Biology Society, EMBC, 2011 Annual International Conference of the IEEE*2011. p. 1600-3.

137. Xu, W., D.H. Xu, and A. Crocombe, *Three-dimensional finite element stress and strain analysis of a transfemoral osseointegration implant.* Proceedings of the Institution of Mechanical Engineers, Part H: Journal of Engineering in Medicine, 2006. **220**(6): p. 661-670.

138. Lippmann, R.K., *THE USE OF AUSCULTATORY PERCUSSION FOR THE EXAMINATION OF FRACTURES.* The Journal of Bone & Joint Surgery, 1932. **14**(1): p. 118-126.

139. Nokes, L.D., *The use of low-frequency vibration measurement in orthopaedics.* Proc Inst Mech Eng H, 1999. **213**(3): p. 271-90.

140. Cunningham, J.L., *Vibration analysis*, in *The Physical Measurement of Bone*, C.M. Langton and C.F. Njeh, Editors. 2003, Taylor & Francis. p. 511-550.

141. Chung, J., G. Pratt, P. Babyn, and R. Poss, *A new diagnostic technique for the evaluation of prosthetic fixation*, in *Procs first annual conference IEEE/ Engineering Medicine and Biological society*1979, IEEE publishing services: New York. p. 158-160

142. Poss, R., G. Pratt Jr, and J. Chung, *An evaluation of total hip replacement cementing technique using sonic resonance.* Engineering in medicine, 1984. **13**(4): p. 191-196.

143. Van der Perre, G., *Dynamic analysis of human bones.* Functional Behaviour of Orthopaedic Materials, 1984: p. 99-159.

144. Smith, S.W., *The scientist and engineer's guide to digital signal processing*. 1997.

145. Rowlands, A., F.A. Duck, and J.L. Cunningham, *Bone vibration measurement using ultrasound: Application to detection of hip prosthesis loosening.* Medical Engineering & Physics, 2008. **30**(3): p. 278-284.

146. Flint, T., L. Nokes, M. Maheson, and J. Woodcock, *Using the Doppler effect to measure the vibration of human bones: in vitro studies.* Proceedings of the Institution of Mechanical Engineers, Part H: Journal of Engineering in Medicine, 1994. **208**(2): p. 127-129.

147. Davies, J.P., M.K. Tse, and W.H. Harris, *Monitoring the integrity of the cement—metal interface of total joint components in vitro using acoustic emission and ultrasound.* The Journal of Arthroplasty, 1996. **11**(5): p. 594-601.

148. Davies, J.P., M.K. Tse, and W.H. Harris, *IN-VITRO EVALUATION OF BONDING OF THE CEMENT-METAL INTERFACE OF A TOTAL HIP FEMORAL COMPONENT USING ULTRASOUND.* Journal of Orthopaedic Research, 1995. **13**(3): p. 335-338.

149. Nakatsuchi, Y., A. Tsuchikane, and A. Nomura, *The vibrational mode of the tibia and assessment of bone union in experimental fracture healing using the impulse response method.* Medical Engineering & Physics, 1996. **18**(7): p. 575-583.

150. Roberts, S.G. and C.R. Steele, *Efficacy of monitoring long-bone fracture healing by measurement of either bone stiffness or resonant frequency: Numerical simulation.* Journal of Orthopaedic Research, 2000. **18**(5): p. 691-697.

151. Van der Perre, G. and G. Lowet, *Vibration, sonic and ultrasonic wave propagation analysis for the detection of osteoporosis.* Clinical Rheumatology, 1994. **13**(SUPPL. 1): p. 45-53.

152. Puers, R., M. Catrysse, G. Vandevoorde, R.J. Collier, E. Louridas, F. Burny, M. Donkerwolcke, and F. Moulart, *A telemetry system for the detection of hip prosthesis loosening by vibration analysis.* Sensors and Actuators A: Physical, 2000. **85**(1-3): p. 42-47.

153. Clasbrummel, B., B. Jettkant, N. DeLuca, G. Muhr, and G. Möllenhoff, *Endoprothesenlockerungen.* Trauma und Berufskrankheit, 2007. **9**(2): p. 84-87.

154. Marschner, U., H. Gratz, B. Jettkant, D. Ruwisch, G. Woldt, W.J. Fischer, and B. Clasbrummel, *Integration of a wireless lock-in measurement of hip prosthesis vibrations for loosening detection.* Sensors and Actuators a-Physical, 2009. **156**(1): p. 145-154.

155. Sauer, S., U. Marschner, H. Graetz, and W.J. Fischer. *Medical Wireless Vibration Measurement System for Hip Prosthesis Loosening Detection*. in *SENSORDEVICES ,The Third International Conference on Sensor Device Technologies and Applications*. 2012.

156. Paech, A., A. Schulz, R. Nassutt, J. Keine, M. Wenzl, and C. Jurgens, *Acoustic Properties of Femoral Components of Hip Endoprostheses Analysis Using Frequency-Resonance-Measurement in a Soft Tissue Simulation Model.* Research Journal of Medical Sciences, 2007. **1**(2): p. 118-123.

157. Ewald, H., C. Ruther, W. Mittelmeier, R. Bader, and D. Kluess. *A novel in vivo sensor for loosening diagnostics in total hip replacement*. in *Sensors, 2011 IEEE*. 2011

158. Ewald, H., U. Timm, C. Ruther, W. Mittelmeier, R. Bader, and D. Kluess, *Acoustic sensor system for loosening detection of hip implants*, in *Sensing Technology (ICST), 2011 Fifth International Conference on*2011 p. 494-497.

159. Ruther, C., Ewald H, Biemann A, Nierath H, Bader R, and K. D. *A New Concept for Non-Invasive Radiation-Free Detection of Implant Loosening*. in *56th Annual Meeting of the Orthopaedic Research Society,New Orleans, Louisiana, USA*. 2010.

160. Ruther, C., H. Ewald, W. Mittelmeier, A. Fritsche, R. Bader, and D. Kluess, *A novel sensor concept for optimization of loosening diagnostics in total hip replacement.* J Biomech Eng, 2011. **133**(10): p. 104503-5.

161. Ruther, C., H. Ewald, W. Mittelmeier, D. Kluess, A. Fritsche, and R. Bader. *A New Method for Detection of Total Hip Replacement Loosening - Development and First Results of a Novel Mechano-acoustical Sensor*. in *Proceedings of the International Conference on Biomedical Electronics and Devices (Biodevices)*. 2011. Rome, Italy.

162. Ruther, C., C. Gabler, H. Ewald, M. Ellenrieder, M. Haenle, T. Lindner, W. Mittelmeier, R. Bader, and D. Kluess, *In vivo monitoring of implant osseointegration in a rabbit model using acoustic sound analysis.* J Orthop Res, 2014. **32**(4): p. 606-12.

163. Ruther, C., H. Nierath, H. Ewald, J.L. Cunningham, W. Mittelmeier, R. Bader, and D. Kluess, *Investigation of an acoustic-mechanical method to detect implant loosening.* Med Eng Phys, 2013. **35**(11): p. 1669-75.

164. Ruther, C., U. Timm, A. Fritsche, H. Ewald, W. Mittelmeier, R. Bader, and D. Kluess, *A New Approach for Diagnostic Investigation of Total Hip Replacement Loosening*, in *Biomedical Engineering Systems and Technologies*, A. Fred, J. Filipe, and H. Gamboa, Editors. 2013, Springer Berlin Heidelberg. p. 74-79.

165. Harris, W.H., R.D. Mulroy, Jr., W.J. Maloney, D.W. Burke, H.P. Chandler, and E.B. Zalenski, *Intraoperative measurement of rotational stability of femoral components of total hip arthroplasty.* Clin Orthop Relat Res, 1991(266): p. 119-26.

166. Cristofolini, L., E. Varini, I. Pelgreffi, A. Cappello, and A. Toni, *Device to measure intra-operatively the primary stability of cementless hip stems.* Med Eng Phys, 2006. **28**(5): p. 475-82.

167. Lannocca, M., E. Varini, A. Cappello, L. Cristofolini, and E. Bialoblocka, *Intra-operative evaluation of cementless hip implant stability: a prototype device based on vibration analysis.* Med Eng Phys, 2007. **29**(8): p. 886-94.

168. Mulier, M., C. Pastrav, and G. Van der Perre, *Per-operative vibration analysis: a valuable tool for defining correct stem insertion: preliminary report.* Ortop Traumatol Rehabil, 2008. **10**(6): p. 576-82.

169. Pastrav, L.C., S.V. Jaecques, I. Jonkers, G.V. Perre, and M. Mulier, *In vivo evaluation of a vibration analysis technique for the per-operative monitoring of the fixation of hip prostheses.* J Orthop Surg Res, 2009. **4**(10): p. 4-10.

170. Varini, E., E. Bialoblocka-Juszczyk, M. Lannocca, A. Cappello, and L. Cristofolini, *Assessment of implant stability of cementless hip prostheses through the frequency response function of the stem–bone system.* Sensors and Actuators A: Physical, 2010. **163**(2): p. 526-532.

171. Reggiani, B., L. Cristofolini, E. Varini, and M. Viceconti, *Predicting the subject-specific primary stability of cementless implants during pre-operative planning: Preliminary validation of subject-specific finite-element models.* Journal of Biomechanics, 2007. **40**(11): p. 2552-2558.

172. Clift, S.E. *Finite Element Modeling of Uncemented Implants: Challenges in the Representation of the Press-fit Condition*. in *IFMBE Proceedings*. 2009.

173. Crosnier, E.A., P.S. Keogh, and A.W. Miles, *A novel method to assess primary stability of press-fit acetabular cups.* Proceedings of the Institution of Mechanical Engineers, Part H: Journal of Engineering in Medicine, 2014. **228**(11): p. 1126-1134.

174. Mathieu, V., A. Michel, C.-H. Flouzat Lachaniette, A. Poignard, P. Hernigou, J. Allain, and G. Haïat, *Variation of the impact duration during the in vitro insertion of acetabular cup implants.* Medical Engineering & Physics, 2013. **35**(11): p. 1558-1563.

175. Michel, A., R. Bosc, V. Mathieu, P. Hernigou, and G. Haiat, *Monitoring the press-fit insertion of an acetabular cup by impact measurements: influence of bone abrasion.* Proc Inst Mech Eng H, 2014. **228**(10): p. 1027-34.

176. Michel, A., R. Bosc, F. Sailhan, R. Vayron, and G. Haiat, *Ex vivo estimation of cementless acetabular cup stability using an impact hammer.* Medical Engineering & Physics, 2016. **38**(2): p. 80-86.

177. Michel, A., R. Bosc, R. Vayron, and G. Haiat, *In Vitro Evaluation of the Acetabular Cup Primary Stability by Impact Analysis.* Journal of Biomechanical Engineering, 2015. **137**(3): p. 031011-6.

178. Michel, A., G. Haïat, and R. Bosc, *Estimation of the Acetabular Cup Implant Stability via Impact Analysis*, in *The 22nd international congress on sound and vibration (ICSV22)*2015: Florence, Italy. p. 1-8.

179. Henys, P., L. Capek, J. Fencl, and E. Prochazka, *Evaluation of acetabular cup initial fixation by using resonance frequency principle.* Proc Inst Mech Eng H, 2015. **229**(1): p. 3-8.

180. Bender, T., M. Sass, W. Mittelmeier, R. Bader, and D. Kluess. *Finite Element Analysis into Eigenfrequencies of a Total Hip Stem with Different Levels of Loosening*. in *COMSOL*. 2015. Grenoble.

181. Culjat, M.O., D. Goldenberg, P. Tewari, and R.S. Singh, *A Review of Tissue Substitutes for Ultrasound Imaging.* Ultrasound in Medicine & Biology, 2010. **36**(6): p. 861-873.

182. Omari, E., H. Lee, and T. Varghese, *Theoretical and phantom based investigation of the impact of sound speed and backscatter variations on attenuation slope estimation.* Ultrasonics, 2011. **51**(6): p. 758-767.

183. Wells, P.N. and H.D. Liang, *Medical ultrasound: imaging of soft tissue strain and elasticity.* J R Soc Interface, 2011. **8**(64): p. 1521-49.

184. Zell, K., J.I. Sperl, M.W. Vogel, R. Niessner, and C. Haisch, *Acoustical properties of selected tissue phantom materials for ultrasound imaging.* Phys Med Biol, 2007. **52**(20): p. N475-84.

185. Lewis, J. and R. Tarr, *Fracture healing assessment by impact response: clinical results.* J. Bone Joint Surg, 1975. **57**: p. 576.

186. Thompson, G.A., D. Orne, and D.R. Young, *In vivo determination of mechnical properties of the human ulna by means of mechanical impedance tests: Experimental results and improved mathematical model.* Medical and Biological Engineering and Computing, 1976. **14**(3): p. 253-262.

187. Saha, S. and R.S. Lakes, *The effect of soft tissue on wave-propagation and vibration tests for determining the in vivo properties of bone.* J Biomech, 1977. **10**(7): p. 393-401.

188. Ziegert, J.C. and J.L. Lewis, *The Effect of Soft Tissue on Measurements of Vibrational Bone Motion by Skin-Mounted Accelerometers.* Journal of Biomechanical Engineering, 1979. **101**(3): p. 218-220.

189. Nokes, L., J.A. Fairclough, W.J. Mintowt-Czyz, I. Mackie, and J. Williams, *Vibration analysis of human tibia: The effect of soft tissue on the output from skin-mounted accelerometers.* Journal of Biomedical Engineering, 1984a. **6**(3): p. 223-226.

190. Christensen, A., L. Tougaard, C. Dyrbye, and H. Vibe-Hansen, *Resonance of the human tibia. Method, reproducibility and effect of transection.* Acta Orthop Scand, 1982. **53**(6): p. 867-74.

191. Van der Perre, G., R. Van Audekercke, M. Martens, and J.C. Mulier, *Identification of in-vivo vibration modes of human tibiae by modal analysis.* J Biomech Eng, 1983. **105**(3): p. 244-8.

192. Cornelissen, P., M. Cornelissen, G. Van der Perre, A.B. Christensen, F. Ammitzbøll, and C. Dyrbye, *Assessment of tibial stiffness by vibration testing in situ—II. Influence of soft tissues, joints and fibula.* Journal of Biomechanics, 1986. **19**(7): p. 551-561.

193. Tsuchikane, A., Y. Nakatsuchi, and A. Nomura, *The influence of joints and soft tissue on the natural frequency of the human tibia using the impulse response method.* Proc Inst Mech Eng H, 1995. **209**(3): p. 149-55.

194. Bediz, B., H. Nevzat Ozguven, and F. Korkusuz, *Vibration measurements predict the mechanical properties of human tibia.* Clin Biomech (Bristol, Avon), 2010. **25**(4): p. 365-71.

195. Razaghi, H., R. Saatchi, A. Offiah, N. Bishop, and D. Burke. *Spectral analysis of bone low frequency vibration signals*. in *Communication Systems, Networks & Digital Signal Processing (CSNDSP), 2012 8th International Symposium on*. 2012.

196. Pastrav, L., S. Leuridan, K. Denis, H. Delport, P. Debeer, L. De Wilde, G. Van der Perre, W. Desmet, and J. Vander Sloten. *Vibrational techniques to assess the stability of spherical press-fitted implants : preliminary results*. in *International Conference on Noise and Vibration Engineering-Proceedings of ISMA*. 2010. Heverlee: Katholieke Univ Leuven, Dept Werktuigkunde.

197. Rao, S.S. and F.F. Yap, *Mechanical vibrations*. 5th ed. Vol. . 2011 Singapore ; London : Prentice Hall

198. Alshuhri, A.A., T.P. Holsgrove, A.W. Miles, and J.L. Cunningham, *Development of a non-invasive diagnostic technique for acetabular component loosening in total hip replacements.* Med Eng Phys, 2015. **37**(8): p. 739-45.

199. Haidekker, M.A., *Medical imaging technology*. 2013, Springer. p. 97-110.

200. Griffin, M.J., *Handbook of human vibration*. 2012: Academic press.

201. *Chapter 2: Digital signal processing*, in *Power System Protection 4: Digital protection and signalling*, E.T. Association, Editor. 1995, Institution of Engineering and Technology. p. 21-35.

202. Ghasemi, A. and S. Zahediasl, *Normality Tests for Statistical Analysis: A Guide for Non-Statisticians.* International Journal of Endocrinology and Metabolism, 2012. **10**(2): p. 486-489.

203. in *THE 2013 SAWBONES CATALOG*. 2013. p. 74-78.

204. Heller, S., T. Brosh, Y. Kosashvili, S. Velkes, A. Burg, and I. Dudkiewicz, *Locking versus standard screw fixation for acetabular cups: is there a difference?* Archives of orthopaedic and trauma surgery, 2013. **133**(5): p. 701-705.

205. Tabata, T., N. Kaku, K. Hara, and H. Tsumura, *Initial stability of cementless acetabular cups: press-fit and screw fixation interaction—an in vitro biomechanical study.* European Journal of Orthopaedic Surgery & Traumatology, 2014. **25**(3): p. 497-502.

206. Udofia, I., F. Liu, Z. Jin, P. Roberts, and P. Grigoris, *The initial stability and contact mechanics of a press-fit resurfacing arthroplasty of the hip.* J Bone Joint Surg Br, 2007. **89**(4): p. 549-56.

207. Jin, Z., S. Meakins, M. Morlock, P. Parsons, C. Hardaker, M. Flett, and G. Isaac, *Deformation of press-fitted metallic resurfacing cups. Part 1: experimental simulation.* Proceedings of the Institution of Mechanical Engineers, Part H: Journal of Engineering in Medicine, 2006. **220**(2): p. 299-309.

208. Macdonald, W., L. Carlsson, G. Charnley, and C. Jacobsson, *Press-fit acetabular cup fixation: principles and testing.* Proceedings of the Institution of Mechanical Engineers, Part H: Journal of Engineering in Medicine, 1999. **213**(1): p. 33-39.

209. Pitto, R., G. Willmann, and M. Schramm, *Initial Stability of Modular Acetabular Components. Comparative In-vitro Study with Polyethylene and Ceramic Liners-Primärstabilität modularer acetabulärer Komponenten. Eine In-vitro-Vergleichsstudie mit Pfanneneinsätzen aus Polyethylen und Keramik.* Biomedizinische Technik/Biomedical Engineering, 2001. **46**(4): p. 109-112.

210. Mehmanparast, H., J. Mac-Thiong, and Y. Petit, *Compressive properties of a synthetic bone substitute for vertebral cancellous bone.* Int J Med Biol Sci, 2012. **65**: p. 287-290.

211. Jamieson, M.L., R.D. Russell, S.J. Incavo, and P.C. Noble, *Does an enhanced surface finish improve acetabular fixation in revision total hip arthroplasty?* The Journal of arthroplasty, 2011. **26**(4): p. 644-648.

212. Kaneko, K., Y. Inoue, Y. Yanagihara, S. Uta, A. Mogami, and H. Iwase, *The initial fixation of the press-fit acetabular shell–clinical observation and experimental study.* Archives of orthopaedic and trauma surgery, 2000. **120**(5-6): p. 323-325.

213. Baleani, M., R. Fognani, and A. Toni, *Initial stability of a cementless acetabular cup design: experimental investigation on the effect of adding fins to the rim of the cup.* Artificial organs, 2001. **25**(8): p. 664-669.

214. Gupta, A., J.M. Redmond, J.E. Hammarstedt, A.E. Petrakos, S.P. Vemula, and B.G. Domb, *Does Robotic-Assisted Computer Navigation Affect Acetabular Cup Positioning in Total Hip Arthroplasty in the Obese Patient? A Comparison Study.* J Arthroplasty, 2015. **30**(12): p. 2204-7.

215. Matharu, G.S., S.J. Mellon, D.W. Murray, and H.G. Pandit, *Follow-Up of Metal-on-Metal Hip Arthroplasty Patients Is Currently Not Evidence Based or Cost Effective.* The Journal of Arthroplasty, 2015. **30**(8): p. 1317-1323.

216. Matharu, G.S., R. Mansour, O. Dada, S. Ostlere, H.G. Pandit, and D.W. Murray, *Which imaging modality is most effective for identifying pseudotumours in metal-on-metal hip resurfacings requiring revision.* ultrasound or MARS-MRI or both?, 2016. **98-B**(1): p. 40-48.

217. Maradit Kremers, H., D.R. Larson, C.S. Crowson, W.K. Kremers, R.E. Washington, C.A. Steiner, W.A. Jiranek, and D.J. Berry, *Prevalence of Total Hip and Knee Replacement in the United States.* The Journal of Bone & Joint Surgery, 2015. **97**(17): p. 1386-1397.

218. Stambough, J.B., G. Pashos, F.C. Bohnenkamp, W.J. Maloney, J.M. Martell, and J.C. Clohisy, *Long-Term Results of Total Hip Arthroplasty with 28-Millimeter Cobalt-Chromium Femoral Heads on Highly Cross-Linked Polyethylene in Patients 50 Years and Less.* J Arthroplasty, 2016. **31**(1): p. 162-7.

219. Sennerby, L. and N. Meredith, *Implant stability measurements using resonance frequency analysis: biological and biomechanical aspects and clinical implications.* Periodontology 2000, 2008. **47**(1): p. 51-66.

220. Mjoberg, B., *The theory of early loosening of hip prostheses.* Orthopedics, 1997. **20**(12): p. 1169-75.

221. Mohler, C.G., J.J. Callaghan, D.K. Collis, and R.C. Johnston, *Early loosening of the femoral component at the cement-prosthesis interface after total hip replacement.* J Bone Joint Surg Am, 1995. **77**(9): p. 1315-22.

222. Katzer, A. and J.F. Lœhr, *Early loosening of hip replacements: causes, course and diagnosis.* Journal of Orthopaedics and Traumatology, 2003. **4**(3): p. 105-116.

223. Garcia-Cimbrelo, E. and L. Munuera, *Early and late loosening of the acetabular cup after low-friction arthroplasty.* J Bone Joint Surg Am, 1992. **74**(8): p. 1119-29.

224. Dahl, M.C., P.A. Kramer, P.G. Reinhall, S.K. Benirschke, S.T. Hansen, and R.P. Ching, *The efficacy of using vibrometry to detect osteointegration of the Agility total ankle.* J Biomech, 2010. **43**(9): p. 1840-3.

Appendix A: LabVIEW Code

A code was developed using LabVIEW sound and vibration software to record and post-process the data. The code detail and configuration are illustrated the below figures.

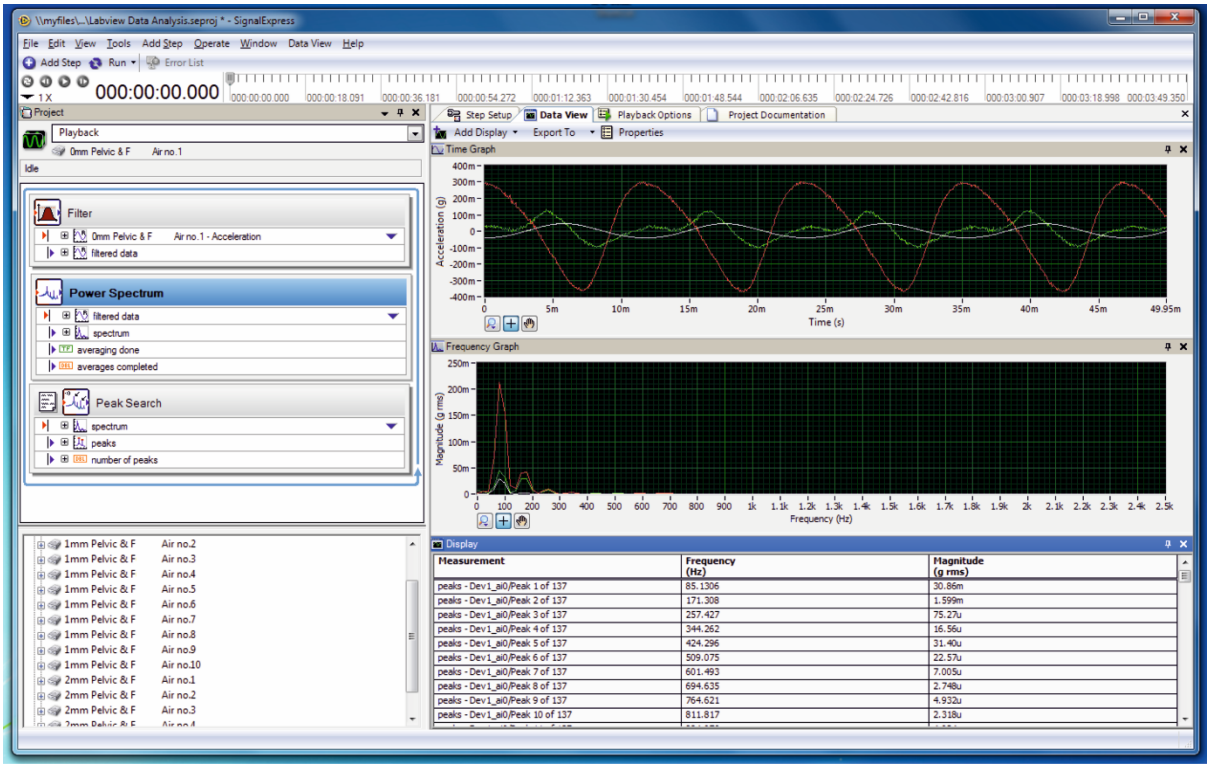

Figure A-1: The LabVIEW code.

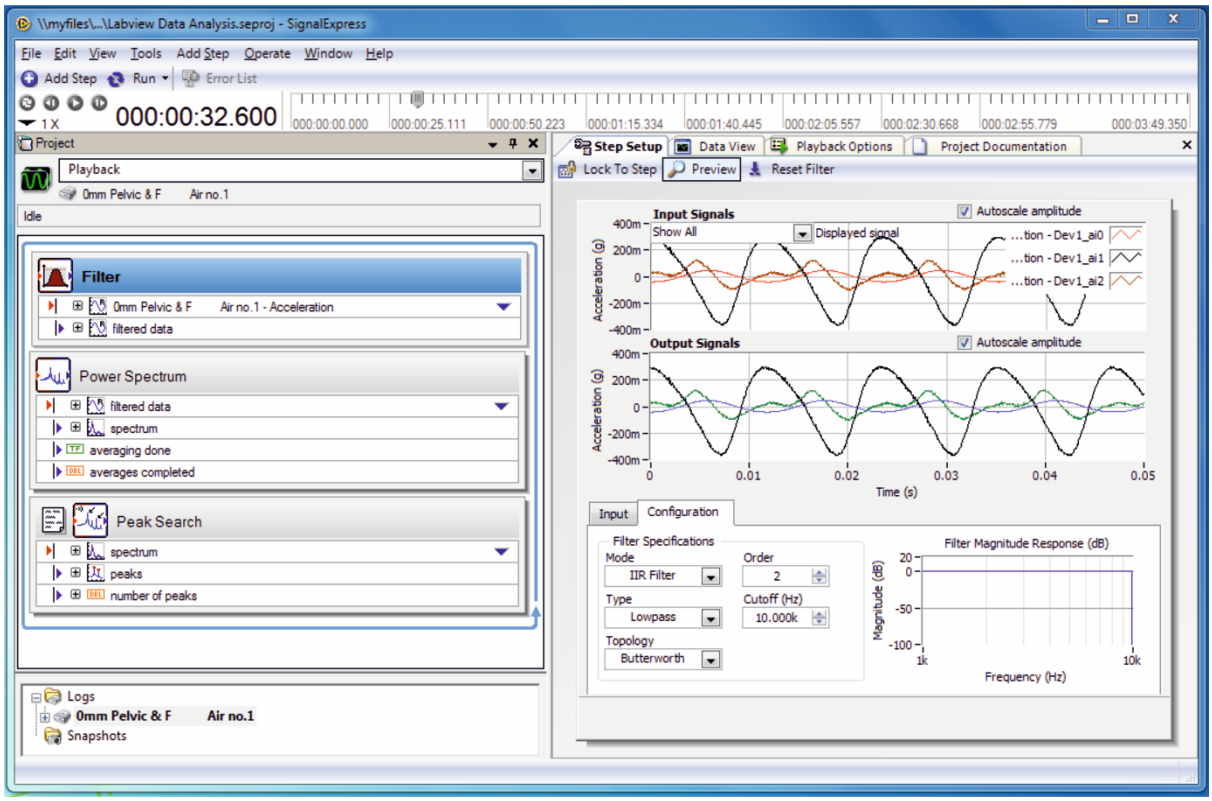

Figure A-2: The LabVIEW code filter configuration.

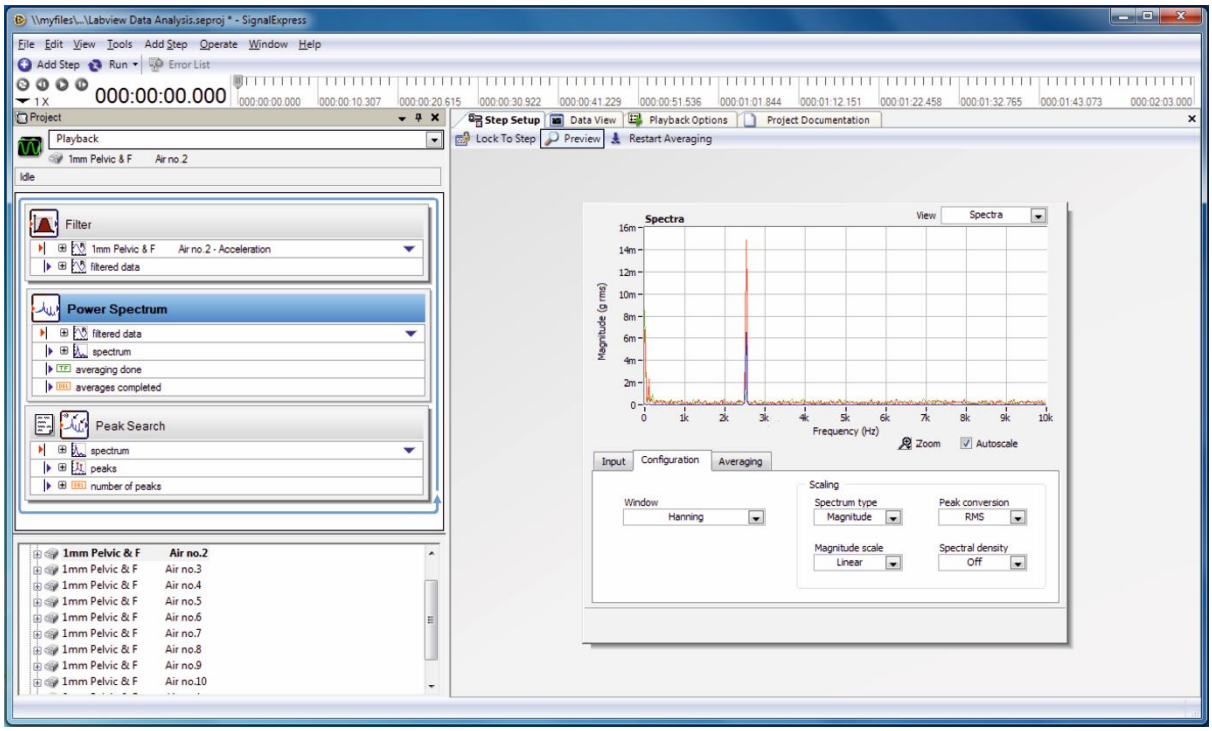

Figure A-3: The LabVIEW code power spectrum configuration.

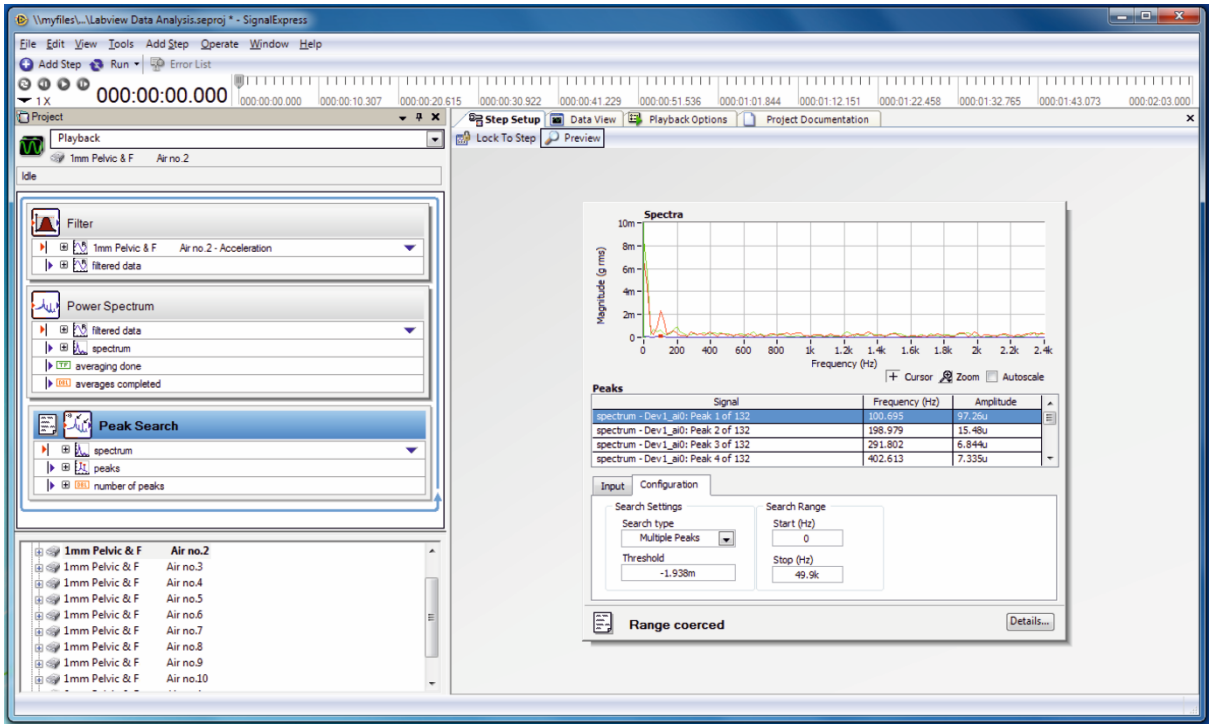

Figure A-4: The LabVIEW code peak search configuration.

Appendix B: FFT Algorithm

B.1-Fast Fourier transform (FFT):

According to the FFT theory, any periodical signal $x(t)$ can be expressed by a continuous sum of a series of sine and/or cosine functions as given blew for a period of $T_\circ$.

$$x(t) = a_0 + \sum_{n=1}^{\infty}(a_n \cos(n\omega_\circ t)\ ) + \sum_{n=1}^{\infty}(b_n \sin(n\omega_\circ t))$$

Where: $\omega_\circ = 2\pi\ /T_\circ$

Fourier coefficients = $a_0, a_n, and\ b_n$

$$a_0 = \frac{1}{T_\circ}\int_{T_\circ} x(t)dt$$

$$a_n = \frac{2}{T_\circ}\int_{T_\circ} x(t)cos(n\omega_\circ t)dt$$

$$b_n = \frac{2}{T_\circ}\int_{T_\circ} x(t)sin(n\omega_\circ t)dt$$

B.2-The Natural frequency:

$$F = \frac{1}{2\pi}\sqrt{\frac{K}{m}}$$

Where; F = natural frequency, K= stiffness, m=mass

Appendix C: Pelvis Specimen Fixation

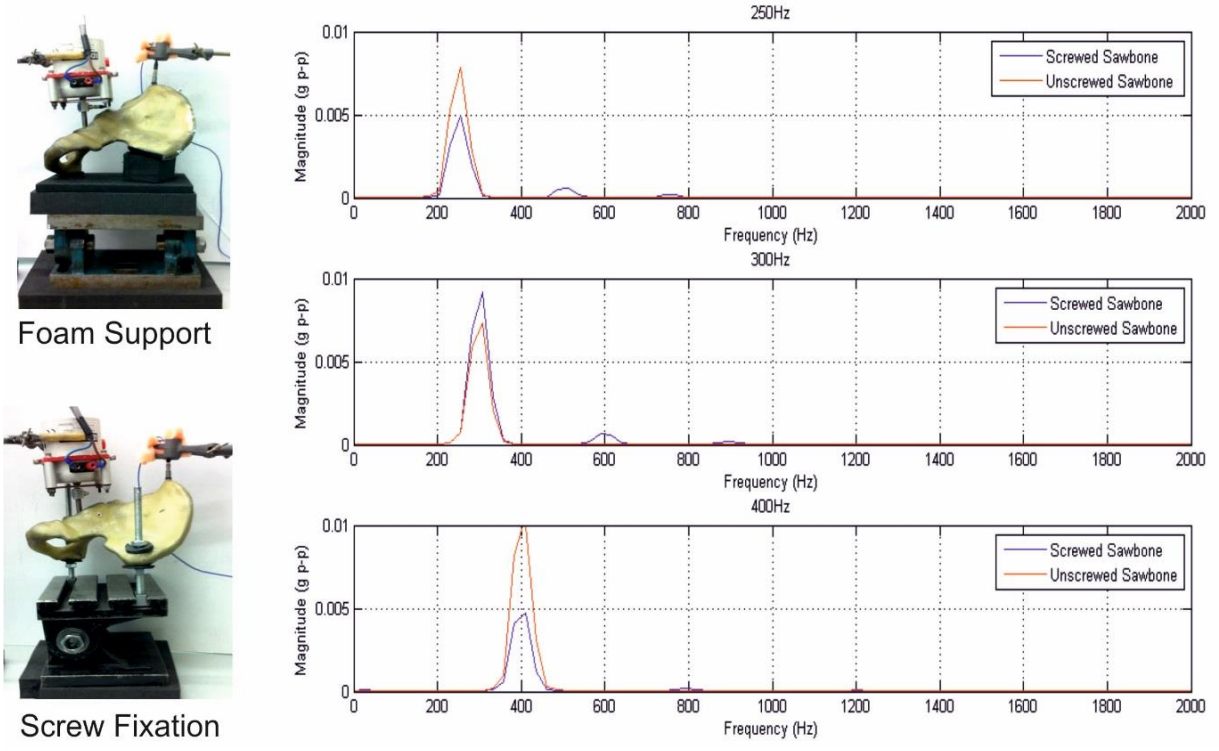

Figure C-1: The FFT analysis for the two pelvis coupling approaches, revealing that the screw fixation give additional unexplained harmonics in the frequency spectrum.

Appendix D: Muscle Simulation Approach

Spring Tension = $(L-L_o)$. K=N

L_o: Initial spring Length

L: Extended spring Length

K: Spring Constant (Rate)

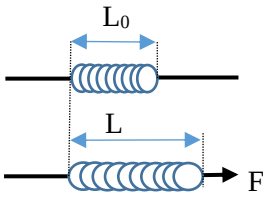

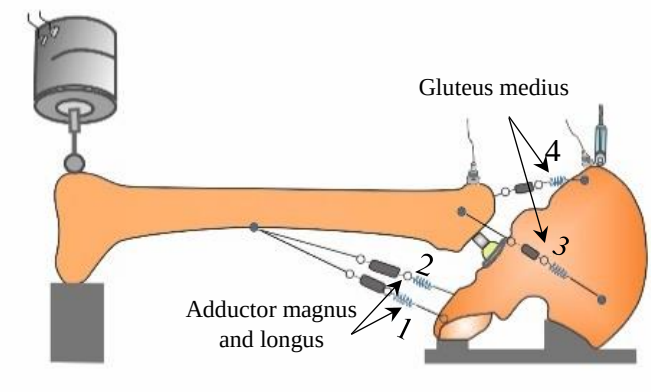

Figure D-1: The muscle simulation set-up

The adductor magnus and adductor longus was simulated by two springs having a spring constant of 2.26N/mm, initial spring length $L_{0=}$2.461cm, extended spring length L=3.13cm.

1 - Spring Tension = $(L-L_0)$. K=N: Spring Tension = (2.8-2.461 cm)* 42.45 N/cm=14.39 N

2 - Spring Tension = (3-2.461 cm)* 42.45 N/cm=22.88 N

The gluteus medius muscle was replicated using two springs having a spring constant = 4.17N/mm, initial spring length $L_{0=}$1.321cm, extended spring length L= 1.9cm.

3 - Spring Tension = (1.9 cm -1.321 cm)* 22.77 N/cm= 13.18N

4 - Spring Tension = (1.9 cm -1.321 cm)* 22.77 N/cm= 13.18N

		Accelerometer - Early Loosening																															
	Driving Frequency (Hz)	100	150	200	250	300	350	400	450	500	550	600	650	700	750	800	850	900	950	1000	1050	1100	1150	1200	1250	1300	1350	1400	1450	1500	#
Fundamental Magnitude	Secure Cup - 1 m Clear Gap	NA	NA	NA	NA	NA	NA	NA	NA	NA	NA	NA	NA	NA	NA	NA	NA	NA	NA	NA	NA	NA	NA	NA	NA	NA	NA	NA	NA	NA	0
	Secure Cup - 1 m Silicon Gap	NA	NA	NA	NA	NA	NA	NA	NA	NA	NA	NA	NA	NA	NA	NA	NA	NA	NA	NA	NA	NA	NA	NA	NA	NA	NA	NA	NA	NA	0
1st Harmonic Magnitude	Secure Cup - 1 m Clear Gap	.023[b]	NA	NA	NA	NA	NA	NA	NA	NA	NA	NA	NA	NA	NA	.000[b]	NA	NA	NA	NA	NA	NA	NA	NA	NA	NA	NA	NA	NA	NA	2
	Secure Cup - 1 m Silicon Gap	NA	NA	NA	NA	NA	NA	NA	NA	NA	NA	NA	NA	NA	NA	NA	NA	NA	NA	NA	.004[b]	.000[b]	.001[b]	NA	NA	NA	NA	NA	NA	NA	3
2nd Harmonic Magnitude	Secure Cup - 1 m Clear Gap	.000[b]	NA	NA	NA	NA	NA	NA	NA	NA	NA	NA	NA	NA	NA	.000[b]	NA	NA	NA	NA	NA	NA	NA	NA	NA	NA	NA	NA	NA	NA	2
	Secure Cup - 1 m Silicon Gap	NA	NA	NA	NA	NA	NA	NA	NA	NA	NA	NA	NA	NA	NA	.001[b]	NA	NA	NA	NA	NA	NA	NA	NA	NA	NA	NA	NA	NA	NA	1
1st Harmonic Ratio	Secure Cup - 1 m Clear Gap	NA	NA	NA	NA	NA	NA	NA	NA	NA	NA	NA	NA	NA	NA	.007[b]	NA	NA	NA	NA	NA	NA	NA	NA	NA	NA	NA	NA	NA	NA	1
	Secure Cup - 1 m Silicon Gap	NA	NA	NA	NA	NA	NA	NA	NA	NA	NA	NA	NA	NA	NA	NA	NA	NA	NA	NA	NA	NA	.003[b]	NA	NA	NA	NA	NA	NA	NA	1
2nd Harmonic Ratio	Secure Cup - 1 m Clear Gap	.000[b]	NA	NA	NA	NA	NA	NA	NA	NA	.011[b]	NA	NA	NA	NA	.000[b]	NA	NA	NA	NA	NA	NA	NA	NA	NA	NA	NA	NA	NA	NA	3
	Secure Cup - 1 m Silicon Gap	NA	NA	NA	NA	NA	NA	NA	NA	NA	NA	NA	NA	NA	NA	.002[b]	NA	NA	NA	NA	NA	NA	NA	NA	NA	NA	NA	NA	NA	NA	1

Table E-1: The accelerometer response comparison between the simulated conditions with the significant value being highlighted, NA = where the signal is not significant or do not support the main finding pattern.

		Ultrsound - Early Loosening																															
	Driving Frequency (Hz)	100	150	200	250	300	350	400	450	500	550	600	650	700	750	800	850	900	950	1000	1050	1100	1150	1200	1250	1300	1350	1400	1450	1500	#
Fundamental Magnitude	Secure Cup - 1 m Clear Gap	NA	NA	NA	NA	NA	NA	NA	NA	NA	NA	NA	NA	NA	NA	NA	NA	NA	NA	NA	NA	NA	NA	NA	NA	NA	NA	NA	NA	NA	0
	Secure Cup - 1 m Silicon Gap	NA	NA	NA	NA	NA	NA	NA	NA	NA	NA	NA	NA	NA	NA	NA	NA	NA	NA	NA	NA	NA	NA	NA	NA	NA	NA	NA	NA	NA	0
1st Harmonic Magnitude	Secure Cup - 1 m Clear Gap	NA	NA	NA	NA	NA	NA	NA	NA	NA	NA	NA	.002[b]	NA	NA	NA	NA	NA	NA	NA	NA	NA	NA	NA	NA	NA	NA	NA	NA	NA	1
	Secure Cup - 1 m Silicon Gap	NA	NA	NA	NA	NA	NA	NA	NA	NA	NA	NA	NA	NA	NA	NA	NA	NA	.000[b]	NA	NA	NA	NA	NA	NA	NA	.001[b]	NA	NA	NA	2
2nd Harmonic Magnitude	Secure Cup - 1 m Clear Gap	NA	NA	NA	NA	NA	NA	NA	NA	NA	NA	NA	NA	NA	NA	.029[b]	NA	NA	NA	NA	.007[b]	NA	NA	NA	NA	NA	NA	NA	NA	NA	2
	Secure Cup - 1 m Silicon Gap	NA	NA	NA	NA	NA	NA	NA	NA	NA	NA	NA	NA	NA	NA	NA	NA	NA	.015[b]	NA	.009[b]	NA	NA	NA	NA	NA	NA	NA	NA	NA	2
1st Harmonic Ratio	Secure Cup - 1 m Clear Gap	NA	NA	NA	NA	NA	NA	NA	NA	NA	NA	NA	NA	NA	NA	NA	NA	NA	NA	NA	NA	NA	NA	NA	NA	NA	NA	NA	NA	NA	0
	Secure Cup - 1 m Silicon Gap	NA	NA	NA	NA	NA	NA	NA	NA	NA	NA	NA	NA	NA	NA	NA	NA	NA	.004[b]	NA	NA	NA	NA	NA	NA	NA	.035[b]	NA	NA	NA	2
2nd Harmonic Ratio	Secure Cup - 1 m Clear Gap	NA	NA	NA	NA	NA	NA	NA	NA	NA	NA	NA	NA	NA	NA	.023[b]	NA	NA	NA	.043[b]	NA	NA	NA	NA	NA	NA	NA	NA	NA	NA	2
	Secure Cup - 1 m Silicon Gap	NA	NA	NA	NA	NA	NA	NA	NA	NA	NA	NA	NA	NA	NA	NA	NA	NA	.011[b]	NA	NA	NA	NA	NA	NA	NA	NA	NA	NA	NA	1

Table E-2: The ultrasound response comparison between the simulated conditions with the significant value being highlighted, NA = where the signal is not significant or do not support the main finding pattern.

Accelerometer - Zone Loosening

	Driving Frequency (Hz)	100	150	200	250	300	350	400	450	500	550	600	650	700	750	800	850	900	950	1000	1050	1100	1150	1200	1250	1300	1350	1400	1450	1500	1550	1600	1650	1700	1750	1800	1850	1900	1950	2000	2050	2100	2150	2200	2250	2300	2350	2400	2450	2500	#
	Secure Cup - 1 m (zone 2)	.000^b	.000^b	.000^b	.000^b	.000^b	.000^b	.000^b	.000^b	.000^b	.000^b	.000^b	.000^b	NA	NA	NA	NA	NA	NA	NA	NA	NA	.000^b	.000^b	.000^b	.000^b	.000^b	.000^b	NA	NA	NA	NA	NA	NA	NA	NA	NA	NA	NA	.000^b	.000^b	.000^b	.000^b	.000^b	NA	.000^b	.000^b	.000^b	NA	NA	26
Fundamental Magnitude	Secure Cup - 1 m (zone 1 and 2)	.000^b	.000^b	.000^b	.000^b	.000^b	NA	NA	NA	NA	NA	NA	.000^b	.000^b	NA	NA	NA	NA	NA	NA	NA	NA	NA	NA	NA	.000^b	.000^b	NA	NA	NA	NA	.000^b	.000^b	.000^b	.000^b	NA	NA	NA	.000^b	.000^b	.000^b	.000^b	.000^b	.000^b	.000^b	.000^b	.000^b	.000^b	.000^b	.000^b	25
	Secure Cup - 1 m (zone 1 and 3)	.000^b	.000^b	.000^b	.000^b	.000^b	NA	NA	NA	NA	NA	.000^b	.000^b	.000^b	.000^b	.000^b	.000^b	.000^b	.000^b	.000^b	.000^b	.000^b	.000^b	.000^b	.000^b	.000^b	.000^b	.000^b	NA	.000^b	.000^b	.000^b	.000^b	.000^b	.000^b	.000^b	NA	NA	.002^b	.000^b	.000^b	.000^b	.000^b	.000^b	.000^b	.000^b	.000^b	.000^b	.000^b	.000^b	41
	Secure Cup - 1 m (zone 2)	NA	NA	NA	.001^b	NA	NA	NA	NA	NA	NA	NA	NA	.000^b	.000^b	.000^b	.000^b	.000^b	.000^b	NA	NA	NA	NA	NA	.000^b	.001^b	.003^b	.029^b	.007^b	NA	NA	.029^b	NA	NA	NA	NA	NA	NA	NA	NA	NA	.001^b	.001^b	.000^b	NA	NA	NA	NA	NA	NA	16
1st Harmonic Magnitude	Secure Cup - 1 m (zone 1 and 2)	NA	NA	NA	.000^b	.000^b	NA	.000^b	.000^b	.000^b	.000^b	NA	NA	NA	NA	NA	NA	NA	.000^b	NA	NA	NA	NA	NA	NA	NA	.000^b	.000^b	.000^b	NA	.000^b	.000^b	.015^b	NA	NA	NA	NA	NA	NA	.003^b	NA	.002^b	.000^b	.000^b	.000^b	NA	NA	NA	NA	NA	18
	Secure Cup - 1 m (zone 1 and 3)	NA	NA	NA	.000^b	.043^b	NA	.000^b	NA	NA	NA	NA	.000^b	.000^b	.000^b	.000^b	.000^b	.000^b	.000^b	.015^b	NA	NA	NA	NA	.000^b	.000^b	.000^b	NA	.000^b	NA	.000^b	.000^b	.000^b	NA	NA	.001^b	.000^b	NA	.000^b	.000^b	.000^b	.000^b	.000^b	.000^b	NA	NA	NA	NA	NA	NA	26
	Secure Cup - 1 m (zone 2)	NA	.000^b	.000^b	.000^b	.000^b	.000^b	NA	.000^b	.000^b	.000^b	NA	.000^b	NA	.000^b	.000^b	.000^b	.000^b	.000^b	.000^b	.000^b	.002^b	.000^b	NA	NA	NA	NA	.000^b	.000^b	NA	NA	NA	NA	NA	NA	NA	NA	NA	NA	NA	NA	NA	NA	.002^b	NA	.035^b	.000^b	.000^b	.000^b	.000^b	26
2nd Harmonic Magnitude	Secure Cup - 1 m (zone 1 and 2)	NA	.000^b	.000^b	.000^b	.000^b	.000^b	.000^b	NA	.000^b	NA	.000^b	.000^b	NA	NA	NA	NA	.000^b	.000^b	.000^b	.000^b	.000^b	.000^b	.000^b	.000^b	.000^b	.000^b	.000^b	.000^b	.000^b	NA	NA	NA	NA	NA	NA	NA	NA	NA	NA	NA	.029^b	NA	NA	NA	NA	.023^b	.003^b	.001^b	.000^b	27
	Secure Cup - 1 m (zone 1 and 3)	NA	.000^b	.000^b	.000^b	.000^b	.000^b	.000^b	.000^b	.000^b	.000^b	.000^b	.000^b	NA	.000^b	.000^b	.000^b	.000^b	.000^b	.000^b	.000^b	.000^b	.000^b	.000^b	.000^b	.000^b	.000^b	.000^b	.002^b	NA	NA	NA	NA	NA	NA	NA	NA	NA	NA	NA	NA	NA	NA	NA	NA	.000^b	.000^b	.023^b	NA	NA	29
	Secure Cup - 1 m (zone 2)	NA	NA	NA	.000^b	.002^b	.000^b	.002^b	.000^b	.002^b	.019^b	NA	.002^b	.000^b	.000^b	.000^b	.000^b	.000^b	.000^b	.000^b	NA	NA	NA	NA	.000^b	.000^b	.000^b	.000^b	NA	NA	NA	NA	NA	NA	NA	NA	NA	NA	NA	.000^b	.000^b	.000^b	.000^b	.000^b	NA	.000^b	.000^b	NA	NA	NA	26
1st Harmonic Ratio	Secure Cup - 1 m (zone 1 and 2)	NA	NA	NA	.000^b	.000^b	NA	.000^b	.000^b	.000^b	.000^b	NA	NA	.000^b	NA	NA	NA	NA	NA	NA	NA	NA	NA	NA	NA	.015^b	.000^b	.002^b	.000^b	NA	.000^b	.000^b	.000^b	NA	NA	NA	NA	NA	.000^b	.000^b	.000^b	.000^b	.000^b	.000^b	.000^b	.000^b	.000^b	.000^b	.000^b	.000^b	26
	Secure Cup - 1 m (zone 1 and 3)	NA	NA	NA	.000^b	.000^b	NA	.000^b	NA	NA	NA	NA	.000^b	.000^b	.000^b	.000^b	.000^b	.000^b	.000^b	.000^b	NA	NA	.000^b	.000^b	.000^b	.000^b	.000^b	.001^b	.000^b	NA	.000^b	.000^b	.000^b	NA	NA	.000^b	.000^b	NA	.000^b	.000^b	.000^b	.000^b	.000^b	.000^b	.000^b	.011^b	NA	.000^b	.000^b	.000^b	34
	Secure Cup - 1 m (zone 2)	NA	.000^b	.000^b	.000^b	.000^b	.000^b	NA	.000^b	.000^b	.000^b	.000^b	.000^b	NA	.000^b	.000^b	.000^b	.000^b	.000^b	.000^b	.000^b	.002^b	.000^b	NA	.043^b	NA	.015^b	.000^b	.000^b	NA	NA	NA	NA	NA	NA	NA	NA	NA	NA	.000^b	.000^b	.000^b	.000^b	.000^b	NA	.000^b	.000^b	.000^b	.000^b	NA	32
2nd Harmonic Ratio	Secure Cup - 1 m (zone 1 and 2)	NA	.000^b	.000^b	.000^b	.000^b	.000^b	.000^b	NA	.009^b	NA	.000^b	.000^b	NA	NA	NA	NA	NA	.000^b	NA	.000^b	NA	.000^b	.000^b	.000^b	.000^b	.000^b	.000^b	.000^b	.000^b	NA	NA	NA	.000^b	NA	NA	NA	NA	NA	.000^b	.000^b	.000^b	.000^b	.000^b	.000^b	.000^b	.000^b	.000^b	.000^b	.000^b	31
	Secure Cup - 1 m (zone 1 and 3)	NA	.000^b	.000^b	.000^b	.000^b	.000^b	.000^b	.000^b	.000^b	.000^b	.000^b	.000^b	.000^b	.000^b	.000^b	.000^b	.000^b	.000^b	.000^b	.000^b	.000^b	.000^b	.000^b	.000^b	.000^b	.000^b	.000^b	.002^b	NA	NA	NA	NA	NA	NA	NA	NA	NA	NA	.000^b	.000^b	.000^b	.000^b	.000^b	.000^b	.000^b	.000^b	.000^b	.000^b	.000^b	38

Table E-3: The accelerometer response comparison between the simulated conditions with the significant value being highlighted, NA = where the signal is not significant or do not support the main finding pattern.

Ultrasound - Zone Loosening

	Driving Frequency (Hz)	100	150	200	250	300	350	400	450	500	550	600	650	700	750	800	850	900	950	1000	1050	1100	1150	1200	1250	1300	1350	1400	1450	1500	1550	1600	1650	1700	1750	1800	1850	1900	1950	2000	2050	2100	2150	2200	2250	2300	2350	2400	2450	2500	#
Fundamental Magnitude	Secure Cup - 1 m (zone 2)	NA	NA	.000^b	.000^b	.002^b	.023^b	.023^b	.001^b	.023^b	.023^b	NA	NA	NA	NA	NA	NA	NA	NA	NA	NA	NA	NA	NA	NA	NA	NA	NA	NA	.000^b	NA	NA	NA	NA	NA	.009^b	.002^b	.000^b	.000^b	.000^b	.000^b	.000^b	.000^b	.000^b	.000^b	.000^b	.000^b	.000^b	.000^b	NA	23
	Secure Cup - 1 m (zone 1 and 2)	NA	NA	NA	NA	NA	NA	NA	NA	NA	NA	NA	NA	NA	NA	NA	NA	NA	NA	NA	NA	NA	NA	NA	NA	NA	.000^b	.000^b	NA	.000^b	NA	NA	NA	NA	NA	NA	.001^b	.000^b	.000^b	.002^b	.000^b	.000^b	.000^b	.000^b	.000^b	.000^b	.000^b	.000^b	.000^b	.000^b	17
	Secure Cup - 1 m (zone 1 and 3)	NA	NA	NA	NA	NA	NA	NA	NA	NA	NA	NA	NA	NA	NA	NA	NA	NA	NA	NA	NA	NA	NA	NA	NA	NA	NA	NA	NA	NA	NA	NA	NA	NA	NA	NA	.019^b	.000^b	.000^b	NA	.000^b	.000^b	.000^b	.000^b	.000^b	.000^b	.000^b	.000^b	.001^b	.001^b	13
1st Harmonic Magnitude	Secure Cup - 1 m (zone 2)	NA	NA	NA	NA	NA	NA	NA	NA	.002^b	NA	.002^b	.000^b	.000^b	.000^b	.000^b	.000^b	.002^b	NA	.000^b	NA	NA	.000^b	.011^b	.000^b	.001^b	.023^b	.000^b	NA	NA	.000^b	.000^b	.000^b	.003^b	.000^b	.000^b	NA	NA	NA	.003^b	NA	NA	NA	NA	.007^b	NA	NA	NA	NA	.000^b	24
	Secure Cup - 1 m (zone 1 and 2)	NA	NA	NA	NA	NA	.000^b	.000^b	.000^b	.000^b	.000^b	.000^b	.000^b	.000^b	.000^b	.000^b	.000^b	.000^b	.000^b	.000^b	.000^b	.000^b	.000^b	NA	.000^b	.000^b	.035^b	NA	NA	NA	.007^b	.004^b	NA	NA	NA	NA	NA	NA	NA	NA	NA	NA	NA	NA	NA	NA	NA	NA	NA	.000^b	23
	Secure Cup - 1 m (zone 1 and 3)	NA	NA	NA	NA	.002^b	.000^b	.000^b	.000^b	.000^b	.000^b	.002^b	.000^b	.000^b	.000^b	.000^b	.000^b	.000^b	.043^b	.000^b	NA	NA	NA	NA	.000^b	.000^b	.009^b	NA	.000^b	NA	.002^b	NA	.000^b	.000^b	NA	NA	NA	NA	NA	.000^b	.000^b	NA	NA	NA	NA	NA	NA	NA	.011^b	.000^b	26
2nd Harmonic Magnitude	Secure Cup - 1 m (zone 2)	NA	NA	NA	NA	NA	NA	NA	NA	.002^b	NA	NA	NA	NA	.003^b	.000^b	.000^b	.000^b	.000^b	.000^b	.000^b	NA	NA	NA	NA	.002^b	NA	.001^b	.000^b	NA	NA	NA	NA	.000^b	.000^b	NA	NA	NA	NA	.011^b	.023^b	NA	.043^b	.005^b	.000^b	.000^b	NA	.015^b	.019^b	.011^b	22
	Secure Cup - 1 m (zone 1 and 2)	NA	NA	NA	NA	NA	NA	NA	NA	.000^b	.000^b	NA	NA	NA	.000^b	.000^b	.000^b	.000^b	.000^b	.000^b	.000^b	.000^b	NA	.007^b	NA	.002^b	NA	.000^b	.000^b	.000^b	NA	NA	NA	.009^b	NA	.011^b	NA	NA	NA	.002^b	NA	NA	.023^b	.007^b	.000^b	.029^b	.000^b	.000^b	.000^b	.000^b	26
	Secure Cup - 1 m (zone 1 and 3)	NA	NA	NA	.029^b	.000^b	.000^b	.000^b	.000^b	.000^b	.000^b	.000^b	.002^b	NA	.000^b	.000^b	.000^b	.000^b	.000^b	.000^b	.000^b	.000^b	.005^b	.000^b	.000^b	.000^b	.000^b	.000^b	.000^b	NA	NA	NA	NA	.001^b	.000^b	.000^b	NA	NA	NA	.000^b	.001^b	NA	.001^b	.005^b	.005^b	.023^b	.000^b	NA	.000^b	.000^b	36
1st Harmonic Ratio	Secure Cup - 1 m (zone 2)	NA	NA	.023^b	.019^b	.023^b	.023^b	.023^b	.023^b	.023^b	.023^b	.002^b	.023^b	.002^b	.023^b	.000^b	.000^b	NA	NA	NA	NA	NA	NA	NA	.002^b	.023^b	NA	.005^b	.000^b	NA	NA	NA	NA	NA	.000^b	.000^b	NA	NA	.000^b	.000^b	.000^b	.000^b	.000^b	.000^b	.000^b	.000^b	.000^b	.000^b	.000^b	.007^b	32
	Secure Cup - 1 m (zone 1 and 2)	NA	NA	NA	NA	NA	NA	.029^b	.000^b	.000^b	.000^b	.000^b	.019^b	NA	NA	.002^b	.002^b	NA	NA	NA	NA	NA	NA	NA	NA	.009^b	.000^b	.000^b	NA	NA	NA	NA	NA	NA	NA	NA	NA	NA	NA	.002^b	.000^b	.001^b	.000^b	.000^b	.000^b	.000^b	.000^b	.000^b	.000^b	.000^b	22
	Secure Cup - 1 m (zone 1 and 3)	NA	NA	NA	NA	NA	NA	.023^b	.023^b	NA	NA	NA	NA	NA	NA	.000^b	NA	NA	NA	.004^b	NA	NA	NA	NA	NA	NA	NA	NA	NA	NA	NA	NA	NA	NA	NA	NA	NA	NA	NA	.003^b	.000^b	.000^b	.000^b	.000^b	.000^b	.000^b	.000^b	.000^b	.000^b	.000^b	15
2nd Harmonic Ratio	Secure Cup - 1 m (zone 2)	NA	NA	NA	NA	.023^b	.023^b	NA	.023^b	.019^b	.023^b	NA	NA	NA	.023^b	.023^b	.002^b	.015^b	NA	NA	NA	NA	NA	NA	NA	NA	NA	.023^b	.000^b	.004^b	NA	NA	NA	NA	NA	.005^b	.002^b	.000^b	.000^b	.000^b	.000^b	.000^b	.000^b	.000^b	.000^b	.000^b	.000^b	.000^b	.000^b	NA	26
	Secure Cup - 1 m (zone 1 and 2)	NA	NA	NA	NA	NA	NA	NA	NA	.011^b	.002^b	NA	NA	NA	NA	.003^b	.000^b	.000^b	.000^b	.000^b	NA	NA	NA	NA	NA	.002^b	.001^b	.000^b	.000^b	.000^b	NA	NA	NA	NA	NA	.029^b	.002^b	.000^b	.000^b	.002^b	.000^b	.000^b	.000^b	.000^b	.000^b	.000^b	.000^b	.000^b	.000^b	.000^b	27
	Secure Cup - 1 m (zone 1 and 3)	NA	NA	NA	NA	NA	NA	NA	NA	NA	.000^b	NA	NA	NA	.000^b	.000^b	.000^b	.000^b	.000^b	.000^b	.000^b	.002^b	NA	NA	.019^b	.000^b	.000^b	.000^b	.000^b	NA	NA	NA	NA	NA	NA	.015^b	.029^b	.019^b	.005^b	NA	.000^b	.000^b	.000^b	.000^b	.000^b	.000^b	.000^b	.000^b	.000^b	.000^b	28

Table E-4: The ultrasound response comparison between the simulated conditions with the significant value being highlighted, NA = where the signal is not significant or do not support the main finding pattern.

		Accelerometer- Hemi-Pelvis																																
	Driving Frequency (Hz)	100	150	200	250	300	350	400	450	500	550	600	650	700	750	800	850	900	950	1000	1050	1100	1150	1200	1250	1300	1350	1400	1450	1500	#
Fundamental Magnitude	Secure Cup - 1 mm Loose	.000b	.023b	.000b	.000b	.000b	.000b	NA	NA	NA	NA	NA	NA	NA	NA	NA	NA	NA	NA	NA	NA	NA	NA	NA	NA	NA	NA	NA	NA	NA	6
	Secure Cup - 2 mm Loose	.000b	NA	.000b	.000b	.000b	.000b	NA	NA	NA	NA	NA	NA	NA	NA	NA	NA	NA	NA	NA	NA	NA	NA	NA	NA	NA	NA	NA	.000b	.000b	7
	1 mm - 2 mm	NA	NA	.000b	.000b	.000b	NA	.000b	.000b	.000b	.000b	.000b	.000b	.000b	NA	.000b	.000b	.000b	.000b	NA	NA	NA	.000b	NA	NA	.000b	.000b	.000b	.000b	.000b	.000b	20
1st Harmonic Magnitude	Secure Cup - 1 mm Loose	NA	NA	.023b	.000b	.023b	NA	NA	.000b	.000b	.000b	.000b	.000b	.000b	.000b	.000b	.000b	.000b	.000b	NA	NA	NA	NA	.000b	.004b	.000b	.000b	.000b	NA	NA	19
	Secure Cup - 2 mm Loose	NA	NA	NA	NA	NA	NA	.015b	.000b	.000b	.000b	.000b	.000b	.000b	.004b	NA	.000b	.000b	.000b	.000b	.007b	NA	.015b	.000b	.007b	.001b	.004b	.001b	.000b	NA	20
	1 mm - 2 mm	NA	NA	NA	NA	NA	NA	.011b	NA	.000b	NA	NA	NA	NA	NA	NA	NA	.000b	NA	.002b	NA	.009b	NA	.035b	NA	NA	NA	NA	.023b	NA	7
2nd Harmonic Magnitude	Secure Cup - 1 mm Loose	.023b	.000b	.000b	.000b	.000b	.000b	.000b	.000b	NA	.000b	.000b	NA	.000b	NA	.000b	.000b	.000b	.000b	.000b	NA	NA	.000b	.000b	.000b	.000b	.007b	NA	NA	NA	21
	Secure Cup - 2 mm Loose	NA	.002b	.000b	.003b	.000b	.000b	.000b	.000b	.000b	.000b	.000b	NA	.000b	NA	NA	.000b	.000b	.000b	.000b	.000b	.000b	NA	.015b	.000b	.000b	.000b	.011b	NA	NA	NA	20
	1 mm - 2 mm	NA	NA	NA	NA	NA	NA	NA	NA	.000b	.002b	.000b	.000b	.000b	.019b	NA	NA	NA	.000b	.000b	.000b	NA	NA	NA	.000b	.000b	NA	NA	NA	NA	NA	10
3rd Harmonic Magnitude	Secure Cup - 1 mm Loose	.000b	.000b	.000b	.000b	.000b	.000b	.000b	NA	NA	NA	.035b	NA	NA	.015b	NA	.023b	.003b	.043b	NA	NA	NA	NA	.001b	NA	.004b	NA	NA	NA	.043b	15
	Secure Cup - 2 mm Loose	NA	NA	.004b	NA	.000b	NA	.000b	NA	.023b	.000b	.007b	.001b	.002b	.002b	.000b	.029b	.019b	.000b	.002b	NA	NA	.004b	.035b	.035b	.000b	.002b	.043b	.007b	.000b	22
	1 mm - 2 mm	NA	NA	NA	NA	NA	NA	NA	NA	.001b	.002b	NA	.000b	.015b	NA	.019b	NA	NA	.035b	NA	NA	.000b	.015b	NA	.029b	NA	.002b	.043b	NA	NA	11
1st Harmonic Ratio	Secure Cup - 1 mm Loose	NA	NA	.000b	.000b	.000b	NA	NA	NA	NA	.000b	.002b	.000b	.019b	NA	NA	NA	NA	NA	NA	NA	NA	NA	NA	NA	NA	NA	NA	NA	NA	7
	Secure Cup - 2 mm Loose	NA	NA	NA	.002b	.000b	NA	NA	NA	NA	.000b	.000b	.000b	NA	NA	NA	.000b	.000b	.043b	NA	NA	NA	NA	NA	NA	NA	NA	NA	.000b	.043b	10
	1 mm - 2 mm	NA	NA	NA	NA	NA	NA	.000b	NA	.000b	.000b	.000b	NA	NA	NA	NA	.000b	.000b	.000b	NA	NA	NA	.011b	NA	NA	NA	NA	NA	.000b	.005b	10
2nd Harmonic Ratio	Secure Cup - 1 mm Loose	.000b	.000b	.000b	.000b	.000b	.000b	.000b	NA	NA	NA	NA	NA	NA	NA	NA	.000b	.000b	.000b	NA	NA	NA	NA	NA	NA	NA	NA	NA	NA	NA	10
	Secure Cup - 2 mm Loose	NA	NA	.000b	.000b	.000b	.000b	.000b	NA	.000b	.001b	.000b	NA	.000b	NA	NA	.000b	.000b	.000b	.000b	NA	NA	NA	NA	NA	NA	NA	NA	NA	NA	13
	1 mm - 2 mm	NA	NA	NA	NA	NA	NA	NA	.019b	.000b	.000b	.000b	.000b	.000b	.029b	NA	NA	.023b	.000b	.000b	.003b	NA	NA	NA	.003b	NA	.000b	.001b	NA	NA	14
3rd Harmonic Ratio	Secure Cup - 1 mm Loose	.000b	.000b	.000b	.000b	.000b	.000b	.005b	NA	NA	NA	NA	NA	NA	NA	NA	NA	NA	NA	NA	NA	NA	NA	NA	NA	NA	NA	NA	NA	NA	7
	Secure Cup - 2 mm Loose	NA	NA	.000b	.000b	.000b	NA	NA	NA	NA	NA	NA	NA	NA	NA	NA	NA	NA	NA	NA	NA	NA	NA	NA	NA	NA	NA	NA	.001b	.000b	5
	1 mm - 2 mm	NA	NA	NA	NA	NA	NA	NA	.000b	.000b	.000b	.000b	.000b	.002b	NA	.003b	.000b	.000b	.000b	NA	NA	NA	.000b	NA	NA	.000b	.000b	.002b	.000b	.011b	16

Table E-5: The air medium accelerometer response comparison between the simulated conditions with the significant value being highlighted, NA = where the signal is not significant or do not support the main finding pattern.

		Ultraound- Hemi-Pelvis																																					
	Driving Frequency (Hz)	100	150	200	250	300	350	400	450	500	550	600	650	700	750	800	850	900	950	1000	1050	1100	1150	1200	1250	1300	1350	1400	1450	1500	#
Fundamental Magnitude	Secure Cup - 1 mm Loose	NA	NA	.000b	NA	NA	NA	NA	NA	NA	NA	NA	NA	NA	NA	NA	NA	NA	NA	NA	NA	NA	NA	NA	NA	NA	NA	NA	NA	NA	1
	Secure Cup - 2 mm Loose	NA	NA	NA	NA	NA	NA	NA	NA	NA	NA	NA	NA	NA	NA	NA	NA	NA	NA	NA	NA	NA	NA	NA	NA	NA	NA	NA	NA	NA	NA
	1 mm - 2 mm	NA	NA	NA	NA	NA	NA	NA	.019b	NA	.002b	.000b	NA	NA	NA	.007b	NA	NA	NA	NA	NA	NA	NA	NA	NA	NA	NA	NA	NA	NA	4
1st Harmonic Magnitude	Secure Cup - 1 mm Loose	NA	NA	NA	.000b	.000b	.000b	.000b	.000b	.000b	.000b	.000b	.000b	.000b	.000b	NA	NA	NA	.009b	.003b	NA	.003b	.001b	.003b	.001b	.000b	.000b	.005b	.029b	.000b	22
	Secure Cup - 2 mm Loose	NA	NA	.009b	.000b	.000b	.000b	.000b	.000b	.000b	.000b	.000b	.000b	.000b	.000b	.002b	.000b	.000b	.000b	.000b	.000b	.001b	.000b	.001b	.000b	.007b	.000b	.000b	.000b	.000b	27
	1 mm - 2 mm	NA	NA	NA	NA	NA	.000b	NA	NA	NA	NA	NA	NA	NA	NA	NA	.043b	.019b	.035b	.011b	.035b	NA	NA	NA	NA	NA	NA	NA	.007b	.007b	8
2nd Harmonic Magnitude	Secure Cup - 1 mm Loose	NA	NA	.000b	.000b	.000b	.000b	.000b	.000b	.000b	.000b	.000b	.000b	.000b	.000b	.000b	.000b	.000b	.001b	.007b	.000b	.004b	.000b	NA	.007b	.004b	.007b	.001b	.007b	.000b	26
	Secure Cup - 2 mm Loose	NA	NA	.000b	.000b	.000b	.000b	.000b	.000b	.000b	.000b	.000b	.000b	.000b	.000b	.000b	.000b	.000b	.000b	.000b	.000b	.004b	.000b	.000b	.000b	.000b	.003b	.000b	.000b	.000b	27
	1 mm - 2 mm	NA	NA	NA	NA	NA	NA	NA	NA	NA	NA	NA	NA	.002b	NA	NA	NA	NA	NA	.029b	NA	NA	NA	.005b	.023b	.023b	NA	NA	NA	.023b	6
3rd Harmonic Magnitude	Secure Cup - 1 mm Loose	NA	NA	.000b	.000b	.000b	.000b	.000b	.000b	.000b	.000b	.000b	.000b	.000b	.000b	.000b	.009b	.043b	.002b	.003b	.011b	.023b	.001b	.000b	.000b	.000b	NA	.000b	.000b	.035b	.005b	26
	Secure Cup - 2 mm Loose	NA	NA	.000b	.000b	.000b	.000b	.000b	.000b	.000b	.000b	.000b	.000b	.000b	.000b	.000b	.000b	.000b	.000b	.002b	.002b	.000b	.000b	.000b	.000b	.000b	.000b	.000b	.000b	.000b	27
	1 mm - 2 mm	NA	NA	NA	NA	NA	NA	NA	NA	NA	NA	NA	NA	.001b	NA	NA	NA	NA	.019b	NA	NA	.023b	NA	NA	NA	NA	NA	NA	.002b	NA	4
1st Harmonic Ratio	Secure Cup - 1 mm Loose	NA	NA	.000b	.000b	.000b	NA	.000b	NA	NA	NA	NA	NA	NA	NA	NA	NA	NA	NA	NA	NA	NA	NA	NA	NA	NA	NA	NA	NA	NA	4
	Secure Cup - 2 mm Loose	NA	NA	NA	.000b	.000b	.000b	.000b	.009b	NA	NA	NA	NA	NA	NA	NA	NA	NA	NA	NA	NA	NA	NA	NA	NA	NA	NA	NA	NA	.002b	6
	1 mm - 2 mm	NA	NA	NA	NA	NA	.000b	NA	.000b	.015b	NA	NA	NA	NA	NA	.035b	NA	NA	NA	NA	NA	NA	NA	NA	NA	NA	NA	NA	NA	NA	4
2nd Harmonic Ratio	Secure Cup - 1 mm Loose	NA	NA	.000b	.000b	.000b	.000b	.000b	NA	NA	NA	NA	NA	NA	NA	NA	NA	NA	.007b	NA	NA	NA	NA	NA	NA	NA	NA	NA	NA	NA	6
	Secure Cup - 2 mm Loose	NA	NA	.003b	.001b	.043b	NA	.035b	NA	NA	NA	NA	NA	NA	NA	NA	NA	NA	NA	NA	NA	NA	NA	NA	NA	NA	NA	NA	NA	.001b	5
	1 mm - 2 mm	NA	NA	NA	NA	NA	NA	NA	NA	.000b	.003b	NA	NA	.035b	NA	.023b	NA	NA	NA	NA	NA	NA	NA	NA	NA	.011b	NA	NA	NA	NA	5
3rd Harmonic Ratio	Secure Cup - 1 mm Loose	NA	NA	.000b	.000b	.000b	.000b	.000b	NA	NA	NA	NA	NA	NA	NA	NA	NA	NA	NA	NA	NA	NA	NA	NA	NA	NA	NA	NA	NA	NA	5
	Secure Cup - 2 mm Loose	NA	NA	.000b	.000b	.001b	.004b	.000b	NA	NA	NA	NA	NA	NA	NA	NA	NA	NA	NA	NA	NA	NA	NA	NA	NA	NA	NA	NA	.015b	.002b	7
	1 mm - 2 mm	NA	NA	NA	NA	NA	NA	NA	NA	.000b	.043b	.000b	.004b	.000b	NA	NA	NA	NA	NA	NA	NA	NA	NA	NA	NA	.035b	NA	NA	NA	NA	6

Table E-6: The air medium ultrasound response comparison between the simulated conditions with the significant value being highlighted, NA = where the signal is not significant or do not support the main finding pattern.

		Ultraound- Hemi-Pelvis (Water medium)																																
	Driving Frequency (Hz)	100	150	200	250	300	350	400	450	500	550	600	650	700	750	800	850	900	950	1000	1050	1100	1150	1200	1250	1300	1350	1400	1450	1500	#
Fundamental Magnitude	Secure Cup - 1 mm Loose	NA	NA	.000b	.003b	NA	.000b	.000b	.000b	.000b	.019b	.015b	.043b	.029b	.002b	.000b	.000b	.000b	.000b	NA	NA	NA	NA	.001b	.009b	.000b	NA	NA	NA	NA	19
	Secure Cup - 2 mm Loose	NA	NA	NA	NA	NA	NA	NA	NA	NA	NA	NA	NA	NA	NA	NA	NA	.000b	.000b	NA	NA	NA	NA	NA	NA	NA	NA	NA	NA	NA	2
	1 mm - 2 mm	NA	NA	NA	NA	NA	NA	NA	NA	NA	NA	NA	NA	NA	NA	NA	NA	NA	NA	NA	NA	NA	NA	NA	NA	NA	NA	NA	NA	NA	NA
1st Harmonic Magnitude	Secure Cup - 1 mm Loose	NA	NA	NA	NA	NA	NA	NA	NA	NA	NA	.000b	.004b	NA	.000b	NA	NA	NA	.043b	.000b	.000b	.000b	.011b	.019b	.000b	.005b	.000b	.000b	.000b	.003b	15
	Secure Cup - 2 mm Loose	NA	NA	NA	NA	.000b	NA	NA	NA	NA	NA	.002b	.000b	.015b	.000b	NA	NA	NA	.002b	.000b	.000b	.000b	.000b	.000b	.000b	.000b	.000b	.000b	.000b	.000b	17
	1 mm - 2 mm	NA	NA	.002b	NA	.000b	.002b	NA	.023b	.001b	NA	NA	NA	NA	NA	NA	NA	NA	NA	NA	NA	NA	.005b	.009b	NA	.029b	.019b	NA	NA	NA	9
2nd Harmonic Magnitude	Secure Cup - 1 mm Loose	NA	NA	NA	NA	NA	NA	NA	NA	.001b	.002b	.009b	.003b	.000b	NA	.000b	.002b	.000b	NA	.005b	.000b	.009b	.005b	.001b	.000b	.005b	.001b	.000b	.000b	.000b	19
	Secure Cup - 2 mm Loose	NA	NA	NA	NA	NA	NA	NA	NA	.000b	.000b	.007b	.000b	.000b	NA	.000b	.002b	.000b	.009b	.000b	.000b	.000b	.000b	.000b	.000b	.000b	.000b	.000b	.000b	.000b	20
	1 mm - 2 mm	NA	NA	NA	NA	.011b	NA	NA	NA	NA	NA	NA	NA	NA	NA	NA	NA	NA	NA	.007b	NA	.029b	.007b	NA	.043b	NA	NA	NA	NA	NA	5
3rd Harmonic Magnitude	Secure Cup - 1 mm Loose	NA	NA	NA	NA	.002b	.009b	.005b	.005b	.001b	.002b	.000b	.005b	.000b	.000b	.000b	.001b	.000b	.000b	.000b	.015b	.000b	.000b	.000b	.000b	.000b	.003b	.000b	.000b	.000b	25
	Secure Cup - 2 mm Loose	NA	NA	NA	NA	.002b	.000b	.000b	.001b	.000b	.001b	.000b	.001b	.000b	.000b	.000b	.000b	.000b	.000b	.000b	.000b	.000b	.001b	.000b	.000b	.000b	.000b	.000b	.000b	.000b	25
	1 mm - 2 mm	NA	NA	NA	NA	NA	NA	NA	NA	NA	NA	NA	NA	NA	NA	.043b	NA	NA	NA	NA	NA	NA	NA	NA	NA	.029b	NA	NA	NA	NA	2
1st Harmonic Ratio	Secure Cup - 1 mm Loose	NA	NA	NA	.000b	NA	NA	NA	NA	.000b	.019b	.002b	.001b	.005b	.000b	.000b	.000b	.000b	.000b	NA	NA	.009b	.009b	.000b	.000b	.000b	.000b	NA	NA	NA	17
	Secure Cup - 2 mm Loose	NA	NA	NA	NA	NA	NA	NA	NA	NA	NA	NA	NA	NA	NA	.000b	NA	.000b	.000b	NA	NA	NA	.035b	NA	NA	NA	.007b	NA	NA	NA	5
	1 mm - 2 mm	NA	NA	NA	NA	NA	NA	NA	NA	NA	NA	NA	NA	NA	NA	NA	NA	NA	NA	NA	NA	NA	NA	NA	NA	NA	NA	NA	NA	NA	NA
2nd Harmonic Ratio	Secure Cup - 1 mm Loose	NA	NA	NA	NA	NA	NA	.000b	.000b	.000b	.011b	.011b	.001b	.005b	.000b	.000b	.000b	.000b	.000b	NA	.029b	.043b	NA	.000b	.000b	.000b	.000b	.035b	NA	.035b	20
	Secure Cup - 2 mm Loose	NA	NA	NA	NA	NA	NA	NA	NA	NA	NA	NA	NA	NA	NA	.000b	.002b	.000b	.000b	NA	NA	NA	NA	NA	NA	NA	.011b	NA	NA	NA	5
	1 mm - 2 mm	NA	NA	NA	NA	NA	NA	NA	NA	NA	NA	NA	NA	NA	NA	NA	NA	NA	NA	NA	NA	NA	NA	NA	NA	NA	NA	NA	NA	NA	NA
3rd Harmonic Ratio	Secure Cup - 1 mm Loose	NA	NA	.000b	.000b	.019b	.000b	.000b	.000b	.000b	.015b	.001b	.003b	.000b	.001b	.000b	.000b	.000b	.000b	.029b	NA	.005b	.015b	.000b	.001b	.000b	.000b	NA	NA	.009b	24
	Secure Cup - 2 mm Loose	NA	NA	NA	NA	.002b	NA	NA	NA	NA	NA	NA	NA	NA	NA	.000b	.004b	.000b	.000b	NA	NA	NA	NA	NA	NA	NA	NA	NA	NA	NA	5
	1 mm - 2 mm	NA	NA	NA	NA	NA	NA	NA	NA	NA	NA	NA	NA	NA	NA	NA	NA	NA	NA	NA	NA	NA	NA	NA	NA	NA	NA	NA	NA	NA	NA

Table E-7: The water medium ultrasound response comparison between the simulated conditions with the significant value being highlighted, NA = where the signal is not significant or do not support the main finding pattern.

		Accelerometer-Femur																																
	Driving Frequency (Hz)	100	150	200	250	300	350	400	450	500	550	600	650	700	750	800	850	900	950	1000	1050	1100	1150	1200	1250	1300	1350	1400	1450	1500	#
Fundamental Magnitude	Secure Cup - 1 mm Loose	NA	.000b	NA	NA	NA	NA	NA	NA	NA	NA	.000b	.000b	.000b	NA	NA	NA	NA	NA	NA	NA	NA	NA	NA	.000b	.000b	.000b	.000b	NA	NA	8
	Secure Cup - 2 mm Loose	NA	.000b	NA	NA	NA	NA	NA	NA	NA	NA	.000b	.000b	.000b	NA	NA	NA	NA	NA	NA	NA	NA	NA	NA	.000b	.000b	.000b	.000b	NA	NA	8
	1 mm - 2 mm	NA	NA	.002b	NA	.000b	NA	NA	NA	.000b	.000b	NA	NA	NA	NA	NA	NA	NA	NA	NA	.001b	NA	NA	NA	.000b	.000b	.011b	.000b	.000b	NA	10
1st Harmonic Magnitude	Secure Cup - 1 mm Loose	.000b	.000b	.000b	.000b	NA	NA	.000b	.000b	.000b	.000b	.000b	.000b	.000b	.000b	.000b	.029b	NA	NA	.000b	.000b	.000b	.000b	.000b	.000b	NA	.000b	.000b	NA	.035b	23
	Secure Cup - 2 mm Loose	.000b	.004b	.000b	.000b	NA	NA	.002b	.000b	.000b	.000b	.000b	NA	.000b	.000b	.000b	NA	NA	NA	.000b	NA	.000b	.005b	.005b	.000b	NA	.000b	.000b	NA	.019b	20
	1 mm - 2 mm	NA	NA	NA	NA	NA	NA	NA	NA	NA	NA	NA	NA	NA	NA	NA	NA	NA	NA	NA	NA	NA	NA	NA	NA	NA	NA	NA	NA	NA	NA
2nd Harmonic Magnitude	Secure Cup - 1 mm Loose	.000b	.000b	.000b	.000b	NA	.000b	.000b	.029b	.000b	.000b	NA	NA	NA	.000b	.000b	.023b	.000b	.000b	.001b	.000b	.000b	NA	.000b	NA	NA	.000b	NA	.003b	NA	20
	Secure Cup - 2 mm Loose	.000b	NA	.003b	.000b	NA	NA	NA	NA	.000b	.005b	NA	NA	NA	.000b	.005b	NA	.000b	.000b	.002b	.000b	.002b	.001b	.000b	NA	NA	.000b	.000b	.002b	NA	17
	1 mm - 2 mm	NA	NA	NA	NA	NA	NA	NA	NA	NA	NA	.015b	NA	NA	NA	NA	NA	NA	NA	NA	NA	NA	.009b	NA	NA	NA	NA	NA	NA	NA	2
3rd Harmonic Magnitude	Secure Cup - 1 mm Loose	.000b	.000b	.000b	NA	.002b	.000b	.000b	.000b	.000b	.000b	.000b	NA	.000b	.000b	.000b	NA	NA	NA	.007b	NA	.011b	NA	.015b	.003b	NA	.000b	NA	.004b	.005b	20
	Secure Cup - 2 mm Loose	.000b	NA	.000b	NA	NA	NA	NA	.004b	.000b	.000b	.011b	NA	.009b	.000b	.000b	NA	NA	NA	.000b	NA	.003b	NA	.023b	.023b	NA	.002b	NA	.001b	.000b	16
	1 mm - 2 mm	NA	NA	NA	NA	NA	NA	NA	NA	NA	NA	NA	NA	NA	NA	NA	NA	NA	NA	NA	NA	NA	NA	NA	NA	NA	NA	NA	NA	NA	NA
1st Harmonic Ratio	Secure Cup - 1 mm Loose	.000b	.000b	.000b	.000b	NA	NA	.000b	NA	NA	.000b	.000b	.000b	.000b	.000b	.011b	NA	NA	NA	NA	NA	.000b	.000b	.002b	.000b	.000b	.000b	.000b	NA	NA	18
	Secure Cup - 2 mm Loose	NA	.000b	.000b	.000b	NA	NA	NA	NA	NA	.000b	.000b	.000b	.000b	.001b	.000b	NA	NA	NA	NA	NA	.009b	NA	.011b	.000b	.000b	.000b	.000b	.023b	NA	16
	1 mm - 2 mm	NA	NA	NA	NA	NA	NA	NA	NA	NA	NA	NA	NA	NA	NA	.019b	NA	NA	NA	NA	.023b	NA	NA	NA	.000b	.009b	.023b	.000b	.000b	NA	7
2nd Harmonic Ratio	Secure Cup - 1 mm Loose	.000b	.000b	.000b	.000b	NA	NA	NA	NA	.000b	.000b	NA	.000b	.000b	.000b	NA	NA	NA	NA	NA	.000b	.000b	NA	.023b	.043b	.007b	.000b	.000b	NA	NA	16
	Secure Cup - 2 mm Loose	.000b	.015b	NA	NA	NA	NA	NA	NA	NA	NA	NA	.000b	.000b	.000b	NA	NA	.011b	.019b	NA	.000b	NA	NA	.000b	.000b	.000b	.000b	.000b	.000b	NA	14
	1 mm - 2 mm	NA	NA	NA	NA	NA	NA	NA	NA	NA	NA	.003b	.003b	.004b	.029b	NA	NA	NA	.004b	.023b	.000b	NA	NA	NA	.000b	.000b	.009b	.000b	.000b	NA	12
3rd Harmonic Ratio	Secure Cup - 1 mm Loose	.000b	.000b	.000b	NA	NA	NA	.000b	NA	.000b	.000b	.000b	.000b	.000b	.001b	.029b	NA	NA	NA	NA	NA	.015b	NA	NA	.002b	.000b	.000b	.000b	NA	NA	16
	Secure Cup - 2 mm Loose	.002b	NA	.000b	NA	NA	NA	NA	NA	NA	NA	.000b	.000b	.000b	NA	NA	NA	NA	NA	NA	NA	NA	NA	NA	.000b	.000b	.000b	.000b	.000b	NA	10
	1 mm - 2 mm	NA	NA	NA	NA	NA	NA	NA	NA	NA	NA	NA	NA	NA	NA	NA	NA	NA	NA	.007b	.000b	NA	NA	NA	.000b	.000b	NA	.000b	.000b	NA	6

Table E-8: The air medium femur accelerometer response comparison between the simulated conditions with the significant value being highlighted, NA = where the signal is not significant or do not support the main finding pattern.

		Accelerometer-Pelvis																																
	Driving Frequency (Hz)	100	150	200	250	300	350	400	450	500	550	600	650	700	750	800	850	900	950	1000	1050	1100	1150	1200	1250	1300	1350	1400	1450	1500	#
Fundamental Magnitude	Secure Cup - 1 mm Loose	NA	NA	NA	NA	NA	NA	NA	.001b	NA	NA	NA	.000b	.000b	NA	NA	NA	.001b	.000b	.000b	NA	.000b	.000b	.001b	.000b	.000b	.000b	.000b	NA	.000b	14
	Secure Cup -2 mm Loose	NA	NA	NA	NA	NA	NA	NA	NA	NA	NA	.000b	.000b	.000b	NA	NA	NA	.000b	.000b	.000b	NA	NA	.023b	.000b	.000b	.000b	.000b	.000b	.000b	NA	NA	12
	1 mm - 2 mm	.000b	.000b	NA	NA	.000b	NA	.000b	NA	NA	.000b	.000b	.000b	.000b	.000b	NA	.000b	.000b	.000b	NA	.000b	NA	NA	.000b	.000b	NA	NA	NA	.043b	NA	16
1st Harmonic Magnitude	Secure Cup - 1 mm Loose	.000b	.000b	NA	.000b	.000b	.000b	.000b	.000b	.000b	.015b	.000b	.001b	NA	.043b	NA	NA	NA	NA	.000b	NA	.007b	NA	.003b	NA	NA	.035b	.011b	NA	NA	17
	Secure Cup - 2 mm Loose	.000b	NA	.000b	.000b	NA	NA	.000b	NA	.019b	NA	NA	.001b	NA	.000b	.043b	NA	NA	NA	.000b	.019b	.003b	.029b	.005b	NA	.023b	NA	NA	.011b	NA	15
	1 mm - 2 mm	NA	NA	.000b	NA	NA	NA	NA	NA	NA	NA	NA	NA	NA	.001b	.023b	NA	NA	.001b	NA	.023b	NA	NA	NA	NA	NA	NA	NA	NA	NA	5
2nd Harmonic Magnitude	Secure Cup - 1 mm Loose	.000b	.000b	.000b	.000b	NA	.000b	NA	NA	NA	NA	NA	NA	NA	NA	NA	NA	.004b	.015b	NA	NA	NA	.007b	NA	NA	.011b	NA	NA	.000b	.000b	11
	Secure Cup - 2 mm Loose	NA	NA	NA	.000b	NA	.000b	NA	NA	NA	NA	NA	NA	NA	.011b	.035b	NA	NA	.029b	NA	NA	NA	.005b	NA	NA	.000b	NA	NA	.001b	.002b	.000b	9
	1 mm - 2 mm	NA	NA	NA	NA	NA	NA	NA	NA	NA	NA	NA	NA	NA	NA	NA	NA	NA	NA	NA	NA	NA	NA	NA	NA	NA	NA	NA	NA	NA	NA	NA
3rd Harmonic Magnitude	Secure Cup - 1 mm Loose	.000b	.000b	.000b	.015b	NA	NA	.023b	NA	.019b	.000b	NA	NA	.019b	NA	NA	NA	NA	.035b	NA	.011b	.001b	.003b	.035b	.035b	NA	.003b	.000b	.000b	.002b	18
	Secure Cup - 2 mm Loose	.000b	NA	.000b	.000b	.019b	.007b	NA	NA	.023b	.000b	NA	.035b	.011b	NA	.035b	.019b	NA	NA	NA	NA	.009b	NA	.015b	NA	.035b	.004b	.000b	.000b	.011b	.000b	18
	1 mm - 2 mm	NA	NA	NA	.000b	NA	NA	NA	NA	NA	NA	NA	NA	NA	NA	NA	NA	NA	NA	NA	NA	NA	NA	NA	NA	NA	NA	NA	NA	NA	NA	1
1st Harmonic Ratio	Secure Cup - 1 mm Loose	.000b	NA	NA	NA	.001b	NA	.000b	.000b	NA	NA	.000b	.000b	.000b	NA	NA	NA	NA	.002b	.001b	NA	.004b	.000b	.000b	.000b	.000b	.000b	.000b	.000b	.002b	17
	Secure Cup - 2 mm Loose	.000b	NA	NA	NA	NA	NA	.000b	NA	NA	NA	.000b	.000b	.000b	NA	NA	NA	.004b	.000b	.000b	.009b	.007b	.003b	.000b	.000b	.000b	.000b	.000b	.000b	NA	NA	16
	1 mm - 2 mm	NA	NA	.000b	NA	NA	NA	NA	NA	NA	NA	NA	.000b	.000b	.000b	.001b	.000b	.000b	.000b	NA	.000b	NA	NA	.007b	.000b	NA	NA	NA	.009b	NA	12
2nd Harmonic Ratio	Secure Cup - 1 mm Loose	NA	NA	NA	NA	NA	NA	NA	NA	NA	NA	NA	.007b	NA	NA	NA	NA	.002b	.000b	.001b	NA	NA	.001b	.007b	.007b	.000b	.000b	.000b	NA	.000b	11
	Secure Cup - 2 mm Loose	NA	NA	NA	NA	NA	NA	NA	.019b	NA	NA	NA	.000b	.000b	NA	NA	NA	.000b	.000b	.000b	NA	.043b	.003b	.000b	.000b	.000b	.000b	.035b	.000b	NA	NA	13
	1 mm - 2 mm	NA	NA	NA	NA	NA	NA	NA	.000b	.000b	.000b	.000b	.000b	.000b	.001b	.019b	.000b	.000b	.000b	NA	.000b	NA	NA	.000b	.000b	NA	NA	NA	NA	.000b	15
3rd Harmonic Ratio	Secure Cup - 1 mm Loose	NA	NA	.000b	NA	NA	NA	NA	NA	NA	.002b	NA	.004b	.000b	NA	NA	NA	NA	.000b	.007b	NA	.000b	.000b	.000b	.000b	.000b	.000b	.000b	NA	.000b	14
	Secure Cup - 2 mm Loose	NA	NA	NA	NA	.003b	NA	NA	.035b	NA	.001b	.000b	.000b	.000b	NA	NA	.005b	.000b	.000b	.002b	NA	.000b	.005b	.000b	.000b	.000b	.000b	.000b	NA	NA	17
	1 mm - 2 mm	NA	NA	NA	.000b	.009b	NA	NA	NA	NA	NA	.000b	.000b	.000b	.002b	NA	.000b	.000b	.000b	NA	.002b	NA	NA	.023b	.000b	NA	NA	NA	.035b	NA	13

Table E-9: The air medium pelvis accelerometer response comparison between the simulated conditions with the significant value being highlighted, NA = where the signal is not significant or do not support the main finding pattern.

		Ultrsound - Pelvis																																
	Driving Frequency (Hz)	100	150	200	250	300	350	400	450	500	550	600	650	700	750	800	850	900	950	1000	1050	1100	1150	1200	1250	1300	1350	1400	1450	1500	#
Fundamental Magnitude	Secure Cup - 1 mm Loose	NA	NA	.000b	NA	NA	NA	.035b	.001b	NA	NA	NA	NA	NA	NA	NA	NA	NA	NA	NA	NA	NA	NA	NA	NA	.001b	NA	NA	NA	NA	4
	Secure Cup - 2 mm Loose	NA	NA	.000b	.002b	.001b	.000b	.000b	.000b	NA	NA	NA	NA	.001b	NA	NA	NA	.000b	.000b	.000b	.000b	.000b	.002b	.000b	.000b	.000b	.001b	.002b	NA	NA	18
	1 mm - 2 mm	NA	NA	NA	.000b	.000b	.000b	.002b	NA	NA	NA	.000b	.000b	.000b	.000b	.000b	.000b	.000b	.000b	.000b	.000b	.000b	.000b	.000b	.000b	.000b	.000b	.002b	.000b	.000b	23
1st Harmonic Magnitude	Secure Cup - 1 mm Loose	NA	NA	NA	.000b	.000b	.035b	.000b	.000b	.000b	.002b	.000b	.000b	.001b	.000b	.000b	.000b	NA	.002b	.035b	.007b	.000b	.007b	.000b	.007b	.002b	.004b	.035b	.007b	.015b	25
	Secure Cup - 2 mm Loose	NA	NA	NA	.029b	NA	NA	NA	NA	NA	.029b	NA	.019b	NA	NA	.001b	NA	.002b	NA	.002b	.000b	.002b	.000b	NA	NA	.011b	.000b	NA	.009b	NA	12
	1 mm - 2 mm	NA	NA	NA	NA	NA	NA	NA	NA	NA	NA	NA	NA	NA	NA	NA	NA	NA	NA	NA	NA	NA	NA	NA	NA	NA	NA	NA	NA	NA	NA
2nd Harmonic Magnitude	Secure Cup - 1 mm Loose	NA	NA	.035b	.000b	.000b	.000b	NA	NA	.029b	.004b	.004b	.009b	.004b	.002b	NA	NA	.009b	NA	.001b	.000b	.004b	.035b	.002b	NA	NA	.043b	NA	.002b	.011b	19
	Secure Cup - 2 mm Loose	NA	NA	NA	.000b	NA	NA	NA	NA	NA	NA	NA	.004b	.001b	NA	NA	NA	NA	.011b	.015b	.002b	.001b	.035b	.005b	.011b	NA	NA	NA	.007b	.000b	12
	1 mm - 2 mm	NA	NA	NA	NA	NA	NA	NA	NA	NA	NA	NA	NA	NA	NA	NA	NA	NA	NA	NA	NA	NA	NA	NA	NA	NA	NA	NA	NA	NA	NA
3rd Harmonic Magnitude	Secure Cup - 1 mm Loose	NA	NA	NA	.000b	.011b	.019b	NA	NA	NA	NA	.000b	.002b	.043b	.001b	.015b	NA	NA	.001b	.023b	NA	.019b	.029b	.001b	.035b	.000b	NA	.000b	NA	.003b	17
	Secure Cup - 2 mm Loose	NA	NA	NA	NA	NA	NA	NA	NA	.007b	NA	.000b	.002b	.035b	.019b	.003b	NA	NA	.004b	NA	NA	.023b	.001b	.002b	NA	.005b	NA	.004b	.011b	.035b	14
	1 mm - 2 mm	NA	NA	NA	NA	NA	NA	NA	NA	NA	NA	NA	NA	NA	NA	NA	NA	NA	NA	NA	NA	NA	NA	NA	NA	NA	NA	NA	NA	NA	NA
1st Harmonic Ratio	Secure Cup - 1 mm Loose	NA	NA	.001b	NA	NA	NA	.000b	.000b	.001b	.004b	NA	NA	NA	NA	NA	NA	NA	NA	.007b	NA	NA	NA	NA	.000b	.000b	NA	NA	NA	NA	8
	Secure Cup - 2 mm Loose	NA	NA	.000b	.002b	NA	NA	NA	NA	NA	NA	.007b	.002b	.000b	NA	NA	NA	.000b	.000b	.000b	.000b	.000b	.000b	.000b	.000b	.000b	.000b	.000b	NA	NA	16
	1 mm - 2 mm	NA	NA	.002b	.035b	NA	NA	NA	NA	NA	NA	NA	.001b	.001b	NA	.000b	.000b	.000b	.000b	.000b	.000b	.000b	.000b	.000b	.000b	.000b	.000b	.001b	.001b	.000b	.000b	19
2nd Harmonic Ratio	Secure Cup - 1 mm Loose	NA	NA	.000b	NA	NA	NA	.043b	.023b	.005b	NA	NA	NA	NA	NA	NA	NA	NA	NA	.009b	NA	NA	NA	NA	NA	.001b	.029b	NA	NA	NA	7
	Secure Cup - 2 mm Loose	NA	NA	.000b	.000b	NA	NA	NA	.002b	.019b	NA	.043b	.005b	.000b	NA	NA	NA	.000b	.000b	.000b	.000b	.000b	.000b	.000b	.000b	.000b	.000b	.002b	NA	.002b	19
	1 mm - 2 mm	NA	NA	NA	.000b	NA	NA	NA	NA	NA	NA	.000b	.000b	.000b	.007b	.000b	.000b	.000b	.000b	.000b	.000b	.000b	.000b	.000b	.000b	.000b	.001b	.001b	.000b	.000b	20
3rd Harmonic Ratio	Secure Cup - 1 mm Loose	NA	NA	.000b	NA	NA	NA	.004b	.000b	NA	NA	NA	NA	NA	NA	NA	NA	NA	NA	.019b	NA	NA	NA	NA	.023b	.000b	NA	.015b	NA	NA	7
	Secure Cup - 2 mm Loose	NA	NA	.000b	.005b	NA	NA	.023b	.000b	NA	NA	.000b	.000b	.000b	NA	NA	NA	.000b	.000b	.000b	.000b	.000b	.000b	.000b	.000b	.000b	.000b	.007b	.000b	.029b	NA	19
	1 mm - 2 mm	NA	NA	NA	.000b	NA	NA	NA	NA	NA	NA	.000b	.000b	.000b	.000b	.000b	.000b	.000b	.000b	.000b	.000b	.000b	.000b	.000b	.000b	.000b	.009b	.004b	.004b	.000b	.000b	20

Table E-10: The air medium ultrasound response comparison between the simulated conditions with the significant value being highlighted, NA = where the signal is not significant or do not support the main finding pattern.

		Ultrasound - (Water medium)																																						
	Driving Frequency (Hz)	100	150	200	250	300	350	400	450	500	550	600	650	700	750	800	850	900	950	1000	1050	1100	1150	1200	1250	1300	1350	1400	1450	1500	#
Fundamental Magnitude	Secure Cup - 1 mm Loose	NA	NA	NA	NA	NA	NA	NA	NA	NA	NA	NA	NA	NA	NA	NA	NA	NA	NA	NA	.019b	.001b	.001b	.000b	.002b	NA	NA	.011b	.002b	.029b	8
	Secure Cup - 2 mm Loose	NA	NA	NA	NA	NA	.001b	NA	.023b	.000b	.000b	.000b	.000b	.000b	.000b	.000b	.000b	.000b	.000b	.000b	.000b	.000b	.000b	.000b	.000b	.015b	NA	.000b	.000b	.002b	22
	1 mm - 2 mm	NA	NA	NA	NA	NA	.002b	.023b	.000b	.000b	.000b	.000b	.000b	.000b	.001b	.000b	.000b	.000b	.000b	.000b	.000b	.000b	.000b	NA	NA	NA	NA	NA	NA	NA	17
1st Harmonic Magnitude	Secure Cup - 1 mm Loose	NA	NA	.000b	.015b	.003b	NA	.000b	.000b	.000b	.000b	.000b	NA	NA	NA	NA	NA	NA	NA	NA	NA	NA	.019b	NA	NA	.019b	NA	NA	NA	NA	10
	Secure Cup - 2 mm Loose	NA	NA	.000b	.000b	NA	NA	NA	NA	NA	NA	NA	NA	NA	NA	NA	NA	NA	NA	NA	NA	NA	NA	NA	NA	NA	NA	NA	NA	NA	2
	1 mm - 2 mm	NA	NA	NA	.000b	NA	NA	NA	NA	NA	NA	NA	NA	NA	NA	NA	NA	NA	NA	NA	NA	NA	NA	NA	NA	NA	NA	NA	NA	NA	1
2nd Harmonic Magnitude	Secure Cup - 1 mm Loose	NA	NA	.000b	NA	.000b	.000b	NA	.000b	.000b	.009b	NA	NA	NA	NA	.002b	NA	NA	NA	.002b	NA	NA	NA	NA	NA	NA	NA	NA	NA	NA	8
	Secure Cup - 2 mm Loose	NA	NA	.000b	.023b	NA	NA	NA	NA	NA	NA	NA	NA	NA	NA	NA	NA	NA	NA	NA	NA	NA	NA	NA	NA	.043b	NA	NA	NA	NA	3
	1 mm - 2 mm	NA	NA	.001b	.007b	NA	NA	NA	NA	NA	NA	NA	NA	NA	NA	NA	NA	NA	NA	NA	NA	NA	NA	NA	NA	NA	NA	NA	NA	NA	2
3rd Harmonic Magnitude	Secure Cup - 1 mm Loose	NA	NA	.000b	NA	.019b	NA	NA	NA	.005b	.000b	NA	NA	NA	NA	NA	NA	NA	NA	.005b	NA	NA	NA	NA	NA	NA	NA	NA	NA	.035b	6
	Secure Cup - 2 mm Loose	NA	NA	.000b	.000b	NA	NA	NA	NA	NA	NA	NA	NA	NA	NA	NA	NA	NA	NA	NA	NA	NA	NA	NA	NA	NA	NA	NA	NA	.035b	3
	1 mm - 2 mm	NA	NA	.000b	.000b	NA	NA	NA	NA	NA	NA	NA	NA	NA	NA	NA	NA	NA	NA	NA	NA	NA	NA	NA	NA	NA	NA	NA	NA	NA	2
1st Harmonic Ratio	Secure Cup - 1 mm Loose	NA	NA	.000b	NA	.001b	NA	.000b	.000b	NA	.000b	.009b	NA	NA	NA	NA	NA	NA	NA	.043b	.011b	.000b	.000b	.000b	.002b	.007b	NA	.001b	.002b	.023b	16
	Secure Cup - 2 mm Loose	NA	NA	NA	NA	NA	NA	NA	NA	NA	.000b	.001b	.000b	.000b	.000b	.000b	.000b	.000b	.000b	.000b	.000b	.000b	.000b	.000b	.000b	.007b	.043b	.001b	.001b	.023b	20
	1 mm - 2 mm	NA	NA	NA	NA	NA	NA	NA	NA	NA	.000b	NA	.000b	.000b	.002b	.000b	.000b	.000b	.000b	.000b	.000b	.000b	.001b	NA	NA	NA	NA	NA	NA	NA	12
2nd Harmonic Ratio	Secure Cup - 1 mm Loose	NA	NA	NA	NA	.000b	.000b	NA	.023b	NA	NA	NA	NA	.043b	NA	NA	NA	NA	NA	.029b	NA	.002b	.003b	.000b	.007b	.029b	NA	.029b	.005b	NA	12
	Secure Cup - 2 mm Loose	NA	NA	NA	NA	NA	NA	NA	NA	.011b	.000b	.000b	.000b	.000b	.000b	.000b	.000b	.000b	.007b	.000b	.000b	.000b	.000b	.000b	.000b	.029b	NA	.003b	.005b	NA	19
	1 mm - 2 mm	NA	NA	NA	NA	NA	NA	NA	NA	NA	.000b	.000b	.000b	.000b	.007b	.000b	.000b	.000b	.000b	.000b	.000b	.000b	.000b	NA	NA	NA	NA	NA	NA	NA	13
3rd Harmonic Ratio	Secure Cup - 1 mm Loose	NA	NA	NA	NA	.003b	NA	NA	NA	NA	NA	NA	NA	NA	NA	NA	NA	NA	NA	.035b	.019b	.001b	.001b	.000b	.007b	.023b	NA	.002b	.002b	.029b	11
	Secure Cup - 2 mm Loose	NA	NA	NA	NA	NA	.001b	NA	NA	.004b	.000b	.000b	.000b	.000b	.000b	.000b	.000b	.000b	.000b	.000b	.000b	.000b	.000b	.000b	.007b	NA	.000b	.000b	.000b	.000b	21
	1 mm - 2 mm	NA	NA	.023b	NA	NA	.005b	NA	NA	.000b	.000b	.000b	.000b	.000b	.004b	.000b	.000b	.000b	.000b	.000b	.000b	.000b	.002b	NA	NA	NA	NA	NA	NA	NA	16

Table E-11: The water medium ultrasound response comparison between the simulated conditions with the significant value being highlighted, NA = where the signal is not significant or do not support the main finding pattern.

Appendix F: Publications

"A non-invasive diagnosis of acetabular component loosening in total hip replacements (THR)" - PowerPoint presentation.
A.A. Alshuhri, J.L. Cunningham, and A.W. Miles,
Presented at British Orthopaedic Research Society (BORS) meeting 2014: Bath,UK

"Development of a non-invasive diagnostic technique for acetabular component loosening in total hip replacements"
A.A. Alshuhri, T.P. Holsgrove, A.W. Miles, and J.L. Cunningham,
Article in the Medical Engineering and Physics Journal, 2015. **37**(8): p.739-45.

"Development of an acetabular cup loosening detection using vibration analysis"
- PowerPoint presentation.
A.A. Alshuhri, A.W. Miles, and J.L. Cunningham,
Presented at European Orthopaedic Research Society (EORS) 23rd Annual Meeting 2015: Bristol,UK.

"Diagnostic of acetabular cup loosening with a non-invasive diagnostic technique based on vibration analysis" - Poster presentation.
A.A. Alshuhri, A.W. Miles, and J.L. Cunningham,
Presented at 25th Congress of International Society of Biomechanics (ISB) 2015: Glasgow,UK.

"Diagnostic of Uncemented Acetabular Cup Loosening With a Non-Invasive Diagnostic Technique Based On Vibration Analysis" - PowerPoint presentation.
A.A. Alshuhri, T.P. Holsgrove, A.W. Miles, and J.L. Cunningham,
Presented at 8th Saudi Students Conference (SSC) *2014: London,UK.

*The SSC Conference brings together the top Saudi students to stimulate discussion and interest in cutting-edge areas of consequence in the arts and sciences. The 2014 Conference was sponsored by King Abdullah University of Science and Technology (KAUST) in Saudi Arabia, and hosted by Imperial College London in the UK. It is organized by the Scientific Society for Saudi Students in the UK with the collaboration of the Saudi Arabian Cultural Bureau.

OC 21 - A NON-INVASIVE DIAGNOSIS OF ACETABULAR COMPONENT LOOSENING IN TOTAL HIP REPLACEMENTS (THR)

A.A. Alshuhri, J.L. Cunningham, A.W. Miles
Department of Mechanical Engineering, University of Bath, Bath, UK.

Research Summary

Aseptic loosening of the acetabular cup in total hip replacement (THR) remains a major problem even with non-cemented cups. Current diagnostic imaging techniques are ineffective at detecting early loosening, especially of the acetabular component. Thus, new, accurate, and quantifiable, methods are required. The aim of this preliminary study was to assess the viability of using ultrasound vibration analysis technique to accurately detect acetabular component loosening.

A simplified model of acetabular cup loosening, designed to mimic different loosening scenarios of 2, 4 and 14 mm of soft tissue between the cup and the bone, was developed. Each model was exposed to a vibration excitation range of 50 -1500 Hz using a shaker. The resulting natural frequency was observed, and used to define the optimum frequency excitation range and the minimum detectable loosening threshold. The output frequencies were measured using two methods; an ultrasound transducer and an accelerometer. Different patterns in the ultrasound output signal spectra were visible when comparing the stable scenario with the three loosening situations. A 2 mm loosening layer between the cup shell and Sawbone® surface was the minimum detectable at an excitation frequency of 200 Hz and 700 - 900 Hz.

These preliminary findings show that vibration analysis could potentially be a reliable method for detecting acetabular component loosening using either an accelerometer or ultrasound probe. However, the capacity of ultrasound to overcome the attenuating effect of the surrounding soft tissues and its high signal to noise ratio suggest it has the best potential for clinical uses.

Introduction

Vibration analysis is a mechanical nondestructive testing technique that is widely used in the inspection of composite materials and structural integrity and has been successfully expanded into the arena of biomechanics (Shao et al., 2007). Vibration analysis could be an alternative to the present expensive, radiological, invasive and complicated THR loosening diagnostic techniques. However, despite extensive in-vitro and limited in-vivo studies, this technique has yet has to convince the medical practitioner that it is capable of producing measurable and convincingly accurate results. Thus, this study's goal is to assess the viability of using ultrasound vibration analysis technique to accurately detect acetabular component loosening.

Hypothesis

Total hip replacement acetabular component loosening can be accurately diagnosed using vibration based technique.

Methods

A simplified model, was constructed to mimic different acetabular cup loosening scenarios (2, 4 and 14 mm of soft tissue between the cup and the bone), using a Sawbone® block (Sawbones Europe AB, Malmo, Sweden) and three different Stryker acetabular cups sizes (54, 52, 42mm). Each scenario was exposed to a vibration excitation range of 50 -1500 Hz using a mini shaker (V201, LDS Ltd, UK) .The resulting natural frequency spectral was observed using fast Fourier transform (FFT) to define the optimum frequency excitation range and the minimum loosening threshold that can be detected.

A code was developed using LabVIEW (Sound and Vibration Measurement Suite version 11, National Instruments) to record the desired signals via USB data acquisition (USB-4431, National Instruments) using a personal computer (Core2Duo 3.16 GHz, CPU 4 GB RAM). The output signal was measured using two methods; an ultrasound transducer (Mini Dopplex 500 4 MHz, Huntleigh Technology plc, UK) and an accelerometer (Model 353B18, PCB Piezotronics Inc, US).

Results

Different patterns in the ultrasound output signal spectra were visible when comparing the stable scenario with the three loosening situations. There were two frequency zones in which loosening as little as 2 mm was clearly identified; the first was at 200 Hz and the second between 700- 900Hz, as shown in Figure 1A. However, the ultrasound signal appears to have limitations in measuring frequencies ≤150 Hz, due to the probe wall filter.

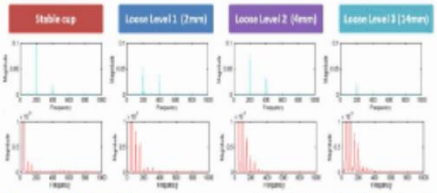

Figure 1: A) The Ultrasound spectral analysis at 200Hz (Blue); B) The Accelerometer spectral analysis at 50Hz (Red).

Spectral analysis of the accelerometer output was also carried out as a control, to compare ultrasound signals and to correlate with previous studies (Tudor et al., 2008; Rieger et al., 2012). Through observing the various frequencies two loosening sensitive zones were noted. The first frequency zone was between 50 -150 Hz, where all loosening levels could be distinguished, as shown in Figure1B. This was followed by a second between 500 -900 Hz, which correlates with the cup loosening sensitive zone of 450 Hz-600 Hz described by Rieger et al. (2012).

Discussion and Conclusions

Experimental testing showed that vibration analysis could be used as a reliable detection method for acetabular cup component loosening using either an accelerometer or ultrasound probe to detect the vibration. However, the capacity of ultrasound to overcome the attenuating effect of the surrounding soft tissues and its high signal to noise ratio suggest it has the best potential for clinical uses. Further experiments will be conducted to achieve more realistic loosening scenarios and develop mathematical models of acetabular cup loosening.

Significance

A non-invasive, ultrasound based, vibration analysis method of diagnosing early acetabular cup loosening is a possible. Preliminary findings have revealed that ultrasound can detect loosening corresponding to a 2 mm of soft tissue layer between the cup shell and Sawbone® surface, at an excitation frequency of 200 Hz and 700 - 900 Hz.

Key References.

Shao et al. Ann Biomed Eng 2007; 35, 817-24, Rowlands et al. Med Eng Phys 2008; 30, 278-284, Tudor et al. Undergraduate Project Report, University of Bath 2008, Rieger et al. Med Eng Phys 2013; 35, 329-37

Acknowledgements

Centre for Orthopaedic Biomechanics, University Of Bath, for their support and help during the development of this Study.

Medical Engineering and Physics 37 (2015) 739–745

Contents lists available at ScienceDirect

Medical Engineering and Physics

journal homepage: www.elsevier.com/locate/medengphy

Development of a non-invasive diagnostic technique for acetabular component loosening in total hip replacements

Abdullah A. Alshuhri*, Timothy P. Holsgrove, Anthony W. Miles, James L. Cunningham

The Centre for Orthopaedic Biomechanics, Department of Mechanical Engineering, University of Bath, Bath, BA2 7AY, United Kingdom

ARTICLE INFO

Article history:
Received 29 September 2014
Revised 10 March 2015
Accepted 3 May 2015

Keywords:
Total hip replacement (THR)
Acetabular cup loosening
Vibrational technique
Loosening diagnostic
Ultrasound
Accelerometer

ABSTRACT

Current techniques for diagnosing early loosening of a total hip replacement (THR) are ineffective, especially for the acetabular component. Accordingly, new, accurate, and quantifiable methods are required. The aim of this study was to investigate the viability of vibrational analysis for accurately detecting acetabular component loosening.

A simplified acetabular model was constructed using a Sawbones® foam block. By placing a thin silicone layer between the acetabular component and the Sawbones block, 2- and 4-mm soft tissue membranes were simulated representing different loosening scenarios. A constant amplitude sinusoidal excitation with a sweep range of 100–1500 Hz was used. Output vibration from the model was measured using an accelerometer and an ultrasound probe. Loosening was determined from output signal features such as the number and relative strength of observed harmonic frequencies.

Both measurement methods were sufficient to measure the output vibration. Vibrational analysis reliably detected loosening corresponding to both 2 and 4 mm tissue membranes at driving frequencies between 100 and 1000 Hz ($p < 0.01$) using the accelerometer. In contrast, ultrasound detected 2-mm loosening at a frequency range of 850–1050 Hz ($p < 0.01$) and 4-mm loosening at 500–950 Hz ($p < 0.01$).

1. Introduction

One million total hip replacement (THR) operations are conducted annually worldwide, and this number is predicted to increase [1]. Within the first ten years of THR, around 10% of all implants are expected to fail, with loosening being the most common reason [2]. The diagnostic approaches to detect loosening are generally categorised into two groups: imaging and non-imaging approaches [3].

Radiology is the most commonly used diagnostic method and consists of different sub-techniques that can be used depending upon need. These techniques generally inspect the bone and implant interfaces to identify osseointegration, failure, or fractures [4]. However, due to the diffraction effects associated with x-ray scattering, it may be difficult to diagnose early loosening using radiological imaging techniques, especially for the acetabular component [5,6]. Even though imaging has a sensitivity and specificity of up to 80% for loosening detection, revision operations on a well-fixed implant may still occur [7].

Vibration analysis is a mechanical non-destructive technique that is widely used to inspect composite materials and structural integrity, and it has been successfully expanded into the arena of biomechanics [5]. This technique predominantly measures the response to low-frequency excitation that is reflected from the targeted surface or structure [8]. In the early 1930s, Lippmann [9] pioneered vibration analysis in medical research, utilising the stethoscope to examine bone fractures and using his fingers to elicit the input vibration. As technology developed, research groups had better tools at their disposal to investigate and develop a clinical diagnostic instrument; this was realised in the works of Chung et al. [10] and Poss et al. [11], who used vibration analysis to study the process of prosthetic fixation using bone cement. They implied that by using vibration analysis and monitoring the resonance frequency shift phenomena, it is possible to estimate implant fixation states. In this scenario, the implant osseointegration process is reflected by a gradual increase in the frequency response. Further studies also were conducted [12–19] to measure the dynamic properties of the implant in order to identify different interference changes.

Rosenstein et al. [20] were one of the first groups to utilise vibration analysis both *in vivo* and *in vitro* in a clinical study. They showed that a secure prosthesis would respond with a single frequency

* Corresponding author. University of Bath, The Centre for Orthopaedic Biomechanics, Department of Mechanical Engineering, Claverton Down, Bath, BA2 7AY, UK. Tel.: +44 01225384187, fax: +44 01225386928.
E-mail addresses: A.Alshuhri@bath.ac.uk, aashuhri@hotmail.com (A.A. Alshuhri), T.P.Holsgrove@bath.ac.uk (T.P. Holsgrove), A.W.Miles@bath.ac.uk (A.W. Miles), J.L.Cunningham@bath.ac.uk (J.L. Cunningham).

http://dx.doi.org/10.1016/j.medengphy.2015.05.012
1350-4533/

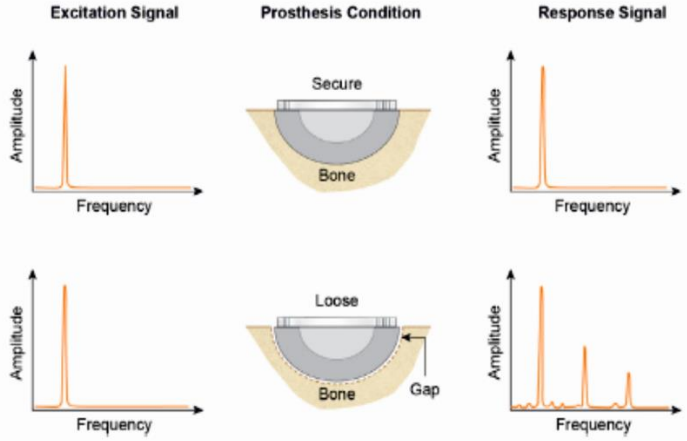

Fig. 1. Vibration analysis concept showing the difference between the secure and loose acetabular cup prostheses.

vibration, whereas a loose prosthesis would vibrate at different frequencies appearing as different peaks in the frequency spectrum; this vibration analysis concept is simplified for the acetabular component, as presented in Fig. 1.

Li et al. [21,22] were the next to explore vibration analysis, showing that the early prosthetic loosening diagnosis has a poor sensitivity (37.5%), but that it could reliably detect late loosening. Georgiou and Cunningham [23] also compared vibration analysis with standard radiological assessment and demonstrated that vibration analysis improved diagnostic precision by 20%; moreover, they were able to detect 13% more cases than radiological diagnosis with 81% sensitivity and 89% specificity. Other research groups have used vibration analysis for different orthopaedic applications such as; the telemetry technique to assess THR femoral loosening [24–26], trans-femoral osseointegration [27–29], intra-operative initial implant stability [6,30–33], THR femoral stability utilising acoustic resonance responses [7,34–41], and complete THR component loosening (femoral and acetabular) [5].

Rowlands et al. [42] investigated replacement of the accelerometer sensor with an ultrasound probe to overcome the effect of soft tissue damping. Their approach used excitation frequencies <1500 Hz on two different types of bone analogues, Sawbones® and Tufnol®. Initially, the Sawbones femur was tested with both a fixed and loose hip prosthesis by using cement fixation. The Tufnol femur was then tested for three interface conditions by using different diameter solid bars of varied fits (fixed, sliding, and loose). Ultrasound distinguished between the secure and loose states with a noticeably higher signal magnitude than the accelerometer.

The majority of previous studies on vibration analysis [20–24,35–42] assessed loosening of the femoral stem. Since a high rate of loosening in the acetabular component has been reported in the clinically [43]; therefore, the aim of the present study was to compare ultrasound and accelerometer methods and to examine the viability of the vibration analysis technique to accurately detect acetabular component loosening.

2. Materials and methods

A simplified model was constructed to mimic different scenarios of acetabular cup loosening. A secure component was represented by a tight press-fit of the acetabular cup in polyurethane solid foam (Sawbones) blocks with a hemispherical cavity. By placing a thin layer of low modulus silicone (EVO-STIK, Bostik Limited, England) between

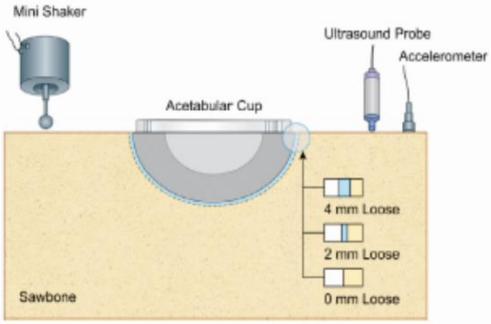

Fig. 2. The Sawbones block showing the excitation and measurement methods.

the acetabular component and the Sawbones block, the loosening effects of 2 and 4 mm soft tissue interfaces were simulated. To represent healthy bone density, blocks with a density of 0.48 g/cm^3 (Sawbones Europe AB, Malmö, Sweden) were used, with two acetabular cups having outside diameters of 54 and 52 mm, respectively (Trident® Hemispherical cup, Stryker Orthopaedics, Mahwah, New Jersey, USA), as shown in Fig. 2.

The secure Sawbones block cavity (diameter 53 mm) was machined using a computer numerically controlled (CNC) milling machine. Subsequent cavities to simulate loosening were created using acetabular reamers to give cup cavity diameters of 56 and 60 mm. This created a gap between the cup shell and the block cavity surface, as shown in Fig. 3. The secure acetabular cup scenario (0-mm loosening) involved using the 54-mm acetabular cup press-fitted in a 53-mm diameter Sawbones block cavity until it was immovable. The 2- and 4-mm loose cup scenarios were produced using the 52-mm acetabular cup placed into Sawbones blocks with cup cavity diameters of 56 and 60 mm, respectively, as shown in Fig. 3. In both loosening scenarios, a silicone layer between the acetabular cup and the Sawbones interface was used to mimic the soft tissue interface in accordance with previous studies [21,22]. Each scenario was exposed to a vibration sweep range of 100–1500 Hz using a mini shaker (V201, LDS Ltd, UK). The Sawbones block setup was lightly suspended to create a repeatable boundary condition, (Fig. 4a).

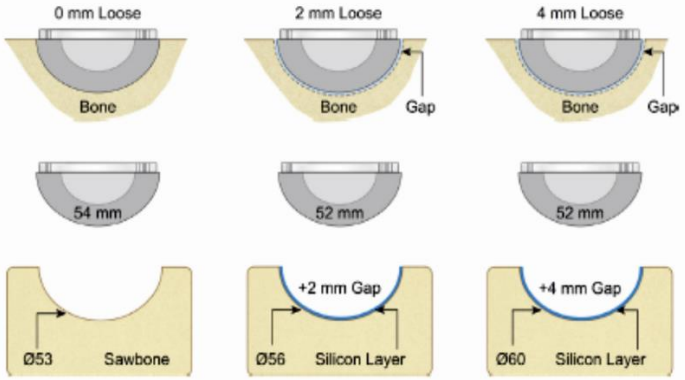

Fig. 3. The three simulated testing conditions of 0, 2, and 4 mm of loosening.

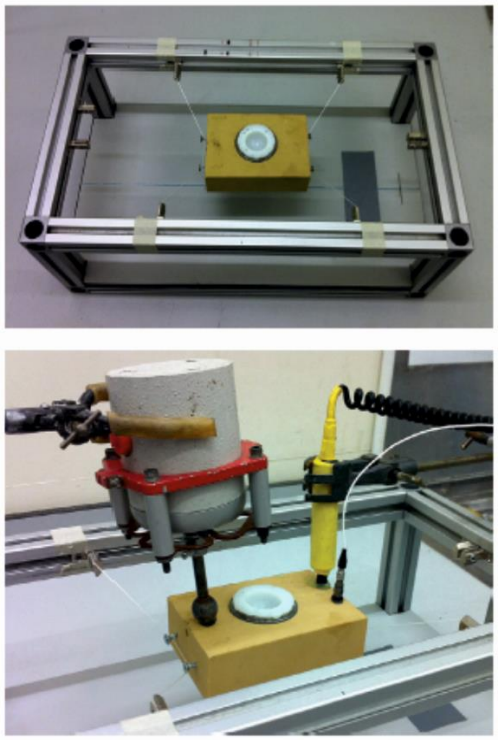

Fig. 4. The experimental setup showing the Sawbones block, excitation, and measurement methods.

2.1. Excitation signal

A function generator (TG230, Thurlby Thandar Ltd, UK) connected to a power amplifier (PA25E, LDS Ltd, UK) was used for vibration excitation via a mini-shaker (V201, LDS Ltd, UK). The excitation signal was a constant amplitude sinusoidal wave with a frequency sweep range of between 100 and 1500 Hz, with incremental steps of 50 Hz. The shaker was positioned in a similar location on the Sawbones block for all tests (Fig. 4b).

2.2. Measurement and analysis

An ultrasound transducer (Mini Dopplex 500 4 MHz, Huntleigh Technology Plc, UK) and accelerometer (Model 353B18; PCB Piezotronics Inc, US) were used to measure the output vibration. Consistent with other orthopaedic vibration studies [5,20–23], the accelerometer was used as a reference measurement method. Ultrasound was chosen as an alternative measurement method due to its capacity to overcome the attenuating effect of the soft tissues surrounding the implant in the clinical environment [42].

The ultrasound and accelerometer data were recorded using a custom code in LabVIEW (Sound and Vibration Measurement Suite version 11, National Instruments) via a USB data acquisition system (USB-4431, National Instruments) using a personal computer (Core2Duo 3.16 GHz, CPU 4 GB RAM). The resulting natural frequency spectrum of both measurement methods was then observed using a fast Fourier transform (FFT) to define the optimum frequency excitation range using two simultaneous measurement methods; twelve measurements were obtained at 50 Hz increments from each of the fixation scenarios (0-, 2-, and 4-mm loose) under the sinusoidal frequency sweep. Insufficient sampling frequency may result in distortion from the original continuous signal, which is known as the aliasing effect. Thus, a sampling frequency of 8 kHz was used to overcome this effect. The accelerometer was coupled to the block surface using a petro-wax, and ultrasound gel was used to couple the ultrasound probe. Each measurement was taken from a specifically defined location on the Sawbone block for accuracy and repeatability (Fig. 4). Analysis was conducted in two stages as explained below: the spectrum analysis and the harmonic ratio.

2.2.1. Spectrum analysis

Real-time spectrum analyses tracked the frequency response and observed relationships between the two loosening scenarios and the secure condition across the different driving frequencies. For the secure implant, vibration analysis implies that the frequency response would be similar to the excitation signal, whereas for the loose condition, the response would be distorted with multiple apparent harmonics. This was accomplished using two frequency variables: the fundamental frequency (F_o) and the first harmonic (F_1). The main response to the driving frequency is the fundamental frequency, whereas the first harmonic is indicative of system nonlinearity.

2.2.2. Harmonic ratio

In an attempt to define the optimum frequency excitation range for the loosening assessment, a sweep analysis was conducted. The resulting frequencies were then analysed as the harmonic ratio, defined as the relative magnitude of the first harmonic to the fundamental frequency (Harmonic Ratio = First Harmonic [F_1] magnitude/Fundamental Frequency [F_o] magnitude). This ratio can then be utilised to show how the different loosening conditions affect the relative magnitude of the first harmonic across the different driving frequencies.

2.3. Statistics

Statistical analysis was performed using SPSS software (version 20.0; SPSS, Chicago, IL, USA). A Shapiro-Wilk test revealed that the harmonic ratio data were not normally distributed; thus, non-parametric analyses were performed. The conditions (0, 2, and 4 mm) were compared at each frequency step using a Kruskal-Wallis test, and Mann-Whitney U-tests were used for post-hoc analysis. Significance was defined as a p value of <0.05.

3. Results

3.1. Spectrum analysis

The initial variable in the FFT spectrum analysis was the fundamental frequency (F_o) magnitude that changed in relation to the cup stability. The frequency magnitude was assessed based on the root mean squared (RMS) value over the excitation period. Fig. 5 shows the output measurement response of three simulated loosening conditions at a driving frequency of 200 Hz for both the ultrasound and accelerometer. It was noted that the secure condition had the highest fundamental frequency magnitude, followed by the 2- and 4-mm loose conditions, respectively. However, when examining the readings for both the ultrasound and accelerometer, the absolute magnitude of the reduction in vibration magnitude with loosening is higher for the ultrasound readings than for the accelerometer readings, as shown in Fig. 5.

The next variable examined was the first harmonic (F_1), which behaves in a manner opposite to the fundamental frequency (F_o). The magnitude of the first harmonic peak increased relative to the degree of acetabular cup loosening. For example, in Fig. 5, the first harmonic with 4-mm loosening had a higher magnitude than for 2-mm loosening. When comparing the absolute magnitude of the first harmonic using the two measurement methods, the ultrasound results were able to discern more harmonics than the accelerometer results, enabling a clear distinction between the loosening scenarios.

The above findings indicated that as the gap between the Sawbones block and cup increased (representing increased loosening), the system became more non-linear, which was reflected in the lower fundamental frequency and higher harmonic peak values. These harmonic readings correlated with the finding of Rowlands et al. [42], who reported that the presence of harmonics can be used as an indication of loosening, which could be detected using either the accelerometer or ultrasound transducers, especially for frequencies <500 Hz with stem component.

3.2. Harmonic ratio

The harmonic ratio measurement for the three simulated conditions by using ultrasound and accelerometer was illustrated alongside each other using the median ± 95% confidence interval for ease of comparison. The Mann–Whitney test was used to determine significance (defined as $p < 0.05$), as shown in Fig. 6.

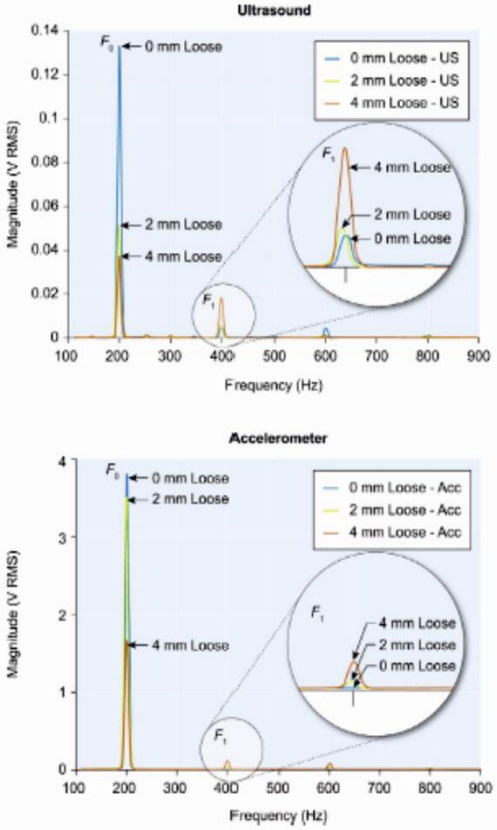

Fig. 5. FFT spectrum analysis at 200 Hz showing the difference between the secure prosthesis, 2 mm loose condition, and 4 mm loose condition for the ultrasound and accelerometer readings.

3.2.1. Accelerometer

The harmonic ratios for the accelerometer are shown in Fig. 6a. The ratios clearly showed a pattern, according to which the secure cup had the lowest value, followed by 2-mm loosening, and 4-mm loosening having the highest harmonic ratio in the frequency range up to 950 Hz. The harmonic ratio for 2-mm loosening was significantly greater ($p < 0.01$) than that in the secure condition in the driving frequency range 100–1050 Hz (Fig. 6c). For 4-mm loosening, the harmonic ratio was significantly greater ($p < 0.01$) than that in the secure condition in the frequency range 100–1000 Hz (Fig. 6e). When comparing the two loosening conditions, the 4-mm loosening condition resulted in a significantly higher harmonic ratio ($p < 0.05$) in the frequency ranges 150–250 Hz and 550–900 Hz.

3.2.2. Ultrasound

The harmonic ratio derived from ultrasound measurements had a higher magnitude than the accelerometer readings, as shown in Fig. 6a–b. The ultrasound measurements were between 200 and 1500 Hz due to the ultrasound system's built-in filter that affected readings below 200 Hz. The same pattern was observed with the accelerometer, with the lowest harmonic ratio observed in the secure

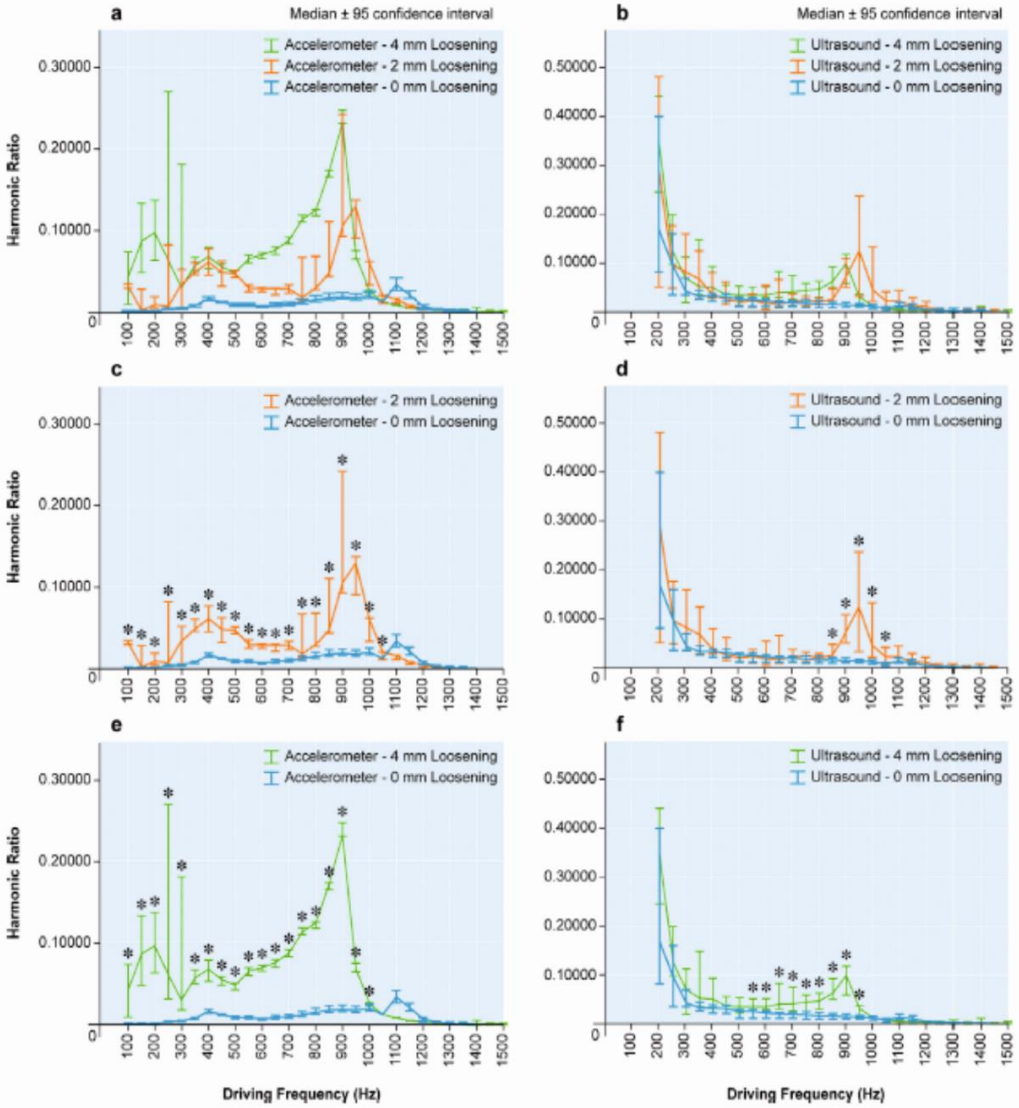

Fig. 6. The harmonic ratio of the different loosening conditions using an accelerometer and an ultrasound probe as the measurement methods. *Graphs a, c,* and *e* used an accelerometer for the loosening conditions of (0, 2 and 4 mm), (0 and 2 mm), and (0 and 4 mm), respectively. *Graphs b, d,* and *f* used an ultrasound for the loosening conditions of (0, 2 and 4 mm), (0 and 2 mm), and (0 and 4 mm), respectively. *Mann–Whitney test $p < 0.05$.

condition and progressively increasing at 2- and 4-mm loosening, respectively. The 2-mm loosening resulted in a significantly higher harmonic ratio ($p < 0.01$) than that in the secure condition at driving frequencies between 850 and 1050 Hz (Fig. 6d). The harmonic ratio of the 4-mm loosening condition was significantly higher ($p < 0.01$) than that in the secure condition between 500 and 950 Hz (Fig. 6f). The harmonic ratio for 4-mm loosening was significantly greater ($p < 0.05$) than that for 2-mm loosening between 500 and 700 Hz and between 800 and 850 Hz.

4. Discussion

Most THR stability assessment studies have focused on the femoral component [20–24,35–42]. Vibration analysis studies on acetabular loosening are limited because the acetabulum has a complex geometry compared to the femur and has a thicker overlaying soft tissue layer, which acts as a signal buffer. Thus, the aim of this study was to explore the viability of vibration analysis to accurately detect acetabular component loosening.

Vibration analysis implies that secure implants respond with a single frequency peak similar to the excitation signal, whereas loose implants vibrate at different frequencies, which appear as multiple harmonics peaks in the frequency spectrum. The resulting frequencies were initially observed using FFT analysis, then analysed as the harmonic ratio, which was subsequently used as a novel method to track frequency responses and observe relationships between the loosening scenarios and the secure condition across frequencies of 100–1500 Hz. Using this approach, the three simulated conditions were distinguishable at an excitation frequency range of 200–950 Hz, using both ultrasound and the accelerometer.

Most orthopaedic vibration studies have used FFT spectrum analysis to assess implant loosening [20–23,42]. However, most examined the stem component and reported that implant instability can be identified through harmonics in the frequency spectrum (Fig. 1). Moreover, they highlighted that the lower frequency range (≤1000 Hz) had the most potential for stability assessment [20,23]. Rieger et al. [5] assessed a complete THR (femoral and acetabular implants in a Sawbones femur and hemi-pelvis) and detected acetabular cup loosening at frequencies of 450 and 600 Hz. At these frequencies, a noticeable resonance shift was observed when the loosening condition was compared with the secure condition using an accelerometer and laser vibrometer. Using an FFT analysis, the present study revealed the same overall conclusions. The difference between the three simulated conditions was observed using two frequency variables: the fundamental frequency (F_0) and the first harmonic (F_1). The fundamental frequency was primarily in response to the driving frequency, and the first harmonic indicated the level of instability. The three simulated conditions examined with FFT analysis at a driving frequency of 200 Hz demonstrated that, as loosening increases, the system becomes increasingly non-linear, which is reflected at the lower fundamental frequency and higher harmonic peak magnitude (Fig. 5).

Another novel contribution of this study is the use of the harmonic ratio to quantify the FFT spectrum analysis frequency response across the 100–1500 Hz range. This ratio represents the relative magnitude of the first harmonic to the fundamental frequency. When analysing the harmonic ratio for the accelerometer and ultrasound measurements at frequencies ≤950 Hz, a clear pattern was observed. The secure cup had the lowest ratios and, as the loosening progressed, this ratio increased. At excitation frequencies of 100–1050 Hz, the accelerometer detected loosening corresponding to 2 mm between the cup shell and the Sawbones surface, while 4 mm loosening was detected at excitation frequencies of 100–1000 Hz. In agreement with the study of Rowlands et al. [42] which examined stem loosening, as opposed to acetabular loosening in the current study, the ultrasound measurements were clearly higher than accelerometer readings throughout the frequency range. However, because of the increased variability of ultrasound measurements compared to measurements with the accelerometer, a significant difference between the secure and loose conditions was only established at the high frequency range. Loosening of 2 mm was detected at driving frequencies of 850–1050 Hz, while 4-mm loosening was detected at 500–950 Hz. Therefore the harmonic ratio was clearly able to discern between the simulated conditions using both measurement methods.

The use of single density Sawbones block to mimic different loosening conditions was an attempt to simplify acetabular cup instability, which could be considered as a limitation. Additionally, the exaction method was positioned closer to the acetabular component than would be possible in a clinical setting. Moreover, the loosening conditions had only press-fit acetabular cups with hard shell components. Future experiments will try to overcome these limitations by moving towards a more clinically realistic setup. Initially, this will involve using a Sawbones hemi-pelvis with an implanted THR cup, followed by a combined pelvis and femur containing a complete THR [5]. On successful completion of these experiments a further aim would be to carry out a pilot clinical study.

5. Conclusion

This work has demonstrated that vibration analysis can be used to detect acetabular cup component loosening in a simplified *in vitro* model using either the accelerometer or ultrasound to measure output vibration. The harmonic ratio is a novel and useful parameter for comparing output signals to easily discern between secure and loose cups. Further experiments will be required to overcome current study limitations and achieve a more realistic setup for loosening scenarios.

Ethical approval

Not required.

Conflict of interest statement

There are no conflicts of interest to declare.

Acknowledgements

This research project is funded by the Saudi Food and Drug Authority-Medical Devices Sector through the Ministry of Higher Education, Saudi Arabia.

References

[1] Pivec R, Johnson AJ, Mears SC, Mont MA. Hip arthroplasty. Lancet 2012;380:1768–77.
[2] Temmerman OP, Raijmakers PG, Deville WL, Berkhof J, Hoeft L, Heyligers IC. The use of plain radiography, subtraction arthrography, nuclear arthrography, and bone scintigraphy in the diagnosis of a loose acetabular component of a total hip prosthesis: a systematic review. J Arthroplasty 2007;22:818–27.
[3] Ruther C, Timm U, Ewald H, Mittelmeier W, Bader R, Schmelzer R, et al. Current possibilities for detection of loosening of total hip replacements and how intelligent implants could improve diagnostic accuracy. In: Foketer S, editor. Recent advances in arthroplasty. InTech; 2012. p. 363–86.
[4] McBride TJ, Prakash D. How to read a postoperative total hip replacement radiograph. Postgrad Med J 2011;87:101–9.
[5] Rieger JS, Jaeger S, Schuld C, Kreuzer JP, Bitsch RG. A vibrational technique for diagnosing loosened total hip endoprostheses: an experimental sawbone study. Med Eng Phys 2013;35:329–37.
[6] Mathieu V, Michel A, Flouzat Lachaniette C-H, Poignard A, Hernigou P, Allain J, et al. Variation of the impact duration during the in vitro insertion of acetabular cup implants. Med Eng Phys 2013;35:1558–63.
[7] Ruther C, Ewald H, Mittelmeier W, Bader R, Kluess D. Localization of uncemented hip Stem loosening with a novel in-vivo sensor system based on vibration analysis. In: Lim CT, Goh JCH, editors. 6th World Congress of Biomechanics (WCB 2010) August 1–6, 2010. Singapore: Springer Berlin Heidelberg; 2010. p. 620–3.
[8] Nondestructive active testing technique for structural composites, MIL-HDBK-793. 1989:2–6.
[9] Lippmann RK. The use of auscultatory percussion for the examination of fractures. J Bone Joint Surg 1932;14:118–26.
[10] Chung J, Pratt C, Babyn P, Poss R. A new diagnostic technique for the evaluation of prosthetic fixation. In: Proceedings of the first annual conference of the IEEE/ Engineering in Medicine and Biological society. New York: IEEE publishing services; 1979. p. 158–60.
[11] Poss R, Pratt Jr G, Chung J. An evaluation of total hip replacement cementing technique using sonic resonance. Eng Med 1984;13:191–6.
[12] Elias JJ, Brunski JB, Scarton HA. A dynamic modal testing technique for noninvasive assessment of bone-dental implant interfaces. Int J Oral Maxillofac Impl 1996;11:728–34.
[13] Meredith N, Alleyne D, Cawley P. Quantitative determination of the stability of the implant-tissue interface using resonance frequency analysis. Clin Oral Impl Res 1996;7:261–7.
[14] Meredith N, Books K, Fribergs B, Jemt T, Sennerby L. Resonance frequency measurements of implant stability in viva: a cross-sectional and longitudinal study of resonance frequency measurements on implants in the edentulous and partially dentate maxilla. Clin Oral Impl Res 1997;8:226–33.
[15] Huang HM, Chiu CL, Yeh CY, Lin CT, Lin LH, Lee SY. Early detection of implant healing process using resonance frequency analysis. Clin Oral Impl Res 2003;14:437–43.
[16] Huang HM, Cheng KY, Chen CF, Ou KL, Li CT, Lee SY. Design of a stability-detecting device for dental implants. Proc Inst Mech Eng H 2005;219:203–11.

[17] Lachmann S, Jager B, Axmann D, Gomez-Roman G, Groten M, Weber H. Resonance frequency analysis and damping capacity assessment. Part 1: an in vitro study on measurement reliability and a method of comparison in the determination of primary dental implant stability. Clin Oral Impl Res 2006;17:75–9.
[18] Lachmann S, Laval JY, Jager B, Axmann D, Gomez-Roman G, Groten M, et al. Resonance frequency analysis and damping capacity assessment. Part 2: peri-implant bone loss follow-up. An in vitro study with the Periotest and Osstell instruments. Clin Oral Impl Res 2006;17:80–4.
[19] Van der Perre G. Dynamic analysis of human bones. Funct Behav Orthop Mater 1984;1:99–159.
[20] Rosenstein AD, McCoy GF, Bulstrode CJ, McLardy-Smith PD, Cunningham JL, Turner-Smith AR. The differentiation of loose and secure femoral implants in total hip replacement using a vibrational technique: an anatomical and pilot clinical study: Proceedings of the Institution of Mechanical Engineers Part H. J Eng Med 1989;203:77–81.
[21] Li PL, Jones NB, Gregg PJ. Loosening of total hip arthroplasty: diagnosis by vibration analysis. J Bone Joint Surg Br 1995;77:640–4.
[22] Li PL, Jones NB, Gregg PJ. Vibration analysis in the detection of total hip prosthetic loosening. Med Eng Phys 1996;18:596–600.
[23] Georgiou AP, Cunningham JL. Accurate diagnosis of hip prosthesis loosening using a vibrational technique. Clin Biomech 2001;16:315–23.
[24] Puers R, Catrysse M, Vandevoorde G, Collier RJ, Louridas E, Burny F, et al. A telemetry system for the detection of hip prosthesis loosening by vibration analysis. Sensors and Actuators A: Physical 2000;85:42–7.
[25] Marschner U, Gratz H, Jettkant B, Ruwisch D, Woldt G, Fischer WJ, et al. Integration of a wireless lock-in measurement of hip prosthesis vibrations for loosening detection. Sensors and Actuators A: Physical 2009;156:145–54.
[26] Sauer S, Marschner U, Graetz H, Fischer WJ. Medical wireless vibration measurement system for hip prosthesis loosening detection. In: SENSORDEVICES, The Third International Conference on Sensor Device Technologies and Applications; 2012. p. 9–13.
[27] Xu W, Shao F, Ewins D. A resonant frequency measurement system for osseointegration trans-femoral implant. Key Eng Mater 2005;295:139–44.
[28] Shao F, Xu W, Crocombe A, Ewins D. Natural frequency analysis of osseointegration for trans-femoral implant. Ann Biomed Eng 2007;35:817–24.
[29] Cairns N, Pearcy M, Smeathers J, Adam C. Ability of modal analysis to detect osseointegration of implants in transfemoral amputees: a physical model study. Med Biol Eng Comp 2013;51(1–2):39–47.
[30] Varini E, Bialoblocka-Juszczyk E, Lannocca M, Cappello A, Cristofolini L. Assessment of implant stability of cementless hip prostheses through the frequency response function of the stem–bone system. Sensors and Actuators A: Physical 2010;163:526–32.
[31] Lannocca M, Varini E, Cappello A, Cristofolini L, Bialoblocka E. Intra-operative evaluation of cementless hip implant stability: a prototype device based on vibration analysis. Med Eng Phys 2007;29:886–94.
[32] Pastrav LC, Jaecques SV, Jonkers I, Perre GV, Mulier M. In vivo evaluation of a vibration analysis technique for the per-operative monitoring of the fixation of hip prostheses. J Orthop Surg Res 2009;4:4–10.
[33] Michel A, Bosc R, Mathieu V, Hernigou P, Haiat G. Monitoring the press-fit insertion of an acetabular cup by impact measurements: influence of bone abrasion. Proc Inst Mech Eng H 2014;228:1027–34.
[34] Unger AC, Cabrera-Palacios H, Schulz AP, Jurgens C, Paech A. Acoustic monitoring (RFM) of total hip arthroplasty: results of a cadaver study. Euro J Med Res 2009;14:264–71.
[35] Ruther C, Timm U, Fritsche A, Ewald H, Mittelmeier W, Bader R, et al. A new approach for diagnostic investigation of total hip replacement loosening. In: Fred A, Filipe J, Gamboa H, editors. Biomedical engineering systems and technologies; 2013. p. 74–9.
[36] Ruther C, Nierath H, Ewald H, Cunningham JL, Mittelmeier W, Bader R, et al. Investigation of an acoustic-mechanical method to detect implant loosening. Med Eng Phys 2013;35:1669–75.
[37] Ruther C, Schulze C, Boehme A, Nierath H, Ewald H, Mittelmeier W, et al. Investigation of a passive sensor array for diagnosis of loosening of endoprosthetic implants. Sensors (Basel) 2012;13:1–20.
[38] Ewald H, Timm U, Ruther C, Mittelmeier W, Bader R, Kluess D. Acoustic sensor system for loosening detection of hip implants. In: Sensing Technology (ICST), 2011 Fifth International Conference; 2011. p. 494–7.
[39] Ewald H, Ruther C, Mittelmeier W, Bader R, Kluess D. A novel in vivo sensor for loosening diagnostics in total hip replacement. Sensors 2011:89–92.
[40] Ruther C, Ewald H, Mittelmeier W, Fritsche A, Bader R, Kluess D. A novel sensor concept for optimization of loosening diagnostics in total hip replacement. J Biomech Eng 2011;133:104503.
[41] Paech A, Schulz A, Nassutt R, Keine J, Wenzl M, Jurgens C. Acoustic properties of femoral components of hip endoprostheses: analysis using frequency-resonance-measurement in a soft tissue simulation model. Res J Med Sci 2007;1:118–23.
[42] Rowlands A, Duck FA, Cunningham JL. Bone vibration measurement using ultrasound: Application to detection of hip prosthesis loosening. Med Eng Phys 2008;30:278–84.
[43] National joint registry for England and Wales 10th annual report, NJR centre. Retrieved from http://www.njrcentre.org.uk/njrcentre/Portals/0/Documents/England/Reports/10th%20annual%20report/NJR%2010th%20Annual%20Report%202013%20B.pdf; 2013 [Accessed 5 September 2014].

DEVELOPMENT OF AN ACETABULAR CUP LOOSENING DETECTION USING VIBRATION ANALYSIS

A.A. Alshuhri, A.W. Miles, and J.L. Cunningham,

The Centre for Orthopaedic Biomechanics, Department of Mechanical Engineering ,University of Bath, Bath, BA27AY , United Kingdom

Introduction

Aseptic loosening of the acetabular cup in total hip replacement (THR) remains a major problem. Current diagnostic imaging techniques are ineffective at detecting early loosening, especially for the acetabular component [1]. The aim of this preliminary study was to assess the viability of using a vibration analysis technique to accurately detect acetabular component loosening.

Methods

A simplified acetabular model was constructed using a Sawbones® foam block into which an acetabular cup was fitted. Different levels of loosening were simulated by the interposition of thin layer of silicon between the acetabular component and the Sawbones block, as shown in Figure 1. This included a simulation of a secure (stable) fixation and various combinations of cup zone loosening. A constant amplitude sinusoidal excitation with a sweep range of 100–1500 Hz was used. Output vibration from the model was measured using an accelerometer and an ultrasound probe. Loosening was determined from output signal features such as the number and relative strength of the observed harmonic frequencies.

Results

Both measurement methods were capable of measuring the output vibration. Preliminary findings show different patterns in the output signal spectra were visible when comparing the stable cup with the 1mm of simulated spherical loosening at driving frequencies 1050 Hz ,1100 Hz and 1150 Hz ($p < 0.05$) using the accelerometer , whereas for ultrasound at frequencies 950 Hz and 1350 Hz ($p < 0.05$).

Conclusions

Experimental testing showed that vibration analysis could be used as a potential detection method for acetabular cup component loosening using either an accelerometer or ultrasound probe to detect the vibration. However, the capacity of ultrasound to overcome the attenuating effect of the surrounding soft tissues and its high signal to noise ratio suggest it has the best potential for clinical use.

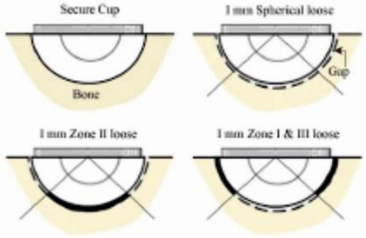

Figure 1: Different fixation models

[1] Ruther et al. 2012, InTech, ISBN: 978-953-307-990-5.

DIAGNOSTIC OF ACETABULAR CUP LOOSENING WITH A NON-INVASIVE DIAGNOSTIC TECHNIQUE BASED ON VIBRATION ANALYSIS

PO-0169

AA AL-Shuhri*, AW Miles*, JL Cunningham *
*Centre for Orthopaedic Biomechanics , University of Bath, Bath, UK.

centre for orthopaedic biomechanics

Introduction

One million total hip replacements (THR) are carried out annually around the world; a number which is likely to increase [1] . The THR procedure is one of the most successful, safe, and cost effective medical interventions with a life expectancy of around 20 years. However, implants can and do fail due to the human, mechanical and biological factors, leaving patients in some cases with unbearable pain and disability. Current diagnostic imaging techniques are ineffective at detecting early loosening, especially of the acetabular component [2]. Accordingly, the aim of this study was to investigate the viability of using vibrational analysis for accurately detecting early acetabular component loosening.

Materials and Methods

Vibration analysis is a mechanical nondestructive testing technique that is widely used in the inspection of composite materials and structural integrity and has been successfully expanded into the arena of biomechanics. Vibration analysis could be an alternative to the present expensive, radiological, invasive and complicated THR loosening diagnostic techniques. However, despite extensive in-vitro and limited in-vivo studies, this technique has yet to convince the medical practitioner that it is capable of producing measurable and convincingly accurate results. Loosening is determined from the response signal features such as the number and relative strength of the observed harmonic frequencies (Figure 1) .

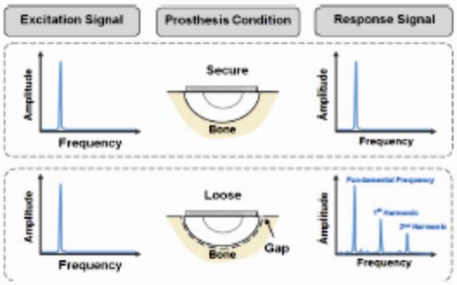

Figure 1: Vibration analysis concept showing the difference between the secure and loose acetabular cup prostheses

A simplified acetabular model was constructed using a Sawbones® (Sawbones Europe AB, Malmö, Sweden) foam block into which an acetabular cup was fitted. Loosening of 1 mm was simulated by the interposition of thin layer of silicon between the acetabular component and the Sawbone block, as shown in Figure 2. Each scenario was exposed to a sinusoidal vibration excitation range of 100 -1500 Hz using a mini shaker (V201, LDS Ltd, UK) .The resulting natural frequency spectral was observed using fast Fourier transform (FFT) to define the optimum frequency excitation range and the minimum loosening threshold that can be detected.

A code was developed using LabVIEW (Sound and Vibration Measurement Suite version 11, National Instruments) to record the desired signals via USB data acquisition (USB-4431, National Instruments) using a personal computer (Core2Duo 3.16 GHz, CPU 4 GB RAM). The output signal was measured using two methods; an ultrasound transducer (Mini Doppler 500 4 MHz, Huntleigh Technology plc, UK) and an accelerometer (Model 353B18, PCB Piezotronics Inc, US) , as shown in Figure 3.

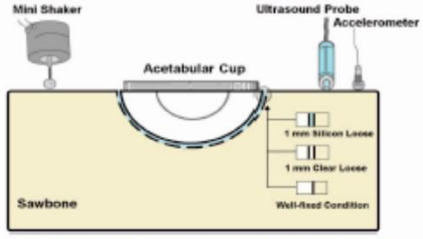

Figure 2: The Sawbone block showing the excitation and measurement methods.

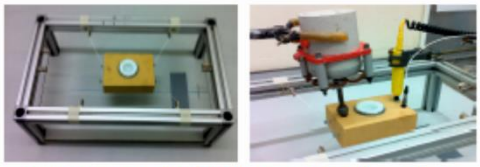

Figure 3: The experimental setup showing the Sawbones block, excitation, and measurement methods.

Results

Different patterns in the ultrasound output signal spectra were visible when comparing the stable scenario with the two 1-mm loosening situations, clear and silicone. It was noted that the loose condition had the higher harmonic frequency magnitude compared to the stable condition. This was the case for the 1-mm clear loosening first harmonic at the driving frequency 650 Hz ($p < 0.05$) and with second harmonic at frequencies 800 and 1050 Hz ($p < 0.05$). While, the 1-mm silicone loosening had significantly greater first harmonic compared to the stable condition at the frequencies 950 and 1350 Hz ($p < 0.05$). Flowed by the second harmonic being also significantly greater at the driving frequencies 950 and 1050 Hz ($p < 0.05$), as shown in Figure 4b.

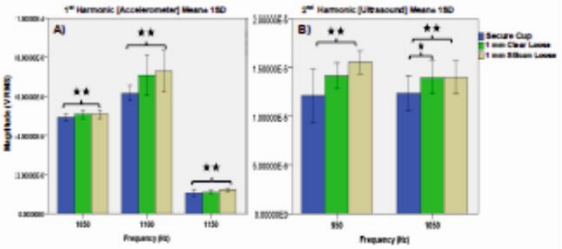

Figure 4: The harmonic comparison between the different conditions ; A) The Accelerometer first harmonic ; B) The Ultrasound second harmonic . Mann-Whitney test $p < 0.05$.

Spectral analysis of the accelerometer output was also carried out as a reference measurement method in consistent with other studies [3]. The first and second harmonic magnitudes for 1-mm loosening, silicone and clear, were significantly greater ($p < 0.05$) than that in the stable condition in the driving frequencies 100 Hz and 800 Hz. Additionally, the 1mm silicone loosening had a significantly greater first harmonics at the frequencies 1050,1100 and 1150 Hz, as seen in Figure 4a.

Discussion and Conclusions

Experimental testing showed that vibration analysis could be used as a reliable detection method for acetabular cup component loosening using either an accelerometer or ultrasound probe to detect the vibration. However, the capacity of ultrasound to overcome the attenuating effect of the surrounding soft tissues and its high signal to noise ratio suggest it has the best potential for clinical uses. Further experiments will be conducted to achieve more realistic loosening scenarios for acetabular cup loosening.

Significance

A non-invasive vibration analysis method of diagnosing early acetabular cup loosening is a possible. Preliminary findings have revealed that loosening corresponding to a 1 mm of soft tissue layer between the cup shell and Sawbones® surface can be detect, at an excitation frequency as low as 800Hz for the accelerometer and 950 Hz for the ultrasound probe.

Acknowledgments

This research project was funded by the Saudi Food and Drug Authority-Medical Devices Sector through the Ministry of Higher Education, Saudi Arabia.

UNIVERSITY OF BATH

References:
[1] Piveo et al. 2012, Hip arthroplasty. The Lancet, 380, 1768-1777.
[2] Ruther et al. 2012, InTech, ISBN: 978-953-307-990-5.
[3] Rieger et al. Med Eng Phys 2012; 329-37.

Corresponding Author: A.Alshuhri@bath.ac.uk
Department of Mechanical Engineering, University of Bath, Bath, BA2 7AY, UK

Title: DIAGNOSTIC OF UNCEMENTED ACETABULAR CUP LOOSENING WITH A NON-INVASIVE DIAGNOSTIC TECHNIQUES BASED ON VIBRATION ANALYSIS

Authors: Abdullah A. Alshuhri[a, 1], Timothy P. Holsgrove[a], Anthony W. Miles[a], and James L. Cunningham[a]

[a]The Centre for Orthopaedic Biomechanics, Department of Mechanical Engineering, University of Bath, Bath, BA2 7AY, United Kingdom, T.P.Holsgrove@bath.ac.uk, A.W.Miles@bath.ac.uk, J.L.Cunningham@bath.ac.uk

[1]Corresponding author:
Abdullah A. Alshuhri
University of Bath
The Centre for Orthopaedic Biomechanics
Department of Mechanical Engineering
Claverton Down, Bath, BA2 7AY, UK
Tel: +44-(0)1225-384187
Fax: +44-(0)1225-386928
E-mail: A.Alshuhri@bath.ac.uk

Abstract

Aseptic loosening of the acetabular cup in total hip replacement (THR) remains a major problem even with non-cemented cups. Current diagnostic imaging techniques are ineffective at detecting early loosening, especially of the acetabular component. The aim of this preliminary study was to assess the viability of using ultrasound vibration analysis technique to accurately detect acetabular component loosening.

A simplified model of acetabular cup loosening, designed to mimic different loosening scenarios of 2 and 4 mm of soft tissue between the cup and the bone, was developed. Each model was exposed to a vibration excitation range of 100 -1500 Hz using a shaker. The output frequencies were measured using two methods; an ultrasound transducer and an accelerometer.

Preliminary experimental testing showed that vibration analysis can reliably detected loosening corresponding to both 2 and 4 mm of soft tissue membrane at driving frequencies between 100 and 1000 Hz ($p < 0.01$).

Keyword:

Total hip Replacement (THR); Aseptic loosening; acetabular cup loosening; vibration analysis

1. Introduction

One million total hip replacements (THR) are carried out annually around the world; a number which is likely to increase. The THR procedure is one of the most successful, safe, and cost effective medical interventions with a life expectancy of around 20 years. However, implants do fail due to the human, mechanical and biological factors, leaving patients in some cases with unbearable pain and disability (Pivec et al., 2012). Current diagnostic imaging techniques are ineffective at detecting early loosening, especially of the acetabular component (Ruther et al., 2012b). Thus, new, accurate, and quantifiable, methods are required. The vibration analysis is one such technique that the current project is examining.

Vibration analysis is a mechanical non-destructive technique that is widely used to inspect composite materials and structural integrity, and it has been successfully expanded into the arena of biomechanics. Where a secure prosthesis would respond with a single frequency vibration, whereas a loose prosthesis would vibrate at different frequencies appearing as different peaks in the frequency spectrum; this is simplified for the acetabular component, as presented in Figure 1

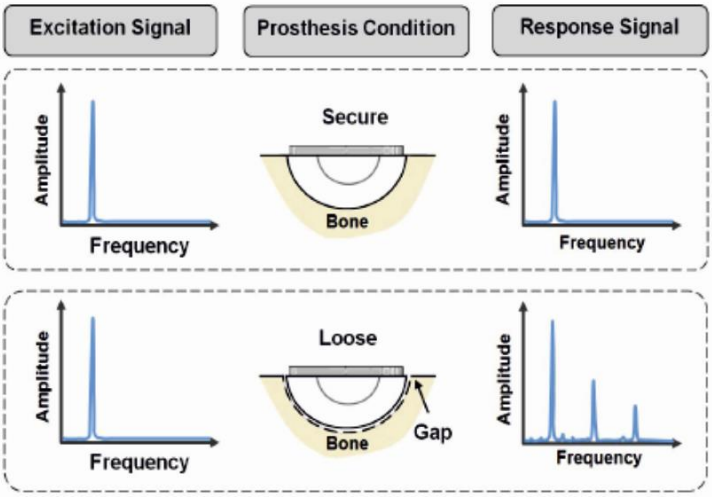

Figure 1 : Vibration analysis concept showing the difference between the secure and loose acetabular cup prostheses

Although the high rate of loosening in the acetabular component has been reported in the clinical scenario (NJR, 2013) , most of THR stability vibration assessment studies have focused on the femoral component (Rosenstein et al., 1989, Li et al., 1995, Li et al., 1996, Puers et al., 2000, Georgiou and Cunningham, 2001, Paech et al., 2007, Rowlands et al., 2008, Ruther et al., 2011, Ewald et al., 2011, Ewald et al., 2011 , Ruther et al., 2012a, Ruther et al., 2013a, Ruther et al., 2013b, Rieger et al., 2013). Thus, the aim of this study was to explore the viability of vibration analysis to accurately detect acetabular component loosening.

2. Materials and Methods

A simplified model, was constructed to mimic different acetabular cup loosening scenarios (secure, 2 and 4 mm of soft tissue between the cup and the bone), using a Sawbone® block with a density of 0.48 g/cm3 (Sawbones Europe AB, Malmö, Sweden) and two different Stryker acetabular cups sizes (54 and 52 mm) with a thin low modulus EVO-STIK silicone layer in between.

A function generator (TG230, Thurlby Thandar Ltd, UK) connected to a power amplifier (PA25E, LDS Ltd, UK) was used for vibration excitation via a mini-shaker (V201, LDS Ltd, UK). The excitation signal was a constant amplitude sinusoidal wave with a frequency sweep range of between 100 and 1500 Hz. The shaker was positioned in a similar location on the Sawbone block for all tests

The resulting natural frequency spectral was observed using fast Fourier transform (FFT) to define the optimum frequency excitation range and the minimum loosening threshold that can be detected. The output signal was measured using two methods; an ultrasound transducer (Mini Dopplex 500, 4 MHz, Huntleigh Technology plc, UK) and an accelerometer (Model 353B18, PCB Piezotronics Inc, US) using a custom code in LabVIEW (Sound and Vibration Measurement Suite version 11, National Instruments) via USB data acquisition (USB-4431, National Instruments) using a personal computer (Core2Duo 3.16 GHz, CPU 4 GB RAM) Figure 2. A sampling frequency of 8 kHz was used to overcome the aliasing effect.

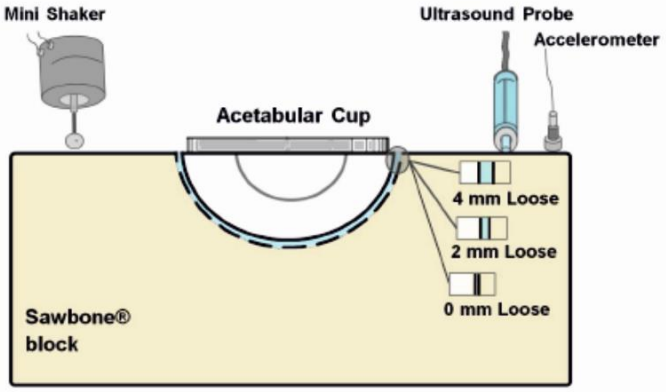

Figure 2: The Sawbone block showing the excitation and measurement methods

Real-time FFT spectrum analyses tracked the frequency response and observed relationships between the two loosening scenarios and the secure condition across the different driving frequencies. In an attempt to define the optimum frequency excitation range for the loosening assessment, a sweep analysis was conducted. The resulting frequencies were then analysed as the harmonic ratio, defined as the relative magnitude of the first harmonic to the fundamental frequency (Harmonic Ratio = First Harmonic magnitude/Fundamental Frequency magnitude). This ratio can then be utilised to show how the different loosening conditions affect the relative magnitude of the first harmonic across the different driving frequencies.

3. Results

The harmonic ratio measurement for the three simulated conditions by using ultrasound and accelerometer was illustrated alongside each for ease of comparison, as shown in Figure 3. The Mann-Whitney test was used to determine significance (defined as $p < 0.05$). Statistical analysis was performed using SPSS software (version 20.0; SPSS,

Chicago, IL, USA). A Shapiro-Wilk test revealed that the harmonic ratio data were not normally distributed; thus, non-parametric analyses were performed.

3.1 Accelerometer

The harmonic ratios for the accelerometer are shown in Figure 3a. The ratios clearly showed a pattern, according to which the secure cup had the lowest value, followed by 2-mm loosening, and 4-mm loosening having the highest harmonic ratio in the frequency range up to 950 Hz. The harmonic ratio for 2-mm loosening was significantly greater ($p < 0.01$) than that in the secure condition in the driving frequency range 100–1050 Hz (Figure 3c). For 4-mm loosening, the harmonic ratio was significantly greater ($p < 0.01$) than that in the secure condition in the frequency range 100–1000 Hz (Figure 3e).

3.2 Ultrasound

The harmonic ratio derived from ultrasound measurements had a higher magnitude than the accelerometer readings, as shown in Figure 3 a-b. The ultrasound measurements were between 200 and 1500 Hz due to the ultrasound system's built-in filter that affected readings below 200 Hz. The same pattern was observed with the accelerometer, with the lowest harmonic ratio observed in the secure condition and progressively increasing at 2- and 4-mm loosening, respectively. The 2-mm loosening resulted in a significantly higher harmonic ratio ($p < 0.01$) than that in the secure condition at driving frequencies between 850 and 1050 Hz (Figure 3d). The harmonic ratio of the 4-mm loosening condition was significantly higher ($p < 0.01$) than that in the secure condition between 500 and 950 Hz (Figure 3f).

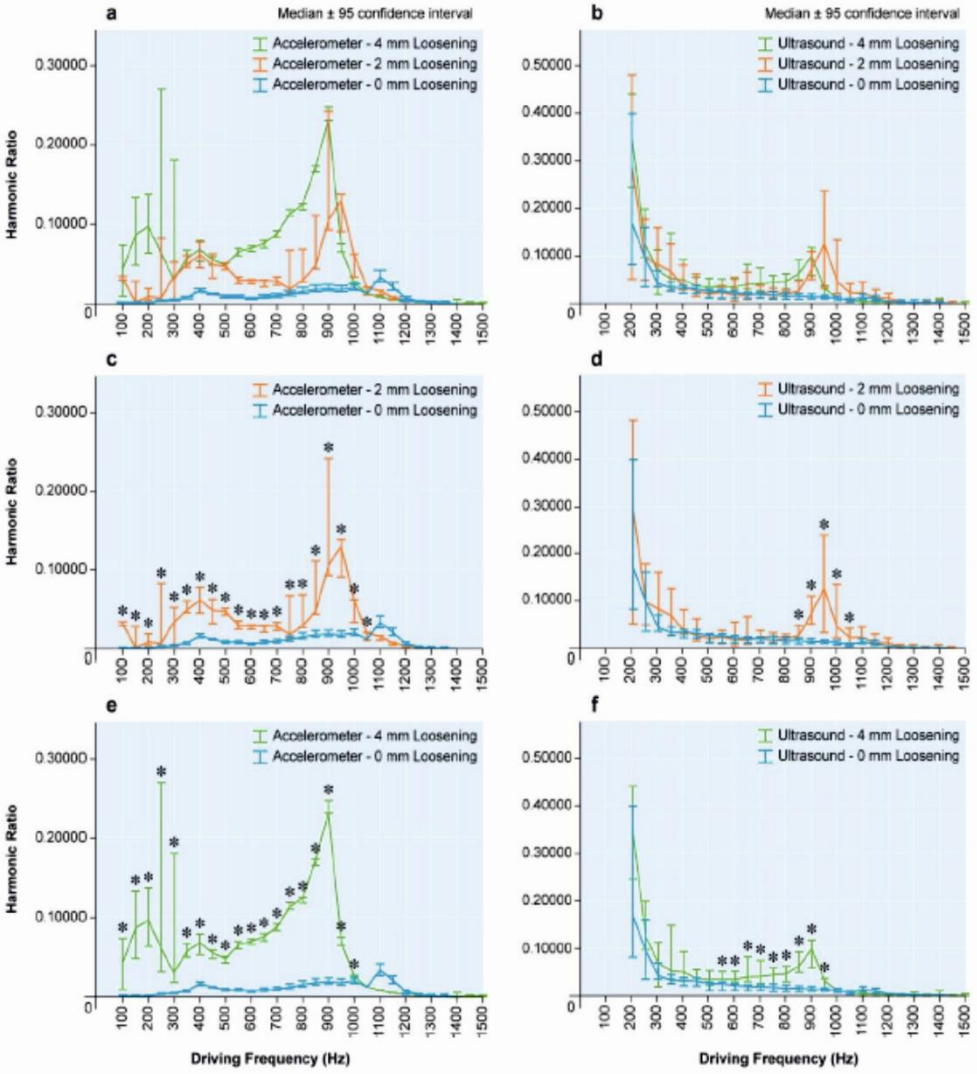

Figure 3: The harmonic ratio of the different loosening conditions using an accelerometer and an ultrasound probe as the measurement methods. Graphs *a, c,* and *e* used an accelerometer for the loosening conditions of (0 mm, 2 mm, and 4 mm), (0 mm and 2 mm), and (0 mm and 4 mm), respectively. Graphs *b, d,* and *f* used an ultrasound for the loosening conditions of (0 mm, 2 mm and 4 mm), (0 mm and 2 mm), and (0 mm and 4 mm), respectively. *Mann-Whitney test $p < 0.05$.

4. Discussion and Conclusions

Vibration analysis implies that secure implants respond with a single frequency peak similar to the excitation signal, whereas loose implants vibrate at different frequencies, which appear as multiple harmonics peaks in the frequency spectrum. The resulting frequencies were initially observed using FFT analysis, then analysed as the harmonic ratio, which was subsequently used as a method to track frequency responses and observe relationships between the loosening scenarios and the secure condition across frequencies of 100–1500 Hz.

When analysing the harmonic ratio for the accelerometer and ultrasound measurements at frequencies < 950 Hz, a clear pattern was observed. The secure cup had the lowest ratios and, as the loosening progressed, this ratio increased. At excitation frequencies of 100–1050 Hz, the accelerometer detected loosening corresponding to 2 mm between the cup shell and the Sawbone surface, while 4 mm loosening was detected at excitation frequencies of 100–1000 Hz. Where for the ultrasound, loosening of 2 mm was detected at driving frequencies of 850–1050 Hz, while 4 mm loosening was detected at 500–950 Hz. Therefore, the harmonic ratio was clearly able to discern between the simulated conditions using both measurement methods.

The use of single density Sawbone block to mimic different loosening conditions was an attempt to simplify acetabular cup instability, which could be considered as a limitation. Additionally, the exaction method was positioned closer to the acetabular component than would be possible in a clinical setting. Moreover, loosening conditions had only press-fit acetabular cups with hard shell components. Future experiments will try to overcome these limitations through achieving a more realistic clinical setup, including a complete

THR Sawbone model with femur and hemi-pelvis, to examine the optimum excitation location and the lowest energy needed to detect loosening.

Preliminary experimental testing showed that vibration analysis could be used as a reliable detection method for acetabular cup component loosening using either an accelerometer or ultrasound probe to detect the vibration. However, the capacity of ultrasound to overcome the attenuating effect of the surrounding soft tissues and its high signal to noise ratio suggest it has the best potential for clinical uses. Further experiments will be conducted to achieve more realistic loosening scenarios for acetabular cup loosening.

5. Ethical approval

Not required.

6. Conflict of interest statement

There are no conflicts of interest to declare.

7. Acknowledgments

This research project was funded by the Saudi Food and Drug Authority-Medical Devices Sector through the Ministry of Higher Education, Saudi Arabia.

References

EWALD, H., RUTHER, C., MITTELMEIER, W., BADER, R. & KLUESS, D. A novel in vivo sensor for loosening diagnostics in total hip replacement. Sensors, 2011 IEEE, 28-31 Oct. 2011 2011 89-92.

EWALD, H., TIMM, U., RUTHER, C., MITTELMEIER, W., BADER, R. & KLUESS, D. Acoustic sensor system for loosening detection of hip implants. Sensing Technology (ICST), 2011 Fifth International Conference on, Nov. 28 2011-Dec. 1 2011 2011. 494-497.

GEORGIOU, A. P. & CUNNINGHAM, J. L. 2001. Accurate diagnosis of hip prosthesis loosening using a vibrational technique. *Clinical Biomechanics,* 16, 315-323.

LI, P. L., JONES, N. B. & GREGG, P. J. 1995. Loosening of total hip arthroplasty. Diagnosis by vibration analysis. *J Bone Joint Surg Br,* 77, 640-4.

LI, P. L., JONES, N. B. & GREGG, P. J. 1996. Vibration analysis in the detection of total hip prosthetic loosening. *Med Eng Phys,* 18, 596-600.

NJR 2013. National Joint Registry for England and Wales 10th Annual Report 2013. *ISSN 1745-1450 (Online).*

PAECH, A., SCHULZ, A., NASSUTT, R., KEINE, J., WENZL, M. & JURGENS, C. 2007. Acoustic Properties of Femoral Components of Hip Endoprostheses Analysis Using Frequency-Resonance-Measurement in a Soft Tissue Simulation Model. *Research Journal of Medical Sciences,* 1, 118-123.

PIVEC, R., JOHNSON, A. J., MEARS, S. C. & MONT, M. A. 2012. Hip arthroplasty. *The Lancet,* 380, 1768-1777.

PUERS, R., CATRYSSE, M., VANDEVOORDE, G., COLLIER, R. J., LOURIDAS, E., BURNY, F., DONKERWOLCKE, M. & MOULART, F. 2000. A telemetry system for the detection of hip prosthesis loosening by vibration analysis. *Sensors and Actuators A: Physical,* 85, 42-47.

RIEGER, J. S., JAEGER, S., SCHULD, C., KRETZER, J. P. & BITSCH, R. G. 2013. A vibrational technique for diagnosing loosened total hip endoprostheses: an experimental sawbone study. *Med Eng Phys,* 35, 329-37.

ROSENSTEIN, A. D., MCCOY, G. F., BULSTRODE, C. J., MCLARDY-SMITH, P. D., CUNNINGHAM, J. L. & TURNER-SMITH, A. R. 1989. The differentiation of loose and secure femoral implants in total hip replacement using a vibrational technique: an anatomical and pilot clinical study. *Proceedings of the Institution of Mechanical Engineers. Part H, Journal of engineering in medicine,* 203, 77-81.

ROWLANDS, A., DUCK, F. A. & CUNNINGHAM, J. L. 2008. Bone vibration measurement using ultrasound: Application to detection of hip prosthesis loosening. *Medical Engineering & Physics,* 30, 278-284.

RUTHER, C., EWALD, H., MITTELMEIER, W., FRITSCHE, A., BADER, R. & KLUESS, D. 2011. A novel sensor concept for optimization of loosening diagnostics in total hip replacement. *J Biomech Eng,* 133, 104503.

RUTHER, C., NIERATH, H., EWALD, H., CUNNINGHAM, J. L., MITTELMEIER, W., BADER, R. & KLUESS, D. 2013a. Investigation of an acoustic-mechanical method to detect implant loosening. *Medical Engineering & Physics,* 35, 1669-1675.

RUTHER, C., SCHULZE, C., BOEHME, A., NIERATH, H., EWALD, H., MITTELMEIER, W., BADER, R. & KLUESS, D. 2012a. Investigation of a passive sensor array for diagnosis of loosening of endoprosthetic implants. *Sensors (Basel),* 13, 1-20.

RUTHER, C., TIMM, U., EWALD, H., MITTELMEIER, W., BADER, R., SCHMELTER, R., ARMIN, AND, L. & KLUESS, D. 2012b. Current Possibilities for Detection of Loosening of Total Hip Replacements and How Intelligent Implants Could Improve Diagnostic Accuracy, Recent Advances in Arthroplasty , Dr. Samo Fokter (Ed.),. *InTech,* ISBN: 978-953-307-990-5.

RUTHER, C., TIMM, U., FRITSCHE, A., EWALD, H., MITTELMEIER, W., BADER, R. & KLUESS, D. 2013b. A New Approach for Diagnostic Investigation of Total Hip Replacement Loosening. *In:* FRED, A., FILIPE, J. & GAMBOA, H. (eds.) *Biomedical Engineering Systems and Technologies.* Springer Berlin Heidelberg.